# Bioremediation Potential and Molecular Characterization of Heavy Metal-resistance Profiles of Bacterial Isolates from Industrial Effluents in Mojo and Bishoftu area, Ethiopia

**Duguma Dibbisa Itana**

**A Dissertation Submitted to the Department of Applied Biology, College of Applied Natural Sciences**
**Presented in Partial Fulfillment of the Requirements for the Degree of Doctor of Philosophy in Biotechnology (Specialization in Environmental Biotechnology)**

**School of Graduate Studies**
**Adama Science and Technology University**

**October, 2025**
**Adama, Ethiopia**

# Bioremediation Potential and Molecular Characterization of Heavy Metal-resistance Profiles of Bacterial Isolates from Industrial Effluents in Mojo and Bishoftu area, Ethiopia

**PhD Candidate:**

**Duguma Dibbisa Itana**

**Supervisors**

**Tadessa Daba (PhD)**

**Seid Mohammed (PhD)**

**A Dissertation Submitted to the Department of Applied Biology, College of Applied Natural Sciences**

**Presented in Partial Fulfillment of the Requirements for the Degree of Doctor of Philosophy in Biotechnology (Specialization in Environmental Biotechnology)**

**School of Graduate Studies**

**Adama Science and Technology University**

**October, 2025**

**Adama, Ethiopia**

# DECLARATION

I hereby declare that the dissertation entitled "**Bioremediation Potential and Molecular Characterization of Heavy Metal-resistance Profiles of Bacterial Isolates from Industrial Effluents in Mojo and Bishoftu area, Ethiopia**" is my original work. That is, it has not been submitted for the award of any academic degree, diploma, or certificate in any other university. All sources of materials used for this thesis have been duly acknowledged

| Duguma Dibbisa Itana | _____ | _____ |
|---|---|---|
| Name of student | Signature | Date |

## RECOMMENDATION OF ADVISORS

We, the undersigned supervisors, confirm that we have read and revised the dissertation entitled "**Bioremediation Potential and Molecular Characterization of Heavy Metal-resistance Profiles of Bacterial Isolates from Industrial Effluents in Mojo and Bishoftu area, Ethiopia**" prepared under our advice by Duguma Dibbisa Itana, submitted in partial fulfillment of the requirements for the degree of Doctor of Philosophy in Biotechnology (Specialized in Environmental Biotechnology). Therefore, we recommend the submission of the dissertation to the department for further review and defense

| | | |
|---|---|---|
| Tadessa Daba (PhD) |  | _____ |
| Major Supervisor | Signature | Date |
| Seid Mohammed (PhD) | _____ | _____ |
| Co-Supervisor | Signature | Date |

# APPROVAL SHEET

We hereby certify that the recommendations and suggestions made by the board of examiners are appropriately incorporated into the final version of the dissertation entitled "**Bioremediation Potential and Molecular Characterization of Heavy Metal-resistance Profiles of Bacterial Isolates from Industrial Effluents in Mojo and Bishoftu area, Ethiopia**" by Duguma Dibbisa.

| | | |
|---|---|---|
| Tadessa Daba (PhD) | 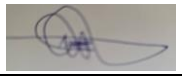 | _____ |
| Major Supervisor | Signature | Date |
| Seid Mohammed (PhD) | _____ | _____ |
| Co-supervisor | Signature | Date |

## APPROVAL OF THE BOARD OF EXAMINERS

We, the undersigned, members of the Board of Examiners of the dissertation open defense by Duguma Dibbisa Itana, have read and evaluated the dissertation entitled "**Bioremediation Potential and Molecular Characterization of Heavy Metal-resistance Profiles of Bacterial Isolates from Industrial Effluents in Mojo and Bishoftu area, Ethiopia**" and examined the candidate during the open defense. This is, therefore, to certify that the dissertation is accepted for partial fulfillment of the requirements of the degree of Doctor of Philosophy in Biotechnology (Specialization in Environmental Biotechnology).

| | | |
|---|---|---|
| Chairperson | Signature | Date |
| Internal Examiner 1 | Signature | Date |
| Internal Examiner 2 | Signature | Date |
| External Examiner 1 | Signature | Date |
| External Examiner 2 | Signature | Date |

Finally, the dissertation's approval and acceptance are contingent upon the candidate submitting its final copy to the School of Postgraduate Studies (SPGS) through the candidate's Department Graduate Council (DGC) and College of Graduate Studies (CGS).

| | | |
|---|---|---|
| Department Head | Signature | Date |
| College Dean | Signature | Date |
| School of Postgraduate Studies | Signature | Date |

# DEDICATIONS

I dedicate this dissertation to my beloved family: my mother, **Negase Gadissa**, my wife, **Hawi Tujuba**, my brother, **Gari Dibbisa**, and my beloved children, **Nimona**, **Monera**, and **Raga** Duguma. Their unwavering support and encouragement were instrumental in my academic journey.

# BIOGRAPHICAL SKETCH

The author was born in the West Shewa Zone of Oromia Regional State to his father, Dibbisa Itana, and his mother, Nagase Gadissa, on May 10/1988. He attended Bosha Elementary School in Bako Tibe Woreda and completed his Secondary & Preparatory School at Ambo Senior Secondary and Comprehensive Preparatory School. After finishing Preparatory School, he directly joined Ambo University in 2007 and graduated on June 24, 2010, with a BSc degree in Applied Biology (Ecological and Environmental Sciences stream). Upon graduation, he was directly hired by the Ministry of Education (MOE). He then started working as a graduate assistant at Haramaya University. After serving for two years, he enrolled in Haramaya University's postgraduate program in 2013, completing his MSc in Biotechnology in 2015. Then, he returned to the Department of Biology, now the School of Biological Science and Biotechnology, where he served as a lecturer, offering various courses for undergraduates and assisting the postgraduate programs. He served the school as a program coordinator for the Molecular Biology and Biotechnology for three years and as a registrar head for the College of Natural and Computational Sciences for a year. After spending five years in the School of Biological Science and Biotechnology, he joined Adama Science and Technology University, College of Applied Natural Science, Department of Applied Biology to pursue his PhD in Biotechnology (Specialization in Environmental Biotechnology) in 2020/21, dedicating himself to advanced research in environmental biotechnology. Over the past five years, he has worked tirelessly to refine his expertise and contribute to his disciplines. His PhD dissertation, the product of dedicated work, is now ready for presentation, showing his commitment to environmental biotechnology. He has conducted his research work at both Haramaya University and Adama Science and Technology University.

# ACKNOWLEDGMENTS

I am profoundly thankful to the Almighty God for His continuous guidance and blessings throughout my academic journey. Without His divine intervention, this dissertation would not have been possible.

My heartfelt gratitude goes to my supervisors, **Dr. Tadessa Daba Bedada** and **Dr. Seid Mohammed Ebu**, whose expert mentorship, generous support, and encouragement were essential to my academic development and the successful completion of this research.

I'm incredibly grateful to the faculty of ASTU for their unwavering dedication, inspiration and guidance. Their commitment laid a strong foundation for my academic journey. I also want to extend a special thanks to my fellow PhD cohort in Applied Biology (2020/2021) at ASTU; their collaborative spirit and intellectual contribution truly enriched my experience.

I express my gratitude to friends, **Mr. Bane Kebede**, **Mr. Gadissa Kefeyalew**, **Dr. Abdissa Jabessa**, **Dr. Habtamu Alemayehu**, **Dr. Zewdu Bezu**, **Mr**. **Deressa Boja, Mr. Fuad Yusuf** and **Ms. Haimanot Buzuneh**, from Haramaya University for their sympathetic support and assistance throughout the laboratory activities. I also appreciate the laboratory support from **Mr. Sirnessa Faye** and **Mr. Wondosen Sime,** both from ASTU. Their contributions have been invaluable in ensuring the successful execution and analysis of my experiments.

Last, not least, I would like to express my deepest gratitude to my beloved wife, **Hawi**, and our beloved daughters and families for their unwavering love, support, and belief in me. Their constant encouragement and sacrifices have been instrumental in helping me overcome challenges and persevere throughout my academic journey. Their generous support has given me the strength and motivation to complete my dissertation. I am eternally grateful for their love and understanding. I would like to extend my sincere thanks to Adama Science and Technology University and Haramaya University for their financial support.

# LIST OF TABLES

**Lists of Tables** **Pages**

# LIST OF FIGURES AND ILLUSTRATIONS

**Lists of Figures** **Pages**

# LISTS OF APPENDICES IN TABLES

**Appendix Tables** **Pages**

# LISTS OF APPENDICES IN FIGURES

**Appendix in Figures** **Pages**

# LIST OF ACRONYMS AND ABBREVIATIONS

| | |
|---|---|
| ASTU | Adama Science and Technology University |
| BEIZ | Bishoftu Effluent Industrial Zone |
| BSS | Bishoftu Soil Sample |
| $Cd^{2+}$ | Cadmium |
| CGview | Circular Genome Viewer |
| CNS | Central Nervous System |
| $Co^{2+}$ | Cobalt |
| $Fe^{2+}$ | Iron |
| HM | Heavy Metal |
| HMRBI | Heavy Metal-Resistant Bacteria Isolate |
| HMRG | Heavy Metal Resistant Gens |
| MALDTOF-MS | Matrix Assisted Laser Desorption/Ionization Time of Flight Mass Spectrometry |
| $Mn^{2+}$ | Manganese |
| MTED | Mojo Tannery Effluent Discharges |
| MWWS | Mojo Waste Water |
| NCBI | National Center of Biotechnology Institute |
| $Ni^{2+}$ | Nickel |
| NNPP | Neural Network Promoter Prediction |
| OrthoANI | Orthologous Average Nucleotide Identity |
| $Pb^{2+}$ | Lead |
| ROS | Reactive Oxygen Species |
| TF | Transcriptional Factor |
| TSS | Transcriptional Start Site |
| WGE | Whole Genome Sequence |
| $Zn^{2+}$ | Zinc |

## Summary

*Various heavy metals (HM) can be removed from the environment by various bacterial species, which are developing resistance and reduction through various mechanisms. Bacteria bioaccumulate Heavy metals (HMs) inside their cell structures. This study aimed to isolate and characterize heavy metal–resistant bacterial isolates (HMRBI) from environmental samples collected in Ethiopia's Bishoftu Eastern Industrial Zone and Mojo Tannery Industry, with the objective of mitigating environmental pollution. Soil and wastewater samples were collected and transported to the Molecular biology and Biotechnology laboratory, Haramaya University. The HMRBIs were subsequently screened and identified based on their resistance to selected heavy metals. These isolates were characterized and identified using biochemical assays, protein profiling through matrix-assisted laser desorption/ionization time-of-flight mass spectrometry (MALDI-TOF MS), and molecular analysis based on 16S rRNA gene sequencing. Furthermore, several computational approaches were employed to investigate the expression patterns and regulatory mechanisms of heavy metal resistance genes (HMRG). These included comparative genomes, predicting promoter regions, & common sequence motifs, identifying transcriptional sites, re-annotating genes, and identifying transcriptional factors. The Multiple Em Motif FOR Elicitation (MEME Suite), Rapid Annotation using Subsystem Technology (RAST), Orthologous Average Nucleotide Identity (OANI), and EziBIO databases were key tools utilized in this analysis. Cell deformation, bio-absorption, and infrared spectra corresponding to heavy metal uptake by cells were examined using scanning electron microscopy with energy-dispersive X-ray spectroscopy (SEM-EDX) and Fourier transform infrared spectroscopy (FTIR). Atomic Absorption Spectrophotometry (AAS) was also utilized to assess the biodegradability of HMRBI. Among seventeen characterized bacterial isolates, Pseudomonas putida-HMRBI-2 showed the highest ability to bioaccumulate cobalt, with removal rates of 67.38%. Exiguobacterium aurantiacum strain HMRBI-7 was the most effective at removing copper and chromium, with bioaccumulation rates of* 65.02 ± 0.002% and 70.04 ± 0.001%, *respectively. Aeromonas hydrophila strain HMRBI-12 and Delftia acidovorans-HMRBI strain 7 demonstrated good cadmium and zinc removal abilities, with bioaccumulation rates of 65.02% and 70.32%, respectively. Although each bacterial isolate exhibited variable levels of HM resistance, they all showed unique capabilities for the bioaccumulation of HMs. It is believed that the isolate most likely possesses a combination of intracellular and extracellular biosorption mechanisms to degrade HMs. The study, which utilized*

*eight 16 rRNA gene sequences, successfully identified three microbial isolates: P. benzoelyticum strain HMRBI-1, Citrobacter strain HMRBI-5, and Klebsiella strain HMRBI-14 as having the highest HM removal capacity. Furthermore, the minimum inhibitory concentration (MIC) results highlighted that Klebsiella spp. exhibited an MIC of 700 ppm, whereas Citrobacter spp. presented an MIC of 800 ppm. Moreover, the* maximum *bioaccumulation efficiencies were noted at 89.74, 85.21,* and *79.27% for Klebsiella strain HMRBI-14, Citrobacter strain HMRBI-5, and P. benzoelyticum strain HMRBI-1, respectively. Additionally, 14 transcription factors were identified and predicted from the reliable and lowest candidate motif with an e-value of 3.0e-009. Further investigation was conducted on the 14 identified transcription factors concerning activation, repression, and dual functions and regulation in microorganisms to thrive in harsh environmental conditions. As the data suggest, the identified transcription factors were used for the activation of gene regulation rather than repression. Therefore, the study highlights the importance of bacteria in HM bioremediation at contaminated sites due to the genes they possess. Analyzing regulatory elements provides a crucial foundation for understanding the genes the key to HM bioremediation, and the combined approach of laboratory experiments and bioinformatics effectively harnesses native microorganisms to clean heavy metal-contaminated environments*

***Keywords***: Biosorption, Common Motif, MEME Suite, Pollution, Promoters, and RAST

# TABLE OF CONTENTS

# 1. BACKGROUND OF THE STUDY

## 1.1. Introduction

Heavy metals are elements with high atomic weights, high densities, and high toxicity at low concentrations. Some HMs are essential micronutrients that play critical roles in the metabolic activities of living things. These include $Co^{+2}$, $Cu^{+2}$, $Fe^{+2}$, $Mg^{+2}$, $Mn^{+2}$, $K^{+2}$, $Na^{+2}$, and $Zn^{+2}$. The most toxic HMs are $As^{+2}$, $Cd^{+2}$, $Cr^{+6}$, $Hg^{+2}$, and $Pb^{+2}$ (Ali et al., 2011). Environmental pollution, is arises from both natural occurrences and pervasive human activities, presents a critical and complex threat that jeopardizes global sustainable development. Due to their wide range of applications in different industries, agricultural practices, and technological activities, heavy metals are widely distributed in the natural environment. This raises concerns about their potential effects, particularly on human health and the environment (Tchounwou et al., 2012).

Heavy metals such as arsenic, cadmium, chromium, mercury, and lead are discharged into the environment by industry, mining activities, and poor waste management, posing risks to the ecosystems, human health. These metals can persist in the environment for a long time and contaminate the air, soil, and water bodies. They can disrupt ecosystem functioning, damage plant diversity, reduce biodiversity, and affect food chains Kutty & Al-Mahaqeri, (2016). When people are exposed to a concentration of HMs, either through inhalation, ingestion, or skin contact, they can experience various health problems. Likewise, HM can enter water bodies, be absorbed by aquatic organisms, accumulate in their tissues, and move up the food chain (Kinuthia et al., 2020). This bioaccumulation can lead to the poisoning of various bird families, fish, and other wildlife. They can also disrupt the reproductive systems of animals, impair their growth and development, and cause population declines (Alengebawy et al., 2021).

Studies have shown that some HMs are essential micronutrients that play critical roles in the processes of microorganisms. Metals such as $Co^{+2}$, $Cr^{+6}$, $Cu^{+2}$, $Fe^{+2}$, $Mg^{+2}$, $Mn^{+2}$, $K^{+2}$, $Ni^{+2}$, $Na^{+2}$, and $Zn^{+2}$ are essential metals. The most referred HMs are usually $As^{+2}$, $Cd^{+2}$, $Cr^{+6}$, $Hg^{+2}$, and $Pb^{+2}$ in this context. As essential micronutrients, these HMs perform several vital functions, including regulating osmotic pressure and facilitating redox reactions. Additionally, they stabilize biological molecules through electrostatic connections, act as cofactors in the enzyme reaction. However, ions like $Cd^{+2}$,

$Hg^{+2}$, and $Pb^{+2}$ pose a risk due to their potential toxicity (Ali et al., 2011). HM toxicity occurs when heavy metals accumulate in the body and interfere with normal biological function. This happens through various routes of exposure, including ingestion, inhalation, and skin contact. Furthermore, evidence shows that some HMs become toxic or polluting agents in the environment when dissolved in water. This is a common phenomenon of toxicity due to $Cd^{+2}$, $Cu^{+2}$, $Cr^{+6}$, and $Zn^{+2}$ ions. Due to their inherent toxicity, high concentration of heavy metals poses a significant threat to human health and the environment. Furthermore, these metals are persistent in the environment because they resist biotransformation processes (Sall et al., 2020).

Heavy metals pose a significant environmental threat due to their non-biodegradable and long-term persistence in the environment (Syed et al., 2015). Released from various industries, the toxic nature of these metals harms humans and the environment alike, leading to negative global effects (Mishra et al., 2020). Environmental pollution, which arises from both natural occurrences and pervasive human activities, presents a critical and complex threat that jeopardizes global sustainable development. The rapid expansion of industrialization and urbanization over the past century has had a profound impact on environmental pollution, making it a major concern worldwide (Marzan *et al*., 2017; Swain, 2024). There is also evidence that environmental pollution from industrial processes can release a mixture of pollutants, for example, those from the manufacturing industries, like HMs (Adnan et al., 2024). Unregulated industrial waste and mining operations are major contributors to environmental degradation, especially concerning the contamination of soil and water with heavy metals (Girma, 2021). These contaminants can have a devastating effect on ecosystems, human health, and the overall sustainability of our planet (Deng et al., 2022).

On the other hand, pesticides and herbicides are indispensable tools widely used in modern agriculture, helping to manage pests and weeds that can reduce crop yields; they are also a source of HM pollution. However, the extensive application of pesticides and herbicides has given rise to considerable apprehension regarding environmental contamination (Alengebawy et al., 2021). Human activities are also the primary heavy metal pollution sources (Deng *et al*., 2022), introducing toxic elements into the environment through numerous pathways. Industrial processes are the major source of their effluents frequently contain high concentrations of HMs. When industrial effluents are discharged without adequate treatment, they severely contaminate vital water sources, including

groundwater, rivers, lakes, and oceans (Afzaal *et al*., 2022). This effluent creates significant environmental risks across all aquatic ecosystems. Similarly, agricultural practices can also contribute to heavy metal pollution (Srivastava et al., 2017). The routine application of inorganic fertilizers and various pest control chemicals directly contributes to the introduction of harmful HMs into both the soil and water bodies. Over time, the accumulation of HMs in the soil and water bodies can negatively impact soil health, hinder plant growth, and potentially enter the food chain (Alengebawy et al., 2021). Therefore, effective environmental management must target both industrial discharges and agricultural runoff to mitigate the widespread danger posed by these contaminants.

Bioremediation is a technique that employs living microorganisms such as bacteria, fungi, & occasionally plants, to eliminate, break down, transform, or neutralize environmental contaminants present in polluted soil, water, and air. Nowadays, it is a promising field to clean industrially polluted areas. Bacteria are the primary and most versatile agents used in bioremediation to clean up environmental pollutants. They are crucial because of their vast metabolic diversity, which allows them to break down an extensive range of contaminants. Bacteria have evolved several sophisticated mechanisms to protect themselves from the toxicity of environmental pollutants such as metal ions. The strategy involves extracellular and intracellular sequestration, where components like the cell wall, outer membrane, & capsule bind to metal ions to change surface groups such as carboxyl, amino acid, and phosphate, preventing their entry. If metal ions enter, bacteria use active transport (efflux), utilizing protein pumps to actively export metal ions out of the cell. They also reduce the toxicity of certain HMs through enzymatic reduction of metal ions, converting highly toxic forms like chromate, molybdate, and vanadate into less harmful states (Benmarrlek & Fardeau, 2016). The metabolic versatility of bacteria, which enables them to efficiently absorb and convert nutrients, is crucial for their survival and functionality in severe environments. They play a substantial role in heavy metal clean up by detoxification and immobilization strategies, which effectively remove the metal ions from the environment or convert them into a less harmful form. This is achieved through the possession of gene diversity, which allows them to adapt & thrive in the toxic environments.

Such knowledge can be harnessed to improve biological waste management processes, enabling more efficient and sustainable cleanup of contaminated sites. Heavy metal-resistant bacteria have a key to bioremediation, offering a natural method of detoxifying polluted sites. However, their prevalence

poses a public concern because they frequently possess antibiotic resistance genes (Pham et al., 2022). Due to industrialization, soils, water resources, and biological entities have been adversely affected, resulting in an overall imbalance in the natural environment. This environmental pressure changes the microbial community structure, favoring HMR bacteria and decreasing overall microbial diversity. Bacteria can accumulate metals because their surface area to volume ratios are high, along with some active sites in cell walls (Mosa et al., 2016). For instance, soil bacteria, which have metal resistance mechanisms, are: *Pseudomonas*, *Bacillus*, *Acinetobacter*, *Micrococcus*, *Hafnia*, *Gemella*, *Nocardia*, & *Deinococcus* (Parisa et al., 2011), whereas *Aspergillus* and *Penicillium species are* some of the fungal *spp.* reported to have heavy metal bioaccumulation (El-Bondkly et al., 2022). In addition, brown algae and *cyanobacteria* exhibit resistance to heavy metals (Chugh et al., 2022).

Bishoftu Industrial Zone, a major industrial hub located in a town southeast of Addis Ababa, Ethiopia, plays an important role in the country's industrialization efforts. This is one of several industrial zones developed by the Ethiopian government to attract foreign direct investment and boost domestic manufacturing. This industrial zone is designed to accommodate a diverse range of industries, including textiles and garments, steel, agro-processing, and pharmaceuticals. On the other hand, Mojo, located 73 kilometers East of Addis Ababa, is a town with a thriving industrial sector, ranging from small-scale businesses to large-scale manufacturing.

One prominent industry in Mojo is tanning, the process of transforming raw animal hides and skins into leather. While tanning is essential for leather production, it often faces significant criticism due to its environmental impact of chromium salts. The improper usage of harmful chemicals, such as chromium salts and dyes, in the tanning process can be a principal cause of water contamination if not properly managed. Tanning is widely recognized as one of the most polluting industries globally, posing a serious threat to the environment (Monira & Mostafa, 2023).

Identifying specific DNA sequences across diverse species is essential for understanding genome function because it provides a powerful lens through which to explore evolution, pinpoint critical biological processes. The conserved regions are vital genes and regulatory elements providing insights into gene function relationships within biological systems and highlighting evolutionary processes (Nelson et al., 2003). Comparative genomics is a powerful tool for identifying real genes amidst the vast expanses of DNA. It influences the principles of nucleotide conservation, which states

that genes essential for an organism's survival and reproduction tend to have their DNA sequences preserved across evolutionary time, Sivashankari et al., (2007). Regulatory elements are essential DNA sequences that control gene expression. The discovery of regulatory elements relies on nucleotide conservation patterns and an experimental validation approach. The elements play an important role in the development of cellular processes (Koo et al., 2017). Regulatory elements are useful in environmental biotechnology. They offer a lot of solutions to problems related to the environment and health.

## 1.2. Statement of the problem

Heavy metals discharged from industrial effluents are a major environmental pollutant due to their non-biodegradable nature. This persistent nature allows them to contaminate the aquatic environment, disrupting the food chain and food web energy flow of the aquatic organisms (Kinuthia et al., 2020). Unlike many organic pollutants, heavy metals are difficult to remove from the environment and can persist for many decades in the environment. Heavy metal removal by microorganisms has many advantages compared to physical and chemical methods due to cost-effectiveness, environmental friendliness, and ease of use (Bhattacharjee et al., 2020).

Petrochemical industries are rapidly developing in different parts of Ethiopia. Despite their social and economic benefits, these industries negatively affect environmental pollution. Mojo and Bishoftu are towns found in the Oromia regional state that host numerous industries. Mojo Tannery Industry, which releases wastes with chromium salts, can pollute soil, water & vegetables. (Gebeyehu & Bayissa, 2020) reported that the maximum levels of ($Cr^{+6}$, $Cd^{+2}$, $Zn^{+2}$, $Fe^{+2}$, $Pb^{+2}$, and $Cu^{+2}$) in soil, water and vegetable. Toxic industrial effluents affect the environment and micro-biota that maintain ecosystem services. The waste generated from the Eastern Industrial Zone (Bishoftu), which contributes a major problem of environmental pollution. Heavy metal pollution can also originate from various sources, emissions from industries, the residual effects of pesticides in agricultural soil, and the application of certain chemical fertilizers used by farmers (Alengebawy et al., 2021).

From the viewpoint of the natural environmental pollution approaches, bioremediation is of paramount importance in the current world to save the environment Sundarraj et al., (2022) studied that *Pseudomonas putida* isolated from tannery has a significant bioremediation ability due to the

indigenous ability of the bacterium to biotransformation chromium into harmless compounds by oxidation-reduction reaction. Another research conducted on the phytoremediation of Heavy metal pollution, such as $Cd^{+2}$, $Zn^{+2,}$ and $Pb^{+2}$, is scrutinized from the food industry using forest species of Scots pine (Pinus silvestris L.), Norway spruce (Picea abies L.), and oak (Quercus robur L) (Placek et al., 2016). Although several studies have been undertaken on the industrial and domestic waste waters discharged into the waterbodies around industrial sites of the Akaki-Awash water basin over the last decades, there is still a need for more studies, especially on heavy metal-laden wastes, to fully realize the best bioremediation option with industrial wastes. Therefore, this study focuses on characterizing and profiling the heavy metal resistance potential of bacteria isolated from industrial effluents in Mojo and Bishoftu, Ethiopia, with the following objectives:

## 1.3. Objectives of Study

### 1.3.1. General Objective:

- To evaluate the bioremediation potential and molecular characterization of heavy metal-resistance profiles of bacterial isolates from industrial effluents in Mojo and Bishoftu, Ethiopia

### 1.3.2. Specific Objectives:

- To assess, isolate, and molecular characterize the heavy metal-resistant bacterial strains
- To optimize the growth of the isolates using carbon and nitrogen sources, study the optimum conditions for the potential HMRBI
- To evaluate the metabolic profile of heavy metal resistance bacterial isolates
- In silico, regulatory element analysis and comparative genomics study of the heavy metal resistance gene in the complete genome of *Cupriavidus gilardii* CR3

# 2. LITERATURE REVIEW

## 2.1. Heavy Metals

Heavy metals such as arsenic, lead, mercury, cobalt, and chromium are major hazardous and enduring weapons of environmental menaces owing to their features and prevalence in industrial wastewaters. Unlike the pollutants that are organic, and which can frequently be mineralized into smaller units, the heavy metals are non-degradable (Ayangbenro & Babalola, 2017). The majority of heavy metals are toxic at low concentrations and can enter the food chain, where they accumulate and inflict damage to living organisms. All metals have the potential to exhibit harmful effects at higher concentrations, and the toxicity of each metal depends on the amount available to organisms, the absorbed dose, the route, and the duration of exposure (Jeyakumar et al., 2023). This means they persist indefinitely in the environment, accumulating in the soil, water, and living organisms. The inabilities of natural processes to eliminate these heavy metals necessitate more active remediation strategies to prevent long-term environmental and health challenges.

The toxicity of heavy metals, even at low concentrations, increases their danger. Even in trace amounts, many heavy metals are toxic to living things. Unlike other toxins that are quickly expelled, heavy metals like lead and cadmium are not easily metabolized. This leads to their gradual buildup in tissues and organs, where they interfere with essential biological processes, damage DNA, and disrupt enzyme function. Consequently, what may seem like a harmless exposure can lead to chronic health problems and severe long-term damage, with the risk amplified as these toxins move up the food chain through bioaccumulation. HMs are frequently not effectively eliminated by organisms after consumption; instead, they accumulate in their tissues over time. The concentration of heavy metals rises at each trophic level as predators higher up the food chain eat these organisms, increasing exposure and possibly harming apex predators and eventually humans (Oladimeji et al., 2024;Oros, 2025).

## 2.2. History of heavy metals

The history of HMs is closely tied to the development of human civilization and the discovery and utilization of various metals throughout the ages. Developing mining techniques and smelting metals like iron and mercury was crucial to the starting point of HMs in ancient civilizations. In the Middle

Ages, the discovery of new metal deposits increased the production and use of heavy metals widely used in construction, coinage, and weaponry. The era of industrialization in the 18$^{th}$ and 19$^{th}$ centuries marked a significant turning point in the development of heavy metals. The discovery and extraction of new metal ores, such as zinc and nickel, along with advancements in metallurgical processes, also led to the further development of HMs. Since their early usage in modern industrial manufacturing applications, HMs have been an integral part of human civilization. Heavy metals were instrumental in the advancement of industries such as manufacturing, transportation, and telecommunications, playing a crucial role in shaping the modern world (Zhou et al., 2020).

Over the past decades, the term HMs has been more frequently utilized in different publications and legislation related to chemical risks and appropriate utilization of chemicals, driven by advances in scientific understanding of the toxic effects of these substances and rising public awareness of the importance of chemical safety and the environment. Csuros and Duffus have defined HMs as metals with a density greater than 5 g/cm$^3$. The term "heavy metals" is often used to refer to a group of metals and metalloids that are associated with environmental pollutants and toxicity (Duffus, 2002). In the current scenario, HM has been defined as a naturally occurring metal with an atomic number greater than 20 and an elemental density greater than 5g/cm$^3$ (Ali et al., 2019). As the industry has grown, waste has been discharged into the environment, primarily into soil and water containing heavy metals. Due to factors like industrial activities and waste disposal, urban areas have become hotspots for the accumulation of HMs, posing a significant environmental challenge. Studies have also shown that they slowly moved deep into the environment through processes like leaching, erosion, and wind erosion. The uncontrolled release of HMs into soil and water is a major global health apprehension. These metals cannot be broken down easily into less harmful substances, leading to long-term environmental damage and posing risks to human health (Bibi et al., 2019). Many heavy metals, including arsenic, cadmium, chromium, copper, lead, mercury, nickel, selenium, silver, and zinc, are toxic even at very low concentrations. Not only are they harmful to cells, but they can also cause cancer and genetic mutations (Dixit et al., 2015).

## 2.3. Classification of heavy metals

HMs can be divided into two categories: essential and non-essential, based on their biological applications. Essential HMs are used in biochemical and physiological functioning in animals and

plants. They are key components of several enzymes and play a significant role in many redox reactions. For instance, the essential heavy metals include $Cu^{+2}$, $Fe^{+2}$, $Mn^{+2}$, and others that play an important role in redox reactions. On the other hand, non-essential HMs have no known biological application in living organisms. These include $Cd^{+2}$, $Hg^{+2}$, and $Pb^{+2}$, which are toxic and biologically non-biodegradable, described as non-essential HMs (Ramírez, 2013). Copper is one of the commonly known essential HMs that functions as an important cofactor for several enzymes. Enzymes such as catalase, cytochrome oxidases, dopamine β-monooxygenases, peroxidases, monoamine oxidases, and superoxide dismutase are associated with the role of copper in redox reactions. It is also involved in metabolism, biosynthesis, and hemoglobin formation. Copper's ability to switch between an oxidized state ($Cu^{2+}$) and a reduced state ($Cu^{1+}$) is influenced by cuproenzymes that participate in redox reactions (Stern, 2010).

Essential and non-essential HMs can be absorbed and harm biodiversity at certain concentrations. Studies have shown that both aquatic and non-aquatic organisms can be affected by heavy metal concentrations at certain levels. For instance, fish are significantly impacted by the accumulation of heavy metals in their food chains, which can be released from external sources (Yilmaz et al., 2017). The transfer of both essential and non-essential heavy metals can occur through food chains, from soil to plants and ultimately to humans, potentially impacting human health. As a result, once metals accumulate in body tissues, they are difficult to remove, especially non-essential metals (Ali et al., 2019). In food chains, all non-essential heavy metals are not biomagnified. Studies have shown that methylmercury is biomagnified in food chains, while $Cd^{+2}$ and $Pb^{+2}$ are not biomagnified in primary producers. However, bioaccumulation of non-essential heavy metals does occur in specific food chains of primary consumers, like fish (Garelick et al., 2008).

## 2.4. Sources of heavy metal pollution

There are two sources of HM pollution: natural and anthropogenic. Natural processes, such as the weathering of metal-bearing rocks, volcanic eruptions, and aerosol formation, contribute to the release of HMs into the environment. Human activities are the primary cause of a dramatic increase heavy metal pollution. Unlike naturally occurring contextual levels, anthropogenic sources release large concentrated quantities of heavy metals that contaminate the air, water and soil, presenting

severe risks to the environment and human health (Xu et al., 2024). Below are some sources of heavy metal pollution presented (Figure 1).

### 2.4.1. Anthropogenic sources of heavy metal pollution

Environmental pollution triggered by HM concentration remains a significant global challenge. HMs, which are naturally occurring elements, can become harmful contaminants when introduced into the environment in excessive amounts. There are several types of environmental contaminants: biological waste disposal, inorganic, and organic substances, which are major sources of environmental contaminants (Garelick et al., 2008). Regardless of their specific category, all pollutants pose a significant threat to the natural environment. As the worldwide population is significantly growing, so too is the amount of waste generated, leading to increased environmental pollution if not properly controlled. This learning has made contamination a major global environmental challenge impacting ecosystems, public health, and contributing a climate change (Manisalidis et al., 2020).

Industrial activities such as the production of chemicals, mining, metallurgy, and wastewater disposal release various pollutants into the environment, including HMs, releasing substantial concentrations. Anthropogenic activities have significantly increased the release of HMs beyond natural levels of concentration. The high concentrations of HMs in the environment can severely disrupt ecosystem services and pose a significant threat to biodiversity by compromising the fundamental processes that support life (Mathivanan et al., 2021). Human activities significantly contribute to HM pollution in the environment, far surpassing natural sources in both scale and impact. For example, the automotive industry releases lead into the atmosphere, while agricultural practices introduce copper and zinc through pesticide and herbicide applications. Additionally, the combustion of fossil fuels releases HMs like nickel and mercury into the environment. To meet the demands of a growing population, industries are compelled to continuously produce goods, resulting in heightened influx of population from different sources. These industrial activities significantly release harmful, untreated industrial effluents that threaten environmental health and biodiversity (He et al., 2005).

The effluents from manufacturing industries, as well as the disposal of untreated hazardous wastes, have contributed to a larger amount of HM pollutants. Although several sources can release heavy metals into the environment, the most common source affecting the natural environment is mining

activities. Mining activities, such as searching, exploration, construction, operation, maintenance, development, and decommissioning, can have a variety of negative impacts, as well as direct and indirect effects on the environment. It is a common economic activity in both the industrialized and non-industrialized worlds and has undeniable negative environmental consequences. The major consequence of mining activities is the release of HM contaminants, which affects surface water more than groundwater. Surface water is a major concern because all life forms rely on it, and it is required to sustain life (Haddaway et al., 2019).

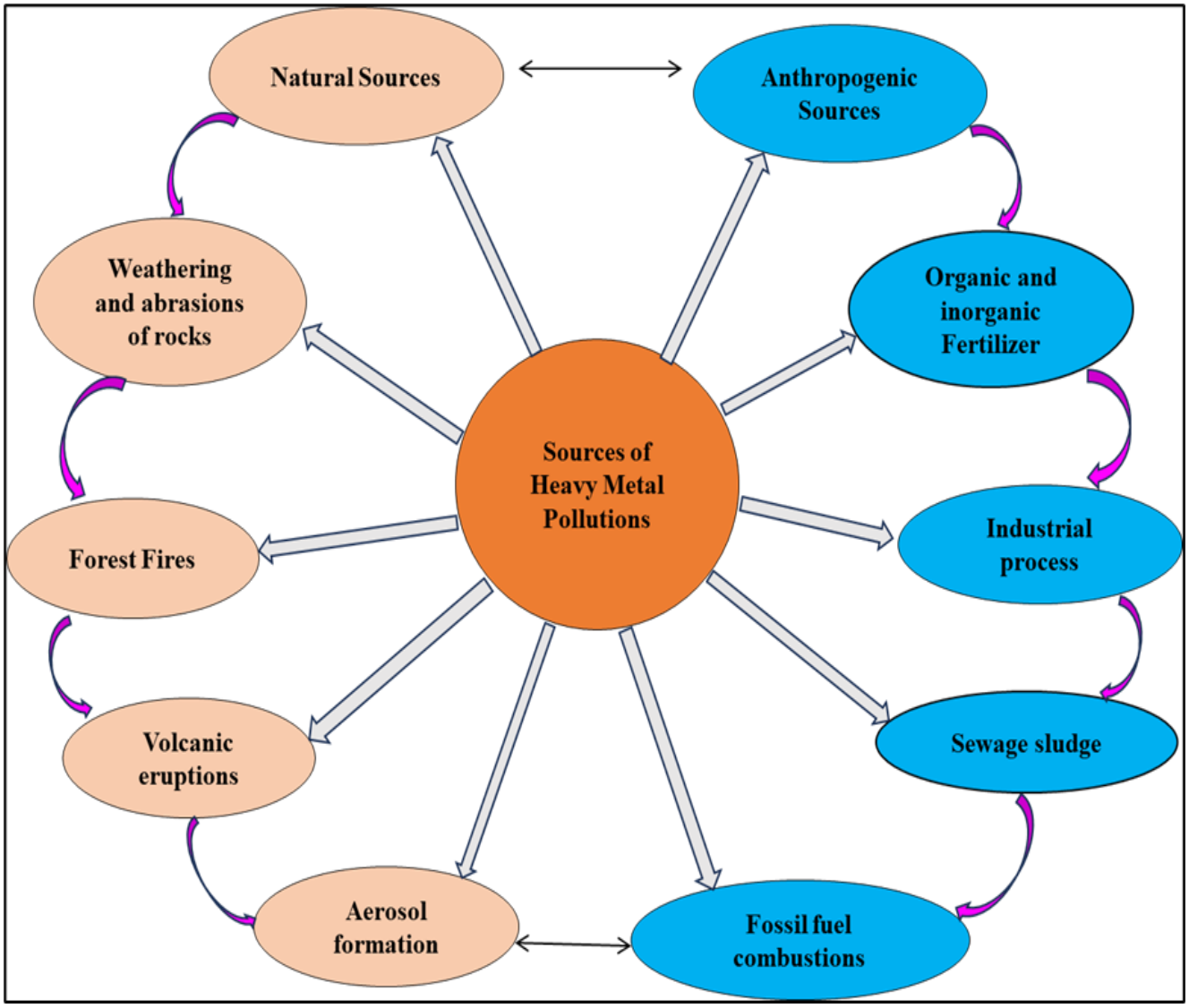


**Figure 1: A schematic diagram illustrating the primary sources of heavy metal pollution (Bishnu et al., 2024)**

### 2.4.2. Natural sources of heavy metal pollution

The sources of HM pollution in the environment have originated from natural processes (Figure 1). Natural processes, such as biogenic activities, metal corrosion, geological weathering, and atmospheric phenomena like wind erosion and volcanic eruptions, contribute to heavy metals in the environment. These natural sources, while often occurring at lower rates, can significantly contribute to the overall accumulation of heavy metals in certain regions (Gomaa & El-Meihy, 2019). Natural weathering, a gradual geological process, breaks down rocks and minerals over time. As this occurs, naturally occurring heavy metals are released into the environment, including soil, water, and air. While this process is slow, it contributes to the overall background levels of heavy metals. This natural release of heavy metals can potentially harm biodiversity. Heavy metals can naturally occur in hydroxides, oxides, organics, phosphates, silicates, sulfates, and sulfides {Formatting Citation}.

## 2.5. Impacts of heavy metals on soil health

Due to their non-biodegradable nature and potential toxicity, HMs pose serious challenges to soil health. Unlike organic pollutants, which can degrade over time, HMs persist in the environment for extensive periods, resisting biotransformation processes. This persistence allows these toxic elements to accumulate in the soil, often reaching concentrations that exceed the threshold for safe environmental functioning. Over time, this accumulation disrupts the balance of the soil ecosystem, impairing its ability to support plant growth, regulate water, and sustain microbial activity. The persistent presence of HMs not only affects soil quality but also exacerbates long-term environmental degradation. Soils contaminated with these metals lose their resilience, making it difficult for natural remediation processes to restore their health. Consequently, HM pollution presents a significant environmental challenge, requiring proactive measures to prevent accumulation and mitigate its impacts on soil ecosystems (El-sharkawy et al., 2025).

One of the primary ways HMs impact soils is by altering their physical structure, leading to significant degradation through time. The metals can disrupt soil aggregation, breaking down the bonds that hold soil particles together. This degradation disrupts the soil's texture, making it more compact or fragmented, which reduces its porosity and prevents the circulation of air (Kalsoom et al., 2023). Reduced soil porosity has a detrimental impact on soil health, as it restricts the availability of

vital resources like water and air, which are critical for root development and the activity of beneficial soil microorganisms.

HMs can inhibit the soil's natural process to form stable aggregates, further diminishing its water infiltration capacity. These physical changes severely compromise the soil's functionality, making it less effective at providing the necessary environment for plant growth. Crops grown in such degraded soils may experience stunted root systems and reduced access to water and nutrients. Over time, these issues can reduce the soil's productivity, posing serious challenges to agricultural sustainability. Besides, the loss of soil functionality due to heavy metal contamination can have long-term consequences for the broader ecosystem, as the soil becomes less capable of supporting the diverse organisms and processes essential for ecological balance (Angon et al., 2024).

Chemically, HMs interfere with essential soil processes, leading to significant disruptions in soil chemistry and nutrient dynamics. One of the primary effects is their ability to compete with vital nutrients for adsorption sites on soil particles. These adsorption sites, typically occupied by essential nutrients such as calcium, magnesium, and potassium, are critical for maintaining nutrient availability for plant uptake. When HMs like $Pb^{+2}$, $Cd^{+2}$, or $Hg^{+2}$ occupy these sites, they displace essential nutrients, rendering them less accessible to plants (Collin et al., 2022;Angon et al., 2024). This nutrient displacement creates deficiencies that can impair plant metabolism and growth. Additionally, the accumulation of HMs in the soil can significantly alter soil pH, either acidifying or alkalizing the soil depending on the type of metal and its concentration. Changes in pH destabilize the chemical environment, affecting nutrient solubility and cycling (Zhao et al., 2024). For example, an acidic shift caused by HMs can increase the solubility of toxic elements, further worsen contamination, while reduce the availability of beneficial nutrients like phosphorus. Conversely, an increase in soil alkalinity may lead to nutrient precipitation, further limiting nutrient uptake by plants (Bouida et al., 2024).

## 2.6. Impacts of heavy metals on water quality

Urbanization and industrialization are the primary sources of water pollution. Runoff from populated and industrial areas carries metals that accumulate in the sediment of water bodies. Even small amounts of these metals can be highly toxic to humans and ecosystems. Heavy metal toxicity varies

depending on the specific metal, its chemical form, its biological function, the exposed organism, and the organism's developmental stage. Contamination of one organism can impact the entire food chain, with humans at the top accumulating higher concentrations of heavy metals. Industrial and domestic waste typically enter the sewage system (Hossen et al., 2023).

Raw sewage is a major source of HM pollution, as these metals persist through standard sewage treatment. While treatment processes do remove HMs, they end up either in the treated wastewater (effluent) or the resulting sludge. The quality of wastewater discharged into the environment is directly related to the level of sewage treatment it receives. Recognizing the environmental damage caused by untreated sewage discharge, governments have implemented stricter regulations and spurred the development of improved treatment technologies to minimize water pollution (Briffa et al., 2020). Sewage treatment typically involves three stages: primary, secondary, & tertiary. Primary treatment begins with filtering out large debris, followed by sedimentation to remove solids, creating sludge. This sludge, containing roughly half of the initial suspended solids, is then processed further, often in a digester. Secondary treatment uses oxidation to further purify the wastewater, employing methods like biofiltration, aeration, or oxidation ponds. Tertiary treatment, the final stage, removes remaining pollutants, particularly phosphates and nitrates, often using activated carbon and sand filtration. These treatment steps are adapted based on the specific sewage composition and treatment facility. Concerns about untreated sewage discharge have led to stricter regulations and the development of advanced technologies to reduce water pollution (Mokarram et al., 2020).

Pollutants in surface waters can be dissolved, suspended, or exist as particulate matter. Water transports these pollutants, sometimes over long distances. Particulate matter can settle to the bottom, while liquid droplets may either sink or float. River transport depends on water flow, pollutant stability, and its physical state. In oceans, wind and currents further disperse pollutants, with seawater density (influenced by salinity and temperature) also playing a role (Aziz et al., 2023). Persistent pollutants like HMs can accumulate in marine organisms, entering the food chain and impacting predators at higher trophic levels, including humans. Migratory species can then spread these pollutants across different ecosystems (Zamora-Ledezma et al., 2021).

## 2.7. Harmful effects of heavy metal concentration on human health

Certain HMs, such as iron, zinc, copper, and selenium, are essential micronutrients for human health (Deng et al., 2022). These elements play crucial roles in various biological processes. However, heavy metals can be toxic to many living organisms, impacting metabolic activities. Therefore, a thorough understanding of their harmful effects on human health, including specific concentrations and oxidation states of these metals, is important and useful Sall et al., (2020). Understanding the origins of HMs, how they are released into the environment through processes like leaching, and how their chemical properties change as they move through ecosystems is a crucial application in fighting environmental pollution. Various human diseases, such as breathing problems, kidney failure, neurological disorders, and ultimately cancers, are caused by certain concentrations of HMs. Studies have shown that chromium is a carcinogenic HM, even at low concentrations (Parui et al., 2023).

Studies have shown that HM exposure can have detrimental impacts on human health, including delays in growth and development in children (Zeng et al., 2019). HM can inhibit different body functions, disrupt regulatory systems, and lead to a range of health problems. For example, chronic fatigue syndrome, Alzheimer's disease, and neurodegenerative disorders can be linked to exposure to high concentrations of HM. Intoxication by certain HMs, such as lead and mercury, can bring about autoimmune disorders in which the patient's immune system attacks its cells. As described by (Sall et al., 2020), inhaling certain concentrations of HMs, such as $Pb^{+2}$ and $Hg^{+2}$, can cause joint disease, circulatory problems, and other nerve system issues. Inhalation of cadmium creates accumulation in parts of the body, leading to organ failure and various diseases. After absorption and subsequent transport into the body, deposited traces of $Cd^{+2}$ can reach the kidneys, and upper and lower respiratory tract, and finally impair human metabolic activities (Kumar et al., 2021).

According to Gaur et al., (2014), mercury is a powerful neurotoxin that primarily affects the central nervous system (CNS). It can cause hearing disorders and muscle weakness. The lungs absorb metallic mercury through the breathing process bringing about breathing difficulties. The metallic mercury is also used to cause biochemical damage to tissues. As it was researched, metallic mercury can induce toxicity by forming free radicals and generating oxidative stress consequently causing DNA damage (Arroyo et al., 2013). However, cadmium is a toxin HM, and toxicity weakens

antioxidant defense by lowering intracellular glutathione levels. Glutathione inhibits the activity of various antioxidant enzymes such as superoxide dismutase and catalase, along with the formation of reactive oxygen species. The increased level of reactive oxygen species (Manousi et al., 2020) causes damage to DNA repair, leading to mutations. Studies also show that the effects of heavy metals on human health, such as arsenic causing carcinogenic effects, copper causing anemia, chromium causing mental disturbance and ulcers, cancer, lead causing neurotoxicity, and nickel causing skin allergies, lung fibrosis, and cardiovascular disease (Arroyo et al., 2013). Some health effects of heavy metals are presented one by one as follows.

### 2.7.1. Lead

Lead is a highly toxic heavy metal whose widespread use has resulted in extensive environmental contamination from industrial wastewater discharges. It is a significant problem across the globe. In a dry environment, lead looks like a bright silver-blue metal. But this appearance doesn't last long when exposed to air; it quickly tarnishes, creating a complex mixture of compounds based on the surrounding atmospheric conditions. There are many ways humans can be exposed to lead contamination. The main sources include industrial activities, contaminated food and drinking water, as well as domestic processes (Jaishankar et al., 2014). Lead is an extremely toxic metal that, unlike essential metals like zinc, copper, and manganese, serves no biological function in plants. When plants absorb high concentrations of lead, it triggers a rapid increase in reactive oxygen species. These harmful molecules damage the plant's cell membrane, which in turn leads to the destruction of chlorophyll and disrupts photosynthesis that ultimately suppressing the plant's overall growth and development (Najeeb et al., 2017).

Lead causes toxicity in living cells through two main pathways: by acting as an ion and by creating oxidative stress. Studies have found that this oxidative stress occurs when there is an imbalance between the production of harmful free radicals and the cell's ability to produce antioxidants to neutralize them and repair the resulting damage (Jaishankar et al., 2014). The attack of lead disrupts the balance between harmful reactive oxygen species and protective antioxidants. Normally, antioxidants such as glutathione protect the cell by neutralizing free radicals such as hydrogen peroxide. However, under the influence of lead, the level of damaging ROS increases while the level of protective antioxidants decreases. This disrupts a crucial protective mechanism. The reduced form

of glutathione donates electrons form its thiol functional group to stabilize ROS. With the help of the enzyme glutathione peroxidase, two molecules of glutathione then bind together forming oxidized glutathione disulfide after they have donated their electrons. This process is essential for keeping the cell healthy, but lead presence overwhelms this defence system (Singh & Sharma, 2025).

### 2.7.2. Chromium

High levels of chromium (VI) exposure are found in industries such chromate manufacturing, chromate plating, ferrochrome production and stainless-steel welding. This occupational exposure is a key known causes of respiratory cancer (Sawicka et al., 2021). Chromium (VI) is a proven toxic, mutagen and carcinogen. It is considered more dangerous than chromium (III) because of its higher solubility and mobility. Chromium (VI) exposure can lead to a range of severe health problems. Inhalation is a major route of exposure, particularly in industrial settings like electroplating and welding. This phenomenon can cause respiratory tract irritation and increase the risk of lung cancer. Chronic exposure can lead to liver and kidney damage, affecting their ability to filter waste and detoxify the body (Jomova et al., 2025). Further, chromium (VI) can disrupt the circulatory system leading to cardiovascular issues. The conversion of chromium (VI) into reactive form generates ROS which causes oxidative stress and damage to cellular components including DNA, proteins and lipids (Yin & Phung, 2015;Chatterjee et al., 2020).

### 2.7.3. Cadmium

Cadmium is a highly toxic heavy metal that is a byproduct of zinc production. It is ranked as the seventh most toxic substance on the Agency for Toxic Substances and Disease Registry (ATSDR) priority list. Its widespread use in industrial applications and its presence in the environment make it a significant public health concern. When it is released into the environment through industrial activities and waste disposal poses a significant threat. The toxic heavy metal has a remarkable ability to persist, accumulating in soils and aquatic sediments for decades. This long-term environmental presence creates a reservoir of contamination, leading to a prolonged risk of exposure for both human and wildlife through contaminated water, crops, and seafood. The persistence of cadmium in these environmental sinks makes it a chronic and difficult-to-manage public health and ecological concern, as it can continue to cycle through ecosystems long after the initial source of pollution has been removed (George et al., 2023).

Cadmium is considered a metal of the 20th century, primarily because of its widespread use in modern industrial applications. As a by-product of zinc production, it is naturally present in small amounts in the soils, rocks, coal, and mineral fertilizers. It is utilized in many products, including batteries, pigments, plastics, and metal coatings, as widely used in electroplating. The International Agency for Research on Cancer (IARC) classifies cadmium and its compounds as a group one carcinogen, meaning they are known to cause cancer in humans (Yang et al., 2025).

## 2.8. Harmful effects of heavy metals on ecosystem biodiversity

An ecosystem is an open thermodynamic system, meaning it exchanges both energy and matter with its surroundings. This exchange allows for a dynamic balance between the biotic (living) and abiotic (non-living) components of the ecosystem. This balance is essential for the stability and resilience of the ecosystem. However, the introduction of heavy metals, either from natural sources or human activities, can disrupt this delicate equilibrium. HM can be bioaccumulated in the environment and organisms leading to various ecological and health problems. The bioavailability of materials in the ecosystem, such as organic matter and nutrients, can significantly influence the uptake of HMs by organisms. For example, the presence of organic matter can bind to HMs, reducing their availability for uptake by plants and animals. Conversely, certain nutrients can increase the uptake of HMs by plant growth promotion and root development. Therefore, understanding the complex interactions between heavy metals, bioavailability, and ecosystem processes is crucial for assessing the potential risks and developing effective strategies for mitigating the impacts of heavy metal pollution (Boshoff et al., 2014).

HMs can exist in the environment in both ionic and elemental forms. In their ionic form, HMs have a positive charge (cations) and can interact with negatively charged particles, such as organic matter, in the environment. This interaction can lead to the adsorption of HMs onto organic matter, which can reduce their mobility and bioavailability. HM pollution has a significant negative impact on microbial communities, which play a vital role in the ecosystem and its function. According to Tovar-Sánchez et al. (2018). Heavy metals can significantly disrupt the growth, development, and biochemical processes of microorganisms due to their toxic effects, which interfere with cellular and molecular function. HM pollution disrupts ecosystem balance by interfering with key processes like organic and inorganic matter decomposition and nutrient cycling. This interference reduces the availability of

essential nutrients in the food chains and webs. Ultimately, these changes affect the overall health and functionality of ecosystems, impacting the services they provide to humans and the environment (Das et al., 2023).

## 2.9. Effects of heavy metals on microorganisms and wildlife

Heavy metal pollution can harm microorganisms, leading to changes in their cellular structure and a decrease in biodiversity (Das et al., 2023). These changes disrupt the metabolic processes of living organisms, potentially reducing nutrient availability & making it harder for plants to absorb nutrients. This impacts food chains and energy flow in ecosystems, accumulates in organisms, disrupts their metabolism and other essential processes, and transfers through various trophic levels within the ecosystem (Gall et al., 2015). Soil invertebrates can accumulate HMs in their bodies as they consume organic matter and leaf litter contaminated with these metals. Crustaceans, earthworms, and snails are examples of invertebrates that are particularly vulnerable to heavy metal accumulation (Tovar-Sánchez et al., 2018). Human activities, such as physical alterations to the environment, sewage discharge, nutrient runoff, sediment erosion, and pollution from persistent organic pollutants, hydrocarbons, and HMs, are increasingly harming marine and coastal ecosystems (Yang et al., 2020; Lu et al., 2018).

Prolonged experience with HMs can have devastating consequences for wildlife populations and their natural habitats. As HMs accumulate in the environment, they can disrupt ecosystems, leading to a decline in biodiversity. HMs can bioaccumulate in organisms, meaning they build up in tissues over time. This can lead to a variety of health problems, including impaired growth, reproductive issues, and neurological disorders (Tovar-Sánchez et al., 2018). For example, bioaccumulation of nickel in the *Alyssum pintodalsivae* (*Brassicaceae*) affects locusts and spiders in the food chains and food webs. Therefore, the transfer of these pollutants at each trophic level leads to harmful effects on biodiversity (Kaur et al., 2021).

## 2.10. Effects of heavy metal concentrations on plant cells

HM contamination poses a significant threat to plant health by adversely affecting their growth, development, and overall physiological processes (Vasilachi et al., 2023). When exposed to high concentrations of HMs, plants experience different adverse effects. It may interfere with several

physiological processes, including photosynthesis, respiration, and nutrient uptake (Srivastava et al., 2017). One of the primary mechanisms of HM toxicity is oxidative stress. It is characterized by an imbalance in the formation of ROS and the body's ability to detoxify these intermediates. HM can generate reactive oxygen species (ROS) within plant cells, damaging cellular components such as DNA, proteins, and lipids. This oxidative stress can lead to a decline in plant growth, reduced photosynthesis, and impaired nutrient uptake. Furthermore, HM might upset the balance of vital nutrients in plants. They can compete with essential nutrients for absorption, resulting in food deficits. For instance, $Cd^{+2}$ concentrations can inhibit iron uptake, both of which are essential for plant growth and development (Ali et al., 2022). Additionally, HMs can accumulate in plant tissues, making them toxic to animals and humans who consume them. This bioaccumulation can have long-lasting consequences for food chains and human health. To discuss the negative impacts of HM contamination on plants, it is essential to implement sustainable agricultural practices, reduce industrial pollution, and develop effective remediation strategies (Vácha, 2021).

Studies have shown that the absorption and bioaccumulation of HMs in plant tissue are affected by temperature, moisture, organic matter, nutrient availability, and pH (Raize et al., 2004). Heavy metal phytotoxicity reduced nutrient uptake, plant metabolism disorders, germination delays, and reduced molecular nitrogen in leguminous plants used for nitrogen fixation (Jin et al., 2018). For example, high Pb concentrations in soil can reduce productivity, and low Pb concentrations can inhibit some important processes in plants, such as photosynthesis, mitosis, and water absorption mechanisms, resulting in plant diseases like dark green leaves, wilting, and brown, short roots. This consequently brings about a loss of production and productivity (Bhattacharyya et al., 2008).

## 2.11. Bioremediation using microorganisms

Bioremediation is a process by which microorganisms, such as bacteria, archaea, and fungi, transform contaminants in polluted environments. It is a cost-effective and environmentally beneficial approach to cleaning up or reducing pollutants in soil and water. The studies have been conducted to characterize bacterial populations, determine their susceptibility to contaminants, and identify genes that facilitate pollutant removal released from industrial effluents (Das et al., 2016). Microorganisms can contribute to bioremediation by cleaning different contaminants, including petroleum hydrocarbons, herbicides, insecticides, and HMs. Some commonly reported organisms for the

detoxification of pesticides and heavy metals include *Pseudomonas* sp., *Bacillus* sp., *Klebsiella* sp., *Pandoraea* sp., *Phanerochaete chrysosporium*, and *Mycobacterium* sp. Rashid et al., (2023). The degradation abilities of bacterial species to pollutants depend on the nature of the pollutants they encounter. For instance, microorganisms isolated from brewery waste samples can efficiently degrade brewery effluents compared to those from other wastes (Bhattacharjee et al., 2020).

Microbial diversity is crucial for maintaining ecosystem stability and functioning, Palit et al., (2022). Different microorganisms play countless roles in the decomposition of environmental pollutants through various mechanisms. Numerous studies show that culture-independent approaches are the only way to detect a wide range of unidentified bacteria that assist in the bioremediation of polluted areas (Das et al., 2016). These cutting-edge molecular methods, such as metagenomics sequencing, allow researcher bypass the need for laboratory cultivation by directly extracting and analyzing genetic material from environmental samples. This capability is critical because traditional culturing methods capture less than 2% of total microbial diversity, thereby overlooking the specialized, uncultured strains that are often the dominant in-situ degraders of contaminants like hydrocarbons and heavy metals. This leads to discoveries of new species, insight into microbial community structure, and a deeper understanding of their roles in various ecosystems, including bioremediation potential. Some prominent examples of heavy metal bioremediation through bacterial species are: *P. mendoca*, *Cellulosmicrobium cellulans*, *Arthrobacter* sp., *Agrobacter* sp., and *P. aeruginosa* S128. These microbes have a promising potential for cleaning up HM contamination (Sundarraj et al., 2022).

Microbes can break down contaminants in both natural and human-made environments. In natural habitats, some microbes have evolved the ability to metabolize specific pollutants. Some bacteria, for example, may break down petroleum hydrocarbons, while certain fungi can transform compounds in organic and inorganic substances such as insecticides, herbicides, pesticides, and HMs Kumar et al., (2011). Aside from decomposing hydrocarbons, microorganisms can also remove industrial wastes and reduce the toxic cations of HMs into less toxic soluble form, through biotransformation mechanisms as reported by Zhao et al., (2021). To increase the rate of contaminant breakdown, specific microorganisms can be introduced, or existing microbial communities can be stimulated.

However, in some cases of toxic heavy metals, microorganisms can only alter the form of the metal or change its location (Pande et al., 2022; Briški et al., 2019).

Microbial communities are immensely diverse and complex, often comprising bacteria, archaea, fungi, and microalgae that influence microbial interactions. Each group contributes uniquely to the degradation processes through specialized metabolic activities. For instance, certain bacteria possess enzymes capable of breaking down hydrocarbons, pesticides, herbicides, and heavy metals. Archaea, a unique class of microorganisms, exhibits considerable promise for bioremediation (Mainka et al., 2021). Methanogenic archaea are essential contributors to breaking down intricate organic substances in anaerobic conditions. They participate in the decomposition of organic materials, such as petroleum hydrocarbons, by generating methane as a secondary product of their metabolism. Moreover, specific species of archaea can carry out denitrification, a mechanism that effectively lowers the concentration of nitrate and nitrite in the polluted environment. Fungi also play a vital role in degrading recalcitrant pollutants such as lignin, polycyclic aromatic hydrocarbons (PAHs) (Yang et al., 2020; Lu et al., 2018), and synthetic dyes, which have their own extracellular enzyme systems like peroxidase. Moreover, microalgae can absorb heavy metals and contribute to phytoremediation in aquatic systems (Omar et al., 2024).

The synergistic interactions among those microbial communities further enhance contaminant degradation, as one group may transform a pollutant into intermediate products that serve as a substrate for others, resulting in incomplete mineralization. Advances in molecular biology, metagenomics, and systems biology have revealed the immense functional potential hidden within these microbial diversities, allowing scientists to better understand their roles and harness them more effectively for targeted bioremediation strategies. Thus, the microbial community can serve as the cornerstone for bioremediation, and their ecological diversity, metabolic flexibility, and ability to adapt to contaminated environments make them indispensable allies in addressing environmental pollution and restoring ecosystem health (Bhattacharjee et al., 2020).

## 2.12. Mechanism of bacteria toward heavy metal bioremediation

Bacteria have been found to survive in a wide range of conditions, including the cold poles, hot deserts, damp swamps, and aquatic systems. Their distinctive characteristics include small size, high

surface area to volume ratio, rapid transfer of genetic traits, and flexibility. Bacteria contribute significantly to heavy metal bioremediation through a variety of processes. One of the easiest techniques is to transform organic pollutants into non-toxic molecules by utilizing them as a carbon source. However, in the case of heavy metal contamination, bacteria have developed three resistance mechanisms: efflux of toxic metals outside a cell via transporters, conversion of the metals into non-toxic or less toxic forms, and biosorption. Biosorption and enzymatic alteration of heavy metals into another form are frequently linked. For example, once a metal has been absorbed into the cell, enzymes work on it, precipitating the metal as a salt (Das et al., 2016).

### 2.12.1. Biosorption

Biosorption is the process by which microorganisms like bacteria, fungi, and algae bind HMs to their cell surfaces. This binding occurs through different processes, including ion exchange, complexation, and precipitation. It is an efficient and environmentally friendly approach to remove HMs from contaminated wastewater and soil. The process has different advantages over traditional technologies, including cost-effectiveness, efficiency, and the ability to treat the enormous amounts of wastewater and soil (Pham et al., 2022). The cellular surface of bacteria contains functional groups like carboxyl, amino, and phosphate groups on which HMs ions can bind (Figure 2). The metal ions can then be removed from the environment along with the bacterial biomass (Zhao et al., 2017). The process consists of a solid phase (biosorbent, a biological substance) and a liquid phase (solvent) containing the dissolved species to be sorbed. The binding of a sorbent to a sorbate continues until a balance is reached between the amount of sorbate bound to the solid phase and the amount remaining in the solution. At this point, the sorbate is essentially removed from the solution. In the case of bacteria, the binding of metals is often mediated by a class of proteins called metallothioneins. These are small proteins rich in cysteine amino acids, and they play a crucial role in regulating and storing heavy metals within cells. They are found in a wide range of bacteria, fungi, plants, and animals that have a high affinity for binding to HM ions, particularly $Zn^{+2}$, $Cu^{+2}$, $Cd^{+2}$, and $Hg^{+2}$ (Chatterjee et al., 2020).

Biosorption technologies influence the binding properties of different biological materials to achieve their desired outcomes. It enables the bioaccumulation of HMs in living cells through a metabolically mediated process (Wang et al., 2006). Metal sequestration during the biosorption mechanism depends on the complex phenomenon of ionic interactions between the metal cations and the cell wall matrix

of the microorganisms (Raize et al., 2004). Studies have shown the biosorption mechanism of different HMs by brown marine macroalgae, which attach to chemical groups containing oxygen, carbon, nitrogen, and sulfur to form complexes with $Cd^{+2}$. However, the binding process did not alter the magnesium and calcium concentrations in the solution, indicating that ion exchange might not be the main mechanism for $Cd^{+2}$ biosorption on brown marine macroalgae, called *Sargassum Vulgaris* (Raize et al., 2004).

### 2.12.2. Bio-attenuation

Bio-attenuation is an in-situ bioremediation development that depends on naturally occurring microorganisms to reduce the concentration or toxicity of pollutants. In HM contamination, bio-attenuation fosters the growth of native bacteria that can immobilize or transform them into less toxic forms. This can be achieved by optimizing environmental conditions such as pH, oxygen levels, and nutrient availability, which promote microbial activity (Das et al., 2016). This approach uses natural processes to control the spread of pollution from chemical spills and reduce the concentration of pollutants at contaminated sites (Emenike et al., 2018). As a result, the environmental contaminants remain undisturbed, providing an opportunity for natural degradation, reduction, or conversion. The effectiveness of bio-attenuation depends on the dominant biological activity at environmentally contaminated sites. However, bio-attenuation effectiveness varies depending on the nature of the pollutants and the physical, chemical, and biological properties of the affected soil and wastewater (Vasilachi et al., 2023). Bio-attenuation can reduce the mass of pollutants by lowering the concentration of pollutants or by binding pollutants to soil particles, thus preventing their spread or migration. It is an effective, inexpensive, and appropriate approach for pollution removal strategies (Emenike et al., 2018).

Studies have shown the success of bio-attenuation as a treatment for hydrocarbons, chlorinated solvents, pesticides, and even some heavy metals in groundwater and soil regimes. For example, indigenous bacteria like *Pseudomonas*, *Mycobacterium*, and *Rhodococcus* naturally biodegrade petroleum hydrocarbons via aerobic metabolic pathways (Abbasian et al., 2015). Compounds that are chlorinated can also be dechlorinated, such as trichloroethene (trichloroethylene, TCE), which can be dechlorinated reductively by bacteria like *Dehalococcoides* (Dutta et al., 2022). Factors important to bio-attenuation include the presence of electron donors and acceptors, nutrients, pH, temperature, and

the bioavailability of the contaminant. Biogeochemical conditions play an especially important role in whether aerobic or anaerobic processes occur. The development of complex molecular tools such as metagenomics, as well as isotopic tools, has advanced our understanding of how bio-attenuation relates to microbial pathways and community interactions (Haripriyan et al., 2022).

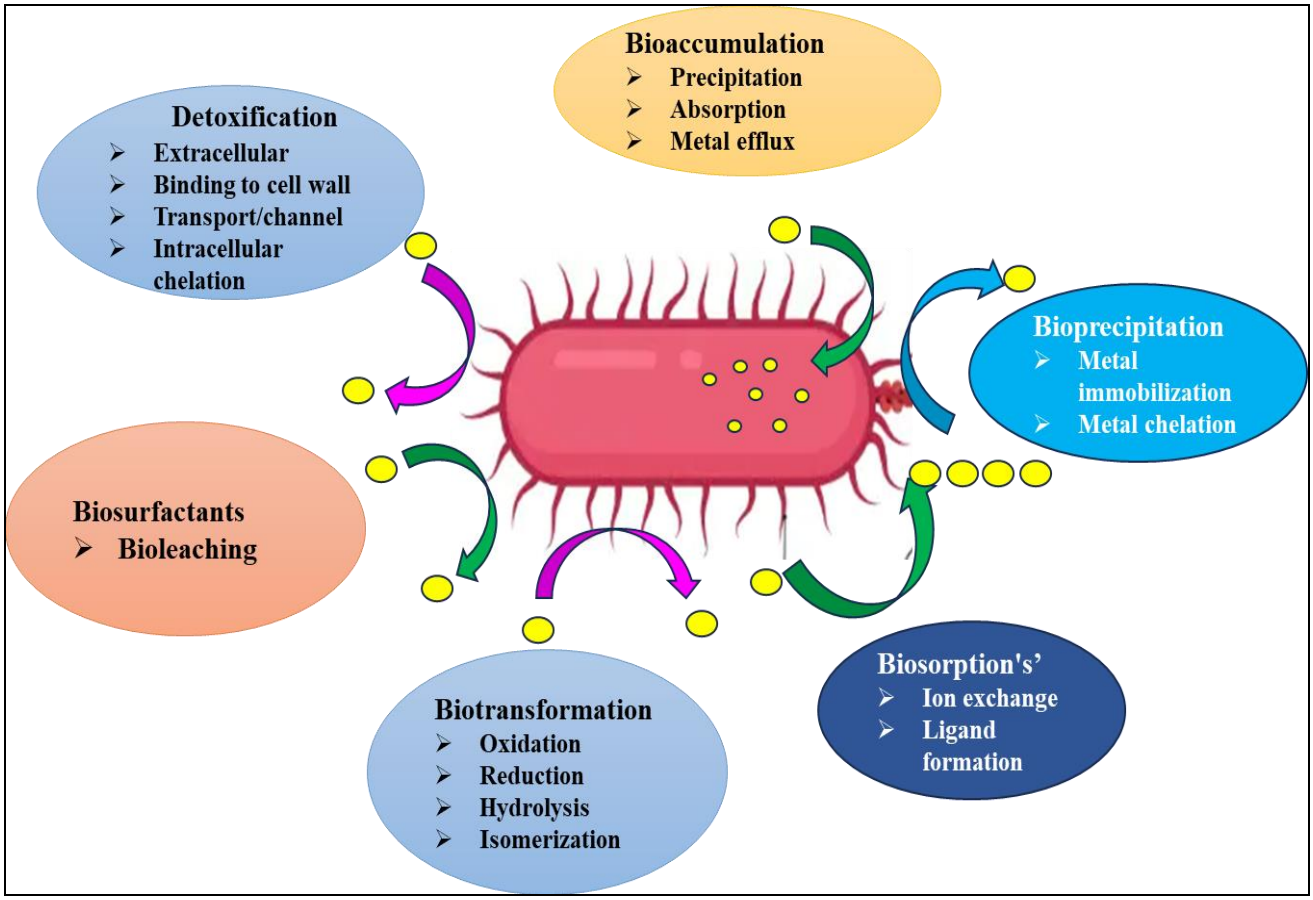


**Figure 2: An Overview of essential mechanisms responsible for heavy metal bioremediation in contaminated environments by Bacteria (Pham et al., 2022; Zhao et al., 2017)**

Bio-attenuation is the cheapest and most environmentally friendly; however, implementation is difficult when using this as the only remediation technique. Such reasons include the fact that it takes quite some time, it can be difficult to know how it will turn out after a long period, and oftentimes in rare cases, the intermediates are not fully degraded and accumulate as by-products. Recent research is exploring o make bio-attenuation more reliable by developing better monitoring methods and a better understanding of symbiotic interrelationships in microbial consortia. The feasibility of controlling

complex contamination situations may be greatly improved by utilizing bio-attenuation in conjunction with other remediation technologies, such as bio-stimulation and bioaugmentation (Haripriyan et al., 2022).

### 2.12.3. Bioaugmentation

Bioaugmentation is a bioremediation technique that involves introducing specific microorganisms into a contaminated environment to accelerate the biotransformation or removal of pollutants. In the context of HM pollution, bioaugmentation involves the addition of microorganisms that can bioaccumulate, biotransform heavy metals. By introducing these specialized microorganisms, biotransformation processes can be accelerated, leading to more efficient removal of HM pollutants. This technique is particularly useful for sites with low microbial activity or where indigenous microorganisms are not effective in degrading the pollutants Mrozik & Piotrowska-Seget, (2010). This process involves the addition of specific cultured bacteria to sewage effluent. These bacteria can effectively degrade pollutants such as HMs concurrently through biotransformation and biosorption processes. Through bioaugmentation, researchers have identified strains of *B. subtilis* that exhibit remarkable tolerance to high temperatures and resistance to heavy metals. These findings have significant implications for bioremediation applications, especially in environments with extreme conditions (Al-Gheethi et al., 2016; Herrero & Stuckey, 2015).

Bioaugmentation, while effective in cleaning up aromatic hydrocarbon contaminants, faces limitations when applied to heavy metal pollution. One major challenge in bioaugmentation is ensuring the survival and growth of introduced microorganisms in the often harsh and competitive environment of polluted sites. These microorganisms may face competition from native microbial populations, exposure to toxic pollutants, and unfavorable environmental conditions. Additionally, the number of familiarized microorganisms frequently experiences a decline following inoculation. This decline, while often observed, is a complex phenomenon influenced by heavy metal toxicity. Furthermore, bioaugmentation alone may not be enough for complete HM removal due to difficulties in separating the metals from a treated medium. The effectiveness of bioaugmentation is also influenced by various abiotic factors, including temperature, moisture, pH, organic matter content, aeration, nutrient availability, and soil type. These factors can significantly impact the efficiency of the bioremediation process (Sundarraj et al., 2022).

### 2.12.4. Biotransformation

The biotransformation of HMs is important for the restoration of damaged ecosystems such as wetlands, abandoned mining sites, agricultural lands, and residential areas. These approaches are particularly valuable in areas experiencing rapid industrialization and where environmental concerns are significant. By employing biotransformation techniques, it is possible to clean up polluted sites and promote ecological recovery (Emenike et al., 2018). For instance, the *Micrococcus luteus* strain AS2 bacterium shows a high degree of resistance to HMs like arsenic from contaminated sites by possessing different genes and their products. Studies have also shown that the presence of the *acr3* gene in the *Micrococcus luteus* strain AS2 can accumulate arsenite in the cell and plays a significant role in transporting arsenite from the AS2 strain cells to the outside of the cell (Sher et al., 2020).

Biotransformation of HMs refers to the use of biological systems, typically microorganisms, to alter the chemical state, and mobility in the environment. The process is attracting much notice because of its potential uses in bioremediation and environmentally sound stabilizations. Microorganisms, including bacteria, fungi, and algae, possess extraordinary metabolic versatility and they can interact with HMs through biotransformation. For example, *Pseudomonas*, *Bacillus*, and *Saccharomyces* spp. have been extensively investigated for their metal-transforming abilities of cadmium, lead, arsenic, and chromium (Aftab, 2022). These are the transformations of metals into less toxic or less soluble forms, such as the reduction of Cr (VI) to the less toxic trivalent state, Cr (III). Biotransformation efficiency is dependent upon pH, temperature, and metal concentration, as well as the presence of co-contaminants that may affect microbial activity. Genomics and proteomics advances have contributed to the elucidation of molecular mechanisms underlying microbial heavy metal transformation, thus allowing the development of designer bioremediation approaches (Lata et al., 2023).

### 2.12.5. Extracellular and intracellular sequestration

Extracellular HM sequestration is a process in which certain bacterial species bind and immobilize heavy metal ions outside their cell membrane (Figure 2). This ability allows these bacteria to protect themselves from toxic metals and contribute to the cleanup of contaminated environments (Gupta et al., 2017). This mechanism enables bacteria to live in harsh, HM-contaminated environments and can be applied to bioremediation efforts. Bacteria employ various strategies to bind and immobilize HMs

outside their cells (Etesami, 2018). The most common technique involves producing metal-binding proteins called metallothioneins or metallothionein-like proteins. These proteins have a strong affinity for HM ions and can effectively remove them from the environment. Once bound, the metal ions form stable complexes with the metallothioneins, reducing their toxicity and facilitating their removal from the system. Exopolysaccharides (EPS) produced by bacteria can also contribute to heavy metal sequestration into bacterial cells. These exopolysaccharides, a complex sugar molecule, form gel-like matrices around bacteria. These matrices can trap heavy metal ions through electrostatic interactions, preventing their dispersion into the environment (Chatterjee et al., 2020).

Intracellular sequestration is another bacterial policy for acquiring and storing HMs. This mechanism is often triggered by high concentrations of HM contaminants, as these metals can be toxic to living organisms. Bacteria have evolved different methods to sequester HM within cells. One common approach involves the production of metal-binding proteins. These proteins, often synthesized in response to HM exposure and to the metals, effectively shield the bacteria from their toxic effects. For instance, such proteins include metallothioneins and phytochelatins. These proteins can bind a significant amount of HM, reducing their bioavailability and toxicity within the cell. Bacteria can trap HMs by turning them into solids like metal sulfides, which store HMs inside the bacteria's cells (Huang et al., 2019).

## 2.13. Gene diversity associated with heavy metal bioremediation

Genetic diversity within a population can influence how organisms respond to HM exposure. Different individuals may possess genetic variations that affect their ability to detoxify HMs, transport them within their bodies, defend against oxidative stress, or repair DNA damage. These genetic differences can lead to varying levels of tolerance and susceptibility to heavy metal toxicity (Oves et al., 2016). This genetic change can result in alterations in susceptibility or tolerance to heavy metal toxicity in harsh environmental conditions. A study of gene diversity associated with heavy metal exposure can help researchers understand the genetic factors that contribute to the variation in susceptibility and responses to heavy metal toxicity. This knowledge can have implications for risk assessment, environmental monitoring, and the development of personalized approaches to prevent or mitigate the health effects of heavy metal exposure. It is expected that microbes living in heavy metal-contaminated environments will exhibit greater gene diversity than those in uncontaminated

areas (Oves et al., 2016). While HM pollution can harm plant growth and reduce the diversity and activity of soil microbes, the stress it imposes significantly impacts and likely alters the genetic structure of the surviving population (Xie et al., 2016).

### 2.13.1. Gene diversity associated with mercury bioremediation

Mercury (Hg) is a naturally occurring element referred to as "quicksilver." It is one of the few metals that are liquid at normal temperatures. This silvery-white metal, while beautiful, poses a considerable health and environmental risk due to its toxicity. Mercury can be ingested, inhaled, or absorbed via the skin. It can harm the neurological system, kidneys, and lungs, and, in severe cases, cause death. Because of its toxicity, many traditional applications of mercury, such as thermometers and barometers, have been phased out. However, it is still present in the environment due to industrial processes and natural sources. It is critical to handle mercury with extreme caution and be aware of its potential risks. According to studies, mercury is a widespread environmental pollutant. It is a naturally occurring heavy metal found in rock, the earth's crust, and coal deposits (Priyadarshanee et al., 2022). Due to their toxic effects, bioremediation methods are often preferred over other remediation techniques for mercury contamination. Mercury-resistant bacteria possess a genetic sequence called the *mer* operon, which enables them to thrive and break down mercury in contaminated environments (Dash et al., 2012). Studies indicated bacterial *mer* operons play a crucial role in mercury biogeochemistry and bioremediation. These genetic sequences allow bacteria to convert various forms of mercury, both inorganic and organic, into less harmful, volatile elemental mercury. The presence of *mer* genes influences the overall mercury cycle in the environment. The effectiveness of this mercury transformation process depends on the specific types and diversity of *mer* genes found in mercury-resistant bacteria (Priyadarshanee et al., 2022).

The genes *merA*, *merB*, *merP*, and *merT* play a vital role in mercury resistance and bioremediation. *MerA* encodes a mercuric reductase that reduces toxic $Hg^{2+}$ to less harmful elemental mercury (Hg). *MerB* degrades organic mercury compounds. *MerP* and *MerT* are involved in transporting inorganic and organic mercury, respectively, into bacterial cells for detoxification (Sone et al., 2013). *MerE* and *MerG* genes influence the cell's permeability to phenylmercury. *MerE* is involved in the uptake of organic mercury, while *MerG* facilitates its efflux, contributing to phenylmercury resistance. *MerC*

and *MerF* are inner membrane proteins commonly used in the bioremediation of mercury-contaminated soils. They play a role in transporting mercury ions across the cell membrane. *MerD* and *MerR* genes regulate mercury bioremediation processes. *MerD* negatively regulates mercury resistance genes, while *MerR* positively regulates their expression (Dash et al., 2012). The *merB* gene is particularly valuable due to its ability to detoxify a wide range of toxic mercury compounds, including methylmercury and other organic mercury species. In conjunction with the *merA* gene, *merB* facilitates the enzymatic transformation of both organic and inorganic mercury into less harmful, non-volatile forms. Bacteria possessing the *merB* gene, especially those adapted to harsh environments and capable of tolerating pH fluctuations, are promising candidates for bioremediation applications (Priyadarshanee et al., 2022).

A different study revealed that genes like *merA*, *merB*, and *merG* play an important role in the bioremediation of mercury-contaminated sites. These genes, often clustered together in a single operon, are involved in the detoxification and removal of mercury. *MerA* and *MerB* are responsible for the enzymatic transformation of mercury, while *MerE* facilitates the transport of both organic and inorganic mercury across the bacterial cell membrane (Bizily et al., 1999). Bacteria exposed to mercury-contaminated environments for prolonged periods develop resistance mechanisms. Studies have shown that the *mer* operon, a genetic sequence responsible for mercury detoxification, is present in thermophilic bacteria and even ancient archaea. This indicates that the origin of mercury resistance mechanisms may lie in hydrothermal environments, where high concentrations of mercury ions are present (Barkay et al., 2010).

### 2.13.2. Gene diversity associated with lead bioremediation

Lead (Pb) is a hazardous HM that poses a substantial environmental risk. Traditional techniques of cleansing Pb from wastewater can be expensive and environmentally damaging. Bioremediation, a sustainable approach that utilizes microorganisms to degrade or remove pollutants, has emerged as a promising alternative. By employing microorganisms capable of absorbing, bioaccumulating/ transforming lead, bioremediation offers a cost-effective and eco-friendly solution to clean up lead-contaminated wastewater Naik & Dubey, (2013). It is a widely used heavy metal in various industries, including electronics, glass manufacturing, and battery production. The increasing demand for lead, especially in countries like China, has led to concerns about environmental contamination.

Certain bacteria, such as *Arthrobacter* spp., *B. megaterium*, *C. freundii*, *E. coli*, *P. marginalis*, and *Staphylococcus aureus*, have been recognized as potential bioremediation agents for lead-contaminated environments. These bacteria can remove or immobilize lead through various mechanisms, including adsorption, biosorption, and bioaccumulation. To address the issue of lead pollution, it is essential to implement effective control measures to reduce lead emissions and remediate contaminated sites. Studies have shown that the *Cupriavidus metallidurans* CH34 plasmid pMOL30 harbors a lead resistance operon, suggesting a potential genetic basis for lead resistance in bacteria (Das et al., 2016).

According to Das et al. (2016), microorganisms have a variety of techniques to deal with HMs, such as lead. These techniques include accumulating the metal inside and outside of their cells, trapping it, binding it to their surfaces (biosorption), turning it into insoluble forms (bio-precipitation), making it less harmful (detoxification), and chemically modifying it (biotransformation). Biosorption, a metabolism-independent process, primarily occurs at the cell-extracellular interface. In this process, microbial cells bind heavy metals to their surface without requiring cellular energy. Metabolism-dependent bioaccumulation involves energy-dependent processes like redox reactions and sequestration. In extracellular sequestration, metal ions form complexes with various compounds within the cell cytoplasm. Subsequently, these metal-ligand complexes are slowly transported into the cell (Akhtar et al., 2013). There is a report in which bacteria can resist lead pollution by ATPase-mediated lead efflux, intracellular sequestration by using metallothionein, exopolysaccharide sequestration, adsorption to the cell surface, and biosorption in the cell wall in the periplasmic space. These are collectively known as bioaccumulation, along with precipitation by sulfate-reducing bacteria, and finally, phosphatase-catalyzing enzymes can be used in lead bioremediation. This mechanism is widely employed in biotechnological applications for lead bioremediation from contaminated sites (Naik & Dubey, 2013).

The *pbr* operon, regulated by the *pbrR* gene, is activated in the presence of $Pb^{+2}$ ions. This operon includes genes like *pbrA*, *pbrB*, *pbrC*, and *pbrT*, each with specific functions. The *pbrA* gene encodes a P-type ATPase that pumps $Pb^{+2}$ ions out of the cell. On the other hand, the *pbrB* gene encodes an integral membrane protein, possibly involved in inorganic phosphate production. The *pbrC* gene encodes a prolipoprotein signal peptidase, while *pbrR* encodes a regulatory protein that activates the

operon in response to $Pb^{2+}$ ions, and *pbrT* encodes a $Pb^{2+}$ uptake protein. The combined action of these genes allows bacteria to resist and potentially remediate lead contamination. The *pbrA* gene plays a crucial role in exporting $Pb^{2+}$ ions from the cell. Additionally, intracellular sequestration of lead using metallothionein proteins, as seen in *P. aeruginosa* WI-1, is another promising strategy for bioremediation (Das et al., 2016).

### 2.13.3. Gene diversity associated with arsenic bioremediation

Arsenic, a naturally occurring heavy metal, is a significant global health and environmental concern, particularly due to its presence in contaminated water sources. This toxic element can infiltrate various environments, including soil, water, and air. Long-term exposure to arsenic-contaminated water can lead to severe health issues, including several types of cancer, skin lesions, cardiovascular diseases, and neurological disorders (Islam et al., 2019). Arsenic is an HM that causes drinking water contamination worldwide. It is a major HM that pollutes drinking water globally. This contamination poses a significant threat to human health, as it is linked to various health issues, including cancer. While both natural geological sources and human activities, like mining and agricultural practices, contribute to arsenic contamination, natural sources are the primary cause. Both developed and developing countries face the challenge of arsenic-contaminated drinking water (Rashid et al., 2023).

Arsenic pollution is a serious environmental issue with significant health implications. The increasing accumulation of arsenic in soil and water bodies has led to its entry into the food chain, posing risks to human health (Selvi et al., 2014). To better understand and address arsenic contamination, scientists are increasingly using molecular techniques to study the microbial communities present in these environments. By identifying specific genes and their functions, researchers can develop genetic models to improve bioremediation strategies. *Enterobacter asburiae* (BC1) and *Enterobacter cloacae* (BC2), two bacterial species commonly found in arsenic-contaminated agricultural soil, are promising candidates for bioremediation due to their arsenic resistance. Additionally, research on bacteria like *Corynebacterium glutamicum*, which is used in industrial bioremediation, is being investigated to further explore their potential for arsenic removal (Mathivanan et al., 2021). While small amounts of heavy metals are essential for cellular processes, excessive levels can be harmful. These metals can generate harmful free radicals, damage cell membranes, and reduce microbial biomass and diversity. To counteract heavy metal toxicity, microorganisms have evolved various

resistance mechanisms, often encoded by specific genes and gene clusters. For instance, the bacterium *Micrococcus luteus* AS2 exhibits high resistance to arsenic due to the presence of genes like acr3. This gene plays a crucial role in both the accumulation and efflux of arsenite, allowing the bacterium to survive in arsenic-contaminated environments (Sher et al., 2020).

Arsenic bioremediation, a sustainable approach to mitigating arsenic pollution, relies on the inherent abilities of microorganisms to tolerate and transform arsenic into less toxic forms. Several mechanisms contribute to this process. These mechanisms include adsorption and biosorption, efflux transport, oxidation-reduction reactions, methylation, and biotransformation via the *AsC1* gene, which helps bacteria reduce arsenic pollution. The *AsC1* gene encodes a protein that facilitates the transport and transformation of arsenic. This gene is often found in arsenic-resistant bacteria and plays a key role in arsenic detoxification. Generally, by understanding the diverse mechanisms employed by microorganisms to tolerate and transform arsenic pollution, scientists can develop innovative bioremediation strategies to mitigate the environmental and health risks associated with arsenic pollution (Sayqal & Ahmed, 2021).

### 2.13.4. Gene diversity associated with copper bioremediation

Copper (Cu) is an important trace element for many organisms, including microorganisms. It plays a vital role in various biological processes, such as respiration and photosynthesis. Due to its broad applications in industries like brewing, agriculture, electronics, and manufacturing, copper can be released into the environment, leading to potential contamination (George et al., 2023). While copper is an essential trace element for microbial growth, acting as a cofactor for various enzymes, it can become toxic at higher concentrations (Huang et al., 2018). To maintain optimal copper levels, bacteria have evolved mechanisms to regulate copper uptake and efflux. These mechanisms often involve the sequestration of copper ions, both inside and outside the cell. Genes associated with these processes play a crucial role in detoxifying copper from polluted environments. Bacteria have developed several mechanisms to resist copper toxicity. For example, *Escherichia coli* and *P. syringae* possess the *Cue*, *Cus*, and *Pco* systems for copper resistance. These systems are responsible for pumping excess copper ions out of the cell, thereby protecting the organism from copper toxicity (Bondarczuk et al., 2013). These copper resistance systems are essential for bacterial survival in copper-rich environments. Bacterial species, such as *Acidithiobacillus ferrooxidans*, *E. coli* strain K-

12, *Metallosphaera sedula,* and *P. aeruginosa*, have been shown to possess such mechanisms (Huang et al., 2018).

Cu is a necessary HM for the normal functioning of entire living organisms. In microorganisms, it serves as a cofactor for several enzymes involved in respiratory and electron transport processes. Cu is toxic to cells at high concentrations, primarily due to its ability to disrupt the integrity of cell membranes (Leite & Mohan, 1990). A trace element is required for the growth of microorganisms because it is a cofactor for several enzymes. However, it can be harmful and toxic even at lower concentrations (Huang et al., 2018). For predicting environmental pollutants and their impact on the environment, screening genes related to copper bioremediation is paramount. The amino acid produced by copper resistance-associated genes depends on the type of bacterial diversity that thrives in copper pollution areas. For instance, amino acid sequences of the *CopA* gene reported from *Arthrobacter* (O4), *Sphingomonas* (O12, A32, and A55), and *Stenotrophomonas* (C21) strains are closely related to the *CopA* gene predicted for *Arthrobacter, Sphingomonas*, and *Stenotrophomonas* strains, respectively, in copper bioremediation (Altimira et al., 2012).

### 2.13.5. Gene diversity associated with cadmium bioremediation

Cadmium (Cd) is a highly toxic HM that poses a substantial threat to both the environment and human health. Primarily sourced from mining, industrial processes, and agricultural practices, cadmium contaminates soil and water bodies. Unlike many other pollutants that can break down over time through biological or chemical processes, HM, like cadmium, is extremely persistent in the environment. This persistence makes their removal from the environment a challenging task. $Cd^{+2}$ accumulation in the environment, particularly in agricultural soils, can enter the food chain and pose serious health threats to humans and animals. Long-term exposure to $Cd^{+2}$ can lead to various health issues. Given the challenges associated with traditional remediation techniques, bioremediation is a promising approach. By utilizing microorganisms with the ability to tolerate and accumulate cadmium, bioremediation can provide an environmentally friendly and cost-effective solution (Ike et al., 2007). $Cd^{+2}$ is primarily used in the manufacturing of pigments and batteries. While battery production has increased the demand for $Cd^{+2}$, its use has decreased in developed countries due to environmental concerns (Chakraborty & Das, 2014). Since the mid-1980s, researchers have investigated the mechanisms of cadmium transport, resistance, and toxicity in microorganisms such

as bacteria, algae, and fungi as a potential approach to bioremediation. The *cad* operon, consisting of the *cadA* and *cadB* genes, plays a crucial role in cadmium resistance and is a key target for bioremediation strategies (Zhao et al., 2021).

In a $Cd^{+2}$-resistant bacterium, the genes *czcA*, *czcB*, and *czcC* encode the components of the membrane-bound cation efflux protein complex CzcABC. It consists of three subunits: *CzcA*, which is localized in the cytoplasmic membrane as a cation/proton antiporter, *CzcB*, found in the periplasm, which is part of a membrane fusion protein, and *CzcC*, an outer membrane protein (Chakraborty & Das, 2014). The main functions are to transport cations through the cytoplasmic membrane, periplasmic space, and outer membrane, respectively, resulting in a decrease in intracellular cations. Bacterial bioremediation of cadmium initially involves metal binding to the bacterial cell wall. Protons are released alongside cadmium, indicating the competitive binding nature of the cell wall. *Pseudomonas* H1 and *Bacillus* H9, which have the same genes, are also confirmed to have intracellular mechanisms of cadmium sequestration to reduce cadmium toxicity, as examined (Roane et al., 2001). The expression of both *MTL4* and *AtPCS* genes affects cadmium accumulation in the nodule plants. These two genes are also introduced with recombinant bacteria in rice paddy soil contaminated with cadmium. The accumulation of $Cd^{+2}$ increased not only in the tubers but also in the roots of *Astragalus sinicus* infected with recombinant rhizobia (Ike et al., 2007).

### 2.13.6. Gene diversity associated with chromium bioremediation

Chromium (Cr) is a versatile element with various oxidation states, ranging from $Cr^{+2}$ (II) to $Cr^{+6}$ (VI). It is naturally present in the environment and is widely used in various industries (Thatoi & Pradhan, 2017). It is a naturally occurring element found in forms including $Cr^{+3}$ (III) and Cr (VI). While $Cr^{+3}$ (III) is relatively less harmful, $Cr^{+6}$ (VI) is an extremely toxic pollutant, particularly recognized for its carcinogenic properties. Human activities, including industrial processes such as metal fabrication, tanning, chromate production, and ferrochrome and pigment manufacturing, are major contributors to $Cr^{+6}$ pollution. The activities release $Cr^{+6}$ into the environment, primarily in the form of Cr (VI), through soil and wastewater pollution. The discharges of $Cr^{+6}$ have led to important environmental pollution, affecting soil and water bodies. This pollution poses serious health risks to humans and ecosystems (Tchounwou et al., 2012).

Bioremediation is a promising technology for cleaning up polluted environments. Microorganisms, particularly bacteria, play an essential role in reducing toxic hexavalent Cr (VI) to less toxic Cr (III). This reduction process involves several mechanisms: oxidation-reduction or using cellular reductase enzymes while indirectly creating reducing conditions in the environment. For instance, certain bacteria can produce organic acids or other reducing agents that facilitate Cr (VI) reduction. The ability of microorganisms to reduce Cr (VI) is influenced by various factors such as environmental conditions, nutrient availability, and the specific bacteria involved. By understanding these factors, experts can optimize bioremediation strategies to effectively clean up Cr-polluted sites. By harnessing the power of microorganisms, bioremediation offers a sustainable and environmentally friendly approach to addressing environmental pollution (Kalsoom et al., 2023). It is crucial to identify and characterize genes involved in chromium bioremediation to ensure the safety and effectiveness of these technologies. These genes facilitate the biosorption of chromium, reducing its environmental impact. Among bacteria, *Pseudomonas* species are particularly effective in detoxifying hexavalent chromium from contaminated environments (Dong et al., 2013).

## 2.14. Factors affecting the bioremediation ability of microorganisms

The task of removing HMs from the environment is a complex and multifaceted challenge. While a variety of biological, chemical, and physical methods exist, each approach comes with its own set of limitations and drawbacks. The use of microorganisms for the removal of HMs, a process known as bioremediation, poses significant ecological and economic constraints. A crucial factor governing microbial response in a polluted environment is the availability of essential nutrients. Nutrients such as nitrogen, phosphorus, sulfur, iron, and potassium play an important role in stimulating microbial growth and cellular metabolism. However, the optimal nutrient balance is essential. An excess or deficiency of any of these nutrients can negatively impact microbial activity and, consequently, bioremediation efficiency. For instance, an excess of nutrients can lead to eutrophication algal bloom, a process that depletes oxygen levels in the environment, harming both the microorganisms and other aquatic organisms. Conversely, a deficiency of essential nutrients can limit microbial growth and reduce their ability to remove heavy metals (Sayqal & Ahmed, 2021).

Nutrients are essential for microbial life and play a pivotal role in bioremediation processes. They serve as the building blocks for microbial cells and the energy source for their metabolic activities.

Specifically, nutrients enable microorganisms to synthesize enzymes, the biological catalysts that break down pollutants into less harmful substances. A source of nutrients, including carbon, nitrogen, phosphorus, and other essential elements, is crucial for optimal microbial growth (Kapur et al., 2024; Mydeen et al., 2024). The nature of pollutants significantly impacts bioremediation strategies. The physical state of a pollutant, including solid, liquid, and volatile, impacts the microbial degradation role. The chemical properties of pollutants, such as toxicity, organic or inorganic nature, and specific functional groups, determine the types of microorganisms and enzymes required for degradation (Mangunwardoyo et al., 2013). For example, HMs, polycyclic aromatic hydrocarbons (PAHs), pesticides, and chlorinated solvents pose unique challenges due to their persistence and toxicity. The environmental conditions (pH, temperature) of the polluted site can significantly influence the success of bioremediation. Factors such as soil or water pH, temperature, oxygen availability, and the presence of other contaminants can affect microbial activity and the rate of pollutant degradation (Atagana et al., 2003). Microbial groups, composed of various species, often work synergistically to biodegrade environmental contaminants. *Pseudomonas* species, *Aeromonas*, *Flavobacterium*, *Corynebacterium*, *Acinetobacter*, *Mycobacterium*, *Streptomyces*, and *Bacillus*, are a few of them (Marzan et al., 2017).

The concentration of pollutants can significantly impact the effectiveness of bioremediation using living organisms to degrade or remove contaminants from polluted environments (Vázquez-Núñez et al., 2020). Bioremediation, a process that utilizes living organisms to degrade or remove pollutants, is most effective within a specific concentration range of contaminants. If the concentration is too low, microorganisms may lack enough substrates to sustain their growth and activity. Conversely, excessively high concentrations can be toxic to microorganisms, inhibiting their growth and reducing their ability to degrade. Optimal concentrations can support microbial growth and degradation, while extremely high or low concentrations can hinder bioremediation processes. The specific response of microorganisms to different pollutants varies depending on the type of pollutant, the microbial community, and environmental conditions. This highlights the importance of careful monitoring and management in bioremediation applications (Sharma, 2012).

# 3. MATERIALS AND METHODS

## 3.1. Description of the Study Area

This study was carried out in Bishoftu and Mojo, located in the Eastern Shewa Zone of the Oromia Region in Ethiopia (Figure 3). Mojo town is situated at 8° 35' North latitude and 39° 07' East longitude, with an elevation ranging from 1,788 to 1,825 meters above sea level (Gebeyehu & Bayissa, 2020). Bishoftu is located at 8° 45' North latitude and 38° 59' East longitude, with an elevation of 1,885 meters above sea level (Beyene et al., 2015). Mojo and Bishoftu, located in the Eastern Shewa Zone of the Oromia Region, are approximately 80 and 40 kilometers from the capital city, Addis Ababa, respectively. Bishoftu is home to the Eastern Industrial Zone, a significant hub of Chinese-operated businesses that contribute substantially to the country's economic growth through foreign currency generation. Similarly, Mojo Town also hosts a variety of industries, ranging from large-scale factories to smaller operations. Notably, the Mojo tanneries process goat and sheepskins, with an annual capacity of 844,000 to 1,656,000 skins. The Mojo tanneries' industrial activity generates a significant amount of waste, estimated to be between 3,500 and 5,500 cubic meters per day (Reda, 2016). It is believed that the industrial effluent discharged from the factories in these towns negatively impacts both natural and human-made environments.

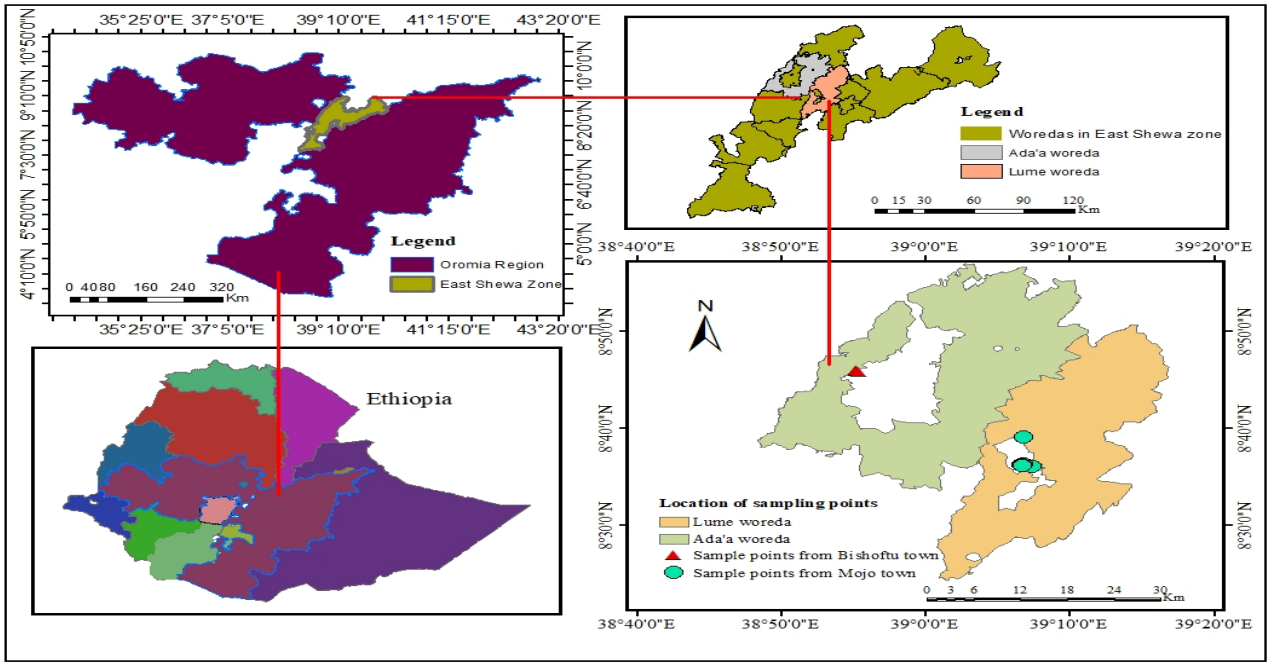


**Figure 3: A Schematic Diagram of the Study Area**

**Table 1: An overview of the Bishoftu Industrial Zone and Mojo Tannery Industries Effluent sampling locations.**

| Sample codes | Locations | Latitudes | Longitudes | Date of Collection |
|---|---|---|---|---|
| BSS-1 | Bishoftu | 8°45'55.0"N | 38°55'12.9"E | 08 June 2023 |
| BSS-2 | Bishoftu | 8°45'54.8"N | 38°55'12.6"E | 08 June 2023 |
| BSS-3 | Bishoftu | 8°45'54.4"N | 38°55'12.3"E | 08 June 2023 |
| BSS-4 | Bishoftu | 8°45'53.9"N | 38°55'13.4"E | 08 June 2023 |
| BSS-5 | Bishoftu | 8°45'52.1"N | 38°55'14.7"E | 08 June 2023 |
| BSS-6 | Bishoftu | 8°45'49.0"N | 38°55'20.7"E | 08 June 2023 |
| MWWSS-1 | Mojo | 8°36'04.5"N | 39°07'21.5"E | 09 June 2023 |
| MWWSS-2 | Mojo | 8°36'19.2"N | 39°06'49.1"E | 09 June 2023 |
| MWWSS-3 | Mojo | 8°39'04.4"N | 39°06'49.6"E | 09 June 2023 |
| MWWSS-4 | Mojo | 8°36'12.1"N | 39°06'36.9"E | 09 June 2023 |
| MWWSS-5 | Mojo | 8°36'12.9"N | 39°06'45.2"E | 09 June 2023 |
| MWWSS-6 | Mojo | 8°36'08.8"N | 39°06'40.2"E | 09 June 2023 |

*BSS-Bishoftu soil sample, MWWSS- Mojo wastewater sample

### 3.2. Soil and Wastewater Sample Collection

Six soil samples, labeled Bishoftu soil sample (BSS-1) through BSS-6, were collected from the Bishoftu Eastern Industrial Zone (BEIZ) in June 2023, as shown in (Figure 1). The sites represent a pollution gradient: BSS-1 is closest to the industry; BSS-2 through BSS-5 are situated mid-canal along the irrigation path; and BSS-6 is an agricultural site (located within a farmer's compound for growing cabbage). Additionally, six wastewater samples, designated MWWS-1 through MWWS-6, were obtained from the Mojo Tannery effluents (Table 1).

Samples were collected sequentially along the effluent discharge path, beginning at the initial discharge site (MWWSS-1). Subsequent points included an intermediate point (MWWSS-2), the middle section (MWWSS-3), a stagnant area (MWWSS-4), the point just before mixing with the river (MWWSS-5), and finally, the site after mixing with the river water (MWWSS-6). All samples were stored in sterile containers and transported under icebox to the molecular and biotechnology laboratory at Haramaya University. Then, after, they were kept at 4 °C until the heavy metal

characterization and bacterial isolation were performed. Some physicochemical analyses of the water were conducted on-site using a pH meter (Model HI98113), while further sample analyses were carried out in the laboratory.

### 3.3.Isolation of heavy metal-resistant bacteria from industrial effluents

Samples were prepared to appropriate dilutions ($10^{-1}$-to $10^{-6}$) using standard methods. From the last dilution, 0.1 ml samples were inoculated into medium containing (28 g/L of nutrient agar, 10 g/L of peptone, and 5 g/L of beef extract, along with 300 µg/mL of each heavy metal, namely cobalt sulfate, copper sulfate, cadmium nitrate, potassium chromate & zinc nitrate) & prepared in a dilution method. The plates were incubated at 37 °C for 24 to 72 h (Elahi et al., 2019). Microbial growth was observed, groups of highly heavy metal-resistant bacterial isolates showing various colonies were picked and subsequently sub-cultured to isolate pure cultures, and preserved at 4 °C for further experimentation. Gram staining and biochemical tests were conducted on the isolates using standard methods (Elahi et al., 2019).

Groups of highly heavy metal-resistant bacterial isolates showing various colonies were observed on the plates. The colonies that showed similarity were well thought out on the identical bacteria, while dissimilar colonies exhibited different heavy metal-resistant isolates. The same agar was used to inoculate the isolated colonies. As a result, various colonies were isolated to achieve pure cultures using the streak plate method (Sneha et al., 2014). The streaking technique successfully obtained a pure bacterial culture on appropriate agar plates. Gram staining and biochemical tests were conducted on the isolates. The pure cultured bacteria were also maintained by sub-culturing regularly and stored under proper media and conditions. Following Gram staining, the motility of each bacterial isolate was observed using a binocular microscope (OPTO-EDU, A11.2601BP), and the result was recorded on a connected computer.

### 3.4. Heavy metal Analysis of Soil and water

Soil samples were processed by crushing, sieving, digestion, and ashing in an oven at 240 °C for 2 hrs. The DTPA extraction method was used. A nitric acid to perchloric acid ratio (3:1v/v) was used to extract HMs from the soil. Five milliliters of a 65% (w/v) nitric acid ($HNO_{3)}$ solution were added to 1g of the soil sample. The mixture was then thoroughly stirred and heated to 140 °C for an h. After

cooling, 4 mL of 70% perchloric acid ($HClO_4$) was added, and the mixture was gently boiled until it formed a white fume. The extracted metals were filtered through Whatman No. 42 filter paper in a 100 mL volumetric flask and diluted for analysis using atomic absorption spectrophotometry (210VGP Buck Scientific). Certified reference materials were analyzed alongside a sample to ensure accuracy and precision. The HM concentrations, such as cobalt, copper, cadmium, zinc, manganese, iron, chromium, and nickel, were determined by measuring their absorbance at specific wavelengths. The specific wavelengths of each HM used were 240.7, 324.7, 228.8, 213.9, 279.5, 248.5, 357.9, and 241.5 nm, respectively. A control sample was also analyzed to validate the digestion process (Uddin et al., 2016).

About 100 ml of wastewater was used and digested with 5 ml of concentrated $HNO_3$ to prepare wastewater samples for HM analysis. The mixture was vaporized to 10 ml. The mixture was then transferred to a 125 ml conical flask and treated with 10 ml of 70% $HClO_4$ (v/v) acid. The mixture was heated until white fumes of perchloric acid appeared, indicating complete digestion. After cooling, the digested samples were filtered using Whatman No. 42 filter paper and diluted with distilled water. HM analysis was conducted using atomic absorption spectroscopy with a Buck Scientific model 210VGP instrument.

### 3.5. Total nitrogen determination of the soil

The Kjeldahl Method was employed to determine the total nitrogen content in the soil sample. About 10 g of the soil was weighed and placed in a digestion flask, where it was subjected to a digestion process. This process involved heating the soil sample with a mixture of 20 ml of concentrated $H_2SO_4$ and a catalyst (such as potassium sulfate) to convert organic nitrogen into $(NH_4)_2SO_4$. A heat source was placed under the flask after the soil sample was added. The temperature was gradually increased to prevent the contents from boiling over. The heating continued until the soil's organic matter was completely oxidized, resulting in a clear yellow solution. This step typically took several hours to complete. After digestion, the flask could cool to room temperature. The contents of the digested flask were then carefully transferred into a 500 mL volumetric flask. Distilled water was added to the flask up to the mark, and the mixture was thoroughly mixed to ensure that the nitrogen content was evenly distributed throughout the solution. A portion of the diluted digested solution was transferred to a separate container to determine the total nitrogen content. A few drops of phenolphthalein

indicator were added to an aliquot. The solution was then distilled, and the resulting distillate was collected in a conical flask containing a known concentration of boric acid ($H_3BO_3$). The boric acid solution acted as a trap to absorb the ammonia gas released during the distillation process. Once the distillation was complete, the boric acid solution was titrated with a standard sodium hydroxide solution. The endpoint of the titration was reached when a permanent pink color appeared, indicating that ammonia had reacted with the sodium hydroxide. The following formula was used to calculate the total nitrogen in the soil sample (Sáez-Plaza et al., 2013):

$$\text{Total Nitrogen (\%)} = \frac{\text{Volume of NaOH x Normality of NaOH x 14.01 x 100}}{\text{Weight of soil sample in gram}}$$

### 3.6. Biochemical characterization of the isolated colonies

**Gelatin hydrolysis test:** The gelatin hydrolysis test was performed on media containing peptone (5 g), beef extract (3 g), and gelatin (12 g). These ingredients were dissolved in distilled water and gently heated until all substances were dissolved. Then about 2 to 3 ml of the medium was dispensed into the test tube culture. The medium was sterilized in an autoclave at 121 °C for 15 min using the autoclave model BEST-PA10L. After sterilization, the medium was cooled in an upright position before use. Then, a heavy inoculum of 18 to 24 hr bacterial isolates was inoculated into test tubes containing nutrient gelatin, along with uninoculated control tubes. Finally, the medium was incubated in the Memmert GmbH + Co. KG incubator, model number DIN12880-2007-Kl, at 37 °C for one week. The results were interpreted as gelatin liquefaction (Phuong et al., 2021).

**Indole production test:** To perform the indole production test, a Sulfide-indole-motility (SIM) medium containing peptone (30 g), beef extract (3 g), ferrous ammonium sulfate (0.2 g), sodium thiosulfate (0.024 g), and agar (3 g) were dissolved in 1000 ml of distilled water, the pH adjusted to 7.3, and autoclaved at 121°C under 15 psi pressure for 15 min. The medium was cooled in an upright position to form agar deep. Following inoculation, the medium was incubated at 37 °C for 24 to 48 h. Five drops of Kovac's reagent were added step by step. A layer formed after the tubes were shaken and allowed to stand for 10 min. Positive results are indicated by a red color at the top of the tube, while a yellow color indicates negative results (Haddaway et al., 2019).

**Methyl red test:** Sterile MR-VP broth medium was prepared in test tubes inoculated with the isolates of fresh culture and incubated at a temperature of 37 ±2 °C for 2 days. After incubation, the tubes were supplemented with 5 drops of methyl red and observed for color changes. The addition of methyl red within 10 to 15 seconds indicates a positive result by changing the color from yellow to red (Shanmugaraj et al., 2021).

**Starch hydrolysis test:** The beef extract (3 g), soluble starch (10 g), and agar (12 g) are thoroughly mixed in 1000 ml of distilled water, and frequent stirring and heating are done to ensure the mixture reaches the desired consistency. The final pH of the medium was adjusted to 7.5 ± 0.2. The dissolved medium was autoclaved at 121 °C for 15 min at 15 psi. After sterilization, the prepared medium was poured into sterilized petri plates and allowed to solidify before use. Colonies of the target bacteria, cultured for 16 to 18 hours, were harvested and sub-cultured onto a plate containing fresh solidified medium. Then, the medium was incubated at 37 °C in the Memmert GmbH + Co. KG incubator, Model number DIN12880-2007-Kl, for 24 to 48 h. The presence of a clear zone around bacterial isolates indicates starch hydrolysis (Velmurugan., 2021).

**Triple sugar analysis:** The combination of media components, including beef extract (3 g), yeast extract (3 g), peptone (20 g), ferrous ammonium sulfate (0.2 g), NaCl (5 g), sodium thiosulfate (0.3 g), phenol red (0.024 g), and nutrient agar (13 g), was dissolved completely in 1000 ml of distilled water. The medium was sterilized at 121 °C for 15 min at 15 psi pressure. The medium was then distributed into sterilized test tubes in a slanted position to create a 2.5 cm butt and a 3.8 cm slant. An 18 to 24-hour bacterial isolate was inoculated and incubated at 37 °C in an incubator for 18 to 24 h to observe a color change (Velmurugan., 2021); Harley and Prescott 2002; Sharma 2012). Yellow butt and red slant colors indicate a positive result for glucose fermentation, while yellow butt and yellow slant indicate the fermentation of glucose, lactose, and sucrose. Finally, red butt and red slant indicate none of the three sugars fermented (Cheeptham & Naowarat, 2016). $H_2S$ gas production is also seen from the agar slant.

**Urease test:** The urea base was prepared by dissolving peptone (1 g), dextrose (1 g), NaCl (5 g), potassium phosphate monobasic (2 g), urea (20 g), phenol red (0.012 g), and nutrient agar (15 to 20 g) in 1000 ml of distilled water. The medium was filtered with Whatman No. 1 filter paper before the addition of nutrient agar. After filtration, the agar medium was added, boiled to completely dissolve,

and sterilized in an autoclave at 121 °C for 15 min at 15 psi pressure. 4 to 5 ml of the urea-based medium was distributed into a sterile test tube and placed in a slant position during cooling until it solidified. A heavy inoculum from 18 to 24 h of pure culture was streaked on the entire slant surface with a control. Then, the medium was incubated at 37 °C. The positive result of a bright pink color on the slant indicated a color change in the time intervals of 6 h, 24 h, and every day for up to 6 days (Dahlén et al., 2018).

**Voges-Proskauer test:** The VP broth medium was prepared from Barritt's reagent A: 5% (wt/vol) α-naphthol in absolute ethanol and Barritt's reagent B: 40% (wt/vol) KOH (16 g of KOH in 100 ml of distilled water) in deionized water, autoclaved, and cooled to room temperature. The 24 h of heavy metal-resistant bacteria isolates were inoculated using a sterilized loop, followed by incubation at 37 °C. After incubation, 1 ml of α-naphthol was added and shaken, followed by the addition of 0.5 ml of 40% KOH to the broth and shaking. The development of a red color after the addition of the reagents within 1 hour was taken as a positive result (Shanmugaraj etal., 2021).

**Catalase Test:** The slide (drop) method was selected for the catalase test for isolated heavy metal-resistant bacteria. For these purposes, 3% hydrogen peroxide (v/v) was used to determine the catalase activity. An overnight bacterial culture was mixed with $H_2O_2$ on the microscopic slide using a sterilized loop. The formation of bubbles during and after the interaction of hydrogen peroxide and isolates was recorded as a positive result (Reiner, 2010).

**Citrate utilization test:** To determine the citrate utilization test, ingredients NaCl (5 g), sodium citrate (dihydrate) (2g), ammonium dihydrogen phosphate (1g), dipotassium phosphate (1g), magnesium sulfate (heptahydrate) (0.2 g), bromothymol blue (0.08 g), and nutrient agar (15 g) were used for bacterial growth culture preparation. The medium was dissolved in 1000 mL of deionized water, and the pH was adjusted to 6.9 before nutrient agar and bromothymol blue were added. After mixing the medium, it was distributed into test tubes and sterilized at 121 °C for 15 min at 15 psi pressure. The test tubes were cooled in slant positions (long slant, shallow, and butt). Streak the slant back and forth with a light inoculum picked from the center of a well-isolated colony. They were incubated at 37 ±2 °C for 4 to 7 days. A clear color change from green to blue, along with the slant, indicated a positive result (Hofwegen et al., 2016).

### 3.7. Growth inhibition percentage rate of heavy metal-resistant isolates

Bacterial growth rate percentage inhibition is measured using Luria-Bertani Broth (LB), which contains 10 g of tryptone, 5 g of yeast extract, 10 g of sodium chloride, and 1 liter of distilled water. The pH of the medium was adjusted to 7.0 with 1 N sodium hydroxide. Different concentrations of heavy metal ions such as $Cd^{2+}$, $Co^{2+}$, $Cr^{3+}$, $Cu^{2+}$, and $Zn^{2+}$ from salts of $CoSO_4 \cdot 2H_2O$, $CuSO_4$, Cd $(NO_3)_2$, $K_2Cr_2O_7$, and Zn $(NO_3)_2$ were used to measure growth inhibition. About 1 mL of an overnight cultured isolate was transferred into 100 mL of freshly prepared medium and incubated at 28 °C on a rotary shaker at 300 rpm. Cell growth was measured at different times by assessing the optical density at 560 nm using a UV-visible spectrophotometer. The percentage of cultured cell growth values was assessed using growth in the absence of heavy metal concentrations as the 100% reference value. The growth inhibition rate caused by heavy metals was measured by comparing the growth rates $\mu(h^{-1})$ of the cultures in the medium with the toxicants (μ, toxicant) to those of the control culture (μ, control) (Heipieper et al., 1995). The growth inhibition of different concentrations of heavy metal forms was calculated as a percentage of the growth rate of cultures in the medium with toxicants, relative to the control cultures, using the following formula (Pepi et al., 2011):

$$\% \text{ Growth inhibition } = \frac{\mu \text{ control} - \mu \text{ toxicants}}{\mu \text{ Control}} \times 100\%$$

### 3.8. Heavy metal utilization assay

HM-resistance bacterial isolates (HMRBI) were cultured in a flask containing LB broth medium (10 g tryptone, 5 g yeast extract, 10 g NaCl) for 6 h in a rotary shaker (REMI-RS-36BL) at 150 rpm. The pH and temperature were maintained at 7.0 and 37 °C, respectively. About 300 μg/ml of sterilized HMs ($Co^{2+}$, $Cu^{2+}$, $Cd^{2+}$, $Cr^{6+}$, and $Zn^{2+}$) from salts of $CoSO_4 \cdot 2H_2O$, $CuSO_4$, Cd $(NO_3)_2$, $K_2Cr_2O_7$, and Zn $(NO_3)_2$ was added separately to each culture flask after the optical density reached 0.6 (k = 600 nm for equal enzyme activity). The cultures were grown for 24 h. The samples were centrifuged (5000 rpm, 15 min). After separation, the supernatants were combined with concentrated HNO3 in a 1:2 volume ratio. The mixtures were then heated to 100 °C on a hotplate stirrer (Stuart Scientific-SM1-13613) to initiate an acid digestion process until the final volume equaled the original supernatant. The extract was filtered using Whatman 42 filter paper to eliminate insoluble materials.

The resulting filtrate was collected in a volumetric flask and diluted with distilled water. The total heavy metal (HM) reduction was assessed using an atomic absorption spectrophotometer (210VGP Buck Scientific). The results were compared to a control group to determine the percentage of HM degradation (Marzan et al., 2017).

$$\% \text{ HM utilized} = \frac{\text{HM utilized (ppm)}}{\text{HM added to the broth (ppm)}} \; x \; 100\%$$

$$\text{HM utilized in (ppm)} = \text{HM added to the broth in (ppm)} - \text{HM at the end of culture in (ppm)}$$

### 3.9. Optimization for heavy-resistant bacteria growth

The impact of pH and temperature on the HMRBI was investigated. These isolates, HMRBI-1, HMRBI-2, HMRBI-7, HMRBI-12, and HMRBI-17, showed resistance to cadmium, chromium, and copper. The bacterium was supplemented with 300 µg/mL of HM concentrations. One milliliter (CFU/ml) of fresh bacterial growth was then inoculated into media with various pH values, including acidic (pH 5.5), neutral (pH 6.5 and 7.5), and basic (pH 8.5). The experiment utilized Luria-Bertani (LB) broth medium supplemented with a carbon source (2%, w/v), including glucose, fructose, and sucrose, as well as various nitrogen sources (0.6%, w/v) such as yeast extract, peptone, ammonium sulfate ($(NH_4)_2SO_4$), and potassium nitrate ($KNO_3$). Similarly, 1 mL of bacteria was added to the growth medium and incubated for 48 h at different temperatures ranging from 25 to 45 °C to evaluate the resistance capacity of the HMRBI. After 48 h of incubation, the optical density (OD) at a wavelength of 600 nanometers (nm) was recorded for these HMRBI. This measurement indicates bacterial growth and can be used to assess the impact of pH and temperature on the resistance of isolates to HMs. Furthermore, the $OD_{600nm}$ was measured for the HMRBI after 48 h of growth, using a double-beam spectrophotometer (Model LV-T5C) (Kalsoom et al., 2023).

### 3.10. Isolation of Heavy Metal by MALDI-TOF MS

A MALDI-TOF MS test was performed at Wudase Diagnostic Center in Addis Ababa. For this test, 17 of 60 colonies of microorganisms were analyzed using a MALDI Biotyper Microflex LT (Bruker Daltonik GmbH, Germany). The instrument generated proteomic spectra, which are unique protein fingerprints. These spectra were then compared against a reference database using Bruker MALDI-TOF MS Biotyper software to identify the microorganisms and assign a confidence score to the result

Koubek et al., (2012). A biotyper score value > 2.0 indicates a species-level identification for the isolates. A score between 1.7 and 1.99 suggests identification at the genus level (Pandey et al., 2019).

### 3.11. Minimum inhibitory concentration detection

The bacterial cells grown on Luria agar medium were evaluated in the presence of different concentrations of heavy metals to determine the minimum inhibitory concentration. Salts such as $CoCl_2 \cdot 6H_2O$, $CuSO_4$, Cd $(NO_3)_2$, $K_2Cr_2O_7$, and Zn $(NO_3)_2$ were used to obtain $Co^{2+}$, $Cd^{2+}$, $Cu^{2+}$, $Cr^{3+}$, and $Zn^{2+}$ ions. Briefly, the medium composition included 10 g/L of peptone, 5 g/L of yeast extract, 5 g/L of sodium chloride, and 12 g/L of pure agar, with a wide range of heavy metal concentrations tested until isolated bacterial colonies failed to grow (Marzan et al., 2017). For this study, heavy metal concentrations ranging from 100 ppm to 1000 ppm were tested on cultures grown by streaking on an agar plate.

### 3.12.FTIR analysis of heavy metal-resistant potential bacteria isolates

FT-IR spectroscopy (JASCO, FT/IR-6600 type A) was conducted to identify a functional group in the bacterial strains that could uptake and exhibit HM resistance during biosorption. For FTIR analysis, HM-resistant bacterial isolates were cultured for 24 h at 37 ± 2 °C with 300 µg/mL of each HM, one culture without HMs as a negative control, following the specified methods (Seyma et al., 2020). The bacterial cells were centrifuged (5000 rpm, 20 min) using a centrifuge (HERMLE-Nr) to collect a pellet. The pellet was air-dried in a hotplate oven (ASI-HO-121212) for 24 h at 45-50 °C after being thoroughly washed with 1xPBS (137 mM NaCl, 2.7mM KCl, 43 mM $Na_2HPO_4$, and 1.47 mM $KH_2PO_4$) buffer solutions at pH 7.4. The dry biomass was crushed with a sterilized mortar and pestle (SKU), and 13-mm pellets were cast after mixing the powder with infrared spectroscopy-grade KBr at a 1:100 ratio. The spectrum was collected by utilizing FTIR spectroscopy (FT/IR-6600typeA) at

standard spatial resolution in the transmission mode between 4000 and 400 cm-1 at a resolution of 4 $cm^{-1}$ after scanning the background by KBr. Each sample underwent 32 scans, with spectral data collected and processed using OPUS 8.2 software. The average spectral data were regulated, and the baseline was corrected for specific bands (Deokar et al., 2013).

### 3.12. Elemental analysis and morphological study of HMRBI biomass by SEM-EDX

Scanning electron microscopy provides useful information on the shape, size, and localization within the biofilm of single bacteria, as well as the steps of the biofilm formation process concerning bacterial interaction with heavy metal concentrations. The analysis of the bacterial strains was done using scanning electron microscopy (COXEM, SEM-EDX, CX-200TM-20kV, Korea) compared with the isolates that did not contain heavy metal concentrations. The bacterial colony was picked and cultured for 24 h with 20 mg/L of each heavy metal ($Co^{+2}$, $Cu^{+2}$, $Cd^{+2}$, $Cr^{+6}$, and $Zn^{+2}$), along with a control, to study alterations in cell morphology. The bacteria were centrifuged at 6,000 rpm for 10 min to form the pellet. After centrifugation, the pellet was washed once with PBS (0.1M) to remove the heavy metal from the suspension. Then, the pellet was fixed with 2.5% (w/v) formaldehyde overnight and subsequently washed three times with 1x PBS (0.1M) buffer (pH 7.2), followed by serial dilution with 30, 50, 70, 90, and 100% ethanol. For each step, 30 minutes were allowed for the bacteria to equilibrate with the dehydrating agent. A bacterial cell was air-dried and crushed using a sterilized mortar and pestle. Finally, the morphological change was observed by SEM-EDX due to the binding of the metal ions (Sodhi et al., 2020).

### 3.13. Genomic DNA extraction for potential HMRBI

Heavy metal-resistant bacterial isolates were cultured overnight in Luria broth. The cells were then recovered by centrifugation at 12,000 rpm for 2 minutes and washed with saline Tris Buffer (pH 4.0). The growing media was discarded, and the bacterial pellets were re-suspended in 200 µL TE buffer. Approximately 18 µL of 50 mg/mL lysozyme was added and stirred thoroughly. After mixing, the pellets were incubated at 30°C for 15 to 30 min. After centrifugation at 5000 rpm for 5 min, the supernatant was removed, leaving 10-20 µL of residual liquid. The microfuge tube was filled with 10 milliliters of protease K, 300 µL of TBA buffer, and 10 µL of RNAse A. Following that, the cell pellet was pipetted into resuspension. The cell pellet was placed in a water bath and incubated for 20 min at 60 °C. The tube was inverted during incubation. After incubation, 300 µL of TBB buffer and 150 µL of 96-100% ethanol was added to the lysate. Again, the tube was inverted 20-25 times. Approximately 650 µL of lysate was put into a DNA spin column and centrifuged at 12,000 rpm for 1 min, repeated multiple times. The column was inserted into the same collecting tube and 600 µL of buffer was added. After addition, it was centrifuged at 10,000 rpm for 1 min before being ejected

through the flow. The empty DNA spin column was placed with the lid open in the same collecting tube and centrifuged at 10,000 rpm for 2 min. After placing the column in a sterile 1.5 mL Eppendorf tube, 30 µL of preheated elution buffer was added and incubated for 5 min. After 1 min of centrifugation at 10,000 rpm, the eluted pure bacterial gDNA was recovered.

### 3.14. PCR amplification of specific HMRBI genes

DNA extraction from bacterial isolates capable of thriving in high concentrations of HMs was performed using the ZymoBIOMICSTM DNA Miniprep kit, following the manufacturer's protocol. Genotyping of the HMRGs was performed using polymerase chain reaction (PCR). Gene-specific forward and reverse primers were designed or selected based on sequences reported in previously published studies and developed in this study (Ojo et al., 2023). These primers were designed to target the genes with similar annealing temperatures of 57 °C, enhancing amplification (Table 2). The PCR reaction conditions were optimized by standard methods to obtain reproducible amplification of the target gene fragments. Following PCR amplification, the resulting products were examined using agarose gel electrophoresis to verify the presence of target DNA fragments. A 1.5% agarose gel was created by dissolving agarose in TAE (Tris-Acetate-EDTA) buffer and was stained with ethidium bromide. PCR products and a molecular weight marker (a DNA ladder) were loaded into the gel wells, and electrophoresis was performed at a constant voltage until adequate separation was achieved. The separated DNA bands were visualized using the UV documentation system.

**Table 2: Specific primers used for the HMRGs amplification**

| HMs | Genes | Primer sequences | P. length | Size in bp | Annealing T °C | References |
|---|---|---|---|---|---|---|
| Cadmium | *cadD* | AATTGCAAGTTGTGGTGCAG<br>CCCACACCAGGAATTCTAGC | 20 | 155 | 57 °C | (Ojo et al., 2023). |
| Copper | *pcoC* | AATTGCAAGTTGTGGTGCAG<br>CCCACACCAGGAATTCTAGC | 20 | 333 | 57 °C | (Ojo et al., 2023). |
| Chromium | *ChrR* | TCACGCCGGAATATAACTAC<br>CGTACCCTGATCAATCACTT | 20 | 591 | 57 °C | This study |

### 3.15. Molecular identification of bacterial isolates and phylogenetic analysis

DNA extracted from the HMRBI samples was amplified using specific primers targeting the 16S rRNA gene. These primers, known as 27F and 1492R, were used to amplify a specific region of the 16S rRNA gene. The PCR amplification was conducted using a Veriti®96-well thermal cycler (Santos et al., 2019). The PCR reaction involved an initial denaturation step at 95°C for 5 min, followed by 32 cycles of denaturation, annealing, and extension. The denaturation step was performed at 95°C for 30 sec, the annealing step at 55°C for 90 sec, and the initial extension step at 72°C for 120 sec. A final extension step at 72°C for 5 min was added to ensure complete DNA synthesis. The PCR products were separated using a 1.8% agarose gel. A single, distinct band of approximately 1500 base pairs (bp) was observed on the agarose gel, confirming successful PCR amplification of the target DNA fragment. The PCR product was purified and then sent for Sanger sequencing. Both forward (27F) and reverse (1492R) primers were used to sequence the DNA, and the sequencing reaction was performed using a BDT v3.1 Cycle sequencing kit on an ABI 3500Dx Genetic Analyzer. The resulting DNA sequences were analyzed using the BLAST search tool to identify the related bacterial species. *Clustal-W* software was used to align DNA sequences of the bacterial isolates with known bacterial sequences in the GenBank database (Higgins et al., 1992). Phylogenetic analysis was conducted to understand the evolutionary relationships between the identified bacterial species. Molecular Evolutionary Genetics Analysis (MEGA11) software was used to construct a phylogenetic tree. The tree was inferred using a suitable method, such as Maximum Likelihood, and the confidence of the tree was assessed using bootstrap analysis (Tamura et al., 2021).

### 3.16. Heavy Metal Resistance Gene Study: A Computational Perspective

#### 3.16.1. Prediction for Transcriptional Start Site (TSS) and Promoter Regions

Heavy metal-resistant genes were retrieved from the National Center for Biotechnology Information (NCBI) genome search engine accessed at https://www.ncbi.nlm.nih.gov/. Fifteen protein-coding gene sequences were selected for this study after a different search (Table 18). To determine the strand orientation of the starting codons, we predicted their presence on both positive and negative strands. Transcriptional start sites (TSS) were analyzed by extracting 1kb sequences flanking the genome coordinates and formatting them as FAST files. The FAST files were then used as input for

promoter prediction using the Neural Network Promoter Prediction (NNPP) tools. About 1kb of the upstream sequences from the start codon were prepared in the FAST file format and submitted to the neural network promoter prediction version 2.2 for promoter prediction search databases retrieved at (https://www.fruitfly.org/seq_tools/promoter.html), tools to obtain a possible TSS. NNPP version 2.2 was utilized with a minimum predictive activator score value of 0.8 (the default threshold for prokaryotic cells) to minimize the false negatives. This setting was expected to reduce the number of zero counts (or undetected promoters) in the input sequences by 80% before further analysis (Reese, 2001). For NNPP output, if multiple transcriptional start sites (TSS) were predicted for a given sequence, the TSS with the highest prediction score values was selected for further analysis to ensure consistency and accuracy. The remaining TSS predictions were retained for basic comparative gene analysis but not used for the primary analysis focused on the highest-scoring TSS (Dinka & Milkesa, 2020; Grant & Stothard, 2008; Aziz et al., 2008).

### 3.16.2. Common motifs and transcriptional factor determination

MEME Suit version 5.5.2 utilized common motif identification and exploration, motif alignment investigation, motif scanning, and motif comparison. Using MEME Suite accessed via the National Biomedical Computational Resource search engine, promoter sequences that met specific criteria were analyzed to identify common motifs (Overbeek et al., 2005). The common candidate motif was identified as the binding sites of transcriptional factors to regulate HMR gene expression (Vázquez-Núñez et al., 2020). The statistically significant candidate motifs predicted by MEME-Suite in the sequence were selected and compared further. Then, the genes found by MEME-suit (known as motifs) that matched the motifs with the lowest e-values (fixed-length and repetitive) were put into a TOMTOM online database to retrieve their corresponding transcriptional factors. This method was used to identify consensus sequences (putative binding sites) of transcription factors that are thought to affect different HMR gene expression steps. Nevertheless, the motif distribution menu's fundamental desired characteristics for searching were outlined before starting to search for the sequences chosen. Including motif distribution, motif positions, the presence of either none or one occurrence per sequence, or multiple occurrences per sequence.

Additionally, it was set at default for the number of motifs and persistent motif width (6-50 bps). After the MEME searches finished, I linked to the MEME HTML output, the search results page. It is

a vital preliminary perspective on integers (i.e., expected value) (e-value) in this stage. As with previously reported studies, the smaller the e-value, the better the result (Vázquez-Núñez et al., 2020). In the MEME HTML output, at the bottom, one or more possible motifs were given for further study. A transcriptional factor common to most was identified using the TOMTOM Web server database tool. The sequences were found that correspond to the top candidate motifs of the different transcription factors, using the imported gene sequences. LOGOS as part of the TOMTOM output. Alignment of candidate motif and TF with p-value and q-value (false discovery rate) links back to the original parent transcription database matches in TOMTOM output (Vázquez-Núñez et al., 2020; Kumar et al., 2004).

### 3.16.3. Comparative genome analysis of *C. gilardii* CR3 genome by Prokka & RAST

The comparative genome analysis of *C. gilardii* CR3 (CP010516.1), *C. metallidurans* CH34 (NC_007973.1), *C. nantongensis* X1 (CP014844.1), *Cupriavidus* ISTL7 (CP066227.1), *Cupriavidus* MP-37 (NZ_CP085344.1), and *Cupriavidus gilardii* WM02 (CP104386.1) for the HMR was performed by using Rapid Annotation utilizing Subsystem Technology (RAST) online engine accessed through (https://rast.nmpdr.org/rast.cgi) after being retrieved from the NCBI database. The Rapid Annotation using Subsystems Technology (RAST) service, a platform for prokaryotic cell genome annotation, was employed to re-annotate the genomes and predict genes used in HMR (Aziz et al., 2008). A circular genome analysis of *C. gilardii* CR3 was conducted using CGView (Circular Genomes Viewer). CGView is a Java application and library that facilitates the construction of high-quality, zoomable maps of circular genomes, allowing for details visualization & analysis of genome features (Grant & Stothard, 2008). Further characterization was performed using SEED, as a subsystem category distribution approach, to analyze gene expression and function. The approach classifies and compares genes based on their involvement in biological processes and pathways defined in the SEED database (Overbeek et al., 2005).

### 3.16.4. Comparative genome analysis of *C. gilardii* CR3 by using OAT Software

This study employed the online Orthologous Average Nucleotide Identity Software Tool (OAT) to determine the OrthoANI values of 16S rRNA sequences (Chalita et al., 2024). The sequences were obtained from the NCBI database and analyzed by the EziBio Cloud genomic database for further confirmation of the selected strains (Lee et al., 2016). The *C. gilardii* CR3 CP010516.1) was

compared with other closely related *C. metallidurans* CH34 (NC_007973.1), *Cupriavidus* ISTL7 (CP066227.1), *Cupriavidus gilardii* WM02 (CP104386.1), *C. nantongensis* X1 (CP014844.1), *Cupriavidus* ISTL7 (CP066227.1), and *Cupriavidus* MP-37 (NZ_CP085344.1), and *P. putida* PD584 was used as an outgroup for the comparisons.

### 3.17. Statistical analysis

Measurement was taken in triplicate for each scenario to observe and evaluate bacterial growth in the presence of various HM concentrations. Statistical analysis included the calculation of the mean and standard deviation for all measured parameters. Differences in bacterial growth rate across the various heavy metal concentrations were determined using a One-Way ANOVA. Results were considered statistically significant when the p-value $\leq 0.05$. Data analysis was performed using Microsoft Excel 2019, OriginPro 2017, GenStat version 2017, and SPSS version 26

# 4. RESULTS AND DISCUSSIONS

## 4.1. Assessing HM pollution and bioremediation potential for bacterial isolates in industrial effluents of Mojo and Bishoftu, Ethiopia

### 4.1.1. Heavy metal assessment from Bishoftu eastern industrial zone (BEIZ) discharges

Heavy metals such as $Co^{+2}$, $Cu^{+2}$, $Cd^{+2}$, $Fe^{+2}$, $Mn^{+2}$, $Ni^{+2}$, and $Zn^{+2}$ were assessed in Bishoftu soil waste using AAS. The analysis revealed that, except for $Cr^{+6}$ and $Pb^{+2}$, the concentration of all detected HMs significantly exceeded the safety limits established by the WHO (WHO, 2017). The evidence in Table 3 provides strong confirmation that the environment was polluted by industrial effluents. The source of this pollution is inferred to be the industrial waste that has been released into the environment. The analysis for $Co^{+2}$ concentrations in the soil samples ranged between 0.189 ± 0.05 mg/kg (BSS-6) and 0.108 ± 0.05 mg/kg (BSS-4). These values were documented in Table 3, which provides a comprehensive overview of HM concentrations detected in the soil waste of the study area. The high concentration of cobalt in the studied area was above its natural threshold. This is primarily due to the anthropogenic activities, especially those related to energy, battery, and electronic manufacturing industries, Dobre et al., (2024). Cobalt can contaminate soil and water bodies like lakes, groundwater, and rivers, adversely impacting aquatic ecosystems and potentially harming aquatic living organisms. This contamination can enter the food chain by consuming contaminated aquatic life (Chatterjee et al., 2020).

**Table 3: The HM concentration measurements (mg/kg) against the Bishoftu soil samples using the AAS method**

| Sampling Sites | Heavy metals | | | | | | | |
|---|---|---|---|---|---|---|---|---|
| | **Co** | **Cu** | **Cd** | **Cr/Pb** | **Ni** | **Mn** | **Zn** | **Fe** |
| BSS-1 | $0.187 \pm 0.05^{b}$ | $0.588 \pm 0.05^{d}$ | $0.026 \pm 0.01^{a}$ | ND | $0.607 \pm 0.13^{a}$ | $6.518 \pm 0.10^{f}$ | $0.830 \pm 0.01^{b}$ | $2.199 \pm 0.04^{b}$ |
| BSS-2 | $0.167 \pm 0.08^{b}$ | $0.849 \pm 0.03^{e}$ | $0.044 \pm 0.02^{ab}$ | ND | $0.830 \pm 0.13^{ab}$ | $5.399 \pm 0.05^{e}$ | $0.843 \pm 0.04^{b}$ | $4.245 \pm 0.41^{d}$ |
| BSS-3 | $0.183 \pm 0.05^{b}$ | $0.371 \pm 0.03^{ab}$ | $0.040 \pm 0.01^{a}$ | ND | $0.681 \pm 0.13^{ab}$ | $3.661 \pm 0.06^{c}$ | $0.437 \pm 0.01^{a}$ | $1.442 \pm 0.04^{a}$ |
| BSS-4 | $0.108 \pm 0.05^{a}$ | $0.400 \pm 0.04^{bc}$ | $0.062 \pm 0.03^{b}$ | ND | $0.978 \pm 0.22^{ab}$ | $3.208 \pm 0.02^{b}$ | $0.419 \pm 0.05^{a}$ | $2.250 \pm 0.08^{b}$ |
| BSS-5 | $0.179 \pm 0.05^{b}$ | $0.487 \pm 0.04^{cd}$ | $0.044 \pm 0.00^{ab}$ | ND | $0.830 \pm 0.13^{ab}$ | $4.065 \pm 0.10^{d}$ | $0.419 \pm 0.01^{a}$ | $3.336 \pm 0.11^{c}$ |
| BSS-6 | $0.189 \pm 0.05^{b}$ | $0.284 \pm 0.03^{a}$ | $0.037 \pm 0.02^{a}$ | ND | $1.052 \pm 0.13^{b}$ | $2.899 \pm 0.02^{a}$ | $0.479 \pm 0.01^{a}$ | $1.215 \pm 0.04^{a}$ |
| CV% | 7.9% | 7.4% | 16.3% | ND | 17.9% | 1.6% | 4.4% | 7.4% |
| Ave. mg/kg | 0.176 | 0.497 | 0.038 | ND | 0.830 | 4.292 | 0.57 | 2.448 |
| WHO | 0.010 | 2.0 | 0.003 | 0.1 | 0.05 | 0.01 | - | - |
| $P \leq 0.05$ | 0.851 | 0.953 | 0.894 | ND | 0.473 | 0.996 | 0.969 | 0.960 |

The values represent the means of three independent experiments carried out in triplicate with standard deviations. ND is not detected.

Key: CV% = Coefficient variation percentage, Ave = average mean; the same letters down the column do not significantly differ between the means, where BSS-Bishoftu Soil Sample

Copper pollution can arise from various sources, including metal manufacturing industries, copper-based pesticides, and fungicides (Panagos et al., 2018). This study found that copper concentration in soil samples ranged from 0.284 ± 0.03 to 0.849 ± 0.03 mg/kg as detailed in (Table 3). While these levels are below the WHO standards of 2.0 mg/kg (WHO, 2017) they indicate copper contamination within the study area in some extents. The minimum copper concentration was detected against BSS-6 soil samples, while the maximum was perceived for BSS-2 samples (Table 3). Exceeding permissible copper levels can affect the environment, including soil, microorganisms, nutrient cycling, and plant growth. Previous researchers have demonstrated that excessive copper can inhibit plant growth, development, and finally cause death (Panagos et al., 2018). Given the use of released wastewater for irrigation, higher copper bioaccumulation is anticipated in fruits and vegetables (Amin et al., 2013) posing potential health risks to consumers. Moreover, excessive copper bioaccumulation in aquatic organisms such as fish can enter the human food chain and present significant health (Ali & Khan, 2018). The continuous monitoring of irrigation water quality and copper levels in the study is important to mitigate the potential long-term and environmental risks.

Cadmium (Cd) is a significant environmental pollutant that can affect the environment and human health. It enters the environment through various human and industrial activities, including fertilizer usage, pigment, and plastic manufacturing (WHO, 2017). The measured $Cd^{+2}$ concentration (Table 3) in the study area exceeded the permissible limits set by the WHO standards (WHO, 2011). Studies have shown that $Cd^{+2}$ concentrations ranged from 0.026 ± 0.01 to 0.062 ± 0.03 mg/kg. These concentrations exceed the safety limits established by WHO (WHO, 2017). The maximum $Cd^{+2}$ concentration was observed at site BBS-4, while the minimum was recorded at site BBS-1, as depicted in Table 3. Similarly, nickel levels were detected in a range of 1.052 ± 0.13 to 0.607 ± 0.13mg/kg in soil samples collected from industrially polluted areas (Bishoftu).

The BSS-6 and BSS-1 soil samples exhibited the maximum (1.052 ± 0.13 mg/kg) and minimum (0.607 ± 0.13 mg/kg) nickel concentrations, respectively (Table 3). These results also exceeded the permissible limits set by WHO (WHO, 2017). These findings suggested that contamination with copper and nickel was most pronounced in soil samples collected from the study areas, which were affected by the discharged wastewater from the industries. The study demonstrated that the measured

levels of all HMs exceeded the standard set by WHO (Table 3). A manganese (Mn) concentration in soil samples ranged from 2.899 ± 0.02 to 6.518 ± 0.10 mg/kg for BSS-1 to BSS-6 sites.

The study revealed the maximum mean concentrations due to Mn (6.518 ± 0.10 mg/kg, BSS-1), $Zn^{+2}$ (0.843 ± 0.04 mg/kg, BSS-2), and $Fe^{+2}$ (4.245 ± 0.41 mg/kg, BSS-2) for all collected soil samples. Our study confirms the similarities with the study of (Lemessa et al., 2022) which assessed HM concentrations in soil, vegetables, and fruit at the Lemi Industrial Park effluent discharge. Particularly, their assessment of the irrigated land found maximum concentration of $Cr^{+6}$ (0.676 mg/kg) and $Cd^{+2}$ (0.0246 mg/kg), respectively. The p-values for each treatment were greater than 0.05 across the group, indicating that there were insignificant differences observed in the soil heavy metal analysis as presented in (Table 3) (Appendix Table 1).

The concentration of $Ni^{+2}$ in the analyzed soil samples varied significantly across different sampling sites. The maximum concentration of Ni was found at location BSS-6 (1.052 ± 0.13 mg/kg), while the minimum was recorded at BSS-4 (0.607 ± 0.13 mg/kg). This variation in $Ni^{+2}$ levels suggests potential differences in soil contamination due to industrial effluents in the study area (Table 3). Similarly, the concentration of $Co^{+2}$ was also assessed in the eastern industrial zone, revealing notable variation across different sampling sites. The maximum concentration of $Co^{+2}$ was detected at BSS-6 (0.189 ± 0.05), indicating a potential hotspot of industrial contamination. In contrast, the minimum concentration of $Co^{+2}$ was recorded at BSS-4 (0.108 ± 0.05), suggesting relatively minimal $Co^{+2}$ deposition in that area, as depicted in (Table 3). These variations due to $Co^{+2}$ and $Ni^{+2}$ concentration may be attributed to several factors, including the closeness of the sampling sites to the pollution sources, and/or the direct discharge of the wastewater from industries into the agricultural lands during irrigation processes.

### 4.1.2. HM assessment from Mojo Tannery effluent discharges (MTED)

The analysis of the wastewater samples collected from MTED revealed the highest Cr concentration compared to the others. The MWWS-2 sample, the closest to Mojo Tannery, had the highest $Cr^{+6}$ content of 4.133 ± 0.42 mg/kg, whereas the MWWS-6 sample had the lowest $Cr^{+6}$ concentration (3.276 ± 0.16 mg/kg), as shown in (Table 4). The HM levels were in the descending order of $Cr^{+6}$ >$Fe^{+2}$ >$Zn^{+2}$ >$Mn^{+2}$ >$Cd^{+2}$. The findings underscored that $Cr^{+6}$

concentrations were higher in samples obtained closest to the factories, as shown in the samples with 4.038 ± 0.16 mg/kg (MWWS-1) and stagnant water, 4.133 ± 0.42 mg/kg (MWWS-2) as indicated in (Table 4). As the distance from the Mojo Tannery factory increases, the concentration of $Cr^{+6}$ gradually decreases, suggesting that it may be sinking into the soil or becoming diluted. This study demonstrates that the $Cr^{+6}$ concentrations surpass the acceptable standard limits by the WHO, indicating a need for clear action (WHO, 2017).

The $Cd^{+2}$ concentration level in all wastewater was assessed, and the result indicated that it exceeds WHO standards, as perceived in (Table 4). The data indicated that the maximum and minimum $Cd^{+2}$ concentrations were 0.253 ± 0.03 (MWWS-5) and 0.231 ± 0.01 mg/kg (MWWS-1). Additionally, the data revealed that the MWWS-3, MWWS-4, and MWWS-6 exhibited identical $Cd^{+2}$ concentrations, as presented in (Table 4). Manganese (Mn) concentrations in the wastewater were evaluated, revealing levels ranging from 0.930 ± 0.02 mg/kg (MWWS-6) to 0.329 ± 0.03 mg/kg (MWWS-4). The maximum Mn concentration was detected at 0.930 ± 0.02 mg/kg (MWWS-6), and the minimum value was recorded at 0.329 ± 0.03 mg/kg (MWWS-4) (Table 4).

Further analysis focused on $Zn^{+2}$ and $Fe^{+2}$ concentrations in the Mojo Tannery wastewater samples. The maximum $Zn^{+2}$ concentration (1.328 ± 0.05mg/kg) was obtained from the MWWS-2 sample, whereas the minimum $Zn^{+2}$ concentration (0.423 ± 0.04 mg/kg) was recorded from MWWS-4, as indicated in Table 4. For $Fe^{+2}$, the maximum concentration was detected against the MWWS-5 (3.585 ± 0.12 mg/kg) site, and the minimum concentration (1.290 ± 0.05 mg/kg) was recorded against the MWWS-6 site (Table 4). It was noted that no HMs, such as $Co^{+2}$, $Cu^{+2}$, $Ni^{+2}$, and $Pb^{+2}$, were detected in the wastewater effluent from the Mojo Tannery (Table 4). The assessment of HM contamination in wastewater samples revealed a significant difference observed in all treatments at ($P < 0.05$), as presented in (Table 2) (Appendix Table 2), except for Ni treatment, which was varied among the other treatments. In general, concentration levels could have a substantial influence on local communities, indicating the presence of industrial pollution in the studied location. The relationship between the levels and possible industrial activity necessitates a careful investigation of surrounding facilities and waste disposal practices.

The Mn concentration in Mojo Tannery wastewater ranges between 0.930 ± 0.02 ml/L (MWWS-6) and 0.329±0.03 ml/L (MWWS-4). The maximum outcome was detected at 0.930 ± 0.02 ml/L (MWWS-6), and the minimum was recorded at 0.329 ± 0.03 ml/L (MWWS-5). Further analysis was conducted on $Zn^{+2}$ and $Fe^{+2}$. The study revealed that the maximum concentration of $Zn^{+2}$ and $Fe^{+2}$ contents in effluent discharges of wastewater samples was 1.328±0.05 ml/L and 3.585±0.012 ml/L, respectively. The maximum (1.328 ± 0.05 ml/L) and minimum (0.423± 0.01 ml/L) concentrations of $Zn^{+2}$ were recorded for MWWS-2 and MWWS-4. The Fe concentration was measured to be 3.585 ± 0.012 ml/L and 1.290 ± 0.05 ml/L for MWWS-5 and MWWS-6, respectively, as detailed in Table 4. However, certain HMs such as $Co^{+2}$, $Cu^{+2}$, $Ni^{+2}$, and $Pb^{+2}$ were not detected in the Mojo tannery industry wastewater effluents (Table 4). These metals were not detected in the wastewater discharge, a result likely due to the analytical techniques' high method detection limit for the Mojo tannery wastewater (Reda, 2016). The metals are not essential or major reagents in the core pre-tanning processes, which primarily rely on high concentrations of chromium salts. Another reason, their presence, if any, would be minimal, stemming only from trace impurities in other chemicals formed in a specialized metal complex for coloring. The finding suggests that the detection methods employed were reliable and effective in accurately identifying the various constituents of the wastewater. This effectiveness is crucial for ensuring environmental compliance and assessing the potential impacts of Mojo tannery's operations on the local water resources. A statistical analysis of the Mojo industrial wastewater heavy metal treatments found insignificant differences observed. The p-values for all treatments were greater than 0.05, indicating that at $p<0.05$ had a statistically insignificant effects within the group as indicated in Table 4 (Appendix Table 2).

**Table 4: The Heavy Metal Concentration in the Effluents of Mojo Tannery by using the AAS Method**

| Sampling Sites | Heavy metals | | | | | | |
|---|---|---|---|---|---|---|---|
| | **Co/Cu** | **Cd** | **Cr** | **Pb/Ni** | **Mn** | **Zn** | **Fe** |
| MWWS-1 | ND | $0.231 \pm 0.01^{a}$ | $4.038 \pm 0.16^{ab}$ | ND | $0.353 \pm 0.02^{a}$ | $0.804 \pm 0.01^{b}$ | $2.355 \pm 0.05^{c}$ |
| MWWS-2 | ND | $0.238 \pm 0.01^{a}$ | $4.133 \pm 0.42^{b}$ | ND | $0.389 \pm 0.02^{ab}$ | $1.328 \pm 0.05^{c}$ | $3.202 \pm 0.05^{d}$ |
| MWWS-3 | ND | $0.246 \pm 0.02^{a}$ | $3.657 \pm 0.28^{ab}$ | ND | $0.437 \pm 0.03^{ab}$ | $0.440 \pm 0.01^{a}$ | $1.536 \pm 0.05^{b}$ |
| MWWS-4 | ND | $0.246 \pm 0.02^{a}$ | $3.562 \pm 0.16^{ab}$ | ND | $0.329 \pm 0.03^{a}$ | $0.423 \pm 0.04^{a}$ | $2.410 \pm 0.08^{c}$ |
| MWWS-5 | ND | $0.253 \pm 0.03^{a}$ | $3.467 \pm 0.42^{ab}$ | ND | $0.702 \pm 0.03^{bc}$ | $0.423 \pm 0.01$ | $3.585 \pm 0.12^{e}$ |
| MWWS-6 | ND | $0.246 \pm 0.02^{a}$ | $3.276 \pm 0.16^{a}$ | ND | $0.930 \pm 0.02^{c}$ | $0.478 \pm 0.01^{a}$ | $1.290 \pm 0.05^{a}$ |
| CV% | - | 8.2% | 8.2% | - | 3.5% | 4.7% | 3.0% |
| Ave. mL/L | - | 0.243 | 3.689 | - | 0.523 | 0.649 | 2.396 |
| WHO | 0.01/2.0 | 0.003 | 0.05 | 0.01/0.07 | 0.01 | 0.01 | 0.05 - 50 |
| $P \leq 0.05$ | ND | 0.931 | 0.446 | ND | 0.884 | 0.995 | 0.994 |

The values represent the means of three independent experiments carried out in triplicate with standard deviations. ND is not detected.

Key: CV% = Coefficient variation percentage, ave = average mean; the same letters down the column do not significantly differ between the means, where MWWS-Mojo Wastewater Sample

### 4.1.3. Soil Organic Matter properties of soil against Bishoftu (BEIZ)

The assessment of soil organic matter against Bishoftu industrial effluents is a crucial step in understanding the environmental impact of industrial activities in the study area. Accordingly, the results of soil organic matter collected from the BEIZ are presented in Table 5. The nitrogen content in the Bishoftu industrial effluents was between 0.56 ± 0.140 and 1.04 ± 0.200 mg/kg, as shown in Table 5. This study revealed the maximum (1.040 ± 0.200 mg/kg) nitrogen concentration for BSS-2 and the minimum (0.560 ± 0.140 mg/kg) for BSS-6 in Table 5. Assessing the impacts of industrial effluents on soil organic matter is essential for sustainable development. It helps identify potential risks, implement mitigation measures, and ensure the long-term health of the soil and environmental ecosystem (Lemessa et al., 2022). High concentrations of minerals such as N and P in water can negatively affect the water quality in several ways. The measured values showed a statistically significant difference at ($P \leq 0.05$). The nitrogen level at all sampling sites except BSS-6 exceeded the UNU-EHS/UNEP (2013) recommended limit of <0.7mg/kg for ecosystem health (Liu et al., 2018).

The carbon content of the Bishoftu industrial effluent was found to be maximum at BSS-1 (16.19 ± 0.120) and lowest at BSS-6 (6.76 ± 0.030), as shown in (Table 5), indicating a difference in carbon levels across effluent samples taken from various locations surrounding the Bishoftu Industrial Area. This is due to the diverse industrial base in the study area, such as textile and food processing, which may produce effluents with various carbon sources polluting the surroundings. The maximum in BSS-1 could be closer to the industry that emits more carbon compared to the rest of the sampling points. Similarly, maximum (18.40 ± 0.350) and minimum (8.79 ± 1.930) P were detected against BSS-5. It was suggested that BSS-5 has likely a mixture of industries that discharge wastewater with various P content. It might also be close to an industry that releases a high amount of phosphorus. The pH of the industrial soil waste detected ranged between 7.050 and 8.123. The maximum (8.123 ± 0.042) and minimum (7.050 ± 0.010) pH values were documented for BSS-6 and BSS-2, respectively, as observed in Table 5. Bishoftu is presumably home to a variety of industries, each of which discharges wastewater with varying pH levels. BSS-6 may be closer to an industrial process producing a higher alkaline effluent.

**Table 5: The Physiochemical Properties of Soil Samples Determined from BEIZ**

| Sampling sites | Organic Matter Contents | | | |
|---|---|---|---|---|
| | pH | Nitrogen (%) | Carbon (%) | Phosphorus (ppm) |
| BSS-1 | $7.583 \pm 0.106^{c}$ | $0.907 \pm 0.190^{ab}$ | $16.19 \pm 0.120^{c}$ | $8.79 \pm 1.930^{a}$ |
| BSS-2 | $7.050 \pm 0.010^{a}$ | $1.040 \pm 0.200^{b}$ | $14.17 \pm 0.180^{d}$ | $12.27 \pm 2.580^{ab}$ |
| BSS-3 | $7.733 \pm 0.021^{c}$ | $0.700 \pm 0.140^{ab}$ | $9.88 \pm 0.130^{ab}$ | $12.30 \pm 0.310^{ab}$ |
| BSS-4 | $7.343 \pm 0.070^{b}$ | $0.770 \pm 0.070^{ab}$ | $11.38 \pm 0.110^{b}$ | $14.78 \pm 0.880^{bc}$ |
| BSS-5 | $7.240 \pm 0.030^{b}$ | $0.700 \pm 0.140^{ab}$ | $9.10 \pm 0.050^{ab}$ | $18.40 \pm 0.350^{c}$ |
| BSS-6 | $8.123 \pm 0.042^{d}$ | $0.560 \pm 0.140^{a}$ | $6.76 \pm 0.030^{a}$ | $12.08 \pm 0.810^{ab}$ |
| CV% | 0.8% | 19.5% | 8.5% | 10.8% |
| Ave. mean mg/kg | 7.512 | 0.779 | 1.125 | 13.103 |
| $P \leq 0.05$ | 0.987 | 0.028 | <0.001 | <0.001 |

**The values represent the means of three independent experiments carried out in triplicate with standard deviations. CV% = Coefficient variation percentage, ave = average mean; the same letters down the column do not significantly differ between the means**

HM contamination of water and soil due to industrial activities is one of the most significant environmental issues, as it causes detrimental effects on ecosystems and human health. Analysis of the physicochemical properties of the soil and water samples revealed that the pH of all the studied sites ranged between 5.6 and 7.2, while that of the soil samples ranged between 7.05 and 8.123. The pH of soil and water from wastewater effluents was found to be acidic and basic, respectively, as reported by (Ojo et al., 2023) in gold mining areas. The increasing alkalinity of the soil sample in the studied area suggests that an accumulation of HMs, leading to environmental contamination (Ridene et al., 2023).

Both the Eastern Industry Zone and Mojo tannery have big industrial hubs in East Shewa, Ethiopia. These industries play a pivotal role in driving the region's economic development, producing a diverse array of goods, including textiles, leather, and chemicals (Bekele Bahiru, 2021), leading to pollution caused by HMs. Yet such rapid industrialization has come at the great environmental cost of largely HM-polluted soil and water. Currently, these regions are facing pollution mainly due to industrial discharges, which are usually released with little or no

wastewater treatment. Scientists, policymakers, and local communities have become increasingly concerned about the environmental and health effects of this contamination (Lemessa et al., 2022). Some of the main reasons for pollution in the Eastern Industrial Zone and Mojo are the strict enforcement of environmental regulations. Moreover, the swift industrial expansions in these regions usually outpace the development of sustainable waste management systems. Tanning companies, for example, in Mojo, discharge an extremely high amount of $Cr^{+6}$, while textile and chemical factories discharge dyes, solvents, heavy metals like $Pb^{+2}$ and $Cd^{+2}$, etc. These pollutants end up in the nearby soil and bodies of water, slowly infiltrating the surrounding farmland and the people living nearby.

### 4.1.4. Isolation and morphological characterization of the HMRBI

In this study, 120 cultured HMRBI (60 isolates not presented in the document) were obtained from industrial effluent samples from Bishoftu Eastern Industrial Zone and Mojo Tannery waste discharges. The isolates were studied based on their morphological and biochemical characteristics. Many of these isolates were classified as Gram-negative bacteria. Morphological analysis revealed that most bacteria had a rod-shaped structure, while a smaller proportion of the isolates displayed spherical shapes. The detailed morphological and biochemical characteristics of these isolates, including their shapes, Gram-staining results, and other relevant traits, are summarized in the Appendix Tables 10 and 11. The present study obtained heavy metal-resistant bacterial isolates with varying biochemical characteristics. There were 30 (25%) Gram-positive bacteria identified among the 120 tested for biochemical characterization, while 90 (75%) Gram-negative isolates were listed in the Appendix Tables 10 and 11. Bacterial isolates were obtained and characterized from industrial effluent discharges in the Bishoftu Eastern Industrial Zone and the Mojo Tannery.

The HMRBI, which exhibit diverse characteristic features, were screened from industrial effluent that discharges in two significant industrial sites: the Bishoftu Eastern Industrial Zone and the Mojo Tannery. The data analysis further revealed that most HMRBIs were rod-shaped, varying in size between small and large forms. Most of the rod-like bacteria were well adapted and had survival ability in metal-polluted effluent environments. Their survival abilities are attributed to a variety of resistance mechanisms that allow them to detoxify or tolerate high concentrations of

heavy metals (Nnaji et al., 2024). The remaining isolates were non-round, suggesting some morphological diversity in the microbial population in these industrial effluents. This morphological variation could indicate the diverse adaptive strategies used to survive in the harsh environmental conditions caused by heavy metal contamination (Mathivanan et al., 2021). These bacteria are often used in bioremediation, a cost-effective and eco-friendly approach to cleansing up contaminated sites.

### 4.1.5. Biochemical test of HMRBI from BEIZ and Mojo Tannery effluents

About 120 pure cultured HMRBIs were identified and characterized from industrial effluent samples collected from Mojo and Bishoftu industrial effluents. Based on biochemical tests, some of them employed glucose, lactose, and sucrose as carbon sources, some of them are positive for indole, methyl red, starch, triple sugars, hydrogen sulfide, urease, VPK, gelatin hydrolysis, catalase, motility, and citrate utilization test (Appendix Tables 10 and 11). As indicated in Appendix Tables 10 and 11. A notable distinction in bacterial characteristics was observed; while some isolates were determined to be Gram-positive, most heavy metal-resistant bacterial isolates were identified as Gram-negative bacteria. Moreover, morphological analysis revealed that most of the bacteria displayed a rod-shaped (*Bacilli*) structure, whereas a smaller portion of the isolates exhibited spherical (*cocci*) shapes. The present study obtained HMRBI with varying biochemical characteristics. This study emphasizes the diversity of bacterial isolates found in industrial effluents and their potential applications in bioremediation, specifically for mitigating heavy metal contamination (Liang et al., 2025).

The biochemical tests of potential HMRBI are presented in (Appendix Tables 10 and 11). A biochemical test is commonly used to identify and characterize bacteria based on their metabolic activities. Hence, for fifteen parameters of HMRBI, the biochemical tests, namely, Gram-staining (Figure 4), indole test, methyl red, starch, triple sugars (glucose, lactose, and sucrose), hydrogen sulfide, urease, VPK, gelatin hydrolysis, catalase, motility, and citrate utilization test were presented in (Appendix Tables 10 and 11). The data revealed that all heavy metal-resistant bacterial isolates had positive results in motility, urease, and catalase tests. However, not all isolates show a similar phenomenon in motility, urease, and catalase tests. The results showed that about 26.67% of the isolates revealed Gram-positive, while 73.33% revealed Gram-negative

in (Appendix Tables 10 and 11). In addition, the motility of the isolates was evaluated. All HMRBI were motile, as can be observed in (Appendix Tables 10 and 11).

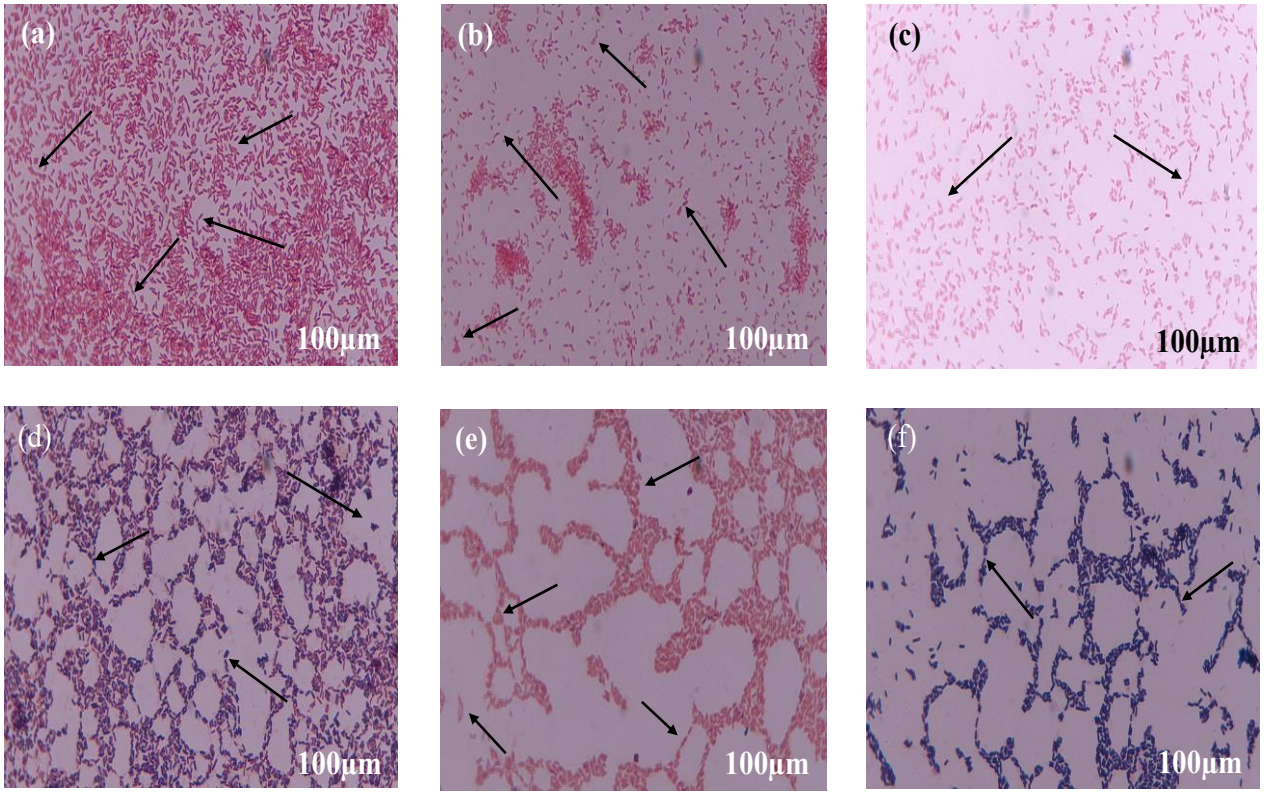


**Figure 4: (a) *P. benzoelyticum*-HMRBI-1, which is a Gram-negative HMRBI with 79.27% biological efficiency for heavy metal removal. (b) *Citrobacter* sp. HMRBI-5, which is a Gram-negative HMRBI with 85.21% % biodegradability efficiency. (c) *Klebsiella* spp.-HMRBI-14, a Gram-negative bacterium with 89.74% biodegradability efficiency (d), *B. pumilis-HMRBI-10,* a Gram-positive bacterium with 66.65% biodegradability efficiency (e), *A. hydrophila*-HMRBI-12, a Gram-negative and (f) *E. aurantiacum*-HMRBI-7, a Gram-positive bacterium with 65.13% of isolated heavy metal bioremediation bacteria viewed under 100x magnifications.**

The morphological features of HMRBI were characterized by Gram staining, and the microscopic appearance was sketched using 100x magnification, as shown in (Figures 4a-f). Data showed that the large microorganisms inhibited the harsh environment of the HM-polluted environment. In this group of isolates, *P. benzoelyticum*, *Citrobacter* spp., *P. putida*, *B. pumilus*, *A. hydrophila*, and *Exigubacterium aurantiacum* were among the best potential HM bioremediation microorganisms. Consistent with the overall findings of this study, most of the

bacterial isolates subjected to Gram staining were definitively characterized as Gram-negative. Consistent with the overall findings of this study, most of the bacterial isolates subjected to Gram staining were definitively characterized as Gram-negative. (74%) Conversely, Gram-positive bacteria represented 27% of the isolates. Further, the data revealed that the presence of Gram-positive and Gram-negative bacteria in a polluted environment shows the complexity and robustness of microbial communities. Their metabolic activities together can be used to improve the degradation ability of pollutants like HMs, with Gram-positive bacteria usually initiating the degradation of larger compounds, larger molecules, and Gram-negative bacteria degrading intermediate contaminants. This interaction is critical for the natural attenuation of contaminants as a means of microbial bioremediation (Qattan, 2025).

### 4.1.6. Identification of isolated HMRBI by MALDI-TOF MS

The present study obtained heavy metal-resistant bacterial isolates with varying biochemical characteristics. The isolates were identified by MALDI-TOF MS based on their unique protein spectra, indicating that they were from different species of bacteria. These include *P. putida*, *Exiguobacterium aurantiacum*, *P. mosselii*, *B. pumilus*, *Aeromonas hydrophila*, *P. mendocina*, *P. oleovorans*, *Delftia acidovorans*, and *P. plecoglossicida*. Among the MALDTO-MS-assisted isolates, we found 8 (47.06%) *Pseudomonas* spp., 2 (11.76%) *Bacillus* spp., 3 (17.64%) *D. acidovorans,* and 1 (5.88%) each of *Exiguobacterium auranticum* and *A. hydrophila*. The *Pseudomonas* sp. was among the dominant species obtained from the heavy metal-resistant bacteria isolates from the discharges of Bishoftu and Mojo industrial effluent, as shown in Table 6, followed by *D. acidovorans* 3 (17.64%), *Bacillus* spp. 2 (11.76%), *E. auranticum,* and *A. hydrophila* 1 (5.88 %). The detailed identification and classification of these isolates are summarized in Table 6. This analysis underscores the utility of MALDI-TOF MS in differentiating microbial species by their protein fingerprints, enabling precise taxonomic identification. The bacterial isolates, exhibiting diverse characteristics, were obtained from industrial effluent discharges in two significant industrial sites: the Bishoftu Eastern Industrial Zone and the Mojo Tannery. The predominance of bacterial isolates among all identified microorganisms highlights their potential use for bioremediation research based on the heavy metal utilization efficiency assay in Table 12.

**Table 6: MALDI-TOF MS protein profile for HMRBI species obtained from Bishoftu and Mojo Tannery Industrial effluents**

| S. N | Sample Id | Genus | Closest species | LSV | Gram r/n | Morphology | Motility | Most likely isolates |
|---|---|---|---|---|---|---|---|---|
| 1. | HMRBI-1 | unidentified | unidentified | 1.44 | -ve | Rode shape | Motile | HMRBI-1 |
| 2. | HMRBI-3 | *Pseudomonas* | *putida* | 1.86 | -ve | Rode shape | Motile | *Pseudomonas* sp. HMRBI-3 |
| 3. | HMRBI-4 | *Pseudomonas* | *putida* | 2.03 | -ve | Rode shape | Motile | *P. putida* HMRBI-4 |
| 4. | HMRBI-5 | unidentified | unidentified | 1.69 | -ve | Rode shape | Motile | HMRBI-5 |
| 5. | HMRBI-7 | *Exiguobacterium* | *aurantiacum* | 2.32 | +ve | Irregular shape | Motile | *E. aurantiacum* HRMWI-7 |
| 6. | HMRBI-8 | *Pseudomonas* | *mosselii* | 2.26 | -ve | Rode shape | Motile | *P. mosselii* HRMWI-8 |
| 7. | HMRBI-10 | *Bacillus* | *pumilus* | 2.20 | +ve | Rod shape | Motile | *B. pumilus* HRMWI-10 |
| 8. | HMRBI-11 | *Bacillus* | *pumilus* | 1.88 | +ve | Rod shape | Motile | *Bacillus* sp. HRMWI-11 |
| 9. | HMRBI-12 | *Aeromonas* | *hydrophila* | 2.04 | -ve | Rode shape | Motile | *A. hydrophila* HRMWI-12 |
| 10. | HMRBI-13 | *Pseudomonas* | *mendocina* | 1.82 | -ve | Rode shape | Motile | *Pseudomonas* sp. HRMWI-13 |
| 11. | HMRBI-14 | *Pseudomonas* | *oleovorans* | 1.73 | -ve | Rode shape | Motile | *Pseudomonas* sp. HRMWI-14 |
| 12. | HMRBI-15 | *Pseudomonas* | *mosselii* | 2.03 | -ve | Rode shape | Motile | *P. mosselii* HRMWI-15 |
| 13. | HMRBI-16 | *Delftia* | *acidovorans* | 2.11 | -ve | Rode shape | Motile | *D. acidovorans* HRMWI-16 |
| 14. | HMRBI-17 | *Delftia* | *acidovorans* | 2.40 | -ve | Rode shape | Motile | *D. acidovorans* HMRBI-17 |
| 15. | HMRBI-18 | *Delftia* | *acidovorans* | 2.15 | -ve | Rode shape | Motile | *D. acidovorans* HMRBI-18 |
| 16. | HMRBI-19 | *Pseudomonas* | *putida* | 1.87 | -ve | Rode shape | Motile | *Pseudomonas* sp. HMRBI-19 |
| 17. | HMRBI-20 | *Pseudomonas* | *plecoglossicida* | 1.72 | -ve | Rode shape | Motile | *Pseudomonas* sp. HMRBI-20 |

Whereas HMRBI-Heavy Metal Resistant Bacteria Isolate

These metal-tolerant/metal-bio-transforming bacteria represent a potentially useful avenue to develop sustainable heavy metal remediation strategies. These rod-shaped bacteria, especially, would be of great interest for bioremediation applications due to their rapid growth and active metabolism. By understanding the mechanisms of HM resistance of each of these isolates, it would be feasible to exploit their potential toxic bioremediation ability via genetic engineering and/or other biotechnological methods.

### 4.1.7. Effects of growth inhibition percentage of bacterial Isolates

A concentration range of 150 to 1050 ppm of HMs was employed to evaluate the growth inhibition effects on selected HMRBIs with notable potential capabilities. This range was to systematically study the tolerance levels and potential inhibitory impacts of varying concentrations of HMs on the growth dynamics of these resistant bacterial isolates. Growth inhibition of the bacterial isolates was consistently observed across all heavy metal HM treatments studied in the Luria-Bertani (LB) medium containing 10 g of tryptone, 5 g of yeast extract, and 10 g of sodium chloride (NaCl) per liter. In this study, we employed cobalt to investigate its specific effects on microbial growth and resistance, as shown in Table 8. All treatments revealed variations in the growth inhibition performance of the bacterial isolates. These differences indicated that each isolate responded differently to the presence of HMs, suggesting variability in their resistance mechanism and tolerance level. For instance, HMRBI-3 (82.91±0.003) exhibited the maximum percentage of resistance at the maximum concentrations, followed by HMRBI-1 (81.83 ± 0.003), as shown in Table 7.

The data further indicated that the lowest growth inhibition percentage in response to cobalt exposure was observed in HMRBI-9 (55.14 ± 0.003), followed closely by HMRBI-8 (57.08 ±0.002). This demonstrated that these isolates exhibited relatively less resistance to cobalt than the other bacterial isolates. The findings highlight the diverse adaptive mechanisms used by the isolates when exposed to HM stress, which may be influenced by factors such as metal type, concentration, and the specific traits of the isolate. In general, a significant inhibition percentage rate of bacterial growth was observed across all HM treatments for the bacterial isolates. The inhibitory effects were consistent and pronounced, with statistically insignificant differences observed between the groups at a confidence level of ($P \leq 0.05$) (Table 7 and Appendix Table 4).

These results suggest potential applications in bioremediation and environmental biotechnology, as certain isolates may be utilized for waste clean-up. Future experiments could investigate the genetic and molecular basis of the observed resistance mechanisms, potentially identifying targets to increase metal tolerance in other bacterial strains. Understanding which characteristics confer this resistance to pollution will enable us to construct more stable microbial communities in polluted environments.

**Table 7: Different concentrations of cobalt inhibited the growth of bacterial isolates from the Bishoftu Industrial Zone waste**

| HM ($Co^{+2}$) Concentration | Growth inhibition in percentage (%) | | | | | | |
|---|---|---|---|---|---|---|---|
| | HMRBI-1 | HMRBI-3 | HMRBI-5 | HMRWI-7 | HMRBI-8 | HMRBI-9 | HMRBI-10 |
| 150ppm | 46.57 ± 0.012[a] | 44.74± 0.01[a] | 31.63 ±0.004[a] | 22.35±0.003[a] | 20.81±.001[a] | 20.29±0.001[a] | 43.79±0.002[a] |
| 250ppm | 48.66 ± 0.019[b] | 55.32± 0.01[b] | 38.71±0.008[b] | 29.10±0.001[b] | 25.39±0.001[b] | 27.10±0.004b | 59.11±0.018[b] |
| 350ppm | 56.50 ±0.002[c] | 67.57±0.02[c] | 52.26±0.001[c] | 52.55±0.002[c] | 47.67±0.003[c] | 37.31±0.005[c] | 61.79±0.002[c] |
| 450ppm | 66.12 ± 0.014[d] | 72.97±0.001[d] | 56.11±0.002[d] | 54.51±0.002[d] | 50.43±.002[d] | 43.15±0.003[d] | 68.83±0.003[d] |
| 550ppm | 70.41 ± 0.004[e] | 78.35±0.004[e] | 60.89±0.001[e] | 56.31±0.002[e] | 52.24±0.001[e] | 43.77±0.001[de] | 69.09±0.001[d] |
| 650ppm | 77.22 ± 0.010[f] | 80.15±0.001[f] | 63.28±0.003[f] | 56.55±0.002[e] | 54.83±0.002[e] | 45.02±0.006[ef] | 71.57±0.002[e] |
| 750ppm | 77.80 ± 0.007[f] | 80.55±0.008[f] | 64.01±.0.013[f] | 58.20±0.001[f] | 52.24±0.001[f] | 45.72±0.002[f] | 71.92±0.002[e] |
| 850ppm | 78.74 ± 0.002[f] | 80.95±0.002[f] | 64.74±0.002[f] | 58.35±0.004[f] | 54.66±0.002[f] | 49.69±0.006[g] | 74.34±0.002[f] |
| 950ppm | 79.13 ± 0.003[f] | 82.85±0.002[g] | 67.93±0.002[g] | 59.14±0.002[f] | 55.27±0.001[f] | 54.13±0.004[h] | 76.53±0.001[g] |
| 1050ppm | 81.83 ± 0.003[g] | 82.91±0.003[g] | 71.51±0.003[h] | 60.63±0.001[g] | 57.08±0.002[g] | 55.14±0.003[h] | 77.00±0.002[g] |
| CV% | 1.5 | 1.2 | 1.9 | 1.0 | 2.0 | 2.2 | 1.3 |
| *P ≤ 0.05* | 0.381 | 0.990 | 0.997 | 1.000 | 0.997 | 0.999 | 0.996 |

The values represent the means of three independent experiments carried out in triplicate with standard deviations. OD was read at 600 nm after 24 hrs. CV% = Coefficient variation percentage, Ave = average mean; the same letters down the column do not significantly differ between the means

The study examined how different concentrations of HMs, ranging from 150 to 1050 ppm, affected the growth of specific HMRBIs with significant potential for environmental impact. In this study, we used copper to investigate its effects on growth inhibition percentage and its resistance effects, as detailed in Table 8. Growth inhibition of the bacterial isolates was consistently observed across all HM treatments studied in the Luria-Bertani (LB) medium. LB medium, a widely used nutrient-rich bacterial growth medium, contains 10 g of tryptone, 5 g of yeast extract, and 10 g of sodium chloride (NaCl) per liter. This medium supports robust bacterial growth under normal conditions, making it an ideal choice for assessing the inhibitory effects of heavy metals. The data particularly revealed how copper exposure influences the growth inhibition of the bacterial isolates.

By analyzing the data presented in (Table 8), the maximum and minimum growth inhibitions of each isolate were assessed. Accordingly, the maximum resistance in percentage was observed for HMRBI-9 (82.18±0.001), followed by HMRBI-10 (72.37±0.003) and HMRBI-1 (71.84±0.001), respectively in (Table 9). The minimum growth inhibition percentage was recorded for HMRBI-7 (64.07±0.002), followed by HMRBI-8 (65.65±0.002), HMRBI-3, and HMRBI-5, which could be inhibited in the presence of copper on average. The recorded results for both isolates were (70.32±0.003 and 68.02±0.001), respectively. The inhibitory effects highlight the dose-dependent nature of HM's toxicity, even in bacteria exhibiting resistance. The overall results suggest that while these isolates can inhibit certain levels of HMs, higher concentration surpass their adaptive mechanisms, leading to reduced growth and metabolic activities. Overall, a notable growth reduction or inhibition in bacterial growth was observed in all HM treatments for each bacterium isolate. The inhibition percentage was both consistent and made with statistically insignificant differences detected at a confidence level of ($P \leq 0.05$) between the groups (Appendix Table 5)**.** Overall, the study highlights the dual nature of bacterial resistance and susceptibility. This shows that while these withstand can tolerate certain concentrations of HMs, their adaptive mechanisms may fail when faced with increased concentrations, leading to prominent reductions in growth & metabolic activities. This has implications for understanding bacterial behavior in contaminated environments and potential applications in bioremediation efforts (Syed et al., 2021).

**Table 8**: Different concentrations of copper inhibited the growth of bacterial isolates from the Bishoftu Industrial Zone waste

| HM ($Cu^{+2}$) Concentration | Growth inhibition in percentage (%) | | | | | | |
|---|---|---|---|---|---|---|---|
| | HMRBI-1 | HMRBI-3 | HMRBI-5 | HMRBI-7 | HMRBI-8 | HMRBI-9 | HMRBI-10 |
| 150ppm | 18.36±0.052$^{a}$ | 28.74±0.001$^{a}$ | 12.03±0.002$^{a}$ | 29.20±0.002$^{a}$ | 22.31±0.001$^{a}$ | 20.52±0.001$^{a}$ | 27.42±0.004$^{a}$ |
| 250ppm | 24.92±0.137$^{b}$ | 36.03±0.003$^{b}$ | 17.64±0.044$^{b}$ | 37.21±0.006$^{b}$ | 30.76±0.005$^{b}$ | 24.70±0.020$^{b}$ | 37.92±0.004$^{b}$ |
| 350ppm | 33.42±0.152$^{c}$ | 38.94±0.001$^{c}$ | 24.29±0.003$^{c}$ | 40.17±0.001$^{c}$ | 36.80±0.001$^{c}$ | 36.92±0.003$^{c}$ | 44.54±0.014$^{c}$ |
| 450ppm | 35.43±0.025$^{c}$ | 50.62±0.001$^{d}$ | 33.84±0.001$^{d}$ | 55.38±0.003$^{d}$ | 38.47±0.002$^{d}$ | 54.64±0.003$^{d}$ | 56.94±0.001$^{d}$ |
| 550ppm | 45.53±0.001$^{d}$ | 56.07±0.001$^{e}$ | 42.91±0.001$^{e}$ | 55.47±0.001$^{d}$ | 39.55±0.003$^{d}$ | 61.33±0.002$^{d}$ | 59.41±0.003$^{e}$ |
| 650ppm | 52.30±0.079$^{e}$ | 57.09±0.004$^{f}$ | 44.16±0.002$^{f}$ | 55.95±0.005$^{de}$ | 41.82±0.001$^{e}$ | 63.04±0.031$^{e}$ | 66.31±0.029$^{f}$ |
| 750ppm | 57.64±0.002$^{f}$ | 59.43±0.006$^{g}$ | 50.78±0.001$^{g}$ | 56.61±0.003$^{de}$ | 52.39±0.001$^{f}$ | 76.09±0.022$^{e}$ | 68.98±0.006$^{g}$ |
| 850ppm | 59.69±0.011$^{f}$ | 67.58±0.009$^{h}$ | 65.82±0.001$^{h}$ | 56.93±0.001$^{e}$ | 56.87±0.002$^{g}$ | 76.48±0.003$^{f}$ | 69.78±0.002$^{gh}$ |
| 950ppm | 71.22±0.001$^{g}$ | 68.87±0.001$^{i}$ | 66.93±0.001$^{i}$ | 57.32±0.002$^{e}$ | 59.80±0.003$^{h}$ | 78.10±0.001$^{f}$ | 71.49±0.002$^{hi}$ |
| 1050ppm | 71.84±0.001$^{g}$ | 70.32±0.003$^{j}$ | 68.02±0.001$^{j}$ | 64.07±0.002$^{f}$ | 65.65±0.002$^{i}$ | 82.18±0.001$^{g}$ | 72.37±0.003$^{i}$ |
| CV% | | 1.0 | 1.4 | 1.5 | 1.5 | 2.5 | 2.3 |
| *P ≤ 0.05* | 0.977 | 0.997 | 1.000 | 0.994 | 0.999 | 0.998 | 0.997 |

The values represent the means of three independent experiments carried out in triplicate with standard deviations. OD was read at 600 nm after 24 hrs. CV% = Coefficient variation percentage, Ave = average mean; the same letters down the column do not significantly differ between the means

**Table 9: Different concentrations of cadmium inhibited the growth of bacterial isolates from the Bishoftu Industrial Zone waste**

| HM ($Cd^{+2}$) Concentration | Growth inhibition in percentage (%) | | | | | | |
|---|---|---|---|---|---|---|---|
| | HMRBI-1 | HMRBI-3 | HMRBI-5 | HMRBI-7 | HMRBI-8 | HMRBI-9 | HMRBI-10 |
| 150ppm | 26.79±0.001$^{a}$ | 17.85±0.005$^{a}$ | 17.18±0.003$^{a}$ | 14.29±0001$^{a}$ | 6.14±0.001$^{a}$ | 11.63±0.0011$^{a}$ | 10.53±0.002$^{a}$ |
| 250ppm | 35.22±0.005$^{b}$ | 22.02±0.007$^{b}$ | 21.73±0.001$^{b}$ | 17.66±0.003$^{b}$ | 8.28±0.003$^{b}$ | 10.70±0.032$^{b}$ | 13.12±0.001$^{b}$ |
| 350ppm | 51.03±0.002$^{c}$ | 31.37±0.007$^{c}$ | 41.88±0.001$^{c}$ | 21.63±0.003$^{c}$ | 11.20±0.001$^{c}$ | 20.10±0.004$^{c}$ | 22.00±0.004$^{c}$ |
| 450ppm | 55.33±0.008$^{d}$ | 34.09±0.007$^{c}$ | 42.98±0.004$^{c}$ | 22.42±0002$^{cd}$ | 15.71±0.003$^{d}$ | 27.30±0.002$^{d}$ | 30.82±0.003$^{d}$ |
| 550ppm | 60.57±0.006$^{e}$ | 42.99±0.004$^{d}$ | 43.10±0.002$^{c}$ | 25.00±0.003$^{de}$ | 16.50±0.001$^{de}$ | 32.78±0.005$^{e}$ | 34.66±0.004$^{e}$ |
| 650ppm | 65.72±0.004$^{f}$ | 51.13±0.001$^{e}$ | 47.25±0.013$^{d}$ | 26.98±0.004$^{ef}$ | 17.96±0.013$^{e}$ | 39.30±0.005$^{f}$ | 42.81±0.006$^{f}$ |
| 750ppm | 67.61±0.003$^{fg}$ | 52.49±0.004$^{e}$ | 47.50±0.002$^{d}$ | 28.97±0.001$^{f}$ | 35.65±0.006$^{f}$ | 40.53±0.001$^{g}$ | 48.71±0.002$^{g}$ |
| 850ppm | 68.13±0.003$^{gh}$ | 52.94±0.003$^{ef}$ | 48.96±0.003$^{d}$ | 29.17±0.004$^{f}$ | 37.71±0.001$^{g}$ | 40.60±0.002$^{g}$ | 50.36±0.004$^{h}$ |
| 950ppm | 69.59±0.003$^{gh}$ | 53.70±0.002$^{ef}$ | 53.48±0.010$^{e}$ | 33.53±0.002$^{g}$ | 41.42±0.010$^{h}$ | 51.44±0.002$^{h}$ | 56.06±0.004$^{i}$ |
| 1050ppm | 70.36±0.002$^{h}$ | 56.41±0.003$^{f}$ | 59.83±0.003$^{f}$ | 47.42±0.002$^{h}$ | 57.59±0.004$^{i}$ | 61.45±0.003$^{i}$ | 59.58±0.005$^{j}$ |
| CV% | 2.2 | 4.7 | 4.0 | 5.9 | 4.4 | 2.0 | 1.7 |
| *P ≤ 0.05* | 0.990 | 0.917 | 0.960 | 0.917 | 1.000 | 0.998 | 0.999 |

The values represent the means of three independent experiments carried out in triplicate with standard deviations. OD was read at 600 nm after 24 hrs. CV% = Coefficient variation percentage, Ave = average mean; the same letters down the column do not significantly differ between the means

The study also examined the effects of cadmium at concentrations ranging from 150 to 1050 ppm. Table 9 provides a detailed analysis of the effects of cadmium concentration on the growth inhibition of HMRBIs. As the Cd concentration increased, the growth inhibition percentage of each bacterial isolate decreased, as observed in all treatments. HMRBI-1 exhibited the maximum growth inhibition percentage was (70.36±0.002), while HMRBI-2 showed the minimum (47.42±0.002). This suggests that the toxicity of cadmium had a direct effect on the ability of these bacteria to grow, but the magnitude of this effect varied among the different isolates.

Particularly, a significant observation was that the isolate HMRBI-1 exhibited the maximum level of growth inhibition percentage, reaching a remarkable 70.36% ± 0.002. This demonstrated that HMRBI-1 is highly sensitive to cadmium, displaying substantial growth suppression at the tested concentrations with the least inhibition. On the other hand, HMRBI-7 displayed the least inhibition at 47.42% ± 0.002, indicating the maximum resistance to cadmium exposure in comparison to the other bacterial isolates in the Table 9. The variation in growth inhibition rates could reflect the differences in the isolates' physiological mechanisms that confer varying degrees of resilience to the toxic effects of cadmium. In general, the observed inhibition proved that the presence of HMs disrupts the physiological processes of the bacterial isolates, even when cultured in a nutrient-rich medium, thereby reflecting the toxic effect of these metals on their growth and survival. Although the bacterial growth rates declined with increased concentrations of HMs, the data show a relatively slow yet sustained growth pattern among the other bacterial isolates within the concentration range of 150 to 1050 ppm. Overall, all HM treatments significantly inhibited the growth of all bacterial isolates, as evidenced by a remarkable decrease in growth. This inhibitory effect was statistically insignificant ($P \leq 0.05$) across all treatments (Table 9 and Appendix Table 6).

Studies have shown that high concentrations of zinc can be toxic to bacterial growth. While zinc is an essential trace element for bacteria, required for the activity of various enzymes and cellular functions, excessive levels can have detrimental effects. Various concentration ranges from 150 to 1050 ppm were used for this study to test the growth inhibition of bacteria isolated from the Bishoftu and Mojo Industrial areas. The data revealed that as the concentration increases, the growth inhibition of bacterial isolates decreases, as predicted in Table 10. At the lower

concentrations, the inhibition percentage rates were lower compared to all bacterial isolates. However, variation in growth inhibition was observed among the isolates with varying degrees of inhibition. For instance, at lower Zn concentrations, 49.90±0.002, 41.55±0.003, 36.76±0.001, 41.26±0.002, 41.86±0.011, 42.07±0.002, and 26.83±0.002 were recorded for HMRBI-1, HMRBI-3, HMRBI-5, HMRBI-7, HMRBI-8, HMRBI-9, and HMRBI-10, respectively, as shown in the Table 10. This indicates that the lower concentration exhibited lower growth inhibition for each bacterial isolate. However, there was a degree of variation among the treatments at a statistically insignificant level ($P \leq 0.05$) between the groups.

The study also showed that as zinc concentration increased, the extent of the growth inhibition percentage rate increased for each bacterial isolate. This pattern indicates that zinc, at higher concentrations, becomes progressively more toxic to the bacteria, impairing their growth to varying degrees depending on the species. As indicated in Table 10, isolates HMRBI-1, HMRBI-9, HMRBI-10, and HMRBI-7 were especially susceptible to the toxic effects of zinc at high concentrations. These bacterial strains confirmed the most significant decrease in growth at high concentrations, indicating the maximum percentage of growth inhibition. The high sensitivity of each bacterial isolate may be due to a lack of efficient zinc resistance mechanisms, limiting their ability to counteract the toxic effects of excess zinc. Zinc treatments exhibited a significant inhibitory percentage effect on bacterial growth, as directed by a statistically insignificant increase in concentration ($P \leq 0.05$) among the group (Appendix Table 7).

Further study was also conducted on the effects of chromium at varying concentrations on bacterial inhibition growth performance, as indicated in Table 11. The same trends were observed for chromium treatments concerning the growth inhibition percentage of HMBIs. The degree of growth inhibition for each bacterium was very different among the treatments, highlighting the varying levels of effectiveness. Some treatments revealed a significant reduction in growth, suggesting they were highly effective in limiting the development of the target organism, while others showed only mild or negligible effects. This inconsistency could be attributed to factors such as the specific mechanisms of action of each treatment and the concentration or dosage of heavy metal applied.

**Table 10: Different concentrations of Zinc inhibited the growth of bacterial isolates from the Bishoftu Industrial Zone waste**

| HM ($Zn^{+2}$) Concentration | Growth inhibition in percentage (%) | | | | | | |
|---|---|---|---|---|---|---|---|
| | HMRBI-1 | HMRBI-3 | HMRBI-5 | HMRBI-7 | HMRBI-8 | HMRBI-9 | HMRBI-10 |
| 150ppm | 39.32±0.001$^{a}$ | 35.10±0.003$^{a}$ | 31.72±0.001$^{a}$ | 32.10±0.003$^{a}$ | 34.46±0.002$^{a}$ | 35.49±0.001$^{a}$ | 23.64±0.002$^{a}$ |
| 250ppm | 45.90±0.002$^{b}$ | 41.85±0.003$^{b}$ | 36.76±0.001$^{b}$ | 41.26±0.002$^{b}$ | 41.86±0.011$^{b}$ | 42.07±0.002$^{b}$ | 26.83±0.002$^{b}$ |
| 350ppm | 46.31±0.001$^{b}$ | 44.34±0.001$^{c}$ | 38.73±0.001$^{c}$ | 43.84±0.003$^{c}$ | 44.70±0.004$^{c}$ | 42.31±0.003$^{bc}$ | 27.63±0.003$^{b}$ |
| 450ppm | 47.87±0.001$^{c}$ | 46.52±0.001$^{d}$ | 40.56±0.006$^{d}$ | 49.20±0.001$^{d}$ | 45.03±0.002$^{cd}$ | 43.91±0.001$^{cd}$ | 35.50±0.002$^{d}$ |
| 550ppm | 48.29±0.001$^{cd}$ | 49.12±0.001$^{e}$ | 42.52±0.004$^{e}$ | 50.05±0.001$^{de}$ | 45.36±0.001$^{cde}$ | 44.77±0.004$^{d}$ | 37.33±0.002$^{c}$ |
| 650ppm | 49.12±0.001$^{de}$ | 49.43±0.001$^{e}$ | 43.26±0.001$^{e}$ | 50.91±0.006$^{fe}$ | 47.43±0.001$^{ef}$ | 50.43±0.004$^{e}$ | 40.64±0.002$^{d}$ |
| 750ppm | 49.53±0.002$^{e}$ | 51.30±0.002$^{f}$ | 45.59±0.001$^{f}$ | 51.77±0.003$^{fg}$ | 47.43±0.002$^{def}$ | 53.26±0.001$^{f}$ | 43.72±0.001$^{e}$ |
| 850ppm | 52.13±0.005$^{f}$ | 51.40±0.004$^{f}$ | 46.69±0.001$^{f}$ | 52.95±0.001$^{g}$ | 48.85±0.004$^{f}$ | 61.13±0.001$^{g}$ | 43.84±0.002$^{f}$ |
| 950ppm | 55.24±0.004$^{g}$ | 52.65±0.002$^{g}$ | 47.06±0.001$^{f}$ | 57.45±0.002$^{h}$ | 53.55±0.001$^{g}$ | 62.13±0.001$^{g}$ | 51.37±0.004$^{f}$ |
| 1050ppm | 67.81±0.003$^{h}$ | 57.94±0.010$^{h}$ | 54.41±0.002$^{g}$ | 60.45±0.003$^{i}$ | 59.34±0.003$^{h}$ | 65.07±0.002$^{h}$ | 60.84±0.003$^{h}$ |
| CV% | 1.0 | 1.5 | 2.0 | 1.6 | 2.8 | 2.0 | 2.4 |
| *P ≤ 0.05* | 0.993 | 0.972 | 1.000 | 0.691 | 0.999 | 0.998 | 0.999 |

The values represent the means of three independent experiments carried out in triplicate with standard deviations. OD was read at 600 nm after 24 hrs. CV% = Coefficient variation percentage, Ave = average mean; the same letters down the column do not significantly differ between the means

**Table 11: Different concentrations of chromium inhibited the growth of bacterial isolates from the Bishoftu Industrial Zone waste**

| HM ($Cr^{+6}$) Concentration | Growth inhibition in percentage (%) | | | | | | |
|---|---|---|---|---|---|---|---|
| | HMRBI-1 | HMRBI-3 | HMRBI-5 | HMRBI-7 | HMRBI-8 | HMRBI-9 | HMRBI-10 |
| 150ppm | 21.05±0.001[a] | 25.61±0.001[a] | 17.80±0.002[a] | 15.30±0.001[a] | 30.15±0.004[a] | 8.47±0.004[a] | 12.55±0.003[a] |
| 250ppm | 24.14±0.006[b] | 29.96±0.023[b] | 21.69±0.002[b] | 17.46±0.012[b] | 38.54±0.005[b] | 10.77±0.033[b] | 15.73±0.019[b] |
| 350ppm | 36.90±0.004[c] | 42.27±0.003[c] | 25.78±0.010[c] | 30.47±0.018[c] | 41.45±0.004[c] | 18.37±0.030[c] | 22.57±0.007[c] |
| 450ppm | 49.21±0.003[d] | 43.03±0.007[c] | 37.34±0.011[d] | 35.24±0.003[d] | 43.80±0.004[d] | 45.84±0.006[d] | 49.06±0.014[d] |
| 550ppm | 53.79±0.006[e] | 47.20±0.001[d] | 44.16±0.010[e] | 37.38±0.007[d] | 54.11±0.002[e] | 46.93±0.008[d] | 51.98±0.010[e] |
| 650ppm | 59.74±0.006[f] | 47.36±0.006[d] | 56.19±0.004[f] | 46.67±0.014[e] | 54.22±0.003[e] | 49.82±0.002[e] | 53.66±0.015[f] |
| 750ppm | 62.58±0.008[g] | 53.91±0.007[e] | 57.52±0.002[ef] | 48.18±0.008[f] | 55.10±0.003[f] | 57.70±0.009[f] | 55.58±0.005[g] |
| 850ppm | 64.88±0.010[h] | 56.81±0.007[ef] | 58.41±0.004[ef] | 57.26±0.001[f] | 63.38±0.003[g] | 65.76±0.012[g] | 69.36±0.002[h] |
| 950ppm | 68.33±0.005[i] | 57.73±0.010[g] | 62.58±0.010[g] | 59.83±0.007[h] | 66.67±0.002[h] | 71.33±0.007[h] | 73.96±0.008[i] |
| 1050ppm | 70.35±0.006[j] | 63.61±0.020[h] | 66.94±0.012[h] | 67.14±0.005[i] | 75.27±0.003[i] | 80.01±0.006[i] | 75.23±0.004[j] |
| CV% | 1.2 | 4.4 | 1.8 | 2.3 | 1.0 | 3.5 | 2.1 |
| $P \leq 0.05$ | 0.997 | 0.979 | 0.983 | 0.986 | 0.973 | 0.999 | 0.993 |

The values represent the means of three independent experiments carried out in triplicate with standard deviations. OD was read at 600 nm after 24 hrs. CV% = Coefficient variation percentage, Ave = average mean; the same letters down the column do not significantly differ between the means

As the concentration of chromium increases, the observed growth inhibition of bacterial isolates tends to follow a dose-dependent pattern. Higher concentrations of chromium cause increased toxicity in bacterial cells, resulting in a more substantial decrease in growth. Overall, the maximum results were observed for the HMTBI-9 (80.01±0.006), followed by HMRBI-8 (75.27±0.003) and HMRBI-10 (75.23±0.004), as presented in Table 11.

The minimum inhibitory concentration (MIC) is defined as the minimum concentration of a given agent that inhibits the growth of the isolate, indicated by a lack of visible bacterial growth on the media (Bhardwaj et al., 2018). This parameter serves as a commonly accepted measure of the microbial resistance to different inhibitory reagents, HMs in this case. However, in this study, MIC values were determined for all 10 isolated strains against HMs. This observation very convincingly indicates that the isolated strains have acquired a substantial resistance against that particular HM. The raised MIC signifies that these isolates can grow and reproduce in the presence of normally lethal or inhibitory concentrations of the HM. HM tolerance development may be due to a variety of mechanisms. This takes place through the activation of efflux pumps to pump toxic metal ions out, detoxification, intracellular sequestration of the HMs, alteration of cellular targets so the metals cannot bind to them, or even the secretion of extracellular polysaccharides to form a barrier (Ahamed et al., 2024). These results highlight the need for studies of microbial adaptation to HMs because that type of tolerance may have considerable ecological ramifications. Some examples of these are HM-tolerant bacteria isolates from polluted environments, which may contribute to the bioaccumulation of HMs.

### 4.1.8. Removal efficiency of HMRBIs

The bio-utilization performance of heavy metals (e.g., $Cd^{+2}$, $Co^{+2}$, $Cr^{+6}$, $Cu^{+2}$, and $Zn^{+2}$) was studied using an atomic absorption spectrometer (AAS) to assess the effectiveness of various bacterial isolates. The results showed significant differences in degradation rates among the isolates, especially with cobalt. The bacterial isolate HMRBI-5 exhibited the highest capacity for cobalt reduction, achieving a rate of 79.27%. This suggests that HMRBI-5 has efficient metabolic mechanisms that enable it to effectively bio-absorb cobalt from contaminated environments. Additionally, HMRBI-14 and HMRBI-1 showed high degradation rates of 78.14% and 67.12%, respectively. The study indicates that these two isolates have strong potential for cobalt bioremediation. In contrast, the

lowest degradation capacity was observed with HMRBI-10 at 28.40%, implying a possible deficiency in metabolic efficiency or detoxification ability for cobalt. Overall, the data suggest that most of the isolates exhibit significant potential for cobalt degradation, supporting their use in bioremediation efforts, as shown in Table 12.

Copper removal was evaluated, and the highest degradation rate (59.18%) was achieved by HMRBI-17, indicating a strong copper resistance capacity compared to the others. This suggests that HMRBI-17 possesses robust resistance mechanisms or metabolic pathways that enable effective copper bioremediation. Conversely, HMRBI-2 exhibited a degradation rate of 47.20%, which points to a lower copper resistance ability, implying that this isolate may be less efficient in high-copper environments as shown in Table 12. The results from cobalt and copper degradation tests underscore the potential of the current bacterial isolates for bioremediation. Isolates with higher degradation rates could be utilized in environmental cleanup efforts, particularly in areas heavily contaminated with heavy metals. Further research may reveal the reasons behind the differences in removal capacities, offering a pathway to improve bioremediation strategies and develop more resilient bacterial strains.

Assessment of HMRBI's heavy metal-degrading capacity highlights its potential for future bioremediation in contaminated, heavy metal-polluted environments. An HMRBI-5 isolated bacterial strain showed excellent resistance to cadmium, with an 85.17% resistance rate. This suggests its possible usefulness in bioremediation efforts against cadmium toxicity in contaminated sites. Conversely, the HMRBI-3 isolated bacterial strain exhibited the highest resistance to cadmium among the isolates, yet it was unable to grow under cadmium-enhanced conditions. This difference underscores the distinct adaptive properties of various bacterial strains when facing heavy metal stress.

**Table 12: The removal capacity (%) of bacteria isolates against Heavy metals (HMs)**

| Bacteria Isolates | HMs | | | | |
|---|---|---|---|---|---|
| | Cobalt (%) | Copper (%) | Cadmium (%) | Chromium (%) | Zinc (%) |
| HMRBI-1 | $67.12 \pm 0.002^{bc}$ | $50.54 \pm 0.002^{ab}$ | $43.71 \pm 0.001^{ab}$ | $79.14 \pm 0.004^{bc}$ | $53.53 \pm 0.001^{a}$ |
| HMRBI-2 | $67.38 \pm 0.002^{c}$ | $47.20 \pm 0.001^{a}$ | $62.14 \pm 0.004^{fg}$ | $56.62 \pm 0.002^{cd}$ | $57.91 \pm 0.002^{a}$ |
| HMRBI-3 | $36.62 \pm 0.006^{ab}$ | $61.63 \pm 0.004^{de}$ | $47.27 \pm 0.003^{ab}$ | $45.51 \pm 0.003^{a}$ | $55.77 \pm 0.006^{b}$ |
| HMRBI-4 | $63.93 \pm 0.002^{bc}$ | $65.13 \pm 0.001^{e}$ | $65.02 \pm 0.002^{b}$ | $51.57 \pm 0.003^{bc}$ | $53.63 \pm 0.002^{a}$ |
| HMRBI-5 | $79.27 \pm 0.006^{abc}$ | $57.14 \pm 0.002^{bcd}$ | $85.17 \pm 0.003^{e}$ | $82.53 \pm 0.002^{bc}$ | $72.04 \pm 0.001^{a}$ |
| HMRBI-6 | $62.34 \pm 0.013^{bc}$ | $52.50 \pm 0.003^{abc}$ | $53.52 \pm 0.001^{de}$ | $70.32 \pm 0.001^{e}$ | $55.77 \pm 0.001^{a}$ |
| HMRBI-7 | $56.24 \pm 0.025^{abc}$ | $57.68 \pm 0.002^{bcd}$ | $63.21 \pm 0.054^{fg}$ | $65.13 \pm 0.004^{cd}$ | $61.97 \pm 0.001^{a}$ |
| HMRBI-8 | $59.16 \pm 0.001^{bc}$ | $53.97 \pm 0.009^{abc}$ | $49.52 \pm 0.039^{cd}$ | $59.65 \pm 0.001^{d}$ | $57.83 \pm 0.002^{a}$ |
| HMRBI-10 | $28.40 \pm 0.007^{a}$ | $50.22 \pm 0.003^{ab}$ | $40.15 \pm 0.002^{a}$ | $66.65 \pm 0.003^{e}$ | $62.24 \pm 0.002^{a}$ |
| HMRBI-14 | $78.14 \pm 0.007^{abc}$ | $56.26 \pm 0.003^{bcd}$ | $64.48 \pm 0.001^{b}$ | $89.74 \pm 0.003^{c}$ | $74.32 \pm 0.002^{a}$ |
| HMRBI-17 | $43.78 \pm 0.009^{abc}$ | $59.18 \pm 0.025^{cde}$ | $53.64 \pm 0.006^{e}$ | $66.00 \pm 0.002^{e}$ | $64.10 \pm 0.001^{a}$ |
| CV% | 20.1% | 4.8% | 2.7% | 3.3% | 5.3% |
| $P \leq 0.05$ | 0.816 | 0.970 | 0.931 | 0.182 | 0.944 |

The values represent the means of three independent experiments carried out in triplicate with standard deviations. Absorption spectrophotometers were utilized to evaluate the entire heavy metal deduction percentage. M/D = mean difference, ave = average mean; the same letters down the column do not significantly differ between the means

In addition, the present study applied to the biodegradability of chromium and zinc. HMRBI-14 was identified as the most efficient isolate for chromium degradation, and its reduction capacity was determined to be 89.74%. On the other hand, HMRBI-3 exhibited the minimum effectiveness, again with a 45.51% degradation rate. Interestingly, HMRBI-5 was very close to HMRBI-14, isolated strains, suggesting that it can be effectively used to bioremediate industrial effluent contaminated by chromium. Among zinc degradation, HMRBI-14, HMRBI-5, and HMRBI-17 isolated bacterial strains were identified as the best isolates, demonstrating a strong capacity for removing zinc from polluted sites. Generally, the data reveal that all the bacterial isolates tested possess remarkable heavy metal degradation ability, with insignificant metal removal rate in all treatments ($P \leq 0.05$) between all treatments as presented in (Table 12 and Appendix Table 3). This indicates that these isolates have

great potential in designing the bioremediation process for industrial waste, which will further lead to the bioremediation of industrial effluents and the cleanup of contaminated ecosystems.

**Table 13: Removal Efficiency of HMR Bacterial Strains: Current vs. Previous Studies**

| S. N | Bacteria species | Reduction efficiency % | HM utilized | references |
|---|---|---|---|---|
| 1. | *P. benzoelyticum*-HMRBI-1 | 79.27% | $Cd^{+2}$ | Current study |
| 2. | *Citrobacter*-HMRBI-5 | 85.21% | $Cu^{+2}$ | Current study |
| 3. | *Klebsiella*-HMRBI-14 | 89.74% | $Cr^{+6}$ | Current study |
| 4. | *A. hydrophila,* | 65.02 | $Cd^{+2}$ | Current study |
| 5. | *D. acidovorans* | 70.32%, | $Zn^{+2}$ | Current study |
| 6. | *E. aurantiacum* | 61.63 & 50.43%. | $Cu^{+2}$ &$Cr^{+6}$ | Current study |
| 7. | *P. benzoelyticum* | 60.49% | $Co^{+2}$ | Current study |
| 8. | *Gemella* spp. | 55.16 % | $Pb^{+2}$ | (Marzan et al., 2017) |
| 9. | *Micrococcus* spp. | 36.55 % | $Cr^{+6}$ | |
| 10. | *B. licheniformis* | 50.65% | Municipal waste | (Sonune et al., 2018) |
| 11. | *Pseudomonas* | 10-60% | $Pb^{+2}$, $Cu^{+2}$ | (Selvi et al., 2014) |
| 12. | *E. coli* | 30-70% | $Cu^{+2}$, $Zn^{+2}$ $Hg^{+2}$, $Pb^{+2}$ $Cr^{+6}$ | |
| 13. | *Bacillus* spp. | 30-50% | $Cr^{+6}$, $Pb^{+2}$, $Zn^{+2}$ & $Cu^{+2}$ | |
| 14. | *Flavobacterium* spp. | 55% | $Cr^{+6}$ | |
| 15. | *P. fluorescens (*YPS3*)* | 84% | $Cr^{+6}$ | (Kalaimurugan et al., 2020) |
| 16. | *B. safensis (*YKS2) | 72% | $Cr^{+6}$ | |
| 17. | *B. circulans* | 40% & 78% | $Cr^{+6}$ and $Pb^{+2}$ | (Priyadarshanee & Das, (2021)) |
| 18. | *Stenotrophomonas maltophilia* | 22% | $Cu^{+2}$ | (Balolong et al., 2007) |

The removal efficiency for the *A. hydrophila*, *D. acidovorans*, *E. aurantiacum*, and *P. benzoelyticum* isolates measured using AAS, demonstrated considerable degradation of $Cd^{+2}$, $Zn^{+2}$, $Cu^{+2}$, $Cr^{+6}$, and $Co^{+2}$, as shown in Table 13. The reduction or removal efficiency percentages were 65.02 ± 0.002, 70.04 ± 0.001, 61.63 ± 0.004, 65.03 ± 0.004, and 60.49 ± 0.002, respectively. The results from this study are important for HM bioremediation. Compared with previous investigations, the bacterial isolates observed in this study demonstrate a remarkable ability for heavy metal degradation. Sonune et al., (2018) conducted a study on *B. licheniformis*, finding that this bacterium exhibited a removal

efficiency of 50.65% for $Cr^{+6}$ removal. The chromium degradation observed in the current study with *E. aurantiacum* (65.03%) is remarkably close to the results reported by Sonune et al., (2018) *B. licheniformis*. Selvi et al., (2014) also studied the reduction or removal of $Cr^{+6}$ using *Bacillus* species and $Pb^{+2}$ and $Cu^{+2}$ using *Pseudomonas* spp. The study demonstrated that these bacteria were capable of $Cr^{+6}$ removal, achieving degradation efficiencies ranging from 30 to 50% and 10 to 60%, respectively. This research underscores the potential of various *Bacillus* strains for bioremediating Cr-contaminated environments. However, the $Cr^{+6}$ removal efficiency observed in that study was lower compared to the efficiency achieved with the *A. hydrophila*, *D. acidovorans*, *E. aurantiacum*, and *P. benzoelyticum* isolates in the present study in Table 13.

### 4.1.9. The effects of carbon and nitrogen sources on the HMR bacteria growth

A variety of carbon (i.e., sucrose, and glucose) and nitrogen (i.e., yeast extract, peptone, and $KNO_3$) sources were used for the growth of these HMRBIs as shown in Figure (5a-d). Since bacteria require elements in varying amounts to synthesize essential cellular components, including proteins, nucleic acids, and lipids, the availability and types of carbon and nitrogen sources can significantly impact their growth rates (Belliveau et al., 2021). The results showed that the maximum CDW (0.012 g/L) for *E. aurantiacum* HMRBI-7 and $OD_{600nm}$ were detected against glucose that was supplied as the primary sole carbon source in the salt medium (Figure 5). The minimum CDW (0.002 g/L) and $OD_{600nm}$ were noticed against sucrose and $KNO_3$ for *Pseudomonas* sp. HMRBI-2, *E. aurantiacum* HMRBI-7, *A. hydrophila* HMRBI-12, and *D. acidovorans* HMRBI-17, respectively (Figure 5a-d). Similarly, the effects of nitrogen sources and salt concentration were observed against each HMRBI. As observed from the data, $(NH_4)_2SO_4$ gave maximum CDW (0.002 g/L) for *E. aurantiacum* HMRBI-7, but similar results were observed for the rest of the isolates. The data also revealed that maximum CDW (0.001 g/L) was observed for each HMRBI (Figures 5a-d). The availability of carbon and nitrogen sources directly affects the biomass of various microbial populations. When both elements are abundant, bacteria can rapidly multiply and bioaccumulate in their biomass. However, if either carbon or nitrogen is limited, growth rates and biomass production will be affected (Nair et al., 2021).

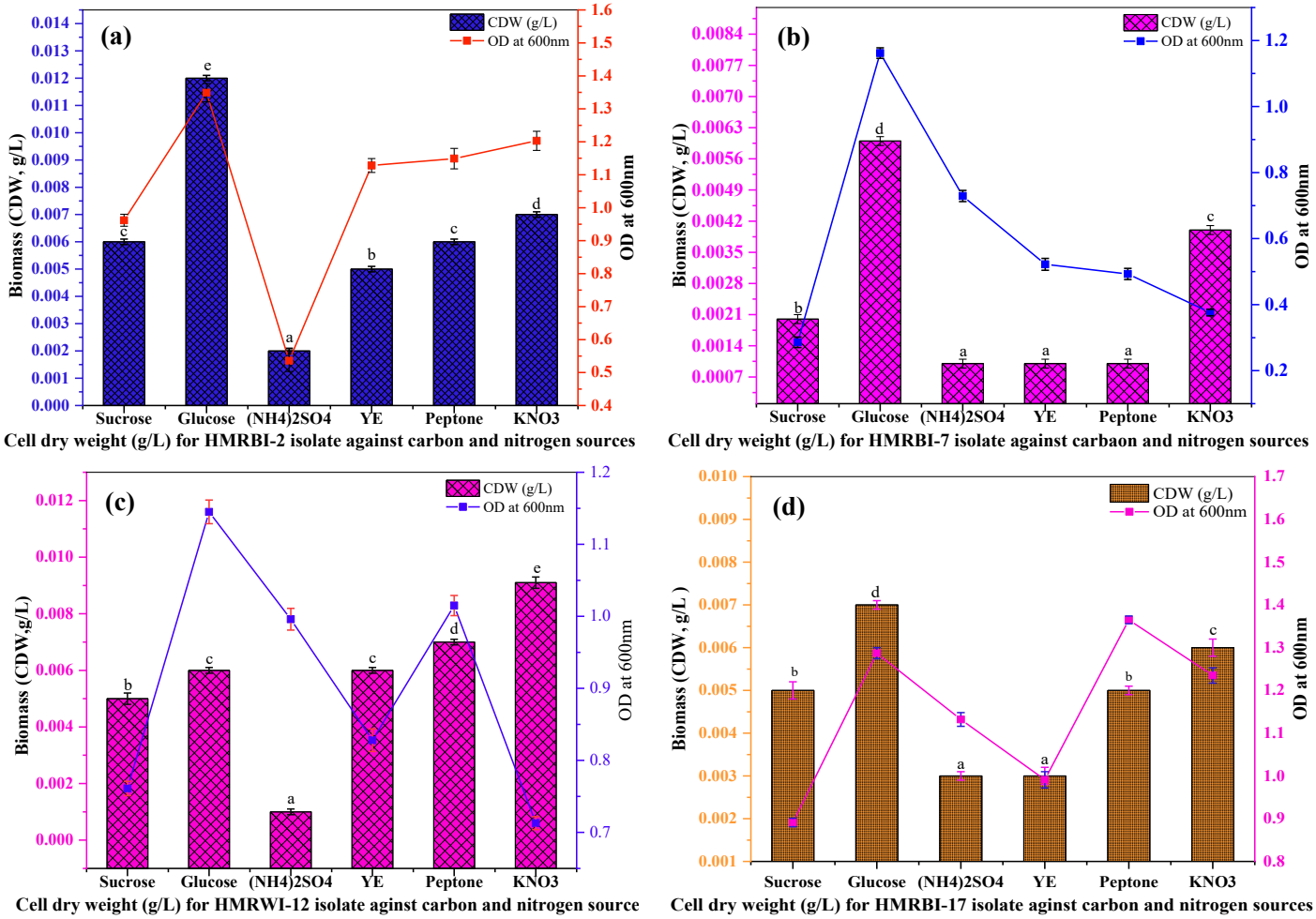


**Figure 5: Effect of carbon & nitrogen sources on the growth of HMRBIs where (a) *P. putida*-HMRBI-2, (b), *E. aurantiacum*-HMRBI-7, (c), *A. hydrophila*-HMRBI-12, and *D. acidovorans*-HMRBI-17 (d). For each experimental condition, measurements were performed in triplicate at $OD_{600nm}$. Data represented as mean ± SEM of three replicate (n = 3) of CDW (g/L)**

## 4.1.13. The effects of pH and temperature values against HMRBIs

The study identified specific bacteria isolates capable of HMR, such as HMRBI-2, *P. putida*, *E. aurantiacum* HMRBI-7, *A. hydrophila*-HMRBI-12, and *D. acidovorans*-HMRBI-17. These isolates can tolerate different HMs concentrations under various pH ranges. The study revealed that pH 6.5 was used to give the optimum $OD_{600nm}$ against HMRBI-2, *P. putida*-(HMRBI-12), *E. aurantiacum*-HMRBI-7, and *D. acidovorans*-HMRBI-17 as indicated in Figure 6. The $OD_{600nm}$ decreases among all treatments as the pH value decreases. However, *E. aurantiacum*-HMRBI-7 (1.003 nm) exhibited

the maximum $OD_{600nm}$ at pH 6.5 compared with *P. putida-HMRBI-2* (0.941 nm) and *A. hydrophila*-HMRBI-12 (0.664 nm) isolates (Figure 6). A considerable amount of $OD_{600nm}$ was also recorded against *D. acidovorans*-HMRBI-17 (nm) and *E. aurantiacum*-HMRBI-7 (nm) at pH 7.5 (Figure 6). This indicates that a slightly acidic environment may influence the growth conditions of these HMRBIs. The recent result revealed that the HMRBIs can tolerate various pH values. A slightly acidic environment is generally conducive to the growth of these HMR isolates. However, as pH increases, the growth rates tend to decline.

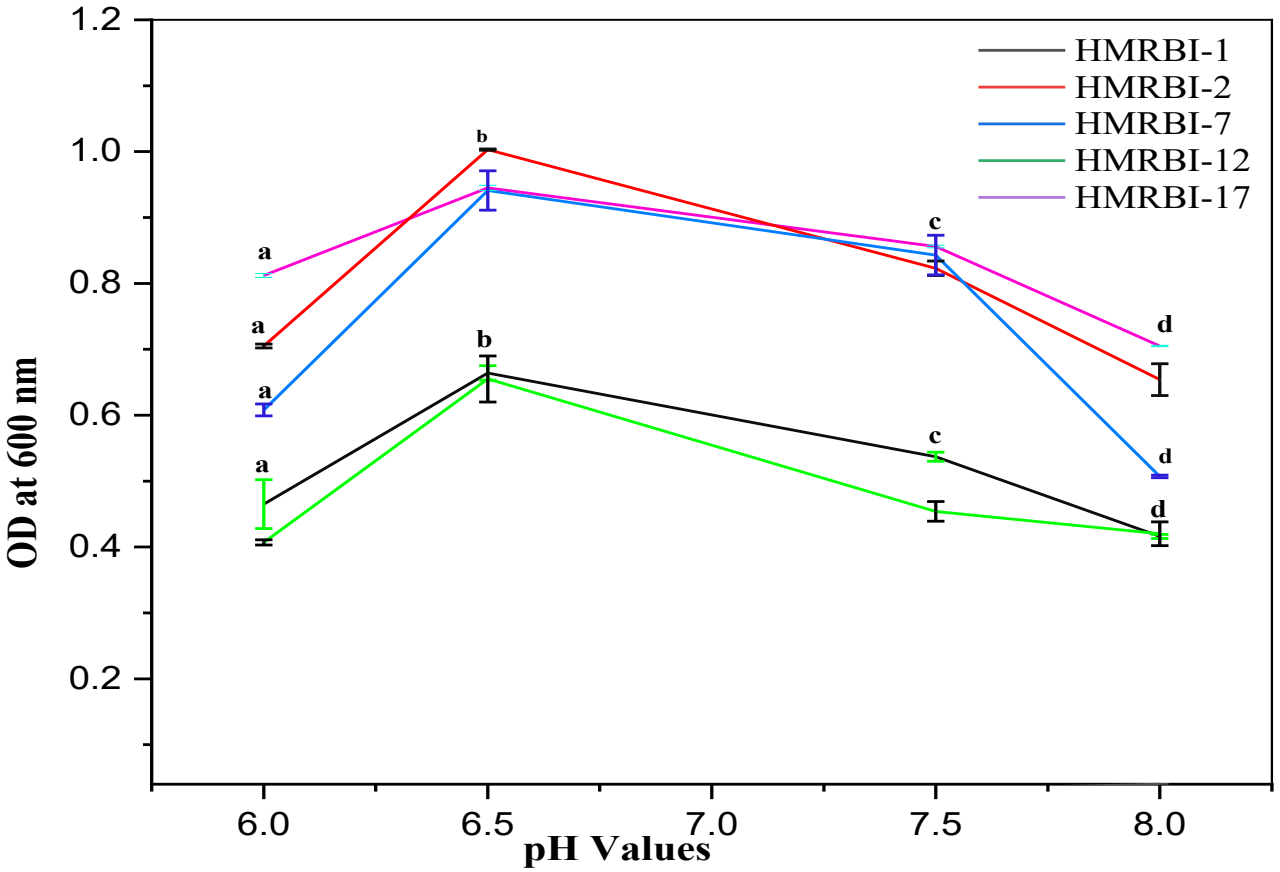


**Figure 6: The effects of various pH values on the growth of HMRBIs (a) *P. putida*-HMRBI-2, (b), *E. aurantiacum*-HMRBI-7, (c), *A. hydrophila-HMRBI-12*, (d), and *D. acidovorans*-HMRBI-17 (d). For each experimental condition, measurements were performed in triplicate at $OD_{600nm}$. Data represented as mean ± SEM of three replicates (n = 3) of pH values.**

Temperature is one of the growth conditions that influence the development of HMRBIs, as shown in Figures 7a-d. The study explored how temperature affects various types of HMRBIs, which can thrive in environments with high levels of heavy metals (Figures 7a-d). The temperature range for

HMRBIs growth was recorded from mild to warm. These isolates were exposed to 300µg/mL HM concentrations and produced various $OD_{600nm}$ readings. The isolates include P. putida-HMRBI-2, *Exiguobacterium aurantiacum*-HMRBI-7, Aeromonas hydrophila-HMRBI-12, and D. acidovorans-HMRBI-17, all of which tolerated $Co^{+2}$, $Cu^{+2}$, $Cd^{+2}$, and $Cr^{+6}$. The results showed a significant variation in response when HMRBIs were exposed to different HM concentrations ($P \leq 0.05$). For instance, P. putida-HMRBI-2 (measured in CDW g/L) exhibited optimal growth at 30°C, indicating that this temperature provides the most favorable conditions for its metabolic processes, cell division, and overall development. This temperature range likely reflects the natural environment where the isolate was sourced. Conversely, the other isolates demonstrated their best growth rate at 35°C, as illustrated in Figures 7a-d.

The isolates resistant to HMs showed the highest growth rates at 40 °C, indicating that their metabolic adaptations not only provide resistance to the toxic effects of chromium but also potentially improve their ability to thrive in such temperatures (Figures 7a-d). This link between chromium resistance and optimal growth at higher temperatures may reflect unique physiological support under stress. The results suggest that the optimal growth conditions for HMRBIs can vary depending on the specific metal they resist. pH optimization was also performed for HMRBIs, as shown in Figures 7a-d. The data indicated that the bacterial isolates had optimal growth in slightly acidic conditions, with the peak at a pH of 6.5. Conversely, isolates adapted to basic environments reached their maximum growth rates at a pH of 7.5 (Figure 7). This divergence in pH preferences highlights the ecological and physiological adaptability of these bacteria to different environmental conditions. Therefore, the ability of HMRBIs to grow under slightly acidic conditions may be connected to the availability of essential nutrients.

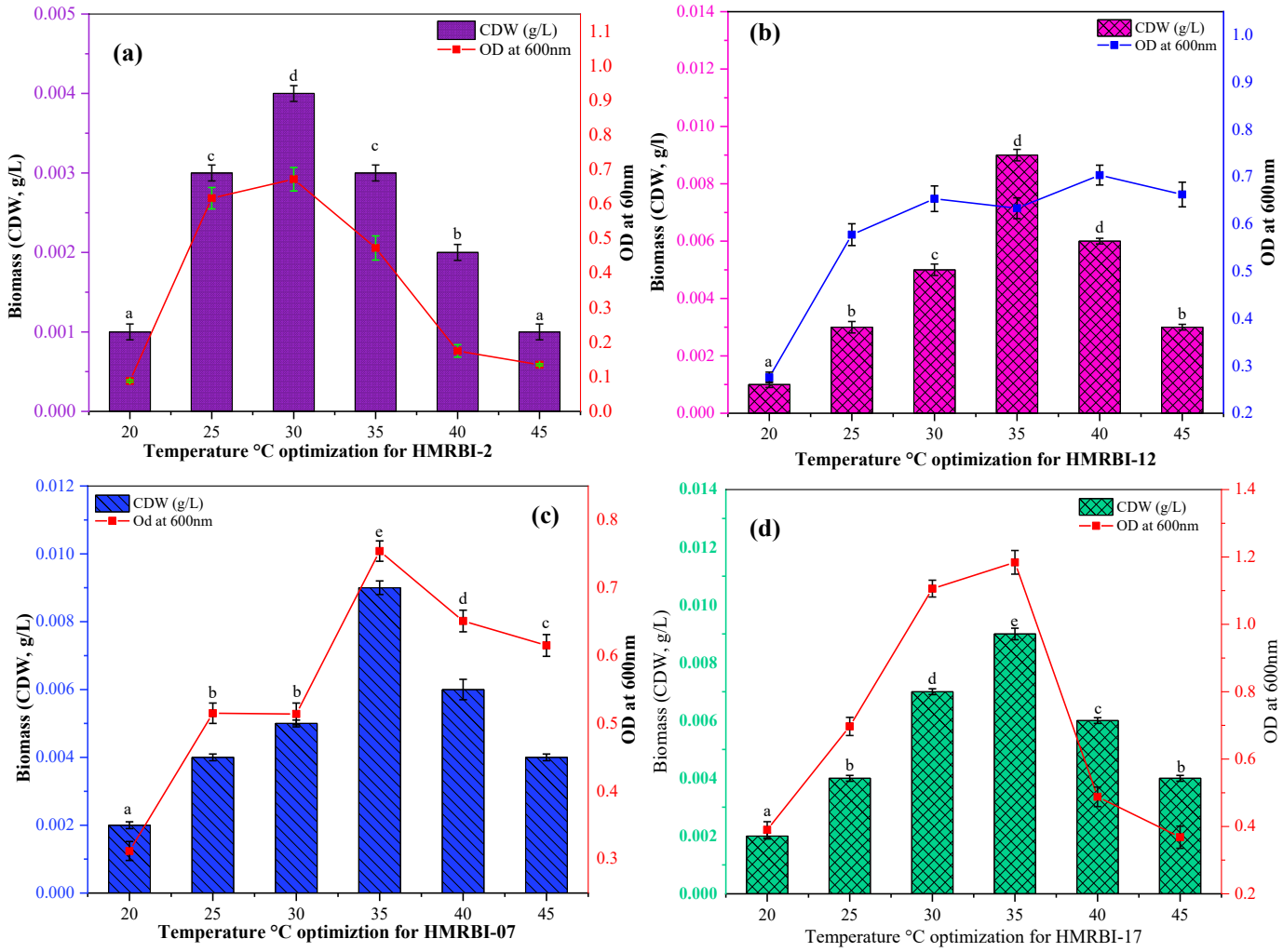


**Figure 7: Effects of Temperature on the growth of HMRBIs where (a) *P. putida*-HMRBI-2, (b), *E. aurantiacum*-HMRBI-7, (c), *A. hydrophila*-HMRBI-12, and *D. acidovorans*-HMRBI-17 (d). For each experimental condition, measurements were performed in triplicate. The $OD600_{nm}$ obtained from certain isolated HMRBIs at various pH values. The results show mean ± SEM of three replicates (n = 3) of CDW (g/L) against pH and temperature.**

### 4.1.14. Assessment of a minimum inhibitory concentration on HMRBIs

The Minimum Inhibitory Concentration (MIC) of each heavy metal was evaluated by assessing its effect on microbial growth across a concentration gradient from 200 ppm to 1000 ppm, as shown in (Table 14). To determine the threshold that restricts microbial growth, heavy metals were tested at both high and low concentrations. By applying incremental adjustments within this range, this study indicated the MIC at which microbial growth is visibly suppressed. Such findings can aid in

developing bacteria-based bioremediation strategies for environmental waste treatment. The data indicated that the MIC for isolate HMRBI-5 was 800 ppm, while for isolate HMRBI-22, the MIC was 1000 ppm. These values correspond to the concentrations of cadmium ($Cd^{+2}$) and cobalt ($Co^{+2}$), respectively, at which the bacterial growth was inhibited. This suggests that isolate HMRBI-5 exhibited a higher resistance to $Cd^{+2}$, as it tolerated a concentration of 800 ppm, whereas isolate HMRBI-22 showed a higher tolerance to cobalt, with the MIC for this metal being 900 ppm. These findings highlight the varying levels of resistance exhibited by the two isolates to different metal pollutants.

**Table 14: The Minimum inhibitory concentration of HMRBI of Bishoftu and Mojo**

| Bacterial strain Code | HMs | | | | | | | | |
|---|---|---|---|---|---|---|---|---|---|
| | 200ppm | 300ppm | 400ppm | 500ppm | 600ppm | 700ppm | 800ppm | 900ppm | 1000ppm |
| HMRBI-1 | **** | **** | *** | ** | ** | * | - | - | - |
| HMRBI-2 | **** | **** | *** | ** | ** | - | - | - | - |
| HMRBI-3 | **** | **** | *** | ** | ** | - | - | - | - |
| HMRBI-4 | **** | **** | *** | ** | ** | - | - | - | - |
| HMRBI-5 | **** | **** | *** | ** | ** | * | * | - | - |
| HMRBI-6 | **** | **** | *** | ** | ** | * | - | - | - |
| HMRBI-7 | **** | **** | *** | ** | ** | * | - | - | - |
| HMRBI-8 | **** | **** | *** | ** | ** | * | - | - | - |
| HMRBI-9 | **** | **** | *** | ** | ** | * | - | - | - |
| HMRBI-10 | **** | **** | *** | ** | ** | * | - | - | - |
| HMRBI-11 | **** | **** | *** | ** | ** | * | - | - | - |
| HMRBI-12 | **** | **** | *** | ** | ** | * | - | - | - |
| HMRBI-13 | **** | **** | *** | ** | ** | * | - | - | - |
| HMRBI-14 | **** | **** | *** | ** | ** | * | - | - | - |
| HMRBI-15 | **** | **** | *** | ** | ** | * | - | - | - |
| HMRBI-16 | **** | **** | *** | ** | ** | * | - | - | - |
| HMRBI-22 | **** | **** | *** | ** | ** | * | * | * | - |

Keynote: High growth (****), Dense growth (**), Slight growth (*), and No growth ()

Most microorganisms were inhibited at the MIC 800 ppm. However, the isolate HMRBI-22 was an exception, requiring a higher concentration of 900ppm. The significance of this 100ppm difference is that HMRBI-22 is less susceptible (or more resistant) to the antimicrobial compound than the other isolates tested, demanding an additional 100 ppm for effective inhibition. As shown in Table 14, bacterial growth in the presence of heavy metals such as $Cd^{2+}$ and $Co^{2+}$ was found to affect the

proliferation of HMBIs at 200–1000 ppm HMs concentration. The data showed that bacterial growth decreased as the concentration of these metals increased. Notably, *C. ferments* HMRBI-5 and *K. oxytoca* HMRBI-22 exhibited sensitivity to $Cd^{2+}$ and $Co^{2+}$ separately at varying concentrations. *C. ferment* HMRBI-5 demonstrated resistance to $Co^{2+}$ with a MIC of 800 ppm, while *K. oxytoca* HMRBI-22 showed resistance to $Cd^{2+}$ with a MIC of 900 ppm (Table 13). The data also revealed that as the concentration of each HM increases, the growth of the HMRBIs population decreases. At lower concentrations (200ppm), these HMRBIs were less inhibited by HMs, suggesting a level of tolerance to HMs. However, as concentrations increased, the toxic effects of $Cd^{2+}$ and $Co^{2+}$ became more pronounced, leading to a sharper decline in these HMRBIs' growth patterns. This trend indicates that higher levels of these HMs disrupt bacterial cell processes. This concentration-dependent inhibition reflects how certain bacteria may initially resist lower levels of metal toxicity but become increasingly susceptible as the concentration rises, ultimately affecting their growth.

### 4.1.10. FTIR Analysis against heavy metal-exposed bacterial biomass

In this study, Figures (8a-d) present the FTIR acquisition spectra of HMRBI's biomass before and after treatment with HMs. Before HM treatment, the FTIR spectra exhibited peaks corresponding to the following functional groups: O-H (hydroxyl), $–NH_2$ (amine), –OH (hydroxyl), C=O (carbonyl), and C=C (alkene). For HMRBI-1, the treated samples displayed a shift in the peak positions to 2614.12 $cm^{-1}$ and 1256.62 $cm^{-1}$. Similarly, the peak of HMRBI-2 shifted to 2614.12 $cm^{-1}$ and 1256.22 $cm^{-1}$. These spectral changes indicate alterations in the functional groups associated with amines, amides, carbohydrates, carboxylic acids, carbonyls, and phosphates. Additional functional groups, such as R−CH=O (aldehydes), C-H (alkanes), C=C (alkenes), (C≡C) alkynes, aromatic compounds, hydroxyls, and ketones, may also interact with the bacterial cell wall. The observed shifts in peak positions suggest cellular composition and biomolecular structure modifications in response to HM stress. The reduction of HMs is believed to occur by a complexation formation involving hydroxyl, carbonyl, and amine moieties located within the spectral region of 1000 to 1100 $cm^{-1}$.

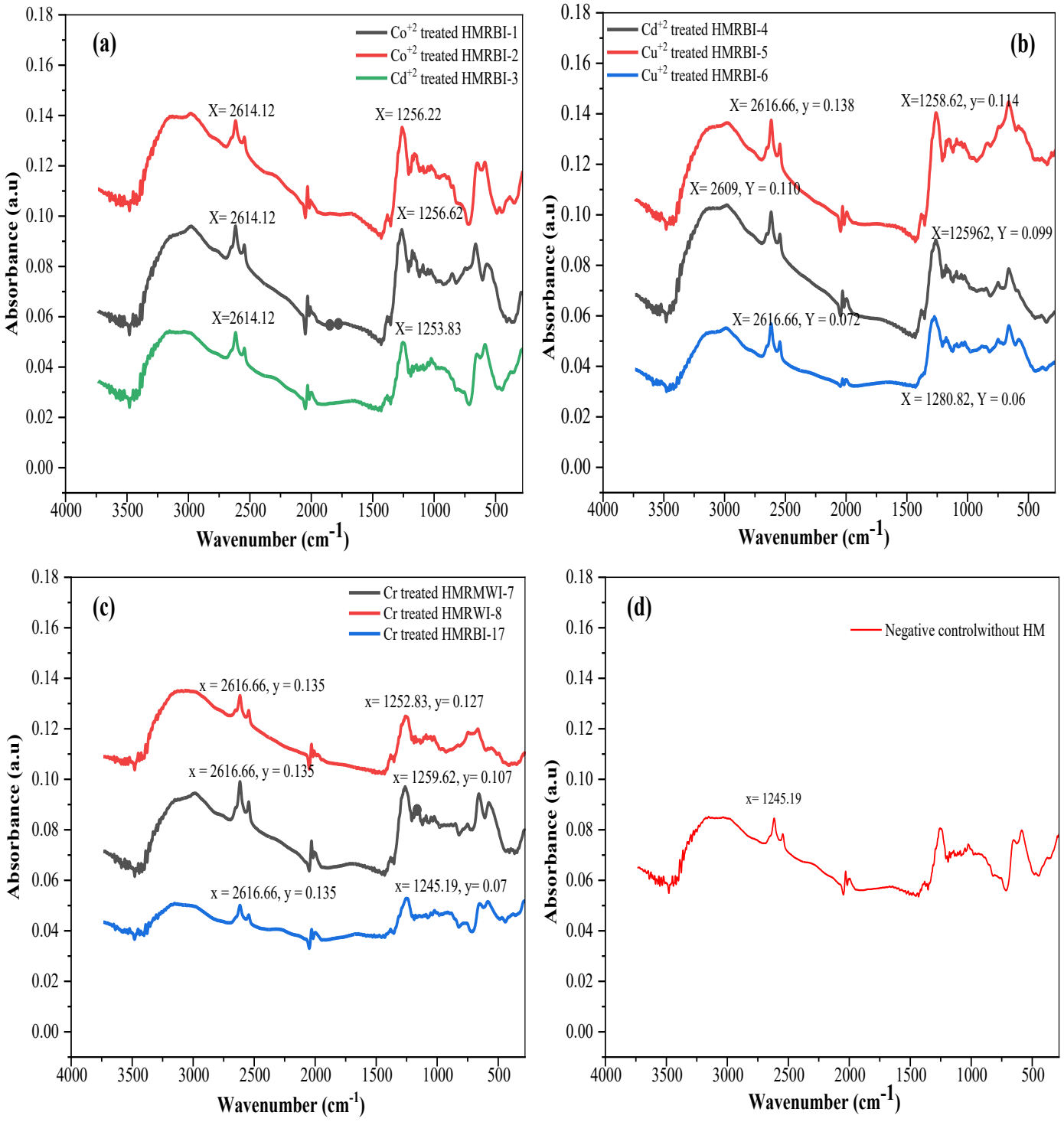


**Figure 8: The Fourier transform infrared spectra of the HMRBIs (a, b, c, and d) treated with 300µg/mL concentration of HMs showed different metabolic profiles compared to the control (d). FT-IR spectra of HMRBI grown in Nutrient broth containing cadmium sulphate, cobalt nitrate, potassium chromate, copper sulphate, and then compared to the control.**

The FTIR spectra of the treated bacterial biomass demonstrated a pronounced peak intensity, suggesting a higher concentration of specific functional groups. This observation is particularly noteworthy for bacterial samples exposed to varying levels of HMs. Figures (8a-d) provide a detailed comparison of the qualitative and quantitative changes in different functional groups within both treated and untreated bacterial species. These findings align with previous research conducted on the *Bacillus* spp. (Idrees et al., 2023). In Pakistan, a study explored the bioremediation of lead contamination using FTIR techniques. A similar study employed FTIR analysis to differentiate between bacterial isolates exposed to varying HM concentrations by identifying changes in the functional groups of biomolecules. The observed variations in the metabolic profiles of bacterial strains highlight the adaptability of these organisms in response to both HM stress and environmental fluctuations (Tiquia-Arashiro et al., 2023). Overall, the FTIR analysis presented in this study provides valuable insights into the impact of HM exposure on bacterial functional groups and metabolic processes. The findings contribute to a deeper understanding of bacterial responses to environmental stressors and have potential implications for bioremediation technologies.

As indicated in (Figures 8a-d), absorption peaks near 2614.12 and 1256.22 $cm^{-1}$ against loaded samples of HMRBI-2 and *P. putida*-HMRBI-4 (2609 $cm^{-1}$) biomasses, which were treated with $Cd^{+2}$, might be suggested for the presence of carboxylic acid O-H stretching and hydroxyl groups on the bacterial surface. Compounds might be employed to accumulate HMs. Previous study (Choudhary & Sar, 2009) also reported that absorption bands ($cm^{-1}$) were predicted between 2500-3300 for $Cd^{2+}$, $Co^{2+}$, $Cu^{2+}$, and $Ni^{2+}$ against *Pseudomonas* sp. J007. New peaks also emerged, which corresponded to HMs like $Co^{+2}$, $Cd^{+2}$, $Cr^{+3}$, and $Cu^{+2}$ (Figures $6_{a, b, c \& d}$). Another study exhibited that the absorption bands ($cm^{-1}$) were detected against Hydroxyl (3,493, *Raoultella* sp. L30; 3,493, *Serratia* sp. L2) and Amine (3,224-3,280, *Klebsiella* sp. R3), which are functional groups (Pagnucco et al., 2023).

Eastern Shewa is an excellent area for industrial development due to its proximity to the country's capital, Addis Abeba, and its location on the main Ethio-Djibouti road. As the industry expanded, cities were confronted with environmental issues. HM effluents discharged by these industries, and anthropogenic activities such as synthetic fertilizers, pesticides, and herbicides, may contaminate water and soil (Rashid et al., 2023). HMs damage ecosystem functions in runoff, which can remain in the environment for a decade and are non-biodegradable. Improper industrial disposal of e-waste and

domestic waste can lead to HM pollution (Kumar et al., 2023). When waste is not effectively managed, HMs can leak into soil and water, endangering the environment and human health. Consequently, a maximum concentration of HMs in the study area has devastating consequences. Chemical and physical methods of environmental pollution control can sometimes create new pollutants as a byproduct (Gunjyal et al., 2023). By contrast, bioremediation is a low-cost, safe, and environmentally friendly means of removing pollution that restores destroyed ecosystems (Sonune et al., 2018).

The fast expansion of industry and the use of effluent from factories in agricultural land have caused worries about the accumulation of HMs in agricultural soils. According to studies, the spatial distribution of HMs in industrial areas is much higher than in urban areas. Developing and developed countries are facing increasing environmental problems due to the contamination of water & soil by different HMs. However, the severe HM accumulation in the environment was higher in developing countries due to poor environmental management (Lemessa et al., 2022). In our study, HM assessments from soil and wastewater discharged from Bishoftu and Mojo with higher accumulation of $Cd^{+2}$, $Co^{+2}$, $Cr^{+6}$, $Cu^{+2}$, $Fe^{+2}$, $Mn^{+2}$, $Ni^{+2}$, $Pb^{+2}$, and $Zn^{+2}$ were recorded, which could affect the surroundings. In the present study, HM assessments from soil and wastewater discharged from Bishoftu revealed higher concentrations of $Cd^{+2}$, $Co^{+2}$, $Cr^{+2}$, $Cu^{+2}$, $Fe^{+2}$, $Mn^{+2}$, $Ni^{+2}$, $Pb^{+2}$, and $Zn^{+2}$, which could affect the environment. The results were compared to WHO standards, and suggestions (WHO, 2017). Soil organic matter, including carbon, phosphorus, and nitrogen, was studied, and findings were obtained. The average mean values for soil organic matter assessed were 0.779, 1.125, & 13.103 mg/kg, subsequently. The data also revealed that the soil organic matter of phosphorus was the maximum compared to the others, followed by carbon and nitrogen, which may be favorable for phosphate-solubilizing bacteria.

Similarly, on average, higher accumulations of HMs were detected. These HMs include Cr (3.689 mL/L), Mn (0.523 mL/L), Zn (0.649 mL/L), and Fe (2.396 mL/L), with their concentrations exceeding WHO standards (WHO, 2017) for the Mojo Tannery industry. The data showed that higher concentrations of these HMs resulted from chemicals used in leather tanning, which convert animal hides into leather and remove unwanted materials. The average chromium concentration in the Mojo tannery industry was higher than that of the other HMs assessed, at about 3.689 mL/L, with Fe

following. A similar study reported an increase in chromium levels in groundwater near industrial areas in Kollam District, Kerala, India (George et al., 2023).

Many colonies of HMRBIs that resist HMs were obtained from soil and wastewater effluents at the study sites. These isolates were proposed for HM bioremediation. These isolates, which resist cobalt and zinc, were identified as *A. hydrophila*, *E. aurantiacum*, *D. acidovorans,* and *P. putida* using MALDITOF-MS analysis at Wudassie Diagnostic Centre, Addis Ababa (Table 6). These isolates could play significant roles in various environmental applications. Bacteria can naturally withstand extreme conditions by actively accumulating HMs, converting these metals from highly toxic forms to less harmful ones. This ability plays a significant role in the cleansing of polluted environments. Studies have also been conducted on lead uptake by bacteria from industrial effluents (Idrees et al., 2023) as a means of bioremediation. According to Idrees et al., (2023), *B. cereus* and *Bacillus* spp. can resist up to 25 mM lead concentrations. It was also suggested that chromium bioremediation was achieved due to *B. paranthracis* and *B. paramycoides* from the polluted industrial sites (Kalsoom et al., 2023).

As shown in the Figures 5&6, the HMRBIs had various degrees of optimum growth conditions based on temperature and pH optimization. To maximize bioremediation, it's crucial to optimize conditions for bacterial growth in HM-contaminated environments. These optimal conditions, which vary based on the specific HM and bacterial species, are key to unlocking the full potential of bacteria to clean up contaminated sites. Figure 7 illustrates five heavy meta-resistance isolates from letters a to d and their optimal growth. For copper-resistant isolates from letters a and d, maximum optimal growth conditions were observed at 30 to 25ºC. Cadmium-resistant bacterial isolates demonstrated maximum growth at a temperature of 30 °C.

According to Syed et al. (2015) HM concentrations can affect bacterial growth. HMs such as arsenic, cadmium, chromium, cobalt, copper, lead, and mercury have toxic effects on bacteria and other organisms. The data presented in Tables 9 to 13 illustrate the growth performance of bacterial isolates to various HM concentrations spanning from 150 ppm, the minimum concentration, to 1050 ppm, the maximum. The data revealed that lower concentrations of HMs favor the growth of microorganisms, while higher concentrations could affect bacterial growth. Bacteria proliferated fastest at a concentration of 150 mg/L, decreasing as the concentration increased. The study also showed that

when bacteria are exposed to a high concentration of HMs, they can experience various detrimental effects. These metals can disrupt cellular processes and damage essential biomolecules such as proteins, enzymes, and DNA. This interference with cellular functions can lead to impaired metabolism, reduced growth rates, and even cell death (Balali-Mood et al., 2021). Bacteria have developed ways to withstand or resist HM toxicity by containing specific genes that encode for metal transporters and metal-binding proteins. This helps regulate and bioaccumulate HMs. These systems enable certain bacteria to grow and thrive in high metal concentrations.

### 4.1.11. SEM-EDX characterization of HMRBI bacterial biomass

The morphology of HMRBI biomass was analyzed and compared with the control after treatment with different HM concentrations. Characterization was performed using scanning electron microscopy (SEM) combined with energy-dispersive X-ray spectroscopy (EDX). The treatment was carried out at Haramaya University Institute of Technology. The cell structure and chemical properties of the bacterial biomass were characterized in (Figures 9a-d). SEM images demonstrated structural and chemical differences induced by treatment with various HMs, suggesting different levels of interactions and possible bioabsorption mechanisms, as shown in the figure. In the untreated/control sample, the surface of the biomass was relatively flat and homogeneous. Nevertheless, significant morphological changes were detected after exposure to cobalt (Co), cadmium (Cd), chromium (Cr), and zinc (Zn), including the presence of irregularities, rough surfaces, and structural deviations. The shifts indicate that the metals interact with each other differently, probably with ionic radii, valency state, and binding affinities. The EDX spectra also complemented the SEM data by yielding elemental composition information, which thereby substantiated the existence of the mentioned HMs on the treated biomass substrates, as shown in (Figures 9a-d). The intensity and the distribution of peaks of $Co^{+2}$, $Cd^{+2}$, $Cr^{+6}$, and $Zn^{+2}$ together reflected the level of metal bio-adsorption. Differences in spectral data between treatments were also evident and provided insight into metal uptake efficiency and possible binding mechanisms at the biomass surface. These findings underscore the significant impact of heavy metal exposure on each HMRBI.

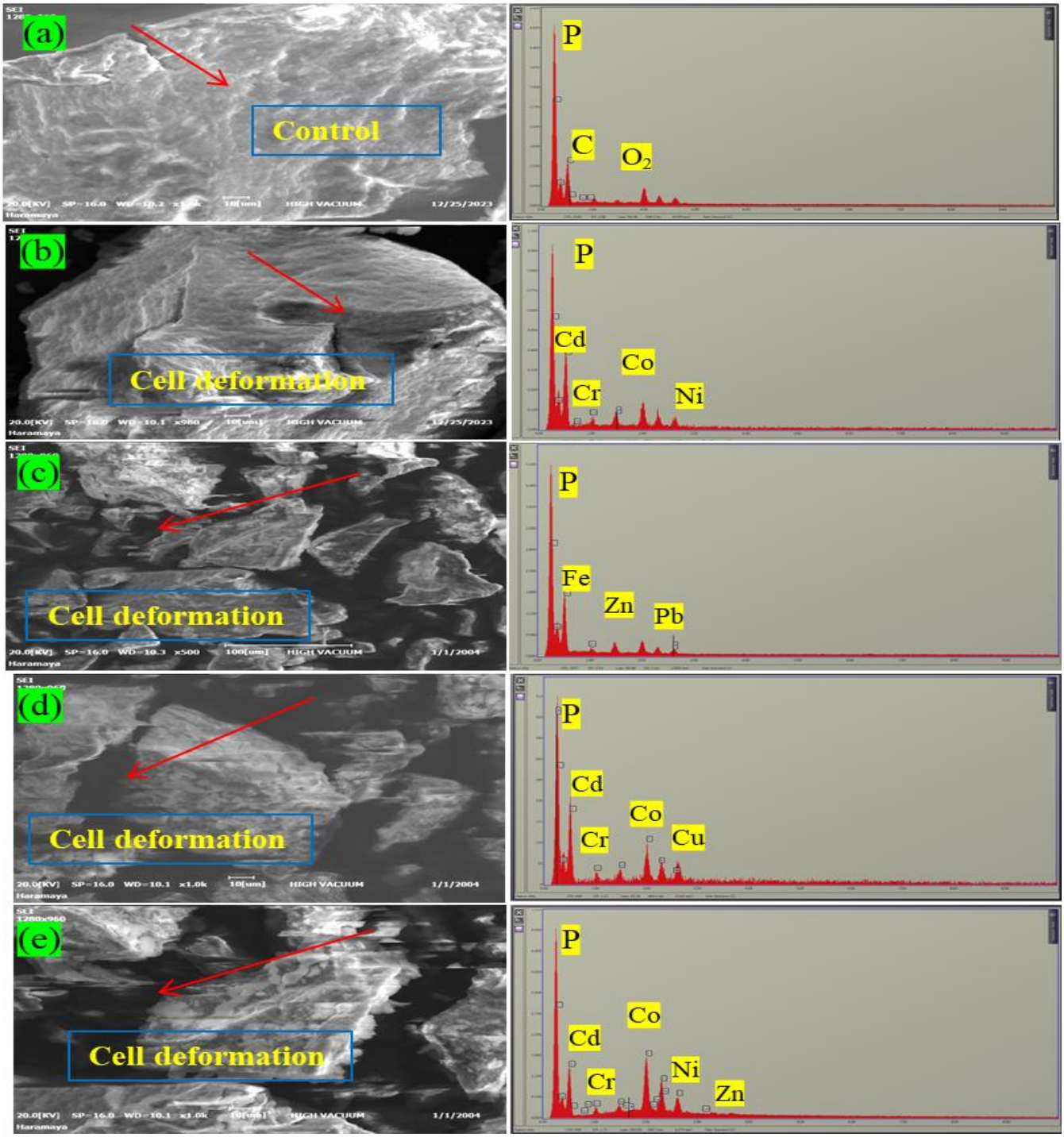


**Figure 9: Scanning electron micrographs (SEM) and Energy Dispersive X-ray (EDX) spectra of HMRBI grown in nutrient broth containing the following conditions: (A) control, (B) cobalt-treated, (HMRBI-1) (C) cadmium-treated, (HMRBI-5) (D) chromium-treated, (HMRBI-10). The EDX spectra peak shows the bioaccumulation of various heavy metals. The results were compared to a control sample with no heavy metals.**

For $Co^{+2}$, $Cd^{+2}$, $Cr^{+6}$, and $Zn^{+2}$ treated biomass (Figure $9_{a-e}$), morphological deformations were noted for cell shape but were less significant than in untreated biomass (A). EDX imaging provides evidence of the existence of $Co^{+2}$ $Cd^{+2}$, $Cr^{+3}$, and $Zn^{+2}$ on the cell surface, as shown in (Figures 9a-e), contrasting with the untreated HMRBI isolates. Overall, the conclusions drawn in (Figures 9a-e) indicated that metal ions are responsible for the change in cell structure and deformation. Bacterial cell shape deformation may be the peptidoglycan layer containing various functional groups with binding affinity to HM ions. For this reason, the peptidoglycan layer is a complex molecule consisting of diverse functional groups such as amino groups, carboxyl groups, and hydroxyl groups. These groups can interact with HM ions through ionic bonds or coordinate covalent bonds. The sensitivity of this deformation is less pronounced in the untreated than in the treated biomass. Firincă et al. (2024) reported that exposure to lead ions ($Pb^{+2}$) caused *B. marisflavi* cells to deform and become irregular in shape, which supports our study. A similar study revealed that the exposure of hexavalent chromium caused *B. licheniformis*, *B. megaterium*, *Byssochlamys* sp., (Itankar & Patil, 2021) and *Candida maltose* were observed from shapes and irregularities during the removal of $Cr^{+6}$ (VI) from tannery waste in India (Aké et al., 2024).

The SEM-EDX spectroscopic analysis of bacterial isolate biomass morphology is observed. The microbial cell biomass of the isolates, upon exposure to HMs, showed significant differences, indicating their structural diversity compared to untreated samples. The changes in microbial structure revealed by SEM indicate that the isolates have a high affinity for HM uptake into the cells, which might pave the way for the detoxification of contaminated sites. The peaks observed in the presence of heavy metals show the complex interactions between the cells and the contaminants, offering insight into the ecological toxicity and possible biotechnological uses of heavy metal exposure. A similar study observed HM removal in the contaminated environment using indigenous bacterial strains, as reported by Firincă et al. (2024). The detection of the peaks in the biomass treated with heavy metals suggests that the elements chromium ($Cr^{+6}$), cadmium ($Cd^{+2}$), and cobalt ions ($Co^{+2}$) are certainly deposited onto the cell surface when one observes the peaks. This enrichment can be caused by surface binding metal ions to the surface of micro-organisms, forming surface complexes that could change the physical and chemical character of the cell surface. Thus, the present study confirms the findings of *B. megaterium* biomasses grown in the presence and absence of chromium, which binds to $Cr^{+6}$ and $Cr^{+3}$ ions (Elahi et al., 2019).

## 4.1.12. Bacterial DNA extraction and 16S rRNA gene sequencing

To investigate the genetic mechanisms underlying bacterial heavy metal resistance, it is crucial to thoroughly profile and extract DNA from bacterial isolates known for their reduction abilities. Detailed analysis of these DNA samples enables scientists to identify specific genes responsible for heavy metal resistance. These genes are thought to play a key role in allowing bacteria to survive and actively break down toxic contaminants. In our study, two bacterial species were utilized to explore the potential for heavy metal bioremediation. *P. benzoelyticum*-HMRBI-1 and *Citrobacter*-HMRBI-5 were selected for their resistance to cobalt and cadmium. Figure 10 is a picture of the bacteria highlighting their DNA bands.

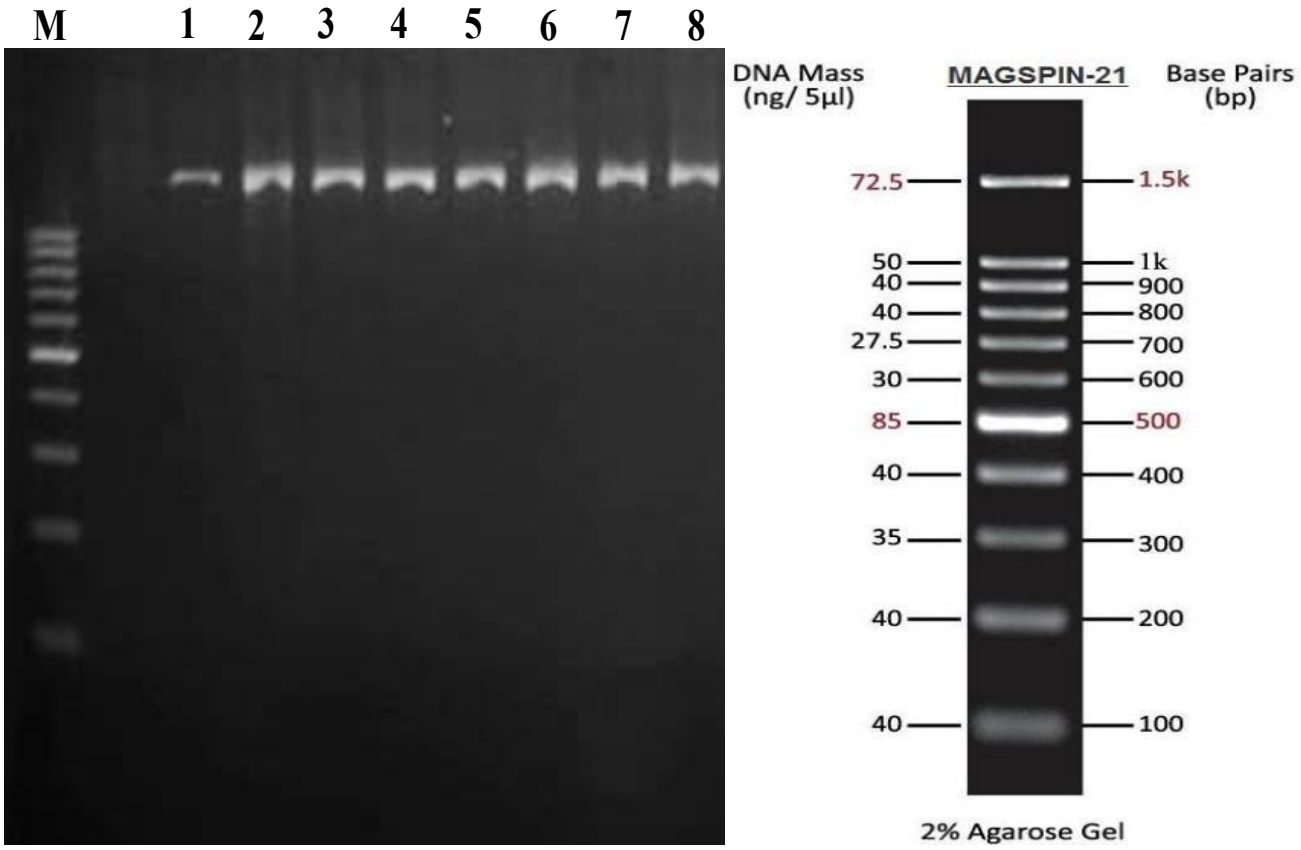


**Figure 10: This figure presents the results of 1.8% Agarose gel electrophoresis showing a single 1500 bp amplicon of the 16S rRNA gene from various HMRBIs. Lines 1, 2, 3, 4, 5, 6, 7, and 8 indicate different HMRBIs for PCR products, while the M line indicates a DNA ladder.**

### 4.4.7. Molecular characterization and phylogenetic tree against HMRBI

HMRBIs that could not be identified based on protein profiles (MALDI-TOF-MS) were further characterized using 16S rRNA gene sequencing. As indicated in Figures 11a-c, the recent isolate exhibited the highest sequence similarity with *P. benzoelyticum* JC272$^T$ (LBBT01000182) (99.79%). Bacterial strains such as *Pbifermentans* PAGU 1678T (LC385716) (99.71%), *Eubacterium tenue* DSM 20695$^T$ (FR749984) (97.80%), *Romboutsia lituseburensis* ATCC 25759$^T$ (M59107) (96.66%), *Intestinibacter bartlettii* DSM 16795$^T$ *(*ABEZ02000021) (96.18%) *Terrisporobacter hibernicus* MCA3$^T$ MZ497377 (95.40%), *Asaccharospora irregularis* DSM 2635$^T$ (X73447) (95.02%) and others were displayed close related with *P. benzoelyticum* HMRBI-1 (Figures 11a-c) and (Table 15). Since the closest sequence similarity of the recent isolate is 99.78% with *P. benzoelyticum* JC272$^T$ (LBBT01000182), the recent isolate could be *P. benzoelyticum* type strain. The strain was designated as *P. benzoelyticum* HMRBI-1(PQ625990) (Figures 11a-c) and (Table 15).

In a recent study, it was confirmed that HRBI-1 also showed sequence similarity with *Clostridioides difficile* DSM 1296$^T$ (CP011968) (94.90%) (Figures 11a-c) and (Table 15), a Gram-positive anaerobic rod-shaped bacterial strain. Table 15 indicates that the recent isolate, identified by 16S rRNA sequencing, shares sequence similarities of 99.71% and 99.65% with *P. bifermentans* subsp. *muricolitidis* PAGU 1678T (LC385716), and *P. bifermentans subsp. bifermentans* ATCC 638$^T$ (AB07576), respectively. The elucidation of this relationship could help unravel the adaptive strategies employed by HMRBI-1 & related bacteria in metal-polluted environments and could provide insight into bioremediation. The GC% contents of *P. benzoelyticum*-HMRBI-1 were predicted to be 53.14 % using a trustworthy online GC calculator, which is somewhat lower than the rest of the organism, as observed in Table 15. This indicates that bacteria with low GC content often have efficient genomes, which may enhance their ability to adapt to stressful environments, such as those contaminated with heavy metals. It also correlates with higher mutation rates, facilitating rapid evolution and the acquisition of resistance or degradation pathways.

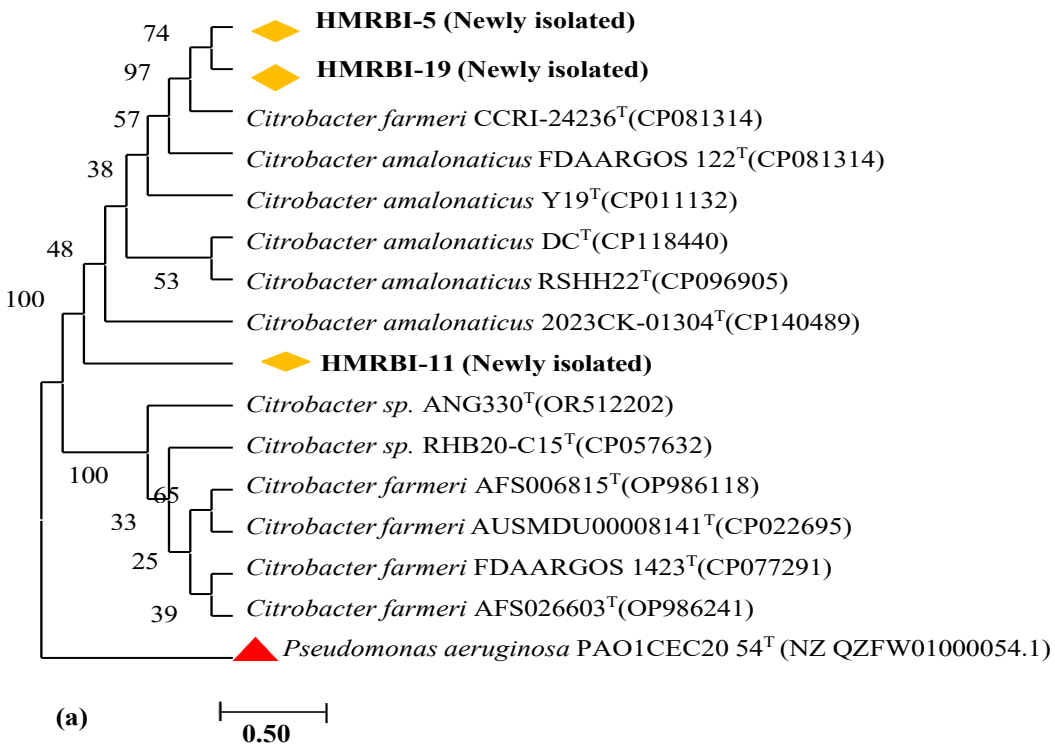
74
97
57
38
48
53
100
100
65
33
25
39
HMRBI-5 (Newly isolated)
HMRBI-19 (Newly isolated)
Citrobacter farmeri CCRI-24236T(CP081314)
Citrobacter amalonaticus FDAARGOS 122T(CP081314)
Citrobacter amalonaticus Y19T(CP011132)
Citrobacter amalonaticus DCT(CP118440)
Citrobacter amalonaticus RSHH22T(CP096905)
Citrobacter amalonaticus 2023CK-01304T(CP140489)
HMRBI-11 (Newly isolated)
Citrobacter sp. ANG330T(OR512202)
Citrobacter sp. RHB20-C15T(CP057632)
Citrobacter farmeri AFS006815T(OP986118)
Citrobacter farmeri AUSMDU00008141T(CP022695)
Citrobacter farmeri FDAARGOS 1423T(CP077291)
Citrobacter farmeri AFS026603T(OP986241)
Pseudomonas aeruginosa PAO1CEC20 54T (NZ QZFW01000054.1)
(a)
0.50

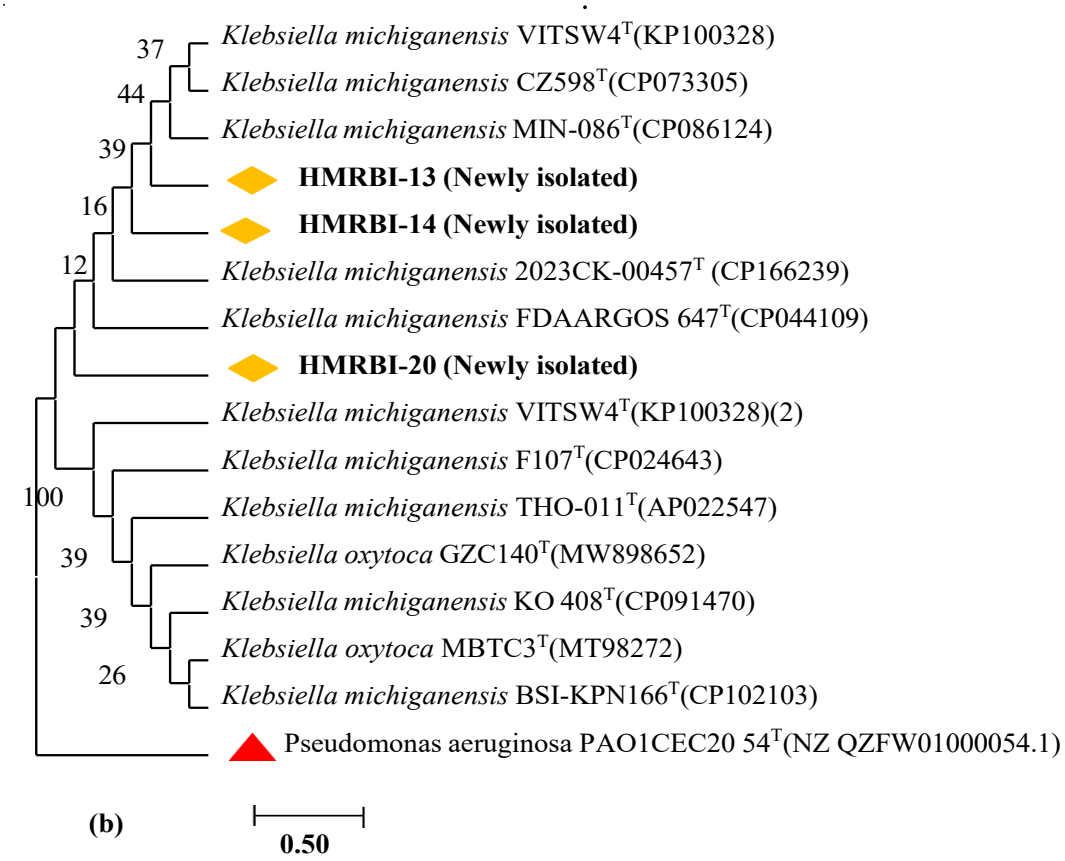
37
44
39
16
12
100
39
39
26
Klebsiella michiganensis VITSW4T(KP100328)
Klebsiella michiganensis CZ598T(CP073305)
Klebsiella michiganensis MIN-086T(CP086124)
HMRBI-13 (Newly isolated)
HMRBI-14 (Newly isolated)
Klebsiella michiganensis 2023CK-00457T (CP166239)
Klebsiella michiganensis FDAARGOS 647T(CP044109)
HMRBI-20 (Newly isolated)
Klebsiella michiganensis VITSW4T(KP100328)(2)
Klebsiella michiganensis F107T(CP024643)
Klebsiella michiganensis THO-011T(AP022547)
Klebsiella oxytoca GZC140T(MW898652)
Klebsiella michiganensis KO 408T(CP091470)
Klebsiella oxytoca MBTC3T(MT98272)
Klebsiella michiganensis BSI-KPN166T(CP102103)
Pseudomonas aeruginosa PAO1CEC20 54T(NZ QZFW01000054.1)
(b)
0.50

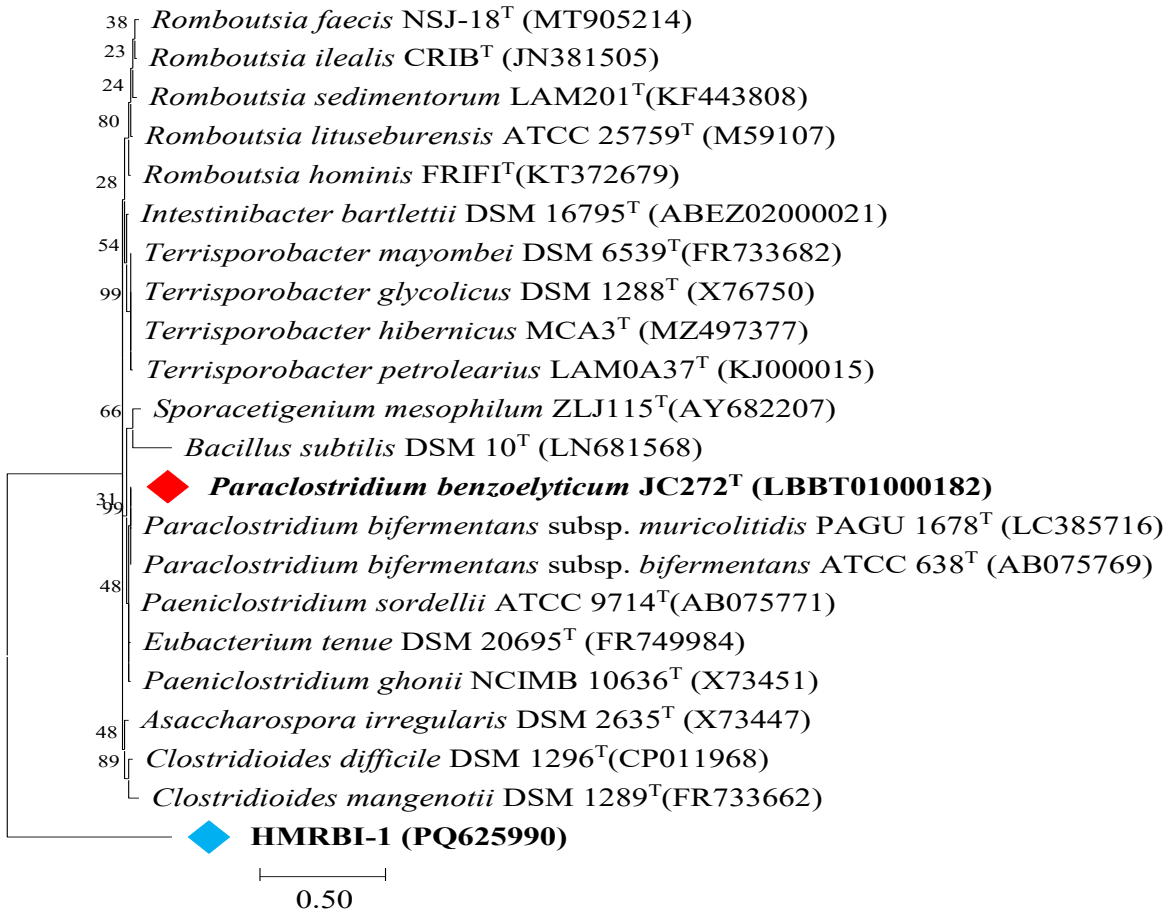


**Figures 11: A phylogenetic tree for identified bacteria isolates. The evolutionary history was inferred by using the Maximum Likelihood method and the Jukes-Cantor (Jukes et al., 1969). The tree with the highest log likelihood (-8030.41) is shown. The percentage of trees in which the associated taxa clustered together is shown above the branches. Initial tree (s) for the heuristic search were obtained automatically by applying Neighbor-Join and BioNJ algorithms to a matrix of pairwise distances estimated using the Jukes-Cantor model and then selecting the topology with the superior log likelihood value. The tree is drawn to scale, with branch lengths measured in the number of substitutions per site. This analysis involved 22 nucleotide sequences. Codon positions included were 1st +2nd +3rd Noncoding. There were a total of 1543 positions in the final dataset. Evolutionary analyses were conducted by (Tamura et al., 2021).**

The comprehensive analysis of these DNA samples enables scientists to detect specific genes associated with HMRB. In this study, isolates HMRBI-5 and HMRBI-14 were identified as *Citrobacter* and *Klebsiella* spp., respectively, based on 16S rRNA gene sequence analysis. These isolates were found to resist $Co^{2+}$ and $Cr^{6+}$, making them valuable for applications during HM

bioremediation. These bacteria have distinctive DNA banding patterns that indicate differences in their genetic structure. For instance, studies have identified heavy metal-resistant bacterial species such as *Pseudomonas*, *Bacillus,* and *Citrobacter* in the contaminated areas (Nnaji et al., 2024; Hassan et al., 2008).

As indicated in (Figure $11_{a\ \&\ b}$), the recent isolate exhibited the highest sequence similarity with *C. fermerii* (99.93%). Bacterial strains such as *C. fermerii* AUSMDU006815 (99.87%), *C. fermerii* CCRI24236 (99.80%), *C. amalonaticus* FDAARGOS-222 (99.77%), *C. fermerii* FDAAGOS-1423 (99.20%) *are very closely related to HMRBI-5* (This study). The findings of this study align with those of (Shan et al., 2022), who also demonstrated the effectiveness of microbial immobilization for heavy metal remediation. *The C. amalonaticus* Y-19 (99.0%), *C. freundii* CFNIH2 (99.01%), *C. fermerii* FS026603 (99.20%), *C. amalonaticus* 2023CK-01304 (98.94%), *C.* sp. cfnih20 (98.94%), *C.* sp. Y3 (98.87%), *C. amalonaticus* C3H (98.87%), *Citrobacter* sp. ANG330 (98.87%), *C. amalonaticus* C71 (98.87%), *Citrobacter* sp. RHB20-C15 (98.81%), *Citrobacter* sp. RHB-C16 (98.81%), *C. amalonaticus* RSHH22 (98.81%), and others displayed a close relation to HMRBI-5 but below 99.20% (Gomaa & El-Meihy, 2019).

On the other hand, HMRBI-14 display close similarity with *K. oxytoca* MBTC3 (99.85%), *K. michiganensis* MINI (99.85%), *K. michiganensis* 2023CK-00457 (99.85%), *K. michiganensis* X2 (99.77%), and close similarity with other (Edet et al., 2023). Both isolates were extremely successful agents for the bioremediation of HMs, dramatically reducing the concentration levels. That indicates how useful they can be in environmental restoration.

In this study, we investigated the species diversity within the genera *Citrobacter* and *Klebsiella* species using comparative genomics and phylogenetic tree approaches. The inclusion of *P. aeruginosa* strain PAO1CEC20 $54^{T}$ (GenBank accession no: NZ_QZFW01000054.1) as an outgroup provided a robust external reference point for tree rooting and evolutionary inference. The use of P. aeruginosa as an outgroup is justified by its placement in its phylogenetic tree outside of the Enterobacteriaceae family, which *Citrobacter* and *Klebsiella,* the newly isolated HMRBI, belong to, while remaining within the *Gammaproteobacteria* class. This taxonomic distance allows for effective polarization of branching patterns, thereby enabling clear distinction of evolutionary relationships among the *Citrobacter* and *Klebsiella* taxa.

**Table 15: 16S rRNA gene sequence for HMRBI-1 and other stains with sequence similarities**

| S.N. | The closest strain to the recent isolate | Strain | Accession Number | Pairwise Similarity (%) | Completeness (%) | GC% Contents |
|---|---|---|---|---|---|---|
| 1. | ***P. benzoelyticum*** | HMRBI-1 | PQ625990 | The recent | recent | 53.14 |
| 2. | *P. benzoelyticum* | JC272$^T$ | LBBT01000182 | 99.78 | 100 | 53.51 |
| 3. | *P. bifermentans subsp. muricolitidis* | PAGU 1678$^T$ | LC385716 | 99.71 | 98.52 | 53.39 |
| 4. | *P. bifermentans subsp. bifermentans* | ATCC 638$^T$ | AB075769 | 99.65 | 100 | 53.23 |
| 5. | *Paeniclostridium sordellii* | ATCC 9714$^T$ | AB075771 | 97.94 | 100 | 53.81 |
| 6. | *E. tenue* | DSM 20695$^T$ | FR749984 | 97.80 | 100 | 53.40 |
| 7. | *P. ghonii* | NCIMB 10636$^T$ | X73451 | 97.79 | 100 | 53.80 |
| 8. | *R. lituseburensis* | ATCC 25759$^T$ | M59107 | 96.66 | 99.86 | 52.88 |
| 9. | *I. bartlettii* | DSM 16795$^T$ | ABEZ02000021 | 96.18 | 100 | 53.75 |
| 10. | *R. faecis* | NSJ-18$^T$ | MT905214 | 95.94 | 95.37 | 52.50 |
| 11. | *R. sedimentorum* | LAM201 $^T$ | KF443808 | 95.73 | 93.96 | 52.88 |
| 12. | *R. hominis* | FRIFI$^T$ | KT372679 | 95.47 | 100 | 52.70 |
| 13. | *T. hibernicus* | MCA3$^T$ | MZ497377 | 95.40 | 100 | 52.28 |
| 14. | *T. mayombei* | DSM 6539$^T$ | FR733682 | 95.26 | 100 | 52.84 |
| 15. | *R. ilealis* | CRIB$^T$ | JN381505 | 95.12 | 100 | 52.90 |
| 16. | *A. irregular* | DSM 2635$^T$ | X73447 | 95.02 | 100 | 53.11 |
| 17. | *C. difficile* | DSM 1296$^T$ | CP011968 | 94.90 | 100 | 52.42 |
| 18. | *T. glycolicus* | DSM 1288$^T$ | X76750 | 94.83 | 99.72 | 52.78 |
| 19. | *T. petrolearius* | LAM0A37$^T$ | KJ000015 | 94.44 | 97.48 | 52.20 |
| 20. | *C. mangenotii* | DSM 1289$^T$ | FR733662 | 93.32 | 100 | 53.02 |
| 21. | *Sporacetigenium mesophilum* | ZLJ115$^T$ | AY682207 | 92.71 | 100 | 53.44 |

### 4.1.13. PCR amplification for certain heavy metal resistance genes (HMRGs)

HMRBI-14 is a bacterium selected for its capacity to grow in the presence of HMs. This property makes it useful for potential bioremediation applications. The HMRGs frequently code for resistance to specific metals, allowing the bacteria to thrive in toxic environments. Thus, in the HMRBI-14 genotype, the study aimed to determine the presence of the following HMRGs: *pcoC* (Cu), *cadD* (Cd), and *cnrA* (Co and Ni). The amplified genes were found to be 333, 155, and 422 bp (Figure 12). The PCR was used to amplify DNA sequences specific to these genes, as shown in Figure 12. This suggests that this isolate has a novel complement of copper, cadmium, cobalt, and nickel-resistance genes. The genes *pcoC*, *cadD*, and *cnrA* indicate adaptation to multiple heavy metal-contaminated environments against HMRBI-14. This suggests that the bacterium must have developed a means of detoxifying or extruding these metals. The strain HMRBI-5 appears to be a highly effective candidate for cleaning up environments, which contaminated by $Cu^{+2}$, $Cd^{+2}$, $Co^{+2}$, and $Ni^{+2}$. Its gene amplification indicates that it can tolerate and possibly detoxify these metals, indicating that the organisms likely employ a mechanism to increase the detoxification, efflux pump (extracellular and intracellular sequestration), enabling it to survive in an environment contaminated with HMs. It is a powerful genetic adaptation that provides a quantitative advantage in a contaminated setting. By having these genes, the bacteria can synthesize a superabundance of protective mechanisms such as detoxification, efflux pumps, and transporters Gaurav et al., (2023). This survival strategy in a hostile environment ultimately enables the organism to tolerate HM concentrations that would be lethal to non-adaptive counterparts. The amplified genes are, therefore, a direct molecular signature of the organism's evolved to HM contamination. Ojo et al. (2023) reported that the *P. aryabhattai* B8W22 strain is known for its ability to thrive in challenging environments and possesses several HMRGs. For example, a study noted the presence of genes such as *cadD*, which is a key component of the cadmium operon that detoxifies cadmium toxicity (Jebril et al., 2022; Zhu et al., 2024; Monsieurs et al., 2011), whereas *cnrA*, is a part of the cobalt-nickel resistance gene found in many bacterial species (Siunova et al., 2025). On the other hand, the *pocC* gene is directly related to functionally heavy metal resistance to copper. Therefore, these findings demonstrate that the key genes that can resist the presence of copper, cobalt, mercury, and nickel were investigated. These recent results confirm the essential nature of these genes for increasing the

capacity of bacteria (particularly isolated from heavy metal-polluted environments) for bioremediation. The genes allow bacteria to survive and even consume these toxins, and such abilities make them ideal candidates for bioremediation. A similar study was conducted, which corroborated the current findings, demonstrating that multiple resistance genes (*czcA*, *czcC*, and *czcS*) confer resistance to $Cd^{+2}$, $Zn^{+2}$, and $Co^{+2}$ as the bacterium *Bradyrhizobium* contained related genes isolated from Slag contaminated soils in Mexico (Montes-Montes et al., 2025).

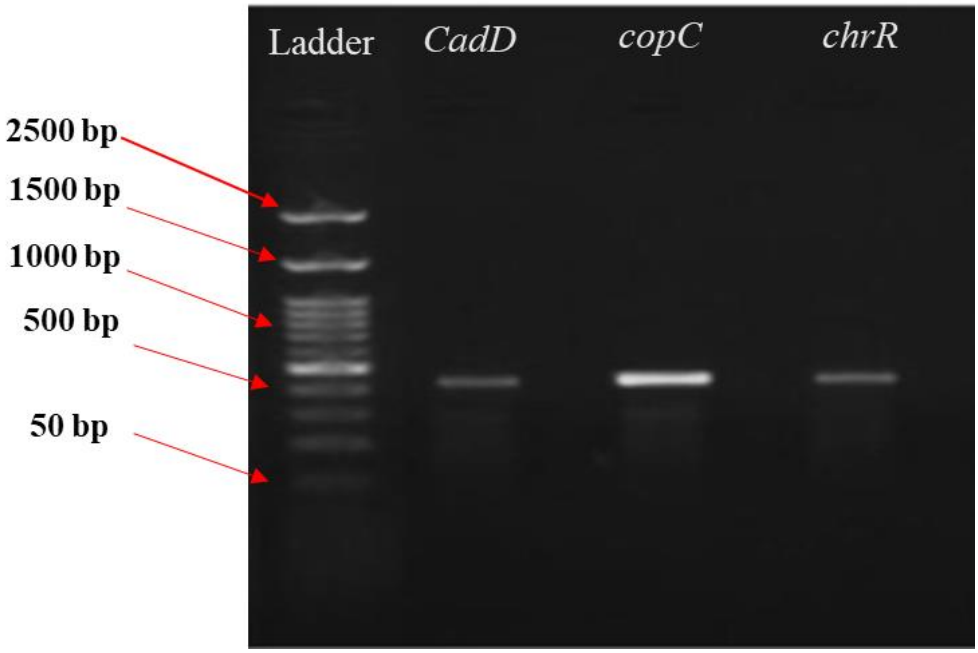


**Figure 12*:* Amplified HMRGs in HMRBI-1, HMRBI-5, and HMRBI-14. Key: A (amplified *cadD, copC,* and *chrR* genes). *CadD amplicon of P. benzoelyticum, copC, amplicon Citrobacter spp., and chrR amplicon Klebsiella spp.***

The capacity of HM to inhibit bacterial isolates likely stems from its significant toxicity. This high level of toxicity can disrupt essential cellular processes within the bacteria, rendering them unable to thrive or reproduce effectively. As a result, the presence of HM acts as a potent inhibitor of bacterial growth and potentially affects the overall microbial community in the environment (Ojo et al., 2023; Zeyaullah et al., 2010). Most of the bacteria isolated in this study exhibited significant resistance to high concentrations of cadmium, $Co^{+2}$, $Cu^{+2}$, $Cd^{+2}$, $Cr^{+6}$, and $Zn^{+2}$. This observation aligns with the findings of Terzi & Civelek, (2021), who similarly reported that their bacterial isolates were capable of tolerating elevated levels of mercury. These

results suggest that certain bacterial strains possess inherent or adaptive mechanisms that allow them to thrive even in environments contaminated with HMs, potentially pointing to their utility in bioremediation efforts. The consistency of these findings across studies underscores the robustness of these bacterial species in withstanding heavy metal stress.

### 4.1.14. Transcriptional start site and promoter determination

Pinpointing the transcriptional start sites (TSS) is essential for interpreting the intricacies of gene expression. The TSS marks the precise nucleotide where transcription begins, and understanding this location is fundamental to understanding how a gene is turned on and off. Conceptually, the TSS is situated downstream of the promoter region, which is the specific stretch of DNA where the RNA polymerase enzyme initially binds. This binding event is a prerequisite for transcription initiation, effectively positioning the enzyme to begin synthesis of RNA at the TSS. Knowing the TSS allows investigators to study regulator elements that control gene expression, such as promoters and enhancers, to understand how these elements can affect gene expression. To accurately predict promoter regions and interpret patterns of gene expression, as well as build and understand genetic regulatory networks, a correct prediction of promoter sites has become a necessary element (Lai et al., 2019).

NNPP version 2.20 databases were utilized to work out the TSS, which is often used in HMRGs. In this investigation, the promoter region focuses on the 1kb stretch of DNA immediately upstream of the TSS, under the assumption that this region contains the key regulatory elements controlling gene activities. As presented in (Table 16), the predicted TSS locations for each of the HMR gene coding sequences. This analysis revealed that individual HMR genes can have multiple TSSs ranging from 1 to 38. Interestingly, the minimum and maximum of the TSS values identified correspond to the specific genes *CzcA*/*CzcB* and *CadD* respectively as shown in (Table 16. The *CzcD* and *CadA* genes exhibited identical TSS, located at the positions -323 and 303 on their respective strands. These TSS were situated at a considerable distance away from the protein-coding regions (codons) of these genes.

The position of the start codon plays a significant role in both the initiation of transcription and the regulation of gene expression. Its locations can either enhance or inhibit gene regulation.

Analysis of the current study revealed that approximately 36.67% of TSS were located on the negative DNA strands, while 73.33% were found on the positive strands, as presented in (Table 16). For genes on the negative strand, the TSS positions ranged from 38 (*CutC*) gene to 550 (*ChrB* gene). On the positive strand, the TSS position varied from 30 (*CadC*) gene to 2994 (*CzcA*) gene. Specifically, *CzcA* and *CzcB* exhibited the highest predicted TSS values (2944 and 1415, respectively), identified using the NNPP tool. The *CadC* gene, conversely, displayed the minimum predicted TSS values of 30.

A deeper analysis revealed that all the identified genes play a crucial role in HM bioremediation. The genes encode proteins involved in a variety of processes related to HM detoxification and resistance. Specifically, the identified genes contribute to functions such as chromate efflux (pumping chromate out of the cell), chromate transport (moving chromate across a membrane), zinc efflux (removing excess zinc), cadmium translocation (moving cadmium with the cell), cadmium resistance (a mechanism that protects the cell from cadmium toxicity), cadmium transport (moving cadmium across cell membrane), copper resistance (mechanisms that protect the cell from copper toxicity), copper bioremediation and arsenate pumping and reduction (removing arsenate from the cell and converting it into a less toxic form) (Table 16) provides a summary of these gene functions.

**Table 16: TSS, its promoter predictive score values, and distance from the 5′UTR region of the corresponding gene predicted**

| S. N | Gene ID | Gene Symbol | No TSS identified | The predictive score cut-off value of 0.80 | L. of TSS from the start codon | Gene Function |
|---|---|---|---|---|---|---|
| 1. | 66323649 | *ChrA* | 5 | 0.97, 0.90, 0.81, 0.98, 0.81 | -45 | Chromate efflux |
| 2. | 66323648 | *ChrB* | 3 | 0.81, 0.98, 0.97 | -550 | Chromate transporter |
| 3. | 60820444 | *CzcA* | 1 | 0.88 | 2994 | Zinc efflux pump |
| 4. | 60820445 | *CzcB* | 1 | 0.88 | 1415 | Zinc efflux pump |
| 5. | 50136911 | *CzcD* | 19 | 1.00,0.94,0.99,0.85,0.83,0.99,0.98,0.89,0.83,0.87,0.98 ,1.00,0.99,1.00,0.99,1.00,0.99,0.90,0.96 | -323 | Zinc transporter |
| 6. | 72447367 | *CadA* | 19 | 0.92,0.95,0.97,0.83,0.97,0.87,0.94,0.99,0.94,0.99,0.93 ,0.93,1.00,0.87,0.83,0.96,0.97,0.98,0.90 | 303 | Cadmium translocating |
| 7. | 69569638 | *CadC* | 16 | 0.95,0.84,0.97,0.98,0.88,0.92,0.95,0.87,0.83,0.97,0.87 ,0.94,0.99,0.94,0.99,0.99 | 30 | sensing metalloregulator transcriptional repressor |
| 8. | 66840924 | *cadD* | 38 | 0.88,0.91,0.99,0.95,0.91,0.91,0.95,0.98,0.99,0.97,0.87 ,0.86,0.99,1.00,0.96,0.96,0.82,1.00,0.91,0.99,100,1.00 ,0.97,1.00,0.89,0.92,0.93,0.81,0.99,0.85,0.90,0 | 379 | Cadmium resistance and transporter |
| 9. | 67467524 | *CutC* | 20 | 0.93,0.98,0.82.0.93,0.90,0.86,0.94,0.93,0.98,0.84,0.85 ,0.96,0.99,0.87,0.81,1.00,0.97,0.92,0.98,1.00 .94,0.99,0.97,0.95,0.99,0.97 | -38 | Copper resistance |
| 10. | 67451619 | *CopC/D* | 4 | 0.83, 0.99, 0.89, 0.90 | 688 | copper resistance |
| 11. | 75085266 | *ZnuA* | 12 | 0.99,0.98,0.85,0.86,0.93,0.95,0.92.0.81,0.86,0.89,1.00 ,0.98 | 99 | Zinc transporter substrate binding |
| 12. | 75088734 | *ArsA* | 10 | 0.95,0.90,0.84,0.90,0.95,0.84,0.95,0.81,0.82,0.83 | 423 | arsenate pump |
| 13. | 68608930 | *ArsB* | 21 | 0.90,0.83,0.93,0.96,0.81,0.88,0.97,0.82,0.95,0.83,0.91 ,0.85,0.92,0.81,0.92,0.99,1.00,0.86,0.98,0.95,0.84 | 440 | arsenate efflux transporter |
| 14. | 68608929 | *ArsC* | 17 | 0.85,1.00,0.92,0.90,0.98,0.83,1.00,0.94,0.99,0.81,0.90 ,0.92,0.89,0.87,0.96,0.95,0.95 | 607 | arsenate reduction |
| 15. | 68610477 | *ArsR* | 24 | 1.00,0.89,0.92,0.99,0.85,0.99,0.98,0.93,0.92,0.99,0.99 ,1.00,0.99,0.97,0.92,0.96.0.82,0.93,0.94,0.82,0.94,0.8 3,0.93,0.97 | 537 | arsenate regulation |

The NNPP tool prediction findings are considered reliable at 0.8 cutoff values for the prokaryotic organism.

### 4.1.15. Prediction of common Motif and TFs

Gene expression is influenced by multiple factors, with sequence motifs playing a critical role. In this study, five essential common motifs were predicted and analyzed using the MEME Suite algorithm (version 5.5.2, available at https://memesuite.org/meme/). The analysis identified CMFs_3 as the top candidate motif. With an e-value of 1.3e-009, CMF_3 was found in seven promoter regions and had a motif width of 50 (Table 17). Compared to 84 motifs in the MEME database, CMFs_3 exhibited the lowest e-values, indicating a high degree of statistical significance, and possessed 63.64% of binding sites. Table 17 further showed that the number of promoter binding sites ranged from 6 to 8, with corresponding e-values between 3.0e-010 and 3.8e-010/3.0e-009. Interestingly, the CMFs-4 candidate motif had a similar number of binding sites as the top candidate motif CMFs_3, as presented in (Table 17).

**Table 17: List of predicted motifs and the number and proportion of promoter-containing motifs**

| S. N | Searched candidates Motifs | The number of promoters % for each motif | e- value [a] | Motifs width | No binding sites |
|---|---|---|---|---|---|
| 1. | CMFs_1 | 8 (72.73%) | 3.0e-010 | 40 | 8 |
| 2. | CMFs_2 | 6 (54.55%) | 3.8e-010 | 50 | 6 |
| 3. | CMFs_3 | 7 (63.64%) | 1.3e-009 | 50 | 7 |
| 4. | CMFs_4 | 7 (63.64%) | 1.6e-010 | 50 | 7 |
| 5. | CMFs_5 | 6 (54.55%) | 3.0e-009 | 50 | 6 |

[a] Possibility of discovery of a similarly well-conserved motif in random sequences.

A motif with a very e-value of 1.3e-009 was discovered, indicating a high degree of statistical significance and strongly suggesting that this motif plays a distinct and important biological role. This highly significant motif was subsequently subjected to analysis using the TOMTOM database version 5.5.2, a freely accessible and widely used software tool. The analysis was used to compare the identified motif against a database of known regulatory elements such as transcriptional factors, and binding sites, and thereby which transcriptional factors might be bound to this novel motif, This comparison allows us to infer the potential regulatory element

function of the motif and understand how it might influence gene expression (Bailey & Elkan, 1994; Bailey et al., 2015).

TOMOTM, a tool that was used in the LOGOSS algorithm, compares discovered sequence motifs against known transcriptional factor binding sites. TOMTOM output provides information about potential interactions with known transcriptional factors, including whether the interaction involves activation, repression, or dual regulatory functions. Additional details regarding the conformation of these transcriptional factors (monomers, dimers, tetramers, etc.) were predicted and summarized in Tables 19 and 20. In this analysis, the motif CMFs_3 showed a high degree of similarity to known transcriptional factor binding sites, exhibiting very low e-values of 1.3e-009, indicating strong statistical significance. Nine transcriptional factors from the database matched this motif with an e-value of 14 or lower. Figure 13 shows a visual representation of the forward and reverse strands of these statistically significant matches of the strands.

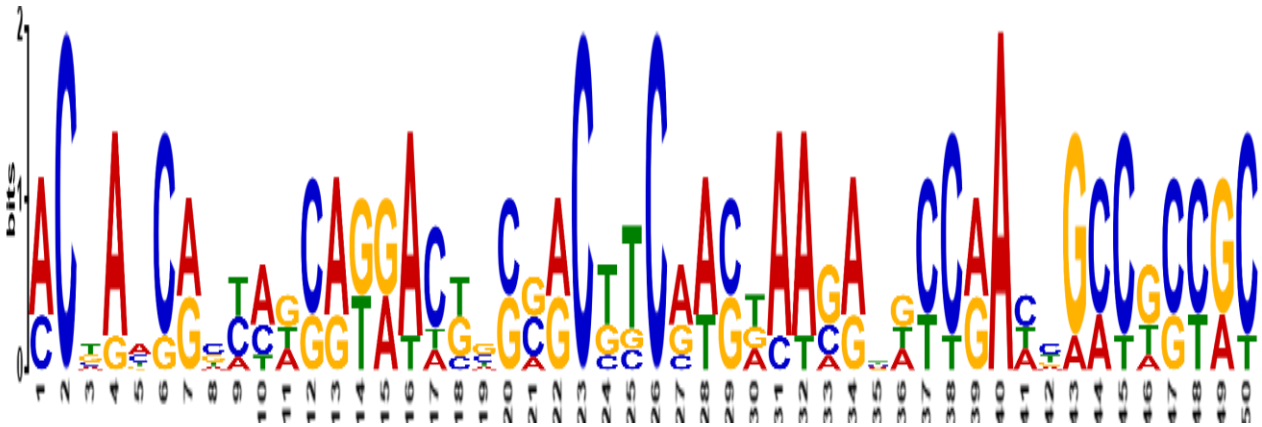

**Figure 13: The Sequence logos for HMR predicted common motifs. MEME suite version 5.5.2 was utilized for the prediction. A sequence logo is a graphical representation of the consensus sequence of a set of aligned nucleotide (DNA) sequences. It provides a visual summary of the conservation and variability of each position within the sequence motif.**

Transcription factors regulate gene transcription, their copying into RNA, on the way to protein making. A TF is a sequence-specific DNA-binding protein that controls the transcription of a set of genes and thus regulates gene expression in a cell (Kim et al., 2021). Thus, for this study about nine transcriptional factors were identified from TOMTOM databases that handle the regulation of gene expression in the bacterium of HMR. *AmrZ*, *ArgR*, *CcpA, Fur, HexR*, *HrpX*,

*IhfA, Lrp, PhhR*, *PvdS*, *RpoN*, and *VqsM*, are transcriptional factors with diverse functions in gene regulation and expression. The primary functions of these transcriptional factors were activation and repression as seen in (Table 18). *P. aeruginosa* PAO1, *Streptococcus pneumoniae*, *P. putida* KT2440, *Xanthomonas oryzae*, *Vibrio cholerae, Shewanella oneidensis, Salmonella enterica, Helicobacter pylori, Lactococcus lactis,* and *E. coli* as revealed in (Table 18). The sequences of all motif-binding sites were obtained from prokaryotic organisms.

**Table 18: Lists of matching candidates from EXPREG transcription factor (TF)**

| S. N | Candidate of TF | Strains that show motif sequence binding | GC (%) | Regulatory Elements | | | | Statistical Significance |
|---|---|---|---|---|---|---|---|---|
| | | | | Activation (%) | Repression (%) | Dual (%) | Not specified (%) | |
| 1. | *HrpX* | *X. oryzae* | 53.20 | 100 | 00 | 0 | 0 | 6.42e-02 |
| 2. | *AmrZ* | *P. aeruginosa* PAO1 | 60.21 | 16 | 31 | 0 | 51 | 4.11e-01 |
| 3. | *RpoN* | *V.cholarae* | 47.75 | 10 | 0 | 0 | 0 | 9.60e-01 |
| 4. | *HexR* | *S. oneidensis* | 21.72 | 30 | 69 | 0 | 0 | 1.69e+00 |
| 5. | *VqsM* | *P. aeruginosa* PAO1 | 59.33 | 7 | 0 | 0 | 92 | 2.02e+00 |
| 6. | *PvdS* | *P. aeruginosa* PAO1 | 48.33 | 100 | 0 | 0 | 0 | 2.23e+00 |
| 7. | *Lrp* | *E. coli* | 40.00 | 1 | 1 | 0 | 97 | 5.34e+00 |
| 8. | *IhfA* | *P. putida* | 10.00 | 100 | 0 | 0 | 0 | 5.82e+00 |
| 9. | *Fur* | *P. pylori* | 14.52 | 13 | 78 | 0 | 8 | 7.33e+00 |
| 10. | *ArgR* | *P. aeruginosa* PAO1 | 50.20 | 61 | 27 | 0 | 11 | 7.57e+00 |
| 11. | *Fur* | *S. enterica* | 28.33 | 26 | 73 | 0 | 0 | 8.08e+00 |
| 12. | *CcpA* | *L. lactis* | 33.46 | 69 | 30 | 0 | 0 | 8.20e+00 |
| 13. | *PhhR* | *P. putida* | 44.67 | 90 | 10 | 0 | 0 | 8.27e+00 |
| 14. | *CcpA* | *S. pneumoniae* | 32.21 | 68 | 31 | 0 | 0 | 9.28e+00 |

*HrpX*: transcriptional regulator, *AmrZ:* Transcriptional activation and biofilm formation, *RpoN*: gene expression*, HexR:* regulation of glucose metabolism, *PvdS:* encodes putative sigma factor*, Lrp*: Leucine-responsive regulatory protein; *IhfA*: Integration host factor subunit alpha; *CcpA*: Catabolite control protein A; *ArgR:* arginine biosynthesis, *Fur* is Ferric uptake regulation protein; *PhhR is* phenylalanine hydroxylase regulator, and *VqsM* is virulence and QS modulator.

Analysis of (Table 18 reveals key insights into the roles of transcriptional factors (TF). Ten specific TFs, *HrpX*, *AmrZ*, *RpoN*, *HexR*, *PvdS*, *Lrp*, *CcpA*, *ArgR*, *PhhR*, and *IhfA,* were predicted to function exclusively as transcriptional activators, each exhibiting 100% activation. While these and other TF were identified, the precise mechanism and target genes of many remain to be elucidated. A significant portion of identified TFs, including *Lrp* and *VqsM*, currently have unknown functions, highlighting a gap in our understanding of the regulatory landscape.

Further investigation, employing a combination of computational and experimental approaches, is crucial to decipher the roles of these uncharacterized TFs. However, none of the identified TFs were observed to possess dual functionality, acting as both activation and repression. This suggests that, at least within this dataset, TFs tend to specialize in both activation and repression. While most identified TFs appear to be activators, the two most potent repressors identified were *Fur* and *HexR*. These TFs demonstrated a strong repressive influence affecting 78% and 69% TF gene expression, respectively. This substantial repressive activity suggests that *Fur* and *HexR* play critical roles in controlling gene expression under specific conditions. However, despite *Fur* and *HexR*, the overall trend observed in the data indicates a greater prevalence of TF activation compared to repression.

Furthermore, the characterized TF *PhhR* stands out due to its versatility and broad applicability in biotechnological applications, particularly in the environmental domain. *PhhR* demonstrated potential in different fields, including agriculture, bioremediation in bioplastic degradation. Specifically, *PhhR* has been successfully employed in conjunction with various organic pollutants. This capability underscores a significant potential of *PhhR* in addressing pressing environmental challenges and promoting sustainable practice (Nelson et al., 2003). Furthermore, the conformational assessment presented in (Table 19) details the application of a TF conformational approach to the identified transcriptional factors, considering their existence as monomers, dimers, and tetramers. For instance, 35.71% of the identified TFs' conformational modes were not known while 7.14 and 21.43% were identified as monomer and dimer TF conformation mode applications. As shown in (Table 19), no transcriptional factors were associated with the tetramer TF conformational mode.

**Table 19: Lists of matching candidates from EXPREG transcription Confirmation Factor**

| S. N | Candidate of TF | Strains that show motif sequence binding | GC (%) | TF Confirmation Mode | | | | Not Specified (%) | Statistical Significance |
|---|---|---|---|---|---|---|---|---|---|
| | | | | Monomer (%) | Dimer (%) | Tetramer (%) | Other (%) | | |
| 1. | *HrpX* | *X. oryzae* | 53.20 | 80 | 20 | 0 | 0 | 0 | 6.42e-02 |
| 2. | *AmrZ* | *P. aeruginosa* PAO1 | 60.21 | 0 | 0 | 0 | 0 | 99 | 4.11e-01 |
| 3. | *RpoN* | *V.cholarae* | 47.75 | 100 | 0 | 0 | 0 | 0 | 9.60e-01 |
| 4. | *HexR* | *S. oneidensis* | 21.72 | 0 | 0 | 0 | 0 | 100 | 1.69e+00 |
| 5. | *VqsM* | *P. aeruginosa* PAO1 | 59.33 | 0 | 0 | 0 | 0 | 100 | 2.02e+00 |
| 6. | *PvdS* | *P. aeruginosa* PAO1 | 48.33 | 0 | 0 | 0 | 0 | 100 | 2.23e+00 |
| 7. | *Lrp* | *E. coli* | 40.00 | 0 | 96 | 0 | 0 | 3 | 5.34e+00 |
| 8. | *IhfA* | *P. putida* | 10.00 | 0 | 50 | 0 | 0 | 50 | 5.82e+00 |
| 9. | *Fur* | *P.pylori* | 14.52 | 0 | 82 | 0 | 0 | 17 | 7.33e+00 |
| 10. | *ArgR* | *P. aeruginosa* PAO1 | 50.20 | 0 | 16 | 0 | 0 | 83 | 7.57e+00 |
| 11. | *Fur* | *S. enterica* | 28.33 | 0 | 100 | 0 | 0 | 0 | 8.08e+00 |
| 12. | *CcpA* | *L. lactis* | 33.46 | 0 | 0 | 0 | 0 | 100 | 8.20e+00 |
| 13. | *PhhR* | *P. putida* | 44.67 | 0 | 100 | 0 | 0 | 0 | 8.27e+00 |
| 14. | *CcpA* | *S. pneumoniae* | 32.21 | 0 | 100 | 0 | 0 | 0 | 9.28e+00 |

***HrpX*: transcriptional regulator, *AmrZ:* Transcriptional activation and biofilm formation, *RpoN*: gene expression, *HexR:* regulation of glucose metabolism, *PvdS:* encodes putative sigma factor, *Lrp*: Leucine-responsive regulatory protein; *IhfA*: Integration host factor subunit alpha; *CcpA*: Catabolite control protein A; *ArgR:* arginine biosynthesis, *Fur* is Ferric uptake regulation protein; *PhhR is* phenylalanine hydroxylase regulator, and *VqsM* is virulence and QS modulator.**

### 4.1.16.Genome re-annotation & genome mapping of *C. gilardii* CR3 genome

Circular genome mapping for *C. gilardii* CR3 genomic DNA was performed using a Prokka online server that can be accessed at https://proksee.ca/which replaced CGView. GC content, open reading frame (ORF), GC skew (+/-), rRNA, starting codon, stop codon, regulatory elements, and CDS were predicted on the genome mapping (Figures 4a, b, and c). The sequence of *C. gilardii* CR3 was obtained via the NCBI database and re-annotated utilizing subsystem category distribution technology. An analysis was performed on the circular genome for *C.*

*gilardii* CR3 which showed the position of GC content, sequence length, and/or contigs, stop, start, ORF, GC skew +, and GC skew (Figures 14a-c). Several genes have been thought to be associated with HMR mechanisms in environments with contamination, following the current investigation. Genes such as *chrA*, *chrB, chrR*, *arsA*, *arsB*, *copC*/*D*, czcA, *czcB*, czcD, czc ABC, *cadiC*, and *cadiC* play a significant role in the polluted environment to clean or decrease pollutant levels after it had been expressed (Figures 14a-c).

Similar investigation of circular genome analysis for the *trehalase* gene from the complete genome of *Shigella* sp. PAMC28760 from Antarctica was predicted with CDS, GC contents, rRNA, tRNA, GC skew$^{+,}$ and GC skew$^{-,}$ and ORFs have been predicted (Shrestha et al., 2022). The RAST server identified genes with their functions, locations, and levels of protein expression for *C. gilardii* CR3 (CP010516.1), and other related strains shown (Figure 14a-c). For the current study, the number of coding sequences (3399), GC contents (67.7), contigs (1), shortest contig size (3539530), media sequence sizes (3539530), mean sequence sizes (3539530.0), longest contig sizes (3539530), the sequence length in base pairs ($N_{50}$ values) (not predicted) and the smallest number of contigs ($L_{50}$) (1) whose length sum makes up half of genome size were predicted.

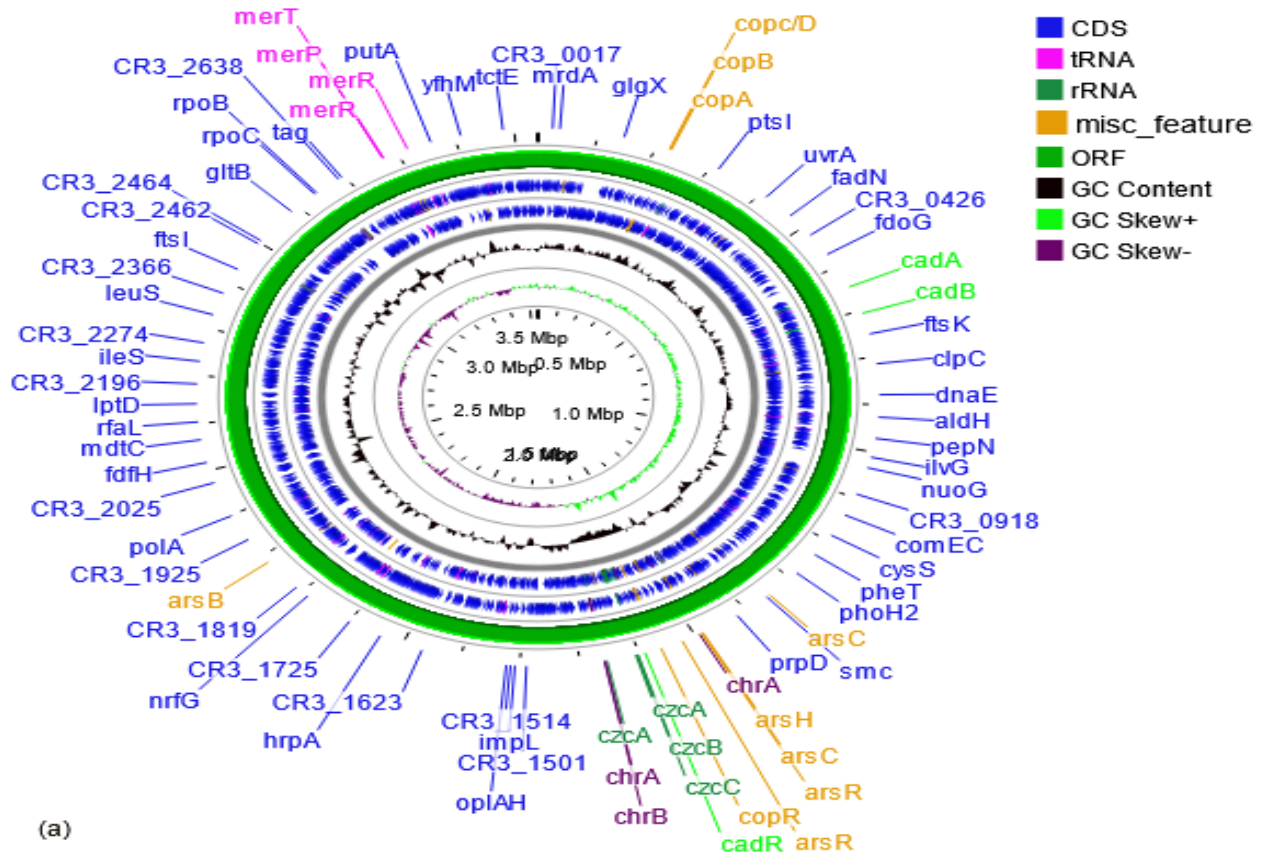
merT
merP
merR
merR
tag
rpoC
rpoB
CR3_2638
putA
yfhM
tctE
CR3_0017
mrdA
glgX
copc/D
copB
copA
ptsI
uvrA
fadN
CR3_0426
fdoG
cadA
cadB
ftsK
clpC
dnaE
aldH
pepN
ilvG
nuoG
CR3_0918
comEC
cysS
pheT
phoH2
arsC
prpD
smc
chrA
czcA
arsH
arsC
arsR
copR
cadR
arsR
czcA
czcB
czcC
chrA
chrB
CR3_1514
impL
CR3_1501
oplAH
hrpA
CR3_1623
CR3_1725
nrfG
CR3_1819
arsB
CR3_1925
polA
CR3_2025
fdfH
mdtC
rfaL
lptD
CR3_2196
ileS
CR3_2274
leuS
CR3_2366
ftsI
CR3_2462
CR3_2464
gltB
3.5 Mbp
3.0 Mbp
0.5 Mbp
2.5 Mbp
1.0 Mbp
1.5 Mbp
CDS
tRNA
rRNA
misc_feature
ORF
GC Content
GC Skew+
GC Skew-
(a)

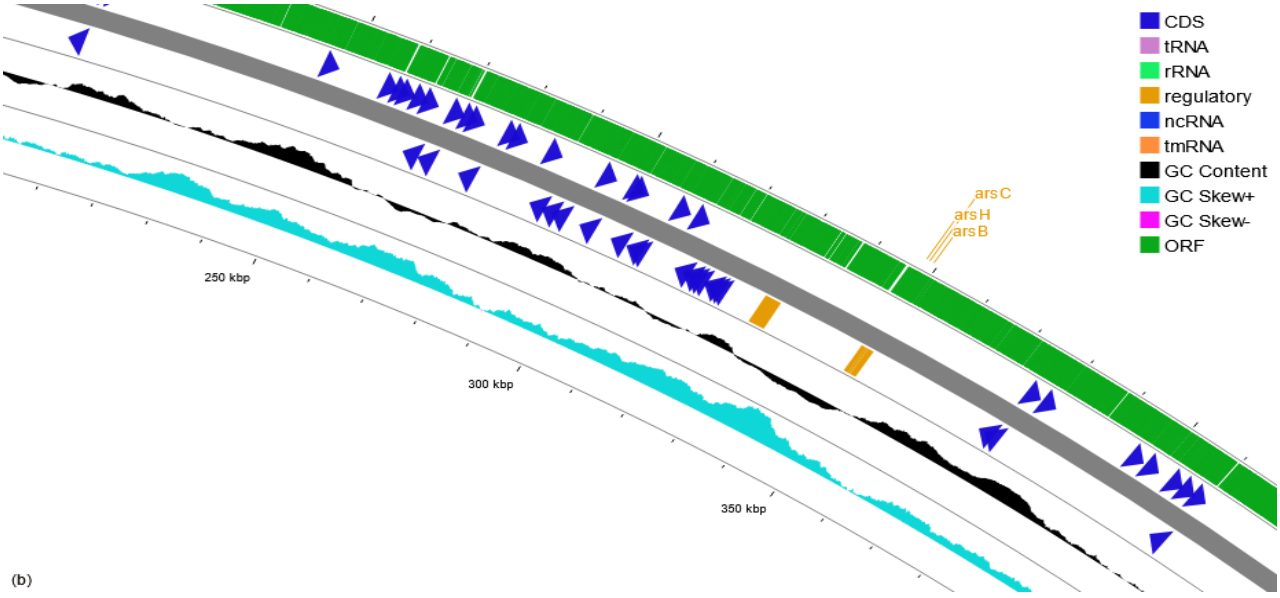
arsC
arsH
arsB
250 kbp
300 kbp
350 kbp
CDS
tRNA
rRNA
regulatory
ncRNA
tmRNA
GC Content
GC Skew+
GC Skew-
ORF
(b)

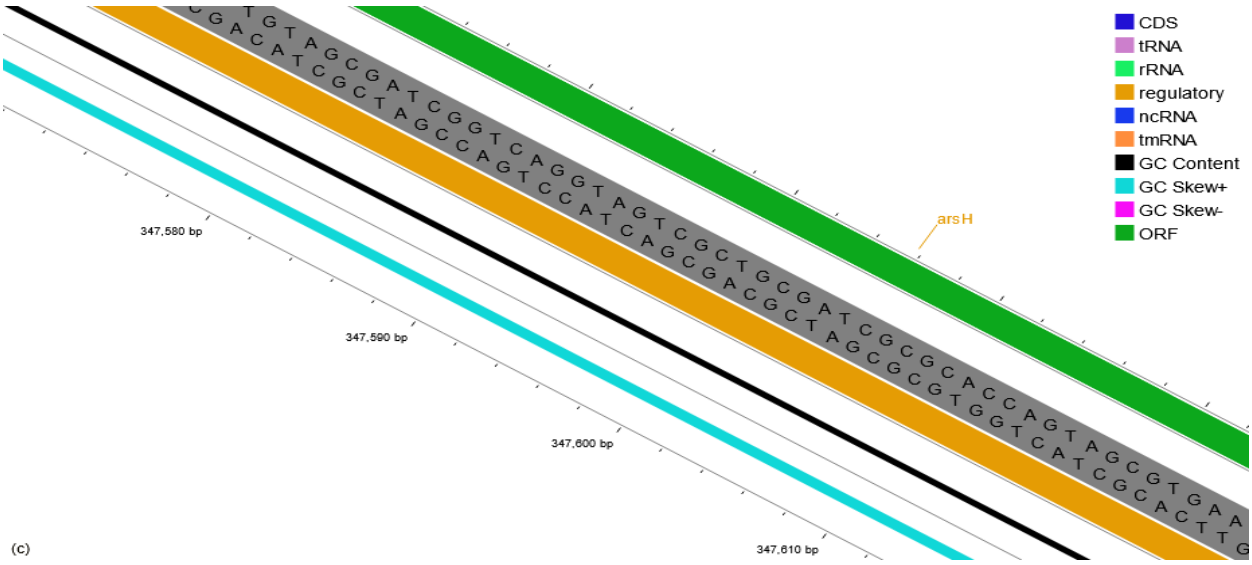


**Figure 14: (a) Graphic circular genome mapping for *C. gilardii* CR3 and a sequence obtained from the NCBI database with accession number CP010516.1. (b) Zoomed circular genome map for *C. gilardii* CR3 obtained from NCBI. (C) Zoomed circular genome map with the location of sequence length and/or contigs, stop, start, ORF, GC skew $^{+}$, and GC skew $^{-}$**

The prediction revealed that the genome contains multiple genes involved in co-factor production, chromosomal replication initiator protein DnaA, vitamin biosynthesis, protein metabolism, nitrogen metabolism, RNA metabolism, nucleosides and nucleotide biosynthesis, stress response and aromatic compound metabolism, copper-sensing two-component system response regulator, mercuric resistance operon regulatory protein, lead, cadmium, zinc and mercury transporting ATPase, and chromate transport protein in (Figure 15a.)

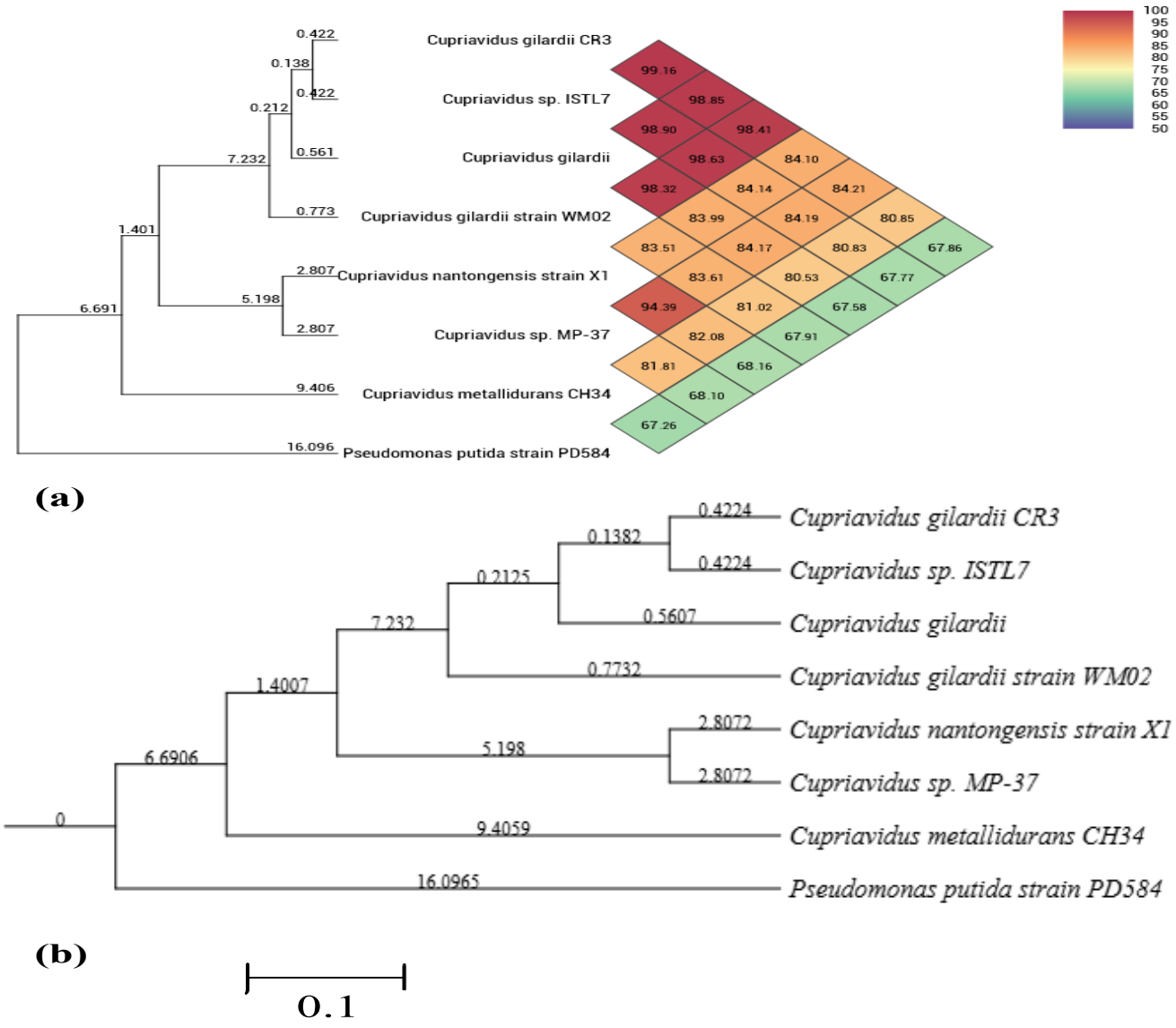


Comparative genome analysis, primarily by using OrthoANI provide definite evidence for classifying different bacterial isolates. The highest degree of similarity is directly correlated to taxonomic rank, allowing to accurately place an unknown isolate within the phylogenetic tree. For 95−96%, the isolates are considered to belong to the same species. This is the standard threshold for species classification in modern prokaryotic taxonomy. For 99−100%, the isolates are very closely related strains of the same species. The minimal difference is likely minor strain-level variation. 70−95%, the isolates belong to the same genus, but are clearly different species. And <70%, the isolates are likely from different genera or even higher taxonomic ranks (Chun et al., 2018).

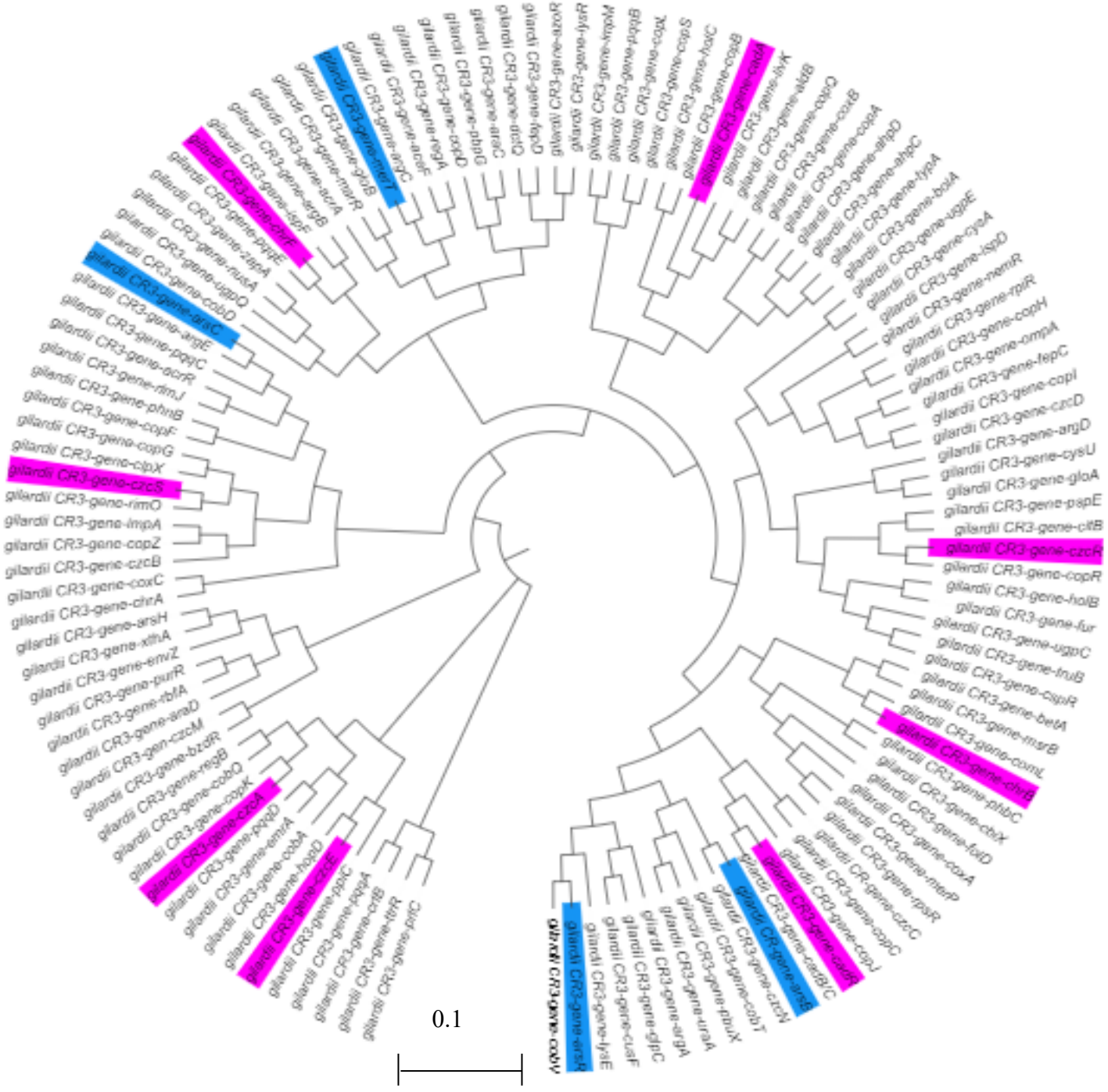


**Figure 15: (a) Sequence similarity of OrthoANI and the other closely related strains, (b). Phylogenetic tree and evolutionary relationships of taxa for *Cupriavidus gilardii* CR3, (c). A circular phylogenetic analysis of the complete genomes of *C. gilardii* CR3. The phylogenetic tree shows various heavy metal resistance gene locations in the complete genomes.**

### 4.1.17. Comparative genome analysis by using OAT Software tools

The 16S rRNA sequences were obtained from WGS of *C. gilardii* CR3 (CP010516.1) and related other strains such as *C. metallidurans* CH34 (NC_007973.1), *C. nantongensis* X1 (CP014844.1), *Cupriavidus sp.* ISTL7 (CP066227.10156), and *Cupriavidus sp.* MP-37 (NZ_CP085344). The phylogenetic tree was constructed using the OAT offline server. The sequences were aligned with ClustalW. *P. putida* PD584 (CP115665.1) was used as an out-group in (Figure 15a-b).

The neighbor-joining method was used to infer evolutionary history (Saitou et al., 1987). The investigation connected eight nucleotide sequences as one nucleotide sequence was used as an out-group. All locations having gaps & missing data were eliminated. Finally, the evolutionary relationship investigation was performed with the OAT offline server (Felsenstein, 1985). *P. putida* PD584 (CP115665.1) was selected and used as an outgroup in the evaluation; other related sequences were obtained from the EzTaxon-e server and annotated with the RAST server before tree construction. (b) UPGMA dendrogram, Heatmap for OrthoANI (Lee et al., 2016). OrthoANI values of ≥ 96% show grouped genomes originating from strains of the same species in (Figures 15a and b).

A circular phylogenetic analysis of the complete genome of *C. gilardii* CR3 (CP010516.1) was studied. The phylogenetic tree shows the location of HM resistance genes in the complete genome of the organism in (Figure 15c). The data also shows that *C. gilardii CR3* is 99.41% related to *Cupriavidus* sp. ISTL7. A (Figures 15a-b) shows that *C. gilardii* CR3 (CP010516.1) has a close relationship to *Cupriavidus* sp. ISTL7 (CP066227.10156) and *C. gilardii* MW02 (CP104386.1) and less related to that of *C. nantongensis* X1 (CP014844.1) and *C. metallidurans* CH34 (NC_007973.1. The 16S rRNA gene sequence results of *C. gilardii* CR3 (CP010516.1) were highly evolutionarily related to *Cupriavidus* sp. ISTL7 (CP066227.10156), *C. gilardii*, *C. gilardii* WM02 (CP104386.1), and *Cupriavidus* sp MP-37 (NZ_CP085344.1) as seen in (Table 22).

The data also revealed that less evolution was related to that of *C. metallidurans* CH34 (NC_007973.1). Thus, the evolutionary relationship between the organisms was 99.41, 98.85, 98.41, and 94.39%, respectively (Table 22). OrthoANI again revealed a weak correlation among

*C. metallidurans* CH34 (NC_007973.1) compared with the *C. gilardii* CR3 (Figures 15a-b). As shown in (Figure 15a and b), the sequence similarity of OrthoANI between *C. gilardii* CR3 (CP010516.1) & *Cupriavidus* sp. ISTL7 (CP066227.10156), *C. gilardii CR3* (CP010516.1) *C. gilardii*, *C. gilardii* CR3 (CP010516.1) & *C. gilardii* WM02 (CP104386.1), *C. gilardii* CR3 (CP010516.1) & *C. nantongensis* X1 (CP014844.1), *C. gilardii* CR3 (CP010516.1) & *Cupriavidus* sp. MP-37 (NZ_CP0 85344.1), *C. gilardii* CR3 (CP010516.1), and *C. metallidurans* CH34 (NC_007973.1) were 99.41, 98.85, 98.41, 84.10, 84.21, and 80.85% (Figures 15a-b).

The larger sequence similarities among the current genome annotated sequences of our strains were calculated between *Cupriavidus gilardii* CR3 (CP010516.1) and *Cupriavidus* sp. ISTL7 (CP066227.10156), OrthoANI is a genomic similarity measuring technique. It was utilized to evaluate the same species of the organism with a demarcation cut-off value of 95-96%, and massive comparison tests showed that both algorithms produced identical reciprocal similarities (Figures 15a-b) which confirm our phylogenetic tree. Accordingly, the OrthoANI obtained between *C. metallidurans* CH34 (NC_007973.1) and *P. putida* PD584 (CP115665.1) as well as other related genera in the present investigation were lower than the demarcation cut-off values.

**Table 20: Features of re-annotated genomic DNA for *C. gilardii* CR3 genome, its allied reference strains, and out-group**

| S. N | Part of genomic information | As uploaded and after splitting into scaffolds | | | | | | |
|---|---|---|---|---|---|---|---|---|
| | | *C. gilardii* CR3 | *C. metallidurans* CH34 | *C. nantongensis* X1 | *C.* sp. ISTL7 | *C.* MP-37 | *C. gilardii* WM02 | *P. putida* PD584 |
| 1. | Accession No | CP010516.1 | NC_007973.1 | CP014844.1 | CP066227.1 | NZ_CP085344.1 | CP104386.1 | NZ_CP115665.1 |
| 2. | Taxonomy ID | 82541 | 266264 | 1796606 | 2771360 | 2884455 | 82541 | 303 |
| 3. | Sequence size | 3539530 | 6913352 | 4619400 | 3314946 | 3615976 | 3511514 | 5913415 |
| 4. | No coding sequ. | 3399 | 6603 | 4525 | 3221 | 3354 | 3323 | 5375 |
| 5. | Number of contigs | 1 | 4 | 3 | 207 | 1 | 1 | 1 |
| 6. | GC content (%) | 67.4 | 63.5 | 66.2 | 67.7 | 67.5 | 67.4 | 61.6 |
| 7. | Shortest cont. size | 3539530 | 171459 | 1150655 | 19 | 3615976 | 3511514 | 5913415 |
| 8. | Media seq. size | 3539530 | 2580084 | 1728946 | 564 | 3615976 | 3411514 | 5913415 |
| 9. | Mean seq. size | 3539530 | 172833.0 | 1539800.0 | 16014.2 | 3615976.0 | 3511514.0 | 5913415.0 |
| 10. | Longest cont. size | 3539530 | 3928089 | 1739799 | 169580 | 3615976 | 3511514 | 5913415 |
| 11. | $N_{50}$ values | Not predicted | 3928089 | 17289946 | 71905 | Not predicted | Not predicted | Not predicted |
| 12. | $L_{50}$ values | 1 | 1 | 1 | 16 | 1 | 1 | 1 |
| 13. | Number of RNA | 61 | 74 | 63 | 60 | 67 | 61 | 96 |
| 14. | No of subsystems | 285 | 366 | 316 | 275 | 302 | 289 | 364 |

The data were predicted and generated by RAST and SEED technologies.

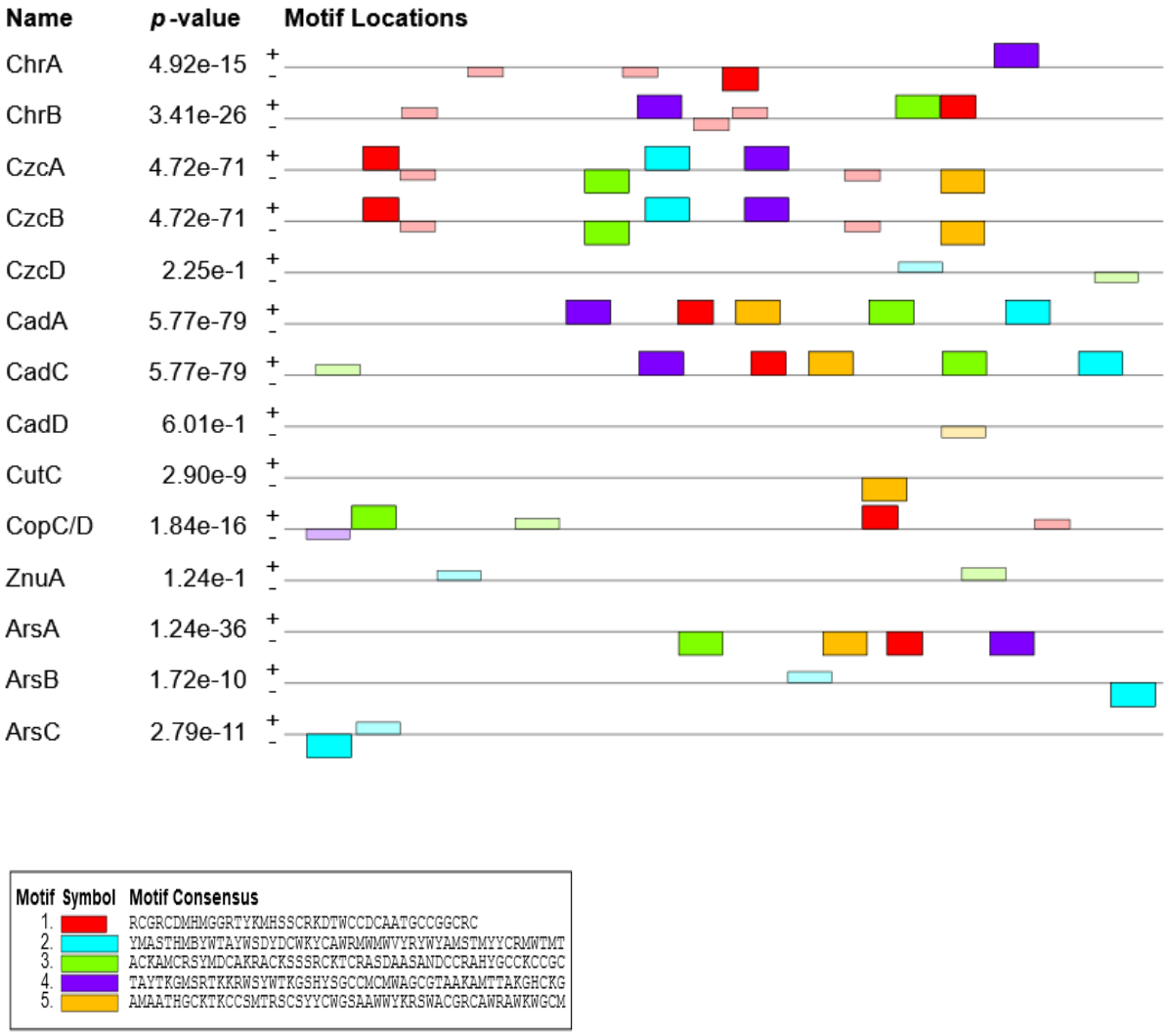


**Figure 16: Block diagrams illustrate the relative location of potential motif + scanned sites in the promoter region relative to TSSs (Transcription Start Sites). The bottom of the graph indicates the locations of nucleotides in the promoter region of heavy metal resistance genes. The locations range from the beginning of the TSS (+1) to upwards of 1 kb (-1 kb) of the MEME suite outcome.**

The objective of this work was regulatory elements analysis and comparative genome analysis of HMR bacteria extracted from *Cupriavidus gilardii* CR3 as a means of HM bioremediation. Sequence-specific DNA-binding, TFs are usually revealed as "main regulators" because they bind to DNA and either activate or suppress gene expression. The identification of a gene's TSS precedes the identification of the upstream promoter region, making gene expression analysis easier. Most of the sequences in this study showed multiple transcriptional start sites, which accounted for about 86.67% (Table 17). As a result, the gene sequence in consideration may have

alternate transcription possibilities. However, TSS with a higher threshold value was evaluated for better prediction, that related to earlier studies reported by (Dibbisa & Wagari, 2022). Genes that have multiple TSS enhance transcription initiation and are more likely to respond to environmental changes, which agrees with the findings of (Dai et al., 2016).

Common motif identification was a core element of TF identification processes. Motifs recruit transcriptional factors, or regulatory elements, to properly target genes in gene expression processes (Alberts et al., 2002). MEME tools were utilized to identify a conserved candidate motif where these 14 transcription factors bind, and motif sites were discovered as shown in (Figure 16). In this study, common candidate motifs with different information content were identified. The densely populated motifs with their locations were found upstream between -100 and -600 (Figure 16). These motifs might take part in the regulation of recognized promoters with contributors to gene expression. In the present investigation, several binding sites were discovered in the promoter region of candidate motifs. These locations might enhance binding interactions and produce different regulatory effects (Aman Beshir & Kebede, 2021; Bantihun & Kebede, 2021).

The data also show that the gene *arsB* at locus_tag=CR3_1877 with CDS located at complement (2282267…2283709) was a membrane protein extracted from *Cupriavidus gilardii* CR3. In addition, the *arsC* and *arsH* genes at locus_tag=CR3_2746 and locus_tag = CR3_1262 were used as arsenate reductase and arsenical resistance functions, respectively. Moreover, the *arsR* gene with CDS complement (1487862...1488218) is in the genome of *C. gilardii* CR3, a family transcriptional regulator protein widely used for arsenate bioremediation capacities. Similar studies were performed in the complete genome of *C. metallidurans* CH34 as a model bacterium of HMR. Resisting heavy metals by tri-component efflux systems was identified in pMOL30, with *czcCBA* present with resistance to $Cd^{2+}$, $Zn^{2+,}$ and $Co^{2+}$ (Mergeay & Van Hroudt, 2021).

Environmental components such as soil and water-contaminated areas with heavy metals are potential sources of HMR bacteria. These microbes could reduce, oxidize, bio-accumulate, and efflux heavy metals through the cell membrane and are widely used in bioremediation processes (Razzak et al., 2022). According to the comparative analysis, the genome of *Cupriavidus sp.* ISTL37 is 99.41% identical to the genomes of *C. gilardii* CR3, as shown in (Figure 14a). A

similar finding was observed on the *C. metallidurans* MSR33 (Rojas et al., 2011), however, it was less related to *C. gilardii* CR3 as seen (Figure 14a).

*MerR* families include *merP*, the *MerT* protein that is widely distributed in the bacterium of the *C. gilardii* CR3, and mercury resistance has also been investigated in this study (Figure 14a). The findings are similar to those identified in the studies that identified the genes from *Eubacteria* (Permina et al., 2006). *C. gilardii* CR3 regulates heavy metals through transcriptional factors controlled by the *MerR*, *CopR*, *CadR,* and *ChrR* protein families. We also studied the cadmium, copper, arsenate, zinc, and chromium resistance genes of *CopB*, *CopC*, *CopCD*, *CopR CadA*, *CadB*, *CadR*, *ArsA*, *ArsB*, *ArsC*, *ArsH*, *ArsR*, *CzcA*, *CzcB*, *ChrA*, *ChrB* in (Figure 14c) resistant systems and demonstrated that the combined protein sequence analysis and analysis of DNA regulatory elements was possible to differentiate the genes involved in the metal resistance, in particular, mercury, copper, cadmium, zinc, and arsenate (Haque et al., 2022; Mutiat et al., 2018; and Saha et al., 2022). Many enzymes contribute to the efficient functions of the genes, including a multicopper oxidase, a cadmium transporter, a zinc transporter, and a copper/zinc/cadmium efflux system (Learman et al., 2019).

The RAST server identified gene calls based on their function, location, and degree of protein expression as presented in (Table 19). Additionally, sequence size, number of coding sequences, number of contigs, GC content percentage, and shortest contig. The RAST server predicted the sequence, mean sequence size, longest contig size, No50 values, L50 values, number of RNA, and several subsystems. The GC content percentage of *C. gilardii* CR3 is like that of *C. gilardii* WM02, which is (67.4%). However, the highest GC% % is documented for *Cupriavidus* sp. ISTL7 (67.7%), while the lowest GC% % is observed for *P. putida* PD584 (61.6%). Similar findings were found in the study on *B. cereus* (Zeng et al., 2020). Following *C. Gilardii* CR3 genomic DNA re-annotation with the RAST online server, subsystem category distribution and subsystem feature counts were anticipated.

These subsystems are supposed to support cellular activity and metabolism. Strengthening our suggestion, it was projected that these subsystems would provide broad metabolic information, increase annotation quality, and provide a framework for determining the statistical qualities required to exploit these tendencies properly. Our results anticipate carbohydrates and other

chemical molecules. OrthoANI, a tool that predicts sequence similarity between *C. gilardii* CR3 and related strains, is an example of an orthologous average nucleotide identity (OAT) tool offline server (Lee et al., 2016). When tested against OrthoANI, *C. gilardii* CR3 (CP010516.1) displayed a genome sequence similarity of 99.16%. *Cupriavidus gilardii* CR3 genomic DNA was found to be most like *Cupriavidus* ISTL7 with 98.85% OrthoANI (Figure 14a), using the OAT tool (Lee et al., 2016). Followed by *Cupriavidus gilardii* MW5 (98.80% OrthoANI), *Cupriavidus gilardii* strain WM02 (98.32% OrthoANI), Cupriavidus sp. MP, 37 (94.39% OrthoANI), *C. nantongensis* X1 (CP014844.1) (83.51% OrthoANI) and *C. metallidurans* CH4.

# 5. SUMMARY, CONCLUSION, AND RECOMMENDATION

Heavy metal pollution poses considerable environmental and health hazards, primarily caused by industrial activities, mining, and inadequate waste management. Bioremediation, especially bacteria-based, has become a promising and eco-friendly method to alleviate HM pollution worldwide. Bacteria have the ability, through biosorption, bioaccumulation, oxidation-reduction, extracellular and intracellular sequestration, and biotransformation, to tolerate and detoxify HMs. Cobalt, copper, cadmium, chromium, zinc, arsenic, mercury, etc., are the most toxic heavy metal ions that are taken up by microbial and plant cells either through cell membranes or by complexing with intracellular molecules, which decreases the bioavailability and toxicity of these metals.

A variety of bacteria were studied for their potential in bioremediation applications. Enhancing the growth conditions of these bacteria can greatly improve their efficiency, allowing them to thrive and function effectively in a wider range of environments. Their ease of adaptation can broaden their use in pollution reduction initiatives, such as contaminated soil and water. By adjusting factors such as temperature, pH, and nutrient levels, one can optimize bacterial performance and potentially increase their utilization in bioremediation across various ecological and industrial situations.

This study investigated HM pollution in soil and wastewater samples from industrial effluents in Bishoftu and Mojo, Eastern Shewa, Ethiopia. The results revealed the following decreasing order of HM concentrations in soil samples: $Mn^{+2} > Fe^{+2} > Zn^{+2} > Ni^{+2} > Cu^{+2} > Co^{+2} >$ Cd, and in wastewater: $Cr^{+6} > Fe^{+2} > Zn^{+2} > Mn^{+2} > Cd^{+2}$. Several bacteria were isolated, and their potential role in HM removal was evaluated. Specifically, isolates HMRMI-1, HMRMI-5, HMRBI-7, and HMRBI-14 demonstrated significant HM reduction abilities. *E. aurantiacum* effectively degraded 65.21% of cadmium and 65.13% of copper. *Citrobacter* and *Klebsiella* isolates using 16S rRNA gene sequencing for species identification. Both *Citrobacter* and *Klebsiella* isolates showed promising effects in removing chromium ($Cr^{+6}$) and cadmium ($Cd^{+2}$), achieving 89.74% and 85.21% respectively. SEM-EDX analysis confirmed that the heavy metal (HM) poisoning caused a deformed structure in the bacterial isolates, providing evidence of a biosorption mechanism within their cellular structure. The study concludes that these bacterial isolates hold

significant promise for future research and can be effectively employed for bioremediation applications to address environmental heavy metal pollution within the industrial zones.

This study investigated heavy metal contamination in soil and wastewater from the Bishoftu Eastern Industrial Zone and Mojo Tannery, identifying high concentrations of $Fe^{2+}$, $Cd^{2+}$, $Co^{2+}$, $Cr^{6+}$, $Cu^{2+}$, $Mn^{2+}$, and $Zn^{2+}$, which are attributed to significant industrial discharge. Recognizing the serious environmental and health risks posed by these pollutants, the research focused on bioremediation as a cost-effective and eco-friendly solution. Specifically, bacterial isolates naturally resistant to high levels of heavy metals were collected from the effluents of these sites in the East Shewa Zone of Oromia. The presence and adaptability of these bacteria, which can integrate both passive and active mechanisms to take up toxic metals like cadmium, cobalt, copper, zinc, and chromium from wastewater, indicate their strong potential as candidates for bioremediation in heavily contaminated industrial areas.

This study also successfully isolated a promising HMRBI candidate from industrial discharge sites heavily polluted with $Co^{+2}$, $Cu^{+2}$, $Zn^{+2}$, $Cd^{+2}$, and $Cr^{+6}$, from the study area of the eastern Shewa zone. The MALD-TOFSM and 16S rRNA gene sequence identified the promising isolates such as *P. putida*, *E. aurontiacum*, *Citrobacter spp.*, and a potentially new strain related to *P. benzoelyticum*. The bacteria demonstrated significant HM degradation efficiency with *Klebsiella* spp., *Citrobacter* spp., achieving 89.74% and 85.21% reduction, respectively, attributed to resistance mechanisms like biosorption or intracellular sequestration.

The findings suggest that this isolate holds great promise for bioremediation processes. Further research is needed to optimize conditions for their large-scale production in real-world applications. Bacterial bioremediation offers a potentially effective and environmentally friendly technology for reducing HM pollution. These inherent abilities form the foundation of natural remediation and can be further enhanced through biotechnological applications. While laboratory studies have shown great promise, translating these findings to real-world applications remains challenging. In actual environments, bacterial efficiency can be affected by a range of complex factors, including fluctuations in metal and contaminant concentrations or variations in pH and temperature.

The conclusion highlights essential recommendations for further evaluation and action

1. Implement trials using the most promising bacteria isolates using lab-scale reactors. To evaluate their performance, adaptability, and efficacy under real-world environmental conditions.
2. Compare the performance of selected isolates with internationally recognized reference strains. To benchmark efficacy, validate results, and enhance global competitiveness.
3. Scale up successful laboratory techniques to large-scale bioremediation formulation. To require a systematic approach that addresses technical and economic changes.
4. Integrating bacterial bioremediation with other techniques represents a sophisticated and environmentally responsible approach to tackling environmental contamination.
5. Effective environmental remediation and management strategies must be meticulously tailored to the unique characteristics of each site. This necessitates a comprehensive assessment and subsequent adaptation of approaches based on a thorough understanding of site-specific environmental conditions.
6. Investigate the genetic and molecular basis of the observed resistance mechanisms, potentially identifying targets to increase metal tolerance in other bacterial strains. Understanding which characteristics confer this resistance to pollution will enable us to construct more stable microbial communities in polluted environments.

# 6. REFERENCES


Adnan, M., Xiao, B., Ali, M. U., Xiao, P., Zhao, P., Wang, H., & Bibi, S. (2024). Heavy metals pollution from smelting activities: A threat to soil and groundwater. *Ecotoxicology and Environmental Safety*, *274*, 116189. https://doi.org/10.1016/j.ecoenv.2024.116189.

Aftab, T. (2022). Environmental Contamination Remediation and Management, Sustainable Management of Environmental Contaminants, Eco-friendly Remediation Approache*s*. *Environmental Contamination Remediation and Management*. https://doi.org/10.1007/978-3-031-08446-1

Afzaal, M., Hameed, S., Liaqat, I., Ali Khan, A. A., Abdul Manan, H., Shahid, R., & Altaf, M. (2022). Heavy metal contamination in water, sediments, and fish of freshwater ecosystems in Pakistan. *Water Practice & Technology*, *17*(5), 1253-1272. https://doi.org/10.2166/wpt.2022.039.

Ahamed, J. M., Dahms, H. U., & Huang, Y. L. (2024). Heavy metal tolerance and metal biosorption by exopolysaccharides produced by bacterial strains isolated from marine hydrothermal vents. *Chemosphere*, *351*, 141170.https://doi.org/10.1016/j.chemosphere.2024.141170.

ké, A. H. J., Rochdi, N., Jemo, M., Hafidi, M., Ouhdouch, Y., & El Fels, L. (2024). Cr (VI) removal performance from wastewater by microflora isolated from tannery effluents in a semi-arid environment: A SEM, EDX, FTIR and zeta potential study. *Frontiers in Microbiology*, *15*, 1423741. https://doi.org/10.3389/fmicb.2024.1423741.

Akhtar, M. S., Chali, B., & Azam, T. (2013). Bioremediation of arsenic and lead by plants and microbes from contaminated soil. *Research in Plant Sciences*, 1(3), 68-73. https://doi.org/10.12691/plant-1-3-4.

Al-Gheethi, A. A., Mohamed, R. M. S. R., Efaq, A. N., Norli, I., Abd Halid, A., Amir, H. K., & Ab Kadir, M. O. (2016). Bioaugmentation process of secondary effluents for reduction of pathogens, heavy metals and antibiotics. *Journal of water and health*, *14*(5), 780-795.https://doi.org/10.2166/wh.2016.046.

Alberts, B., Johnson, A., Lewis, J., Raff, M., Roberts, K., & Walter, P. (2002). Molecular Biology of the Cell. In *Molecular Biology of the Cell*.

https://doi.org/10.1201/9780203833445.

Alengebawy, A., Abdelkhalek, S. T., Qureshi, S. R., & Wang, M. Q. (2021). Heavy metals and pesticides toxicity in agricultural soil and plants: Ecological risks and human health implications. *Toxics*, *9*(3), 42. https://doi.org/10.3390/toxics9030042.

Ali, A. H. A., Hamed, M. A., & Abd El-Azim, H. (2011). Heavy metals distribution in the coral reef ecosystems of the Northern Red Sea. *Helgoland marine research*, *65*(1), 67-80. https://doi.org/10.1007/s10152-010-0202-7.

Ali, B., & Gill, R. A. (2022). Heavy metal toxicity in plants: Recent insights on physiological and molecular aspects, volume II. *Frontiers in plant science*, *13*, 1016257. https://doi.org/10.3389/fpls.2022.1016257.

Ali, H., Khan, E., & Ilahi, I. (2019). Environmental chemistry and ecotoxicology of hazardous heavy metals: environmental persistence, toxicity, and bioaccumulation. *Journal of Chemistry*, *2019*(1), 6730305. https://doi.org/10.1155/2019/6730305.

Altimira, F., Yáñez, C., Bravo, G., González, M., Rojas, L. A., & Seeger, M. (2012). Characterization of copper-resistant bacteria and bacterial communities from copper-polluted agricultural soils of central Chile. *BMC Microbiology*, *12*(1), 193 (2012). https://doi.org/10.1186/1471-2180-12-193.

Aman Beshir, J., & Kebede, M. (2021). In silico analysis of promoter regions and regulatory elements (motifs and CpG islands) of the genes encoding for alcohol production in *Saccharomyces cerevisiaeae* S288C and *Schizosaccharomyces pombe* 972h. *Journal of Genetic Engineering and Biotechnology*, *19*(1). https://doi.org/10.1186/s43141-020-00097-9.

Amin, N. U., Hussain, A., Alamzeb, S., & Begum, S. (2013). Accumulation of heavy metals in edible parts of vegetables irrigated with waste water and their daily intake to adults and children, District Mardan, Pakistan. *Food Chemistry*, *136*(3–4), 1515–1523. https://doi.org/10.1016/j.foodchem.2012.09.058.

Angon, P. B., Islam, M. S., KC, S., Das, A., Anjum, N., Poudel, A., & Suchi, S. A. (2024). Sources, effects, and present perspectives of heavy metals contamination: Soil, plants, and human food chain. *Heliyon*, *10*(7), e28357. https://doi.org/10.1016/j.heliyon.2024.e28357.

Shanmugaraj, C., Anokhe, A., & Kalia, V. (2021). Determination of Fermentation Pathway by Methyl Red and Voges Proskauer (MRVP) Test. *AgriCos e-Newsletter*, *2*(11), 41-43.

Arroyo, V. S., Flores, K. M., Ortiz, L. B., Gómez-Quiroz, L. E., & Gutiérrez-Ruiz, M. C. (2012). Liver and cadmium toxicity. *J Drug Metab Toxicol S*, *5*(001). https://doi.org/10.4172/2157-7609.s5-001.

Atagana, H. I., Haynes, R. J., & Wallis, F. M. (2003). Optimization of soil physical and chemical conditions for the bioremediation of creosote-contaminated soil. *Biodegradation*, *14*(4), 297-307.https://doi.org/10.1023/A:1024730722751.

Ayangbenro, A. S., & Babalola, O. O. (2017). A new strategy for heavy metal polluted environments: A review of microbial biosorbents. *International Journal of Environmental Research and Public Health*, *14*(1). https://doi.org/10.3390/ijerph14010094.

Aziz, H., Hikmat, K., Mustafa, S., F., Omer, M., K., Hama, Sarkawt, Hamarawf, Fayaq, R., Rahman, & Othman, K. (2023). Heavy metal pollution in the aquatic environment: efficient and low-cost removal approaches to eliminate their toxicity: a review. *RSC Advances*, *13*(26), 17595–17610. https://doi.org/10.1039/d3ra00723e.

Aziz, R. K., Bartels, D., Best, A., DeJongh, M., Disz, T., Edwards, R. A., Formsma, K., Gerdes, S., Glass, E. M., Kubal, M., Meyer, F., Olsen, G. J., Olson, R., Osterman, A. L., Overbeek, R. A., McNeil, L. K., Paarmann, D., Paczian, T., Parrello, B., Zagnitko, O. (2008). The RAST Server: Rapid annotations using subsystems technology. *BMC Genomics*, *9*, 1–15. https://doi.org/10.1186/1471-2164-9-75.

Bailey, T. L., & Elkan, C. (1994). Fitting a mixture model by expectation maximization to discover motifs in bipolymers.

Bailey, T. L., & Elkan, C. (1994). Fitting a mixture model by expectation maximization to discover motifs in biopolymers. *Proceedings/International Conference on Intelligent Systems for Molecular Biology ; ISMB. International Conference on Intelligent Systems for Molecular Biology*, *2*(February), 28–36.

Bailey, T. L., Johnson, J., Grant, C. E., & Noble, W. S. (2015). The MEME Suite. *Nucleic Acids Research*, *43*(W1), W39–W49. https://doi.org/10.1093/nar/gkv416.

Balali-Mood, M., Naseri, K., Tahergorabi, Z., Khazdair, M. R., & Sadeghi, M. (2021). Toxic Mechanisms of Five Heavy Metals: Mercury, Lead, Chromium, Cadmium, and Arsenic. *Frontiers in Pharmacology*, *12*(April), 1–19. https://doi.org/10.3389/fphar.2021.643972.

Balolong, M., Trinidad, L., Parungao, M. M., Tacata, P. S., Ray Tanayan, C. G., & Trinidad, L. C. (2007). Biosorption of Copper, Cadmium and Lead by Copper-Resistant Bacteria

Isolated from Mogpog River, Marinduque. *Philippine Journal of Science*, *136*(2), 155–165. https://www.researchgate.net/publication/228971940.

Bantihun, G., & Kebede, M. (2021). In silico analysis of promoter region and regulatory elements of mitogenome co-expressed trn gene clusters encoding for bio-pesticide in entomopathogenic fungus, Metarhizium anisopliae: strain ME1. *Journal of Genetic Engineering and Biotechnology*, *19*(1). https://doi.org/10.1186/s43141-021-00191-6.

Barkay, T., Kritee, K., Boyd, E., & Geesey, G. (2010). A thermophilic bacterial origin and subsequent constraints by redox, light and salinity on the evolution of the microbial mercuric reductase. Journal of *Environmental Microbiology*, *12*(11), 2904–2917. https://doi.org/10.1111/j.1462-2920.2010.02260.x.

Bekele Bahiru, D. (2021). Assessment of Some Heavy Metals Contamination in Some Vegetables (Tomato, Cabbage, Lettuce, and Onion) in Ethiopia: A Review. *Journal of Environmental Protection*, *10*(2), 53. https://doi.org/10.11648/j.ajep.20211002.12.

Belliveau, N. M., Chure, G., Hueschen, C. L., Garcia, H. G., Kondev, J., Fisher, D. S., Theriot, J. A., & Phillips, R. (2021). Fundamental limits on the rate of bacterial growth and their influence on proteomic composition. *Cell Systems*, *12*(9), 924-944.e2. https://doi.org/10.1016/j.cels.2021.06.002.

Benmarrlek, Y., & Fardeau, M. L. (2016). Isolation and characterization of metal-resistant bacterial strain from wastewater and evaluation of its capacity in metal-ion removal using living and dry bacterial cells. *International Journal of Environmental Science and Technology*, *13*(9), 2153–2162. https://doi.org/10.1007/s13762-016-1048-6.

Beyene, T., Kemal, A., Jibat, T., Tadese, F., Ayana, D., & Feyisa, A. (2015). Assessment on Chemicals and Drugs Residue in Dairy and Poultry Products in. *Journal of Nutrition & Food Sciences*. https://doi.org/10.4172/2155-9600.S13.

Bishnu, P., Islam, S., Kc, S., & Das, A. (2024). Heliyon Sources, effects, and present perspectives of heavy metals contamination : Soil, plants, and human food chain. *Heliyon*, *10*(7), e28357. https://doi.org/10.1016/j.heliyon.2024.e28357.

Bhardwaj, R., Gupta, A., & Garg, J. K. (2018). Impact of heavy metals on inhibitory concentration of *Escherichia coli*: A case study of the river Yamuna system. *Environmental Monitoring and Assessment, 190(11),*(674).https://doi.org/10.1007/s10661-018-7061-0.

Bhattacharjee, G., Gohil, N., Vaidh, S., Joshi, K., Vishwakarma, G. S., & Singh, V. (2020).

Microbial bioremediation of industrial effluents and pesticides. In *Bioremediation of pollutants* (pp. 287-302). https://doi.org/10.1016/B978-0-12-819025-8.00013-2.

Bhattacharyya, P., Chakrabarti, K., Chakraborty, A., Tripathy, S., & Powell, M. A. (2008). Fractionation and bioavailability of Pb in municipal solid waste compost and Pb uptake by rice straw and grain under submerged condition in amended soil. *Geosciences Journal*, *12*(1), 41–45. https://doi.org/10.1007/s12303-008-0006-9.

Bibi, T., Manzoor, S., Azhar, S., Saeed, M., Raheem, M. A., Pal, A. K., Singh, J., Soni, R., Tripathi, P., Kamle, M., Tripathi, V., Kumar, P. S. P., Chandran, H., Meena, M., Sharma, K., Shafeeq-ur-Rahman, Xuebin, Q., Yatao, X., Ahmad, M. I.,Dórea, J. G. (2019). Effects and mechanisms of microbial remediation of heavy metals in soil: A critical review. *Applied Sciences*, *8*(3), 1336. https://doi.org/10.3390/app8081336.

Bizily, P., S., Rugh, L., Cl., Summers, O., A., Meagher, & B., and Ri. (1999). Phytoremediation of methylmercury pollution: *merB* expression in Arabidopsis thaliana confers resistance to organomercurials. *Proc. Natl. Acad. Sci. USA*, *96*(June), 6808–6813.

Bondarczuk, Kinga, Piotrowska-Seget, & Lizofia. (2013). Molecular basis of active copper resistance mechanisms in Gram-negative bacteria. In *Cell Biology and Toxicology* (Vol. 29, Issue 6, pp. 397–405). https://doi.org/10.1007/s10565-013-9262-1.

Boshoff, M., De Jonge, M., Dardenne, F., Blust, R., & Bervoets, L. (2014). The impact of metal pollution on soil faunal and microbial activity in two grassland ecosystems. *Environmental Research*, *134*(2014), 169–180. https://doi.org/10.1016/j.envres.2014.06.024.

Bouida, L., Ya'acob, F., Jaafar, M. H., Abdullah, H., & Fadhullah, W. (2024). Human and Ecological Risk Assessment of Soil and Plants Metal Contamination in a Tropical Municipal Solid Waste Dumping Site. *Soil and Sediment Contamination*, *34*(1), 34–70. https://doi.org/10.1080/15320383.2024.2329951.

Briffa, Jessica, Sinagra, Emmanuel, Blundell, & Renald. (2020). Heavy metal pollution in the environment and their toxicological effects on humans. *Heliyon*, *6*(9), e04691. https://doi.org/10.1016/j.heliyon.2020.e04691.

Briški, Felicita, Domanovac, V., & Marija. (2019). Environmental microbiology. *Physical Sciences Reviews*, *2*(11), 1–22. https://doi.org/10.1515/psr-2016-0118.

Chakraborty, J., & Das, S. (2014). Characterization and cadmium-resistant gene expression of biofilm-forming marine bacterium *Pseudomonas aeruginosa* JP-11. *Environ Sci Pollut Res*,

*21*(24), 14188–14201. https://doi.org/10.1007/s11356-014-3308-7.

Chalita, M., Kim, Y. O., Park, S., Oh, H. S., Cho, J. H., Moon, J., Beak, N., Moon, Ch., Lee, K.,Yang, J., Nam, G., Jung, Y., Na S., Bailey, M.J.& Chun, J. (2024). EzBioCloud: a genome-driven database and platform for microbiome identification and discovery. *International Journal of Systematic and Evolutionary Microbiology*, *74*(6), 006421.https://doi.org/10.1099/ijsem.0.006421.

Chatterjee, Shreosi, Kumari, Supriya, Rath, Sonalin, Priyadarshanee, Monika, Das, & Surajit. (2020). Diversity, structure and regulation of microbial metallothionein: Metal resistance and possible applications in sequestration of toxic metals. *Metallomics*, *12*(11), 1637–1655. https://doi.org/10.1039/d0mt00140f.

Choudhary, S., & Sar, P. (2009). Characterization of a metal resistant *Pseudomonas* sp. isolated from uranium mine for its potential in heavy metal ($Ni^{2+}$, $Co^{2}$+, $Cu^{2+}$, and $Cd^{2+}$) sequestration. *Bioresource Technology*, *100*(9), 2482–2492. https://doi.org/10.1016/j.biortech.2008.12.015.

Collin, S., Baskar, A., Geevarghese, D. M., Ali, M. N. V. S., Bahubali, P., Choudhary, R., Lvov, V., Tovar, G. I., Senatov, F., Koppala, S., & Swamiappan, S. (2022). Bioaccumulation of lead (Pb) and its effects in plants: A review. *Journal of Hazardous Materials Letters*, *3*(March), 100064. https://doi.org/10.1016/j.hazl.2022.100064.

Chun, J., Oren, A., Ventosa, A., Christensen, H., Arahal, D. R., da Costa, M. S., ... & Trujillo, M. E. (2018). Proposed minimal standards for the use of genome data for the taxonomy of prokaryotes. *International journal of systematic and evolutionary microbiology*, *68*(1), 461-466.https://doi.org/10.1099/ijsem.0.002516.

Dahlén, G., Hassan, H., Blomqvist, S., & Carlén, A. (2018). Rapid urease test (RUT) for evaluation of urease activity in oral bacteria in vitro and in supragingival dental plaque ex vivo. *BMC Oral Health*, *18*(1), 1–7. https://doi.org/10.1186/s12903-018-0541-3.

Dai, Z., Xiong, Y., & Dai, X. (2016). DNA signals at isoform promoters. *Scientific Reports*, *6*, 1–8. https://doi.org/10.1038/srep28977.

Das, S., Dash, H. R., & Chakraborty, J. (2016). Genetic basis and importance of metal-resistant genes in bacteria for bioremediation of contaminated environments with toxic metal pollutants. *Applied Microbiology and Biotechnology*, *100*(7), 2967–2984. https://doi.org/10.1007/s00253-016-7364-4.

Das, S., Sultana, K. W., Ndhlala, A. R., Mondal, M., & Chandra, I. (2023). Heavy metal pollution in the environment and its impact on health: exploring green technology for remediation. *Environmental health insights*, *17*, 11786302231201259. https://doi.org/10.1177/11786302231201259.

Dash, R., Phirak, Das, & Surajit. (2012). Bioremediation of mercury and the importance of bacterial *mer* genes. *International Biodeterioration and Biodegradation*, *75*, 207–213. https://doi.org/10.1016/j.ibiod.2012.07.023.

Deng, Haoyu, Tu, Yuling, Wang, Han, Ziyi, Wang, Li, Yanyu, Chai, Liyuan, Zhang, Wenchao, Lin, & Zhang. (2022). Environmental behavior, human health effect, and pollution control of heavy metal(loid)s toward full life cycle processes. *Eco-Environment and Health*, *1*(4), 229–243. https://doi.org/10.1016/j.eehl.2022.11.003.

Deokar, A. R., Lin, L. Y., Chang, C. C., & Ling, Y. C. (2013). Single-walled carbon nanotube-coated antibacterial paper: Preparation and mechanistic study. *Journal of Materials Chemistry B*, *1*(20), 2639–2646. https://doi.org/10.1039/c3tb20188k.

Dibbisa, D., & Wagari, G. (2022). In Silico Study of Mercury Resistance Genes Extracted from *Pseudomonas* spp. Involved in Bioremediation: Understanding the Promoter Regions and Regulatory Elements. *International Journal of Genomics*, *2022*. https://doi.org/10.1155/2022/6185615.

Dinka, H., & Milkesa, A. (2020). Unfolding SARS-CoV-2 viral genome to understand its gene expression regulation. *Infection, Genetics and Evolution*, *84*(May). https://doi.org/10.1016/j.meegid.2020.104386.

Dixit, R., Wasiullah, Malaviya, D., Pandiyan, K., Singh, U. B., Sahu, A., Shukla, R., Singh, B. P., Rai, J. P., Sharma, P. K., Lade, H., & Paul, D. (2015). Bioremediation of heavy metals from soil and aquatic environment: An overview of principles and criteria of fundamental processes. *Sustainability*, *7*(2), 2189–2212. https://doi.org/10.3390/su7022189.

Dobre, T., Isopencu, G. O., Bdaiwi Ahmed, S., & Deleanu, I. M. (2024). Heavy metal pollution and solutions for its control: General aspects with a focus on cobalt removal and recovery from aqueous systems. *Chemical Engineering*, *8*(6), 118. https://doi.org/10.3390/chemengineering8060118.

Dong, G., Wang, Y., Gong, L., Wang, M., Wang, H., He, N., Zheng, Y., & Li, Q. (2013). Formation of soluble Cr(III) end-products and nanoparticles during Cr(VI) reduction by

*Bacillus cereus* strain XMCr-6. *Biochemical Engineering Journal*, *70*, 166–172. https://doi.org/10.1016/j.bej.2012.11.002.

Duffus, and J. H. (2002). *" Heavy Metals "a Meaningless Term ? ( IUPAC Technical Report )*. *74*(5), 793–807.https://doi/10.1351/pac200274050793/html.

Dutta, N., Usman, M., Ashraf, M. A., Luo, G., & Zhang, S. (2022). A critical review of recent advances in the bio-remediation of chlorinated substances by microbial dechlorinators. *Chemical Engineering Journal Advances*, *12*(July), 100359. https://doi.org/10.1016/j.ceja.2022.100359.

Edet, U. O., Bassey, I. U., & Joseph, A. P. (2023). Heavy metal co-resistance with antibiotics amongst bacterial isolates from an open dumpsite soil. *Heliyon*, *9*(2), e13457. https://doi.org/10.1016/j.heliyon.2023.e13457.

Vázquez-Núñez, E., Molina-Guerrero, C. E., Peña-Castro, J. M., Fernández-Luqueño, F., & de la Rosa-Álvarez, M. G. (2020). Use of nanotechnology for the bioremediation of contaminants: A review. *Processes*, *8*(7), 826.https://doi.org/10.3390/pr8070826.

El-sharkawy, Mahmoud, Alotaibi, O. M., Li, J., Du, D., & Mahmoud, E. (2025). Heavy Metal Pollution in Coastal Environments : Ecological Implications and Management Strategies : A Review. *Sustainability, 7*(2), 1–29. https://doi.org/10.3390/su17020701.

Elahi, A., & Rehman, A. (2019). Multiple metal resistance and Cr6+ reduction by bacterium, Staphylococcus sciuri A-HS1, isolated from untreated tannery effluent. *Journal of King Saud University-Science*, *31*(4), 1005-1013. https://doi.org/10.1016/j.jksus.2018.07.016.

Emenike, C. U., Jayanthi, B., Agamuthu, P., & Fauziah, S. H. (2018). Biotransformation and removal of heavy metals: a review of phytoremediation and microbial remediation assessment on contaminated soil. *Environmental Reviews*, 1–47.https://doi.org/10.1139/er-2017-0045.

Etesami, H. (2018). Bacterial-mediated alleviation of heavy metal stress and decreased accumulation of metals in plant tissues: mechanisms and future prospects. *Ecotoxicology and environmental safety*, *147*, 175-191.https://doi.org/10.1016/j.ecoenv.2017.08.032.

Felsenstein, J. (1985). Phylogenies and the comparative method. *American Naturalist*, *125*(1), 1–15. https://doi.org/10.1086/284325.

Firincă, C., Zamfir, L. G., Constantin, M., Răut, I., Capră, L., Popa, D., Jinga, M. L., Baroi, A. M., Fierăscu, R. C., Corneli, N. O., Postolache, C., Doni, M., Gurban, A. M., Jecu, L., &

Șesan, T. E. (2024). Microbial Removal of Heavy Metals from Contaminated Environments Using Metal-Resistant Indigenous Strains. *Journal of Xenobiotics*, *14*(1), 51–78. https://doi.org/10.3390/jox14010004.

Gall, J. E., Boyd, R. S., & Rajakaruna, N. (2015). Transfer of heavy metals through terrestrial food webs: a review. *Environmental Monitoring and Assessment*, *187*(4). https://doi.org/10.1007/s10661-015-4436-3.

Garelick, H., Jones, H., Dybowska, A., & Valsami-Jones, E. (2008). Reviews of Environmental Contamination Volume 197. In *Natural History* (Vol. 197). https://doi.org/10.1007/978-0-387-79284-2.

Gaurav, A., Bakht, P., Saini, M., Pandey, S., & Pathania, R. (2023). Role of bacterial efflux pumps in antibiotic resistance, virulence, and strategies to discover novel efflux pump inhibitors. *Microbiology*, *169*(5), 001333.https://doi.org/10.1099/mic.0.001333.

Gaur, N., Flora, G., Yadav, M., & Tiwari, A. (2014). A review with recent advancements on bioremediation-based abolition of heavy metals. *Environmental Sciences: Processes and Impacts*, *16*(2), 180–193. https://doi.org/10.1039/c3em00491k.

Gebeyehu, H. R., & Bayissa, L. D. (2020). Levels of heavy metals in soil and vegetables and associated health risks in Mojo area, Ethiopia. *PLoS ONE*, *15*(1), 1–22. https://doi.org/10.1371/journal.pone.0227883.

George, A., Venugopal, A., & Vashisht, A. K. (2023). Heavy metal contamination in soil and groundwater around industrial areas of Kollam District, Kerala, India. *Environmental Monitoring and Assessment*, *195w*(2). https://doi.org/10.1007/s10661-022-10880-5.

Girma, Bekele. (2021). The Effects of Environmental Pollution of Eastern Industrial Park on Human Health and Comfort of Dukem Town, Ethiopia. *Industrial Polluction Control*, *37*(8), 1–14. www.icontrolpollluction.com.

Grant, J. R., & Stothard, P. (2008). The CGView Server: a comparative genomics tool for circular genomes. *Nucleic Acids Research*, *36*(Web Server issue), 181–184. https://doi.org/10.1093/nar/gkn179.

Gomaa, E. Z., & El-Meihy, R. M. (2019). Bacterial biosurfactant from *Citrobacter freundii* MG812314.1 as a bioremoval tool of heavy metals from wastewater. *Bulletin of the National Research Centre*, *43*(1). https://doi.org/10.1186/s42269-019-0088-8.

Gunjyal, N., Rani, S., Asgari Lajayer, B., Senapathi, V., & Astatkie, T. (2023). A review of the

effects of environmental hazards on humans, their remediation for sustainable development, and risk assessment. *Environmental Monitoring and Assessment*, *195*(6). https://doi.org/10.1007/s10661-023-11353-z.

Gupta, Pratima, Diwan, & Batul. (2017). Bacterial Exopolysaccharide-mediated heavy metal removal: A Review on biosynthesis, mechanism, and remediation strategies. *Biotechnology Reports*, *13*, 58–71. https://doi.org/10.1016/j.btre.2016.12.006.

Haddaway, N. R., Cooke, S. J., Lesser, P., Macura, B., Nilsson, A. E., Taylor, J. J., & Raito, K. (2019). Evidence of the impacts of metal mining and the effectiveness of mining mitigation measures on social-ecological systems in Arctic and boreal regions: A systematic map protocol. *Environmental Evidence*, *8*(1), 1–11. https://doi.org/10.1186/s13750-019-0152-8.

Haque, F., Jabeen, I., Keya, C. A., & Shuvo, S. R. (2022). Whole-genome sequencing and comparative analysis of heavy metals-tolerant *Bacillus anthracis* FHq strain isolated from tannery effluents in Bangladesh. *AIMS Microbiology*, *8*(2), 226–238. https://doi.org/10.3934/microbiol.2022018.

Haripriyan, U., Gopinath, K. P., Arun, J., & Govarthanan, M. (2022). Bioremediation of organic pollutants: a mini review on current and critical strategies for wastewater treatment. *Archives of Microbiology*, *204*(5), 1–9. https://doi.org/10.1007/s00203-022-02907-9.

Hassan, S. H. A., Abskharon, R. N. N., Gad El-Rab, S. M. F., & Shoreit, A. A. M. (2008). Isolation, characterization of a heavy metal-resistant strain of *Pseudomonas aeruginosa* isolated from polluted sites in Assiut city, Egypt. *Journal of Basic Microbiology*, *48*(3), 168–176. https://doi.org/10.1002/jobm.200700338.

He, Z. L., Yang, X. E., & Stoffella, P. J. (2005). Trace elements in agroecosystems and impacts on the environment. *Journal of Trace Elements in Medicine and Biology*, *19*(2–3), 125–140. https://doi.org/10.1016/j.jtemb.2005.02.010.

Heipieper, H. J., Loffeld, B., Keweloh, H., & de Bont, J. A. M. (1995). The cis/trans isomerisation of unsaturated fatty acids in *Pseudomonas putida* S12: An indicator for environmental stress due to organic compounds. *Chemosphere*, *30*(6), 1041–1051. https://doi.org/10.1016/0045-6535(95)00015-Z.

Herrero, M., & Stuckey, D. C. (2015). Bioaugmentation and its application in wastewater treatment: A review. *Chemosphere*, *140*, 119–128. https://doi.org/10.1016/j.chemosphere.2014.10.033.

Higgins, G. D., Bleasby, J. A., Fuchs, & Rainer. (1992). CLUSTAL V: Improved software for multiple sequence alignment. *Bioinformatics*, *8*(2), 189–191. https://doi.org/10.1093/bioinformatics/8.2.189.

Hossen, Anowar, Mostafa, M., & G., M. (2023). Assessment of heavy metal pollution in surface water of Bangladesh. *Environmental Challenges*, *13*(1), 119–124. https://doi.org/10.1016/j.envc.2023.100783.

Huang, F., Wang, Z. H., Cai, Y. X., Chen, S. H., Tian, J. H., & Cai, K. Z. (2018). Heavy metal bioaccumulation and cation release by growing *Bacillus cereus* RC-1 under culture conditions. *Ecotoxicology and Environmental Safety*, *157*, 216–226. https://doi.org/10.1016/j.ecoenv.2018.03.077.

Huang, Ning, Mao, Juan, Hu, M., Wang, X., & Huo, M. (2019). Responses to copper stress in the metal-resistant bacterium *Cupriavidus gilardii* CR3: a whole-transcriptome analysis. *Journal of Basic Microbiology*, *59*(5), 446–457. https://doi.org/10.1002/jobm.201800693.

Idrees, M., Ali, S., Rehman, A., Zajif Hussain, S., & Abbas Bukhari, D. (2023). Uptake of lead by bacteria isolated from industrial effluents and their potential use in bioremediation of wastewater. *Saudi Journal of Biological Sciences*, *30*(8), 103740. https://doi.org/10.1016/j.sjbs.2023.103740.

Ike, A., Sriprang, R., Ono, H., & Murooka, Y. (2007). Bioremediation of cadmium contaminated soil using symbiosis between leguminous plants and recombinant *rhizobia* with the MTL4 and the *PCS* genes. *Chemosphere*, *66*, 1670–1676. https://doi.org/10.1016/j.chemosphere.2006.07.058.

Islam, S., Rahman, M. M., & Naidu, R. (2019). Impact of water and fertilizer management on arsenic bioaccumulation and speciation in rice plants grown under greenhouse conditions. *Chemosphere*, *214*, 606–613. https://doi.org/10.1016/j.chemosphere.2018.09.158.

Itankar, N., & Patil, Y. (2021). Employing waste to manage waste: Utilizing waste biomaterials for the elimination of hazardous contaminant Cr(VI) from aqueous matrices. *Journal of Contaminant Hydrology*, *239*, 103775. https://doi.org/10.1016/j.jconhyd.2021.103775.

Jaishankar, M., Tseten, T., Anbalagan, N., Mathew, B. B., & Beeregowda, K. N. (2014). Toxicity, mechanism, and health effects of some heavy metals. *Interdisciplinary Toxicology*, *7*(2), 60–72. https://doi.org/10.2478/intox-2014-0009.

Jebril, N., Boden, R., & Braungardt, C. (2022). Cadmium-resistant bacteria mediated cadmium

removal: a systematic review on resistance, mechanism, and bioremediation approaches. *IOP Conference Series: Earth and Environmental Science*, *1002*(1). https://doi.org/10.1088/1755-1315/1002/1/012006.

Jin, Y., Luan, Y., Ning, Y., & Wang, L. (2018). Effects and mechanisms of microbial remediation of heavy metals in soil: A critical review. *Applied Sciences (Switzerland)*, *8*(8). https://doi.org/10.3390/app8081336.

Jomova, K., Alomar, S. Y., Nepovimova, E., Kuca, K., & Valko, M. (2025). Heavy metals: toxicity and human health effects. In *Archives of Toxicology* (Vol. 99, Issue 1). Springer Berlin Heidelberg. https://doi.org/10.1007/s00204-024-03903-2.

Kalaimurugan, D., Balamuralikrishnan, B., Durairaj, K., Vasudhevan, P., Shivakumar, S., M., Kaul, T., Chang, S. W., Ravindran, B., & Venkatesan, S. (2020). Isolation and characterization of heavy-metal-resistant bacteria and their applications in environmental bioremediation. *International Journal of Environmental Science and Technology*, *17*(3), 1455–1462. https://doi.org/10.1007/s13762-019-02563-5.

Kalsoom, Batool, A., Din, G., Din, S. U., Jamil, J., Hasan, F., Khan, S., Badshah, M., & Shah, A. A. (2023). Isolation and screening of chromium resistant bacteria from industrial waste for bioremediation purposes. *Brazilian Journal of Biology*, *83*, 1–8. https://doi.org/10.1590/1519-6984.242536.

Kapur, M. A., Yuvarani, M., Shiyamala, G., Sudha, S. S., Janaki, S., Prasanna, J., & Kolar, A. B. (2024). *The Role of Microbes in Environmental Bioremediation: Novel Approaches For Pollution Control*. *April*. https://doi.org/10.53555/jaz.v45i2.3867.

Kaur, M., Sharma, A., & Aditya. (2021). A review on heavy metal accumulation and toxicity in biotic and abiotic components. *IOP Conference Series: Earth and Environmental Science*, *889*(1). https://doi.org/10.1088/1755-1315/889/1/012062.

Kim, G. B., Gao, Y., Palsson, B. O., & Lee, S. Y. (2021). Deep Transcription Factor: A deep learning-based tool for the prediction of transcription factors. *Proceedings of the National Academy of Sciences of the United States of America*, *118*(2), 1–5. https://doi.org/10.1073/pnas.2021171118.

Kinuthia, G. K., Ngure, V., Beti, D., Lugalia, R., Wangila, A., & Kamau, L. (2020). Levels of heavy metals in wastewater and soil samples from open drainage channels in Nairobi, Kenya: community health implications. *Scientific Reports*, *10*(1), 1–13.

https://doi.org/10.1038/s41598-020-65359-5.

Koo, H. J., Ahn, S., Chung, H. Y., Kim, S., Kim, K., Ryu, S., Lee, J. H., Choi, S. H., & Kim, H. (2017). Comparative genomic analysis reveals genetic features related to the virulence of *Bacillus cereus* FORC-013. *Gut Pathogens*, *9*(1), 1–8. https://doi.org/10.1186/s13099-017-0175-z.

Koubek, J., Uhlik, O., Jecna, K., Junkova, P., Vrkoslavova, J., Lipov, J., Kurzawova, V., Macek, T., & Mackova, M. (2012). International Biodeterioration & Biodegradation Whole-cell MALDI-TOF : Rapid screening method in environmental microbiology. *International Biodeterioration & Biodegradation*, *69*(1), 82–86. https://doi.org/10.1016/j.ibiod.2011.12.007.

Kumar, M., Seth, A., Singh, A. K., Rajput, M. S., & Sikandar, M. (2021). Remediation strategies for heavy metals contaminated ecosystems: A review. *Environmental and Sustainability Indicators*, *12*, 100155. https://doi.org/10.1016/j.indic.2021.100155.

Kumar, S., Tamura, K., & Nei, M. (2004). MEGA3: Integrated software for Molecular Evolutionary Genetics Analysis and sequence alignment. *Briefings in Bioinformatics*, *5*(2), 150–163. https://doi.org/10.1093/bib/5.2.150.

Kumar, V., Tyagi, S. K., Kumar, K., & Parmar, R. S. (2023). Heavy metal-induced pollution in the environment through waste disposal. *International Journal of Research Publication and Reviews*, *4*(7), 1205-1210.http://www.ijrpr.com.

Kutty, A. A., & Al-Mahaqeri, S. A. (2016). An Investigation of the Levels and Distribution of Selected Heavy Metals in Sediments and Plant Species within the Vicinity of Ex-Iron Mine in Bukit Besi. *Journal of Chemistry*, *2016*, 1–12. https://doi.org/10.1155/2016/2096147.

Lai, H. Y., Zhang, Z. Y., Su, Z. D., Su, W., Ding, H., Chen, W., & Lin, H. (2019). iProEP: A Computational Predictor for Predicting Promoter. *Molecular Therapy-Nucleic Acids*, *17*(September), 337–346. https://doi.org/10.1016/j.omtn.2019.05.028.

Lata, S., Sharma, S., & Kaur, S. (2023). OMICS Approaches in Mitigating Metal Toxicity in Comparison to Conventional Techniques Used in Cadmium Bioremediation. *Water, Air, and Soil Pollution*, *234*(3). https://doi.org/10.1007/s11270-023-06145-7.

Learman, D. R., Ahmad, Z., Brookshier, A., Henson, M. W., Hewitt, V., Lis, A., Morrison, C., Robinson, A., Todaro, E., Wologo, E., Wynne, S., Alm, E. W., & Kourtev, P. S. (2019). Comparative genomics of 16 *Microbacterium* spp. that tolerate multiple heavy metals and

antibiotics. *PeerJ*, *2019*(1). https://doi.org/10.7717/peerj.6258.

Lee, I., Kim, Y. O., Park, S. C., & Chun, J. (2016). OrthoANI: An improved algorithm and software for calculating average nucleotide identity. *International Journal of Systematic and Evolutionary Microbiology*, *66*(2), 1100–1103. https://doi.org/10.1099/ijsem.0.000760.

Leite, R. P., & Mohan, S. K. (1990). Integrated management of the citrus bacterial canker disease caused by *Xanthomonas* campestris pv. Citri in the State of Paraná, Brazil. *Crop Protection*, *9*(1), 3–7. https://doi.org/10.1016/0261-2194(90)90038-9.

Lemessa, F., Simane, B., Seyoum, A., & Gebresenbet, G. (2022). Analysis of the concentration of heavy metals in soil, vegetables and water around the bole Lemi industry park, Ethiopia. *Heliyon*, *8*(12), e12429. https://doi.org/10.1016/j.heliyon.2022.e12429.

Liu, Y., Zhu, Y., Qiao, X., Zheng, B., Chang, S., & Fu, Q. (2018). Investigation of nitrogen and phosphorus contents in water in the tributaries of Danjiangkou reservoir. *Royal Society Open Science*, *5*(1). https://doi.org/10.1098/rsos.170624.

Lu, Y., Yuan, J., Lu, X., Su, C., Zhang, Y., Wang, C., Cao, X., Li, Q., Su, J., Ittekkot, V., Garbutt, R. A., Bush, S., Fletcher, S., Wagey, T., Kachur, A., & Sweijd, N. (2018). Major threats of pollution and climate change to global coastal ecosystems and enhanced management for sustainability. *Environmental Pollution*, *239*, 670–680. https://doi.org/10.1016/j.envpol.2018.04.016.

Mangunwardoyo, W., Sudjarwo, T., & Patria, M. P. (2013). Bioremediation of effluent wastewater treatment plant Bojongsoang, Bandung, Indonesia, using a consortium of aquatic plants and animals. *Int J Res Rev Appl Sci*, *14*(1), 150-160. https://www.researchgate.net/publication/273756248.

Manisalidis, Ioannis, Stavropoulou, Elisavet, Stavropoulos, Agathangelos, Bezirtzoglou, & Eugenia. (2020). Environmental and Health Impacts of Air Pollution: A Review. *Frontiers in Public Health*, *8*(14), 1–13. https://doi.org/10.3389/fpubh.2020.00014.

Manousi, N., Rosenberg, E., Deliyanni, E., Zachariadis, G. A., & Samanidou, V. (2020). Magnetic solid-phase extraction of organic compounds based on graphene oxide nanocomposites. *Molecules*, *25*(5). https://doi.org/10.3390/molecules25051148.

Mainka, T., Weirathmüller, D., Herwig, C., & Pflügl, S. (2021). Potential applications of halophilic microorganisms for the biological treatment of industrial process brines contaminated with aromatics. *Journal of Industrial Microbiology and Biotechnology*, *48*(1-

2), kuab015.https://doi.org/10.1093/jimb/kuab015.

Marzan, L. W., Hossain, M., Mina, S. A., Akter, Y., & Chowdhury, A. M. M. A. (2017). Isolation and biochemical characterization of heavy-metal resistant bacteria from tannery effluent in Chittagong city, Bangladesh: Bioremediation viewpoint. *Egyptian Journal of Aquatic Research*, *43*(1), 65–74. https://doi.org/10.1016/j.ejar.2016.11.002.

Mathivanan, K., Chandirika, J. U., Vinothkanna, A., Yin, H., Liu, X., & Meng, D. (2021). Bacterial adaptive strategies to cope with metal toxicity in the contaminated environment – A review. *Ecotoxicology and Environmental Safety*, *226*, 112863. https://doi.org/10.1016/j.ecoenv.2021.112863.

Mergeay, M., & Van Hroudt, R. (2021). *Cupriavidus metallidurans* CH34, a historical perspective on its discovery, characterization and metal resistance. *FEMS Microbiology Ecology*, *97*(2), 1–7. https://doi.org/10.1093/femsec/fiaa247.

Mishra, M., Singh, S. K., & Kumar, A. (2020). Environmental factors affecting the bioremediation potential of microbes. In *Microbe Mediated Remediation of Environmental Contaminants* (pp. 47–58). https://doi.org/10.1016/B978-0-12-821199-1.00005-5.

Mokarram, Marzieh, Saber, Ali, Sheykhi, & Vahideh. (2020). Effects of heavy metal contamination on river water quality due to the release of industrial effluents. *Journal of Cleaner Production*, *277*, 123380. https://doi.org/10.1016/j.jclepro.2020.123380.

Monira, U., & Mostafa, M. G. (2023). Leather industrial effluent and environmental concerns: a review. *Sustainable Water Resources Management*, *9*(6), 1–14. https://doi.org/10.1007/s40899-023-00969-1.

Monsieurs, P., Moors, H., Houdt, R. Van, Janssen, P. J., Janssen, A., Coninx, I., Mergeay, M., & Leys, N. (2011). Heavy metal resistance in Cupriavidus metallidurans CH34 is governed by an intricate transcriptional network. *Biometals*, *14*, 1133–1151. https://doi.org/10.1007/s10534-011-9473-y.

Montes-Montes, Gustavo, Muñoz-Ramírez, Y., Z., Cortes-Palacios, Leonor, Carrillo-Campos, Javier, Ramírez-Sánchez, Obed, Ortiz-Aguirre, Ismael, Muñoz-Castellanos, N., L., González-Escobedo, & Román. (2025). Microbial Diversity and Heavy Metal Resistome in Slag-Contaminated Soils from an Abandoned Smelter in Chihuahua, Mexico. *Soil Systems*, *9*(2), 1–17. https://doi.org/10.3390/soilsystems9020030.

Mrozik, A., & Piotrowska-Seget, Z. (2010). Bioaugmentation as a strategy for cleaning up of

soils contaminated with aromatic compounds. *Microbiological Research*, *165*(5), 363–375. https://doi.org/10.1016/j.micres.2009.08.001.

Mutiat, Y., Bello, F., Gbolahan, Babalola, Olu, & Odeyemi. (2018). A comparative study of the wild and mutated heavy metal-resistant *Klebsiella variicola* generated for cadmium bioremediation. *Bioremediation Journal*, *22*(1–2), 1–15. https://doi.org/10.1080/10889868.2018.1445695.

Mydeen, A. K. M., Agnihotri, N., Lytand, W., & Bahadur, R. (2024). *Microbial-Maestros-Unraveling-the-Crucial-Role-of-Microbes-in- Microbial Maestros : Unraveling the Crucial Role of Microbes in Shaping the Environment*. *May*. https://doi.org/10.5281/zenodo.8340009.

Naik, M. M., & Dubey, S. K. (2013). Lead-resistant bacteria: Lead resistance mechanisms, their applications in lead bioremediation and biomonitoring. *Ecotoxicology and Environmental Safety*, *98*, 1–7. https://doi.org/10.1016/j.ecoenv.2013.09.039.

Nair, Abhinav, Sarma, & Jyoti, S. (2021). The impact of carbon and nitrogen catabolite repression in microorganisms. *Microbiological Research*, *251*(September 2020), 126831. https://doi.org/10.1016/j.micres.2021.126831.

Najeeb, U., Ahmad, W., Zia, M. H., Zaffar, M., & Zhou, W. (2017). Enhancing the lead phytostabilization in wetland plant Juncus effusus L. through somaclonal manipulation and EDTA enrichment. *Arabian Journal of Chemistry*, *10*, S3310–S3317. https://doi.org/10.1016/j.arabjc.2014.01.009.

Nnaji, N. D., Anyanwu, C. U., Miri, T., & Onyeaka, H. (2024). Mechanisms of Heavy Metal Tolerance in Bacteria: A Review. *Sustainability (Switzerland)*, *16*(24), 1–22. https://doi.org/10.3390/su162411124.

Nelson, K. E., Weinel, C., Paulsen, I. T., Dodson, R. J., Hilbert, H., Martins Dos Santos, V. A. P., Fouts, D. E., Gill, S. R., Pop, M., Holmes, M., Brinkac, L., Beanan, M., DeBoy, R. T., Daugherty, S., Kolonay, J., Madupu, R., Nelson, W., White, O., Peterson, J.,Fraser, C. M. (2003). Complete genome sequence and comparative analysis of the metabolically versatile *Pseudomonas putida* KT2440. *Environmental Microbiology*, *5*(7), 630-630. https://doi.org/10.1046/j.1462-2920.2003.00480.x.

Ojo, G. J., Onile, O. S., Momoh, A. O., Oyeyemi, B. F., Omoboyede, V., Fadahunsi, A. I., & Onile, T. (2023). Physiochemical analyses and molecular characterization of heavy metal-

resistant bacteria from Ilesha gold mining sites in Nigeria. *Journal of Genetic Engineering and Biotechnology*, *21*(1). https://doi.org/10.1186/s43141-023-00607-5.

Oladimeji, T. E., Oyedemi, M., Emetere, M. E., Agboola, O., Adeoye, J. B., & Odunlami, O. A. (2024). Review on the impact of heavy metals from industrial wastewater effluent and removal technologies. *Heliyon*, *10*(23), e40370. https://doi.org/10.1016/j.heliyon.2024.e40370.

Omar, M., Uddin, S., Mozahar, M., Hossain, S. M. Z., & Abdur, S. (2024). Journal of Hazardous Materials Advances: A comprehensive review on microalgae-driven heavy metals removal from industrial wastewater using living and nonliving microalgae. *Journal of Hazardous Materials Advances*, *16*(September), 100492. https://doi.org/10.1016/j.hazadv.2024.100492.

Oros, A. (2025). Bioaccumulation and Trophic Transfer of Heavy Metals in Marine Fish: Ecological and Ecosystem-Level Impacts. *Journal of Xenobiotics*, *15*(2). https://doi.org/10.3390/jox15020059.

Overbeek, R., Begley, T., Butler, R. M., Choudhuri, J. V., Chuang, H. Y., Cohoon, M., de Crécy-Lagard, V., Diaz, N., Disz, T., Edwards, R., Fonstein, M., Frank, E. D., Gerdes, S., Glass, E. M., Goesmann, A., Hanson, A., Iwata-Reuyl, D., Jensen, R., Jamshidi, N., Krause, L., Kubal, M.., Larsen, N., Linke, B., McHardy, A.C., Meyer, F., Neuweger, G., Olsen, G., Olson, R., Osteman, A., Portnoy, V., Pusch, G.D., Rodionov, A.D., Ruckert, J., Steiner, J., Stevens, R., Thiele, I., Vassieva, O., Ye, Y., Zagnitko, O., and Vonstein, V. (2005). The subsystems approach to genome annotation and its use in the project to annotate 1000 genomes. *Nucleic Acids Research*, *33*(17), 5691–5702. https://doi.org/10.1093/nar/gki866.

Oves, M, M, S., A. K., Qari, H. T., M. N. F., & Almeelbi, A. (2016). Heavy Metals: Biological Importance and Detoxification Strategies. *Journal of Bioremediation & Biodegradation*, *07*(02). https://doi.org/10.4172/2155-6199.1000334.

Pagnucco, G., Overfield, D., Chamlee, Y., Shuler, C., Kassem, A., Opara, S., Najaf, H., Abbas, L., Coutinho, O., Fortuna, A., Sulaiman, F., Farinas, J., Schittenhelm, R., Catalfano, B., Li, X., & Tiquia-Arashiro, S. M. (2023). Metal tolerance and biosorption capacities of bacterial strains isolated from an urban watershed. *Frontiers in Microbiology*, *14*(October), 1–21. https://doi.org/10.3389/fmicb.2023.1278886.

Palit, K., Rath, S., Chatterjee, S., & Das, S. (2022). Microbial diversity and ecological interactions of microorganisms in the mangrove ecosystem: Threats, vulnerability, and

adaptations. In *Environmental Science and Pollution Research* (Vol. 29, Issue 22). Springer Berlin Heidelberg. https://doi.org/10.1007/s11356-022-19048-7.

Panagos, P., Ballabio, C., Lugato, E., Jones, A., Borrelli, P., Scarpa, S., Orgiazzi, A., & Montanarella, L. (2018). Potential sources of anthropogenic copper inputs to European agricultural soils. *Sustainability (Switzerland)*, *10*(7). https://doi.org/10.3390/su10072380.

Pande, Veni, Pandey, Chandra, Satish, Sati, Diksha, Bhatt, Pankaj, Samant, & Mukesh. (2022). Microbial Interventions in Bioremediation of Heavy Metal Contaminants in Agroecosystem. *Frontiers in Microbiology*, *13*(May), 1–16. https://doi.org/10.3389/fmicb.2022.824084.

Pandey, A., Jain, R., Sharma, A., Dhakar, K., Kaira, G. S., Rahi, P., & Dhyani, A. (2019). 16S rRNA gene sequencing and MALDI-TOF mass spectrometry-based comparative assessment and bioprospection of psychrotolerant bacteria isolated from high altitudes under mountain ecosystem. *SN Applied Sciences*, *1*(3), 1–12. https://doi.org/10.1007/s42452-019-0273-2.

Parui, R., Nongthombam, G. S., Hossain, M., Adil, L. R., Gogoi, R., Bhowmik, S., Barman, D., & Iyer, P. K. (2023). Impact of Heavy Metals on Human Health. *Remediation of Heavy Metals: Sustainable Technologies and Recent Advances*, *0530*, 47–81. https://doi.org/10.1002/9781119853589.ch4.

Pepi, M., Gaggi, C., Bernardini, E., Focardi, S., Lobianco, A., Ruta, M., Nicolardi, V., Volterrani, M., Gasperini, S., Trinchera, G., Renzi, P., Gabellini, M., & Focardi, S. E. (2011). Mercury-resistant bacterial strains, *Pseudomonas* and *Psychrobacter* spp. isolated from sediments of Orbetello Lagoon (Italy) and their possible use in bioremediation processes. *International Biodeterioration and Biodegradation*, *65*(1), 85–91. https://doi.org/10.1016/j.ibiod.2010.09.006.

Permina, E. A., Kazakov, A. E., Kalinina, O. V., & Gelfand, M. S. (2006). Comparative genomics of regulation of heavy metal resistance in Eubacteria. *BMC Microbiology*, *6*, 1–11. https://doi.org/10.1186/1471-2180-6-49.

Pham, V. H. T., Kim, J., Chang, S., & Chung, W. (2022). Bacterial Biosorbents, an Efficient Heavy Metals Green Clean-Up Strategy: Prospects, Challenges, and Opportunities. *Microorganisms*, *10*(3), 1–16. https://doi.org/10.3390/microorganisms10030610.

Phuong, N., Linh, N.T., Duy, T.D., Khanh, T.L.N., Giang, D. D.T., Linh, T.T.T., Nga, M. Th.Ph., Huong, T.Th.M., Chung, M.D., Ha, Ch. H., and Binh, L.T. (2021). Identification

and evaluation of enzymes gelatinase, amylase, and catalase produced by rice root endophytic bacteria isolated from Hai Duong with antimicrobial properties against \(\textit{Xanthomonas oryzea}\) *pv*. *Oryzea*. *Academia Journal of Biology*, *43*(2), 107–117. https://doi.org/10.15625/2615-9023/15906.

Priyadarshanee, M., Chatterjee, S., Rath, S., Dash, H. R., & Das, S. (2022). Cellular and genetic mechanisms of bacterial mercury resistance and their role in biogeochemistry and bioremediation. *Journal of Hazardous Materials*, *423*(PA), 126985. https://doi.org/10.1016/j.jhazmat.2021.126985.

Qattan, S. Y. A. (2025). Harnessing bacterial consortia for effective bioremediation : targeted removal of heavy metals, hydrocarbons, and persistent pollutants. In *Environmental Sciences Europe*. Springer Berlin Heidelberg. https://doi.org/10.1186/s12302-025-01103-y.

Raize, O., Argaman, Y., & Yannai, S. (2004). Mechanisms of biosorption of different heavy metals by brown marine macroalgae. *Biotechnology and Bioengineering*, *87*(4), 451–458. https://doi.org/10.1002/bit.20136.

Ramírez, R. (2013). The gastropod Osilinus atrata as a bioindicator of Cd, Cu, Pb and Zn contamination in the coastal waters of the Canary Islands. *Chemistry and Ecology*, *29*(3), 208–220. https://doi.org/10.1080/02757540.2012.735659.

Rashid, Abdur, Schutte, J. B., Ulery, April, Deyholos, K. M., Sanogo, Soum, Lehnhoff, A., E., Beck, & Leslie. (2023). Heavy Metal Contamination in Agricultural Soil: Environmental Pollutants Affecting Crop Health. *Agronomy*, *13*(6), 1–30. https://doi.org/10.3390/agronomy13061521.

Razzak, S. A., Faruque, M. O., Alsheikh, Z., Alsheikhmohamad, L., Alkuroud, D., Alfayez, A., Hossain, S. M. Z., & Hossain, M. M. (2022). A comprehensive review of conventional and biological-driven heavy metals removal from industrial wastewater. *Environmental Advances*, *7*(January), 100168. https://doi.org/10.1016/j.envadv.2022.100168.

Reese, M. G. (2001). Application of a time-delay neural network to promoter annotation in the Drosophila melanogaster genome. *Computers & Chemistry*, *26*(1), 51–56. https://doi.org/10.1016/S0097-8485(01)00099-7.

Reiner, K. (2010). Catalase Test Protocol. *American Society for Microbiology for Microbiology*, *November 2010*, 1–9. http://www.microbelibrary.org/library/laboratory-test/3226-catalase-test-protocol.

Reda, A. H. (2016). *Study on the Pollution Levels of Trace Metals from Modjo Tannery Effluent in Study on the Pollution Levels of Trace Metals from Modjo Tannery Effluent in the Surrounding River Water and Soil*. *January*. https://doi.org/10.11648/j.sjac.20150305.13.

Ridene, S., Werfelli, N., Mansouri, A., Landoulsi, A., & Abbes, C. (2023). Bioremediation potential of consortium *Pseudomonas Stutzeri* LBR and Cupriavidus Metallidurans LBJ in soil polluted by lead. *PLoS ONE*, *18*(6 June), 1–15. https://doi.org/10.1371/journal.pone.0284120.

Roane, T. M., Josephson, K. L., & Pepper, I. L. (2001). Dual-Bioaugmentation Strategy to Enhance Remediation of Cocontaminated Soil. *Applied and Environmental Microbiology*, *67*(7), 3208–3215. https://doi.org/10.1128/AEM.67.7.3208-3215.2001.

Rojas, L. A., Yáñez, C., González, M., Lobos, S., Smalla, K., & Seeger, M. (2011). Characterization of the metabolically modified heavy metal-resistant Cupriavidus metallidurans strain MSR33 generated for mercury bioremediation. *PLoS ONE*, *6*(3). https://doi.org/10.1371/journal.pone.0017555.

Sáez-Plaza, P., Michałowski, T., Navas, M. J., Asuero, A. G., & Wybraniec, S. (2013). An Overview of the Kjeldahl Method of Nitrogen Determination. Part I. Early History, Chemistry of the Procedure, and Titrimetric Finish. *Critical Reviews in Analytical Chemistry*, *43*(4), 178–223. https://doi.org/10.1080/10408347.2012.751786.

Saha, Jayanti, Sarkar, Monalisha, Mandal, Parimal, Pal, & Ayon. (2022). Comparative Study of Heavy Metal Uptake and Analysis of Plant Growth Promotion Potential of Multiple Heavy Metal-Resistant Bacteria Isolated From Arable Land. *Current Microbiology*, *79*(1), 1–13. https://doi.org/10.1007/s00284-021-02704-5.

Saitou, N., & Nei, M. (1987). The neighbor-joining method: a new method for reconstructing phylogenetic trees. *Molecular Biology and Evolution*, *4*(4), 406–425. https://doi.org/10.1093/oxfordjournals.molbev.a040454.

Sall, M. L., Karim, A., Diaw, D., Gningue-sall, D., Aaron, S. E., & Aaron, J. (2020). Toxic heavy metals: impact on the environment and human health, and treatment with conducting organic polymers, a review. *Environ Sci Pollut Res Int.*, *27*(24), 29927–29942. https://doi.org/10.1007/s11356-020-09354-3.

Santos, D., Martins, H. R., Argolo, Suzart, C., Argôlo-Filho, Costa, R., Loguercio, & Lopes, L. (2019). A 16S rDNA PCR-based theoretical to actual delta approach on culturable mock

communities revealed severe losses of diversity information. *BMC Microbiology*, *19*(1), 1–14. https://doi.org/10.1186/s12866-019-1446-2.

Sawicka, E., Jurkowska, K., & Piwowar, A. (2021). Chromium (III) and chromium (VI) as important players in the induction of genotoxicity – Current view. *Annals of Agricultural and Environmental Medicine*, *28*(1), 1–10. https://doi.org/10.26444/aaem/118228.

Sayqal, A., & Ahmed, O. B. (2021). Retracted: Advances in Heavy Metal Bioremediation: An Overview. *Applied Bionics and Biomechanics*, 1–9. https://doi.org/10.1155/2023/9871378.

Selvi, M. S., Sasikumar, S., Gomathi, S., Rajkumar, P., & Sadasivam, S. G. (2014). Isolation and characterization of arsenic resistant bacteria from agricultural soil, and their potential for arsenic bioremediation. *International Journal of Agricultural Policy and Research*, *2*(11), 393–405. http://www.journalissues.org/IJAPR/http://dx.doi.org/10.15739/IJAPR.012.

Seyma, E., Severcan, M., Gul, A., & Severcan, F. (2020). Discrimination of heavy metal acclimated environmental strains by chemometric analysis of FTIR spectra. *Ecotoxicology and Environmental Safety*, *202*, 110953. https://doi.org/10.1016/j.ecoenv.2020.110953.

Shan, Shiping, Cheng, Wei, Li, Yilu, Zhang, Min, Liu, Zhudong, Wang, Yushuang, Wei, Xiaowu, Fu, Zujiao, Wu, Shandong, Du, Zhaohui. (2022). Comparative genomic analysis of Citrobacter sp. XT1-2-2 reveals insights into the molecular mechanism of microbial immobilization of heavy metals. *BMC Genomics*, *23*(1), 1–13. https://doi.org/10.1186/s12864-022-09069-4.

Sharma, S. (2012). Bioremediation : Features , Strategies, and applications. *Asian Journal of Pharmacy*, *2*(2), 202–213.http://www.ajpls.com.

Sher, S., Hussain, S. Z., & Rehman, A. (2020). Phenotypic and genomic analysis of multiple heavy metal–resistant Micrococcus luteus strain AS2 isolated from industrial waste water and its potential use in arsenic bioremediation. *Applied Microbiology and Biotechnology*, *104*(5), 2243–2254. https://doi.org/10.1007/s00253-020-10351-2.

Shrestha, P., Karmacharya, J., Han, S. R., Park, H., & Oh, T. J. (2022). In silico analysis and a comparative genomics approach to predict pathogenic trehalase genes in the complete genome of Antarctic Shigella sp. PAMC28760. *Virulence*, *13*(1), 1502–1514. https://doi.org/10.1080/21505594.2022.2117679.

Siunova, T. V., Filonov, A. E., Gorovtsov, A. V., Akhmetov, L. I., Ivanov, F. D., Rajput, V. D., Minkina, T. M., Sushkova, S. N., Wong, M. H., & Biswas, J. K. (2025). Potential of nickel

and cobalt-resistant microorganisms for effective phytoremediation of heavy metal contaminated soils. *Discover Environment*, *3*(1). https://doi.org/10.1007/s44274-025-00301-y.

Sivashankari, S. and Shanmughavel, P. (2007). Comparative genomics perspective. *Bioinformation*, *1*(9), 376. https://doi.org/10.6026/97320630001376.

Singh, A., Sharma, A., & Sundaram, S. (2025). Bioremediation of hexavalent chromium Cr (VI) in fluoride-contaminated environment by novel bacteria Bacillus albus SSAU-9. *Biodegradation*, *36*(5), 79. https://doi.org/10.1007/s10532-025-10176-8.

Sneha, S., Das, M. P., & Rebecca, L. J. (2014). Isolation and screening of protease producing bacteria from marine waste. *J Chem Pharm Res*, *6*(5), 1157-1159.http://www.jocpr.com/.

Sone, Y., Mochizuki, Y., Koizawa, K., Nakamura, R., Pan-Hou, H., Itoh, T., & Kiyono, M. (2013). Mercurial-resistance determinants in *Pseudomonas* strain K-62 plasmid pMR68. *AMB Express*, *3*(1), 1–7. https://doi.org/10.1186/2191-0855-3-41.

Sonune, Nilesh, Garode, & Anil. (2018). Isolation, characterization and identification of extracellular enzyme producer *Bacillus licheniformis* from municipal wastewater and evaluation of their biodegradability. *Biotechnology Research and Innovation*, *2*(1), 37–44. https://doi.org/10.1016/j.biori.2018.03.001.

Srivastava, V., Sarkar, A., Singh, S., Singh, P., de Araujo, A. S. F., & Singh, R. P. (2017). Agroecological responses of heavy metal pollution with special emphasis on soil health and plant performances. *Frontiers in Environmental Science*, *5*(OCT), 1–19. https://doi.org/10.3389/fenvs.2017.00064.

Stern, B. R. (2010). Essentiality and toxicity in copper health risk assessment: Overview, update and regulatory considerations. *Journal of Toxicology and Environmental Health - Part A: Current Issues*, *73*(2–3), 114–127. https://doi.org/10.1080/15287390903337100.

Sundarraj, S., Sudarmani, D. N. P., Samuel, P., & Sevarkodiyone, S. P. (2022). Bioremediation of hexavalent chromium by transformation of Escherichia coli DH5α with chromate reductase (ChrR) genes of Pseudomonas putida isolated from tannery effluent. *Journal of Applied Microbiology*, *134*(1), 1–11. https://doi.org/10.1093/jambio/lxac019.

Swain, C. K. (2024). Environmental pollution indices: a review on concentration of heavy metals in air, water, and soil near industrialization and urbanisation. *Discover Environment*, *2*(1). https://doi.org/10.1007/s44274-024-00030-8.

Syed, A., Zeyad, M. T., Shahid, M., Elgorban, A. M., Alkhulai, M. M., & Ansari, I. A. (2021). Heavy Metals Induced Modulations in Growth, Physiology, Cellular Viability, and Biofilm Formation of an Identified Bacterial Isolate. *ACS Omega*, *38*(6), 25076–25088. https://doi.org/10.1021/acsomega.1c04396.

Syed, Shameer, Chinthala, & Paramageetham. (2015). Heavy Metal Detoxification by Different *Bacillus* Species Isolated from Solar Salterns. *Scientifica*, *2015*, 1–8. https://doi.org/10.1155/2015/319760.

Tamura, K., Stecher, G., & Kumar, S. (2021). MEGA11: Molecular Evolutionary Genetics Analysis Version 11. *Molecular Biology and Evolution*, *38*(7), 3022–3027. https://doi.org/10.1093/molbev/msab120.

Tchounwou, P. B., Yedjou, C. G., Patlolla, A. K., & Sutton, D. J. (2012). Molecular, clinical and environmental toxicicology Volume 3: Environmental Toxicology. *Molecular, Clinical and Environmental Toxicology*, *101*, 133–164. https://doi.org/10.1007/978-3-7643-8340-4.

Terzi, E., & Civelek, F. (2021). Cu, Cd, As, and Hg resistance levels in *Escherichia coli* isolated from Mediterranean mussel and sea snail in the Southeastern Black Sea. *Marine Science and Technology Bulletin*, *10*(1), 36–41. https://doi.org/10.33714/masteb.776902.

Thatoi, H. N., & Pradhan, S. K. (2017). Detoxification and bioremediation of hexavalent chromium using microbes and their genes: An insight into genomic, proteomic, and bioinformatics studies. *Microbial Biotechnology*, *1*, 287–306. https://doi.org/10.1007/978-981-10-6847-8_13.

Tiquia-Arashiro, S., Li, X., Pokhrel, K., Kassem, A., Abbas, L., Coutinho, O., Kasperek, D., Najaf, H., & Opara, S. (2023). Applications of Fourier Transform-Infrared spectroscopy in microbial cell biology and environmental microbiology: advances, challenges, and future perspectives. *Frontiers in Microbiology*, *14*. https://doi.org/10.3389/fmicb.2023.1304081.

Tovar-Sánchez, E., Hernández-Plata, I., Martínez, M. S., Valencia-Cuevas, L., & Galante, P. M. (2018). Heavy metal pollution as a biodiversity threat. *Heavy metals*, *383*.https://doi: 10.5772/intechopen 74052.

Vácha, R. (2021). Heavy metal pollution and its effects on agriculture. *Agronomy*, *11*(9), 14–16. https://doi.org/10.3390/agronomy11091719.

Vasilachi, I. C., Stoleru, V., & Gavrilescu, M. (2023). Analysis of Heavy Metal Impacts on Cereal Crop Growth and Development in Contaminated Soils. *Agriculture*, *13*(10).

https://doi.org/10.3390/agriculture13101983.

Velmurugan, S., Anokhe, A., & Kalia, V. (2021). Biochemical characterisation of starch-hydrolysing bacteria. *AgriCos e-Newsletter*, *2*, 63-65.www.agricosemagazine.com.

Wang, Jianlong, Chen, & C. (2006). Biosorption of heavy metals by Saccharomyces cerevisiae: A review. *Biotechnology Advances*, *24*(5), 427–451. https://doi.org/10.1016/j.biotechadv.2006.03.001.

WHO. (2017). Guidelines for Drinking-water Quality, fourth. In *Proceedings of the Royal Society of Medicine* (Vol. 55). https://doi.org/10.5005/jp/books/11431_8.

Xie, Y., Fan, J., Zhu, W., Amombo, E., Lou, Y., Chen, L., & Fu, J. (2016). Effect of heavy metals pollution on soil microbial diversity and bermudagrass genetic variation. *Frontiers in Plant Science*, *7*(MAY2016), 1–12. https://doi.org/10.3389/fpls.2016.00755.

Xu, W., Jin, Y., & Zeng, G. (2024). Introduction of heavy metals contamination in the water and soil: a review on source, toxicity, and remediation methods. *Green Chemistry Letters and Reviews*, *17*(1), 1–25. https://doi.org/10.1080/17518253.2024.2404235.

Yang, Y., Hassan, M. F., Ali, W., Zou, H., Liu, Z., & Ma, Y. (2025). Effects of Cadmium Pollution on Human Health: A Narrative Review. *Atmosphere*, *16*(2), 1–23. https://doi.org/10.3390/atmos16020225.

Yang, T., Diao, X., Cheng, H., Wang, H., Zhou, H., Zhao, H., & Chen, C. M. (2020). Comparative study of polycyclic aromatic hydrocarbons (PAHs) and heavy metals (HMs) in corals, sediments, and seawater from coral reefs of Hainan, China. *Environmental Pollution*, *264*, 114719. https://doi.org/10.1016/j.envpol.2020.114719.

Yilmaz, A. B., Yanar, A., & Alkan, E. N. (2017). Review of heavy metal accumulation on aquatic environment in the Northern East Mediterrenean Sea Part I: Some essential metals. *Reviews on Environmental Health*, *32*(1–2), 119–163. https://doi.org/10.1515/reveh-2016-0065.

Yin, R. V., & Phung, O. J. (2015). Effect of chromium supplementation on glycated hemoglobin and fasting plasma glucose in patients with diabetes mellitus. *Nutrition Journal*, *14*(1). https://doi.org/10.1186/1475-2891-14-14.

Zamora-Ledezma, Camilo, Negrete-Bolagay, Daniela, Figueroa, Freddy, Zamora-Ledezma, Ezequiel, Ni, Ming, Alexis, Frank, Guerrero, & H., V. (2021). Heavy metal water pollution: A fresh look at hazards, novel and conventional remediation methods. *Environmental*

*Technology and Innovation*, *22*, 101504. https://doi.org/10.1016/j.eti.2021.101504.

Zeng, Weimin, Li, Fang, Wu, Chenchen, Yu, Runlan, Wu, Xueling, Shen, Li, Liu, Yuandong, Qiu, Guanzhou, Li, J., & Iaokun. (2020). Role of extracellular polymeric substance (EPS) in toxicity response of soil bacteria *Bacillus* sp. S3 to multiple heavy metals. *Bioprocess and Biosystems Engineering*, *43*(1), 153–167. https://doi.org/10.1007/s00449-019-02213-7.

Zeng, X., Xu, X., Qin, Q., Ye, K., Wu, W., & Huo, X. (2019). Heavy metal exposure has adverse effects on the growth and development of preschool children. *Environmental Geochemistry and Health*, *41*(1), 309–321. https://doi.org/10.1007/s10653-018-0114-z.

Zeyaullah, M., Islam, B., & Ali, A. (2010). Isolation, identification, and PCR amplification of the merA gene from the highly mercury-polluted Yamuna River. *African Journal of Biotechnology*, *9*(24), 3510-3514.https://doi.org/10.4314/ajb.v9i24.

Zhao, M. M., Kou, J. bin, Chen, Y. ping, Xue, L. gui, Fan, T. T., & Wang, S. mei. (2021). Bioremediation of wastewater containing mercury using three newly isolated bacterial strains. *Journal of Cleaner Production*, *299*, 126869. https://doi.org/10.1016/j.jclepro.2021.126869.

Zhao, S., Zhao, Y., Cui, Z., Zhang, H., & Zhang, J. (2024). Effect of pH, Temperature, and Salinity Levels on Heavy Metal Fraction in Lake Sediments. *Toxics*, *12*(7). https://doi.org/10.3390/toxics12070494.

Zhao, Yue, Yao, Jun, Yuan, Zhimin, Wang, Tianqi, Zhang, Yiyue, Wang, & Fei. (2017). Bioremediation of Cd by strain GZ-22 isolated from mine soil based on biosorption and microbially induced carbonate precipitation. *Environmental Science and Pollution Research*, *24*(1), 372–380. https://doi.org/10.1007/s11356-016-7810-y.

Zhou, Q., Yang, N., Li, Y., Ren, B., Ding, X., Bian, H., & Yao, X. (2020). Total concentrations and sources of heavy metal pollution in global river and lake water bodies from 1972 to 2017. *Global Ecology and Conservation*, *22*, e00925. https://doi.org/10.1016/j.gecco.2020.e00925.

Zhu, X., Liang, Z., Ma, J., Huang, J., Wang, L., & Yao, H. (2024). The cadDX operon contributes to cadmium resistance, oxidative stress resistance, and virulence in zoonotic streptococci. *Veterinary Research*, 1–15. https://doi.org/10.1186/s13567-024-01371-1.

# 7. LISTS OF APPENDICES

## 1. List of publications and contributions to conferences

a. **Dibbisa D**, Daba T, Mohammed S. (2024). Regulatory Element Analysis and Comparative Genomics Study of Heavy Metal-Resistant Genes in the Complete Genome of *Cupriavidus gilardii* CR3. *Bioinformatics and Biology Insights*. 18. doi:10.1177/11779322241299905.

Bioinformatics and Biology Insights

Impact Factor: 2.4 / 5-Year Impact Factor: 3.8 | Journal Homepage | Submi

Open access | Research article | First published online November 24, 2024

Regulatory Element Analysis and Comparative Genomics Study of Heavy Metal-Resistant Genes in the Complete Genome of *Cupriavidus gilardii* CR3

Duguma Dibbisa, Tadesse Daba, and Seid Mohammed View all authors and affiliations

All Articles | https://doi.org/10.1177/11779322241299905

b. **Dibbisa Itana**, D., Bedada, T. D., & Mohammed Ebu, S. (2025). Exploring the bioremediation potential of *Citrobacter* spp. and *Klebsiella* spp. newly isolated from the industrial effluents of Eastern Shewa, Ethiopia. *Environmental Research Communications*, *7*(7). https://doi.org/10.1088/2515-7620/adec45

ENVIRONMENTAL RESEARCH COMMUNICATIONS

INCLUSIVE PUBLISHING TRUSTED SCIENCE

Part of the ENVIRONMENTAL RESEARCH SERIES

PAPER • OPEN ACCESS

Exploring the bioremediation potential of *Citrobacter* spp. and *Klebsiella* spp. newly isolated from the industrial effluents of Eastern Shewa, Ethiopia

Duguma Dibbisa Itana*, Tadessa Daba Bedada and Seid Mohammed Ebu

Published 15 July 2025 • © 2025 The Author(s). Published by IOP Publishing Ltd

Environmental Research Communications, Volume 7, Number 7

Citation Duguma Dibbisa Itana *et al* 2025 *Environ. Res. Commun.* 7 075015

DOI 10.1088/2515-7620/adec45

Article metrics

423 Total downloads

Submit

Submit to this Journal

Share this article

c. **Dibbisa Itana, D.**, Daba Bedada, T., & Mohammed Ebu, S. (2025). A bioremediation approach of some selected heavy metal detected from Bishoftu and Mojo industrial effluents in Ethiopia. *Egyptian Journal of Aquatic Research*, *51*(3), 395–409. https://doi.org/10.1016/j.ejar.2025.03.002

HOSTED BY ELSEVIER

Egyptian Journal of Aquatic Research

Volume 51, Issue 3, September 2025, Pages 395-409

Full length article

# A bioremediation approach of some selected heavy metal detected from Bishoftu and Mojo industrial effluents in Ethiopia

Duguma Dibbisa Itana [a] [b], Tadessa Daba Bedada [a] [c], Seid Mohammed Ebu [a]

[a] Department of Applied Biology, School of Applied Natural Science, Adama Science and Technology University, P.O. Box 1888, Adama, Ethiopia

[b] School of Biological Science and Biotechnology, Haramaya University, P. O. Box, 138, Dire Dawa, Ethiopia

[c] Ethiopia Institute of Agricultural Research Center, P.O. Box 2003 Addis Ababa, Ethiopia

**Conference participation and Others**

a. First African Biotechnology Congress on Biotechnology for Sustainable Development of Africa. Elilli International Hotel, Addis Ababa, June 4-7, 2024.
b. **Itana, D. D**., & Duguma, A. (2021). The role and impacts of growth hormones in maximizing animal production-a review. *Turkish Journal of Agriculture-Food Science and Technology*, *9*(6), 975-981.
c. **Dibbisa**, D., & Wagari, G. (2022). In *silico* study of mercury resistance genes extracted from *Pseudomonas* spp. involved in bioremediation: understanding the promoter regions and regulatory elements. *International Journal of Genomics*, *2022*(1), 6185615.
d. **Itana, D. D**., & Habib, Z. Y. (2022). *In vitro* micropropagation of apple (Malus domestica) through axillary buds and shoot apices culture. *International Journal of Zoology and Applied Biosciences*, *7*(3), 1-7.

# 2. TABLE IN THE APPENDIX

**Appendix Table 1: Analysis of variance demonstrating differences in HM concentrations among soil samples from contaminated areas of the Bishoftu Eastern Industrial Zone**

| | | ANOVA TABLE | | | | |
|---|---|---|---|---|---|---|
| | | Sum of Squares | df | Mean Square | F | Sig. |
| Co | Between Groups | 0.000 | 2 | 0.000 | 0.163 | 0.851 |
| | Within Groups | 0.016 | 15 | 0.001 | | |
| | Total | 0.016 | 17 | | | |
| Cu | Between Groups | 0.004 | 2 | 0.002 | 0.048 | 0.953 |
| | Within Groups | 0.621 | 15 | 0.041 | | |
| | Total | 0.625 | 17 | | | |
| Cd | Between Groups | 0.000 | 2 | 0.000 | .113 | 0.894 |
| | Within Groups | 0.003 | 15 | 0.000 | | |
| | Total | 0.003 | 17 | | | |
| Ni | Between Groups | 0.066 | 2 | 0.033 | 0.787 | 0.473 |
| | Within Groups | 0.627 | 15 | 0.042 | | |
| | Total | 0.693 | 17 | | | |
| Mn | Between Groups | 0.016 | 2 | 0.008 | 0.004 | 0.996 |
| | Within Groups | 29.276 | 15 | 1.952 | | |
| | Total | 29.291 | 17 | | | |
| Zn | Between Groups | 0.003 | 2 | 0.001 | 0.032 | 0.969 |
| | Within Groups | 0.646 | 15 | 0.043 | | |
| | Total | .649 | 17 | | | |
| Fe | Between Groups | 0.110 | 2 | 0.055 | 0.041 | 0.960 |
| | Within Groups | 20.247 | 15 | 1.350 | | |
| | Total | 20.356 | 17 | | | |

**Appendix Table 2: Analysis of variance demonstrating differences in HM concentrations among wastewater samples from contaminated areas of Mojo industrial effluents**

| | | ANOVA | | | | |
|---|---|---|---|---|---|---|
| | | Sum of Squares | df | Mean Square | F | Sig. |
| Cd | Between Groups | 0.000 | 2 | 0.000 | 0.071 | 0.931 |
| | Within Groups | 0.006 | 15 | 0.000 | | |
| | Total | 0.006 | 17 | | | |
| Cr | Between Groups | 0.282 | 2 | 0.141 | 0.853 | 0.446 |
| | Within Groups | 2.477 | 15 | 0.165 | | |
| | Total | 2.759 | 17 | | | |
| Mn | Between Groups | 0.018 | 2 | 0.009 | 0.124 | 0.884 |
| | Within Groups | 1.062 | 15 | 0.071 | | |
| | Total | 1.079 | 17 | | | |
| Zn | Between Groups | 0.001 | 2 | 0.001 | 0.005 | 0.995 |
| | Within Groups | 1.989 | 15 | 0.133 | | |
| | Total | 1.990 | 17 | | | |
| Fe | Between Groups | 00.009 | 2 | 0.004 | 0.006 | 0.994 |
| | Within Groups | 12.141 | 15 | 0.809 | | |
| | Total | 12.150 | 17 | | | |

**Appendix Table 3: Analysis of variance demonstrating differences in HM reduction**

| | | ANOVA | | | | |
|---|---|---|---|---|---|---|
| | | Sum of Squares | df | Mean Square | F | Sig. |
| Co | Between Groups | 106.343 | 2 | 53.171 | 0.205 | 0.816 |
| | Within Groups | 6998.328 | 27 | 259.197 | | |
| | Total | 7104.671 | 29 | | | |
| Cu | Between Groups | 2.166 | 2 | 1.083 | 0.030 | 0.970 |
| | Within Groups | 974.575 | 27 | 36.095 | | |
| | Total | 976.741 | 29 | | | |
| Cd | Between Groups | 9.341 | 2 | 4.670 | 0.072 | 0.931 |
| | Within Groups | 1746.214 | 27 | 64.675 | | |
| | Total | 1755.555 | 29 | | | |
| Cr | Between Groups | 197.737 | 2 | 98.869 | 1.818 | 0.182 |
| | Within Groups | 1468.387 | 27 | 54.385 | | |
| | Total | 1666.124 | 29 | | | |
| Zn | Between Groups | 7.885 | 2 | 3.943 | 0.058 | 0.944 |
| | Within Groups | 1835.371 | 27 | 67.977 | | |
| | Total | 1843.257 | 29 | | | |

**Appendix Table 4: Analysis of variance of the effects of cobalt on the Growth inhibition of bacterial isolates**

| | | ANOVA | | | | |
|---|---|---|---|---|---|---|
| | | Sum of Squares | df | Mean Square | F | Sig. |
| HMRBI-1 | Between Groups | 153500401.725 | 2 | 76750200.862 | 1.001 | 0.381 |
| | Within Groups | 2070272933.532 | 27 | 76676775.316 | | |
| | Total | 2223773335.257 | 29 | | | |
| HMRBI-3 | Between Groups | 3.548 | 2 | 1.774 | 0.010 | 0.990 |
| | Within Groups | 4615.082 | 27 | 170.929 | | |
| | Total | 4618.631 | 29 | | | |
| HMRBI-5 | Between Groups | 0.866 | 2 | 0.433 | 0.003 | 0.997 |
| | Within Groups | 4508.176 | 27 | 166.969 | | |
| | Total | 4509.043 | 29 | | | |
| HMRMI-7 | Between Groups | 0.099 | 2 | 0.049 | 0.000 | 1.000 |
| | Within Groups | 4920.832 | 27 | 182.253 | | |
| | Total | 4920.931 | 29 | | | |
| HMRMI-8 | Between Groups | 1.106 | 2 | 0.553 | 0.003 | 0.997 |
| | Within Groups | 4549.520 | 27 | 168.501 | | |
| | Total | 4550.626 | 29 | | | |
| HMRMI-9 | Between Groups | 0.331 | 2 | 0.166 | 0.001 | 0.999 |
| | Within Groups | 3380.228 | 27 | 125.194 | | |
| | Total | 3380.559 | 29 | | | |
| HMRMI-10 | Between Groups | 0.842 | 2 | 0.421 | 0.004 | 0.996 |
| | Within Groups | 2788.964 | 27 | 103.295 | | |
| | Total | 2789.806 | 29 | | | |

**Appendix Table 5: Analysis of variance of the effects of copper on the Growth inhibition of bacterial isolates**

| | | ANOVA | | | | |
|---|---|---|---|---|---|---|
| | | Sum of Squares | df | Mean Square | F | Sig. |
| HMRBI-1 | Between Groups | 13.037 | 2 | 6.518 | 0.023 | 0.977 |
| | Within Groups | 6772.567 | 24 | 282.190 | | |
| | Total | 6785.603 | 26 | | | |
| HMRBI-3 | Between Groups | 0.794 | 2 | .397 | 0.003 | 0.997 |
| | Within Groups | 3712.394 | 24 | 154.683 | | |
| | Total | 3713.188 | 26 | | | |
| HMRBI-5 | Between Groups | 0.097 | 2 | 0.048 | 0.000 | 1.000 |
| | Within Groups | 8325.507 | 24 | 346.896 | | |
| | Total | 8325.603 | 26 | | | |
| HMRBI-7 | Between Groups | 0.853 | 2 | 0.426 | 0.006 | 0.994 |
| | Within Groups | 1820.347 | 24 | 75.848 | | |
| | Total | 1821.199 | 26 | | | |
| HMRBI-8 | Between Groups | 0.402 | 2 | 0.201 | 0.001 | 0.999 |
| | Within Groups | 3487.337 | 24 | 145.306 | | |
| | Total | 3487.739 | 26 | | | |
| HMRBI-9 | Between Groups | 1.828 | 2 | 0.914 | 0.002 | 0.998 |
| | Within Groups | 9479.498 | 24 | 394.979 | | |
| | Total | 9481.326 | 26 | | | |
| HMRBI-10 | Between Groups | 1.052 | 2 | 0.526 | 0.003 | 0.997 |
| | Within Groups | 3723.517 | 24 | 155.147 | | |
| | Total | 3724.569 | 26 | | | |

**Appendix Table 6: Analysis of variance of the effects of cadmium on the Growth inhibition of bacterial isolates**

| | | ANOVA | | | | |
|---|---|---|---|---|---|---|
| | | Sum of Squares | df | Mean Square | F | Sig. |
| HMRBI-1 | Between Groups | 4.514 | 2 | 2.257 | 0.010 | 0.990 |
| | Within Groups | 6290.080 | 27 | 232.966 | | |
| | Total | 6294.594 | 29 | | | |
| HMRBI-3 | Between Groups | 35.401 | 2 | 17.700 | 0.087 | 0.917 |
| | Within Groups | 5481.324 | 27 | 203.012 | | |
| | Total | 5516.725 | 29 | | | |
| HMRBI-5 | Between Groups | 14.597 | 2 | 7.299 | 0.041 | 0.960 |
| | Within Groups | 4793.665 | 27 | 177.543 | | |
| | Total | 4808.263 | 29 | | | |
| HMRBI-7 | Between Groups | 15.056 | 2 | 7.528 | 0.087 | 0.917 |
| | Within Groups | 2344.407 | 27 | 86.830 | | |
| | Total | 2359.463 | 29 | | | |
| HMRBI-8 | Between Groups | 0.268 | 2 | 0.134 | 0.000 | 1.000 |
| | Within Groups | 7943.183 | 27 | 294.192 | | |
| | Total | 7943.451 | 29 | | | |
| HMRBI-9 | Between Groups | 1.122 | 2 | 0.561 | 0.002 | 0.998 |
| | Within Groups | 6941.422 | 27 | 257.090 | | |
| | Total | 6942.543 | 29 | | | |
| HMRBI-10 | Between Groups | 0.882 | 2 | 0.441 | 0.001 | 0.999 |
| | Within Groups | 8294.590 | 27 | 307.207 | | |
| | Total | 8295.472 | 29 | | | |

**Appendix Table 7: Analysis of variance of the effects of Zinc on the Growth inhibition of bacterial isolates**

| | | ANOVA | | | | |
|---|---|---|---|---|---|---|
| | | Sum of Squares | df | Mean Square | F | Sig. |
| HMRBI-1 | Between Groups | 4.714 | 2 | 2.357 | 0.007 | 0.993 |
| | Within Groups | 8723.797 | 27 | 323.104 | | |
| | Total | 8728.511 | 29 | | | |
| HMRBI-3 | Between Groups | 8.643 | 2 | 4.322 | 0.029 | 0.972 |
| | Within Groups | 4039.503 | 27 | 149.611 | | |
| | Total | 4048.147 | 29 | | | |
| HMRBI-5 | Between Groups | .142 | 2 | 0.071 | 0.000 | 1.000 |
| | Within Groups | 8904.853 | 27 | 329.809 | | |
| | Total | 8904.996 | 29 | | | |
| HMRBI-7 | Between Groups | 235.143 | 2 | 117.572 | 0.375 | 0.691 |
| | Within Groups | 8473.594 | 27 | 313.837 | | |
| | Total | 8708.737 | 29 | | | |
| HMRBI-8 | Between Groups | 0.293 | 2 | 0.146 | 0.001 | 0.999 |
| | Within Groups | 5237.350 | 27 | 193.976 | | |
| | Total | 5237.643 | 29 | | | |
| HMRBI-9 | Between Groups | 3.119 | 2 | 1.559 | 0.002 | 0.998 |
| | Within Groups | 17018.142 | 27 | 630.302 | | |
| | Total | 17021.260 | 29 | | | |
| HMRBI-10 | Between Groups | 1.123 | 2 | 0.562 | 0.001 | 0.999 |
| | Within Groups | 14658.668 | 27 | 542.914 | | |
| | Total | 14659.791 | 29 | | | |

**Appendix Table 8: Analysis of variance of the effects chromium on the Growth inhibition of bacterial isolates**

| | | ANOVA | | | | |
|---|---|---|---|---|---|---|
| | | Sum of Squares | df | Mean Square | F | Sig. |
| HMRBI-1 | Between Groups | 0.368 | 2 | 0.184 | 0.003 | 0.997 |
| | Within Groups | 1512.927 | 27 | 56.034 | | |
| | Total | 1513.295 | 29 | | | |
| HMRBI-3 | Between Groups | 1.737 | 2 | 0.868 | 0.021 | 0.979 |
| | Within Groups | 1106.482 | 27 | 40.981 | | |
| | Total | 1108.219 | 29 | | | |
| HMRBI-5 | Between Groups | 1.369 | 2 | 0.685 | 0.017 | 0.983 |
| | Within Groups | 1084.458 | 27 | 40.165 | | |
| | Total | 1085.828 | 29 | | | |
| HMRBI-7 | Between Groups | 1.920 | 2 | 0.960 | 0.014 | 0.986 |
| | Within Groups | 1818.583 | 27 | 67.355 | | |
| | Total | 1820.503 | 29 | | | |
| HMRBI-8 | Between Groups | 2.454 | 2 | 1.227 | 0.027 | 0.973 |
| | Within Groups | 1215.064 | 27 | 45.002 | | |
| | Total | 1217.518 | 29 | | | |
| HMRBI-9 | Between Groups | 0.101 | 2 | 0.051 | 0.001 | 0.999 |
| | Within Groups | 2668.339 | 27 | 98.827 | | |
| | Total | 2668.441 | 29 | | | |
| HMRBI-10 | Between Groups | 2.012 | 2 | 1.006 | 0.007 | 0.993 |
| | Within Groups | 3635.814 | 27 | 134.660 | | |
| | Total | 3637.825 | 29 | | | |

**Appendix Table 9: Analysis of variance of DNA quantification results of HMRBI samples**

| Well No | Isolate Name | 260 | 280 | 260/280 | Comment |
|---|---|---|---|---|---|
| 1. | HMR1_01 | 0.155 | 0.084 | 1.845 | QC PASS |
| 2. | HMR1_03 | 0.145 | 0.091 | 1.593 | QC PASS |
| 3. | HMR1_05 | 0.15 | 0.081 | 1.851 | QC PASS |
| 4. | HMR1_11 | 0.125 | 0.068 | 1.838 | QC PASS |
| 5. | HMR1_13 | 0.184 | 0.102 | 1.803 | QC PASS |
| 6. | HMR1_14 | 0.168 | 0.095 | 1.768 | QC PASS |
| 7. | HMR1_19 | 0.088 | 0.047 | 1.872 | QC PASS |
| 8. | HMR1_20 | 0.144 | 0.078 | 1.846 | QC PASS |

**Appendix Table 10: Biochemical Tests for HMRBI Obtained from Bishoftu**

| Biochemical Tests | | | | | | | | | | | | | | |
|---|---|---|---|---|---|---|---|---|---|---|---|---|---|---|
| Isolates code | Gst | Ind | Mer | Str | Triple sugar | | | | Ur | VPK | Gel | Cat. | Mot. | Cit. |
| | | | | | Glu | Lac | Suc | $H_2S$ | | | | | | |
| HMRBI-1 | - | - | + | + | + | - | - | - | + | - | + | + | motile | + |
| HMRBI-2 | - | - | - | - | + | - | - | - | + | - | + | + | motile | - |
| HMRBI-3 | - | - | - | - | - | + | + | + | - | - | + | + | motile | + |
| HMRBI-4 | - | - | - | - | - | + | + | + | - | - | + | + | motile | + |
| HMRBI-5 | - | - | - | + | + | - | - | + | + | - | + | + | motile | + |
| HMRBI-6 | - | - | + | - | - | - | - | - | + | - | + | + | motile | - |
| HMRBI-7 | - | - | + | + | - | - | - | - | + | - | + | + | motile | + |
| HMRBI-8 | - | - | - | - | - | - | - | + | + | - | - | + | motile | + |
| HMRBI-9 | - | - | + | + | + | - | - | - | + | - | + | + | motile | + |
| HMRBI-10 | + | - | - | + | - | - | - | + | + | - | - | + | motile | + |
| HMRBI-11 | + | - | - | - | - | - | - | + | + | - | + | + | motile | + |
| HMRBI-12 | - | + | + | + | + | - | + | + | - | + | + | + | motile | + |
| HMRBI-13 | - | - | - | - | - | + | + | + | - | - | - | + | motile | + |
| HMRBI-14 | - | - | - | - | - | - | - | + | - | - | + | + | motile | + |
| HMRBI-15 | - | + | - | - | - | - | - | + | - | - | + | + | motile | + |
| HMRBI-16 | - | + | - | + | + | - | + | - | - | + | - | + | motile | + |
| HMRBI-17 | - | - | - | + | + | - | + | + | - | + | - | + | motile | + |
| HMRBI-18 | - | - | - | + | + | - | + | + | - | + | - | + | motile | + |
| HMRBI-19 | - | - | - | + | - | - | + | + | - | + | - | + | motile | + |
| HMRBI-20 | - | + | - | - | + | - | + | + | - | - | - | + | motile | + |
| HMRBI-21 | + | + | + | - | + | - | + | - | - | - | - | + | motile | + |
| HMRBI-22 | + | + | + | - | + | - | + | - | - | - | - | + | motile | + |
| HMRBI-23 | + | + | + | - | + | - | + | - | - | - | - | + | motile | + |
| HMRBI-24 | + | + | + | - | + | - | + | - | - | - | - | + | motile | + |
| HMRBI-25 | - | + | - | - | + | - | + | - | - | - | - | + | motile | + |
| HMRBI-26 | - | + | + | - | + | - | - | + | - | + | - | + | motile | + |
| HMRBI-27 | - | + | + | - | + | - | - | + | - | + | - | + | motile | + |
| HMRBI-28 | - | + | + | - | + | - | - | + | - | + | - | + | motile | + |
| HMRBI-29 | - | + | + | - | + | - | - | + | - | + | - | + | motile | + |
| HMRBI-30 | - | + | + | - | + | - | - | + | - | + | - | + | motile | + |

Keywords: Gst -Gram staining, Ind- Indole test Mer- Methylene red, Str-starch hydrolysis, Glu- Glucose, Lac- Lactose, Suc- Sucrose, Ur- urease, Gel- Gelatin hydrolysis, Cat- Catalase, Mot-Motile, Cit-Citrate utilization, HMRBI- Heavy metal resistant bacteria isolates

**Appendix Table 11: Biochemical Tests for HMRBIs Obtained from Mojo Tannery Wastewater**

| Bacteria Isolates code | Biochemical Tests | | | | | | | | | | | | | |
|---|---|---|---|---|---|---|---|---|---|---|---|---|---|---|
| | | | | | Triple sugar | | | | | | | | | Cit. |
| | Gst | Ind | Mer | Str | Glu | Lact. | Suc | $H_2S$ | Ur | VPK | Gel | Cat | Mot. | |
| HMRBI-31 | - | - | - | - | + | - | - | - | - | - | - | + | motile | + |
| HMRBI-32 | - | + | - | - | + | + | - | - | + | - | + | + | motile | + |
| HMRBI-33 | - | - | - | - | - | + | + | + | - | - | + | + | motile | + |
| HMRBI-34 | - | - | - | - | - | + | + | + | - | - | + | + | motile | + |
| HMRBI-35 | - | - | - | + | + | - | - | + | + | - | + | + | motile | + |
| HMRBI-36 | - | - | + | - | - | - | - | - | + | - | + | + | motile | + |
| HMRBI-37 | + | - | + | + | - | - | - | - | + | - | + | + | motile | + |
| HMRBI-38 | - | - | - | - | - | - | - | + | + | - | - | + | motile | + |
| HMRBI-39 | - | - | + | + | + | - | - | - | + | - | + | + | motile | + |
| HMRBI-40 | + | - | - | + | - | + | - | + | + | - | - | + | motile | + |
| HMRBI-41 | + | - | - | - | - | - | - | + | + | - | - | + | motile | + |
| HMRBI-42 | + | + | - | + | - | - | + | + | - | + | - | + | motile | + |
| HMRBI-43 | - | - | - | - | - | - | - | + | - | - | - | + | motile | + |
| HMRBI-44 | - | - | - | - | - | - | - | + | - | - | + | + | motile | + |
| HMRBI-45 | - | + | - | - | - | - | - | + | - | - | + | + | motile | + |
| HMRBI-46 | - | + | + | + | + | + | + | + | + | + | + | + | motile | - |
| HMRBI-47 | - | + | + | - | + | - | - | + | + | + | - | + | motile | - |
| HMRBI-48 | - | + | + | - | + | + | - | + | + | + | - | + | motile | - |
| HMRBI-49 | - | + | + | - | + | - | - | + | + | + | - | + | motile | - |
| HMRBI-50 | - | + | + | - | + | + | - | + | + | + | - | + | motile | + |
| HMRBI-51 | - | + | + | - | + | + | - | + | + | + | - | + | motile | - |
| HMRBI-52 | - | + | + | - | + | - | - | + | + | + | - | + | motile | - |
| HMRBI-53 | - | + | + | - | + | + | - | + | + | + | - | + | motile | - |
| HMRBI-54 | - | + | + | - | + | - | - | + | + | + | - | + | motile | |
| HMRBI-55 | + | - | + | + | + | + | - | - | | + | - | + | motile | + |
| HMRBI-56 | + | - | + | + | + | + | - | - | | + | - | + | motile | + |
| HMRBI-57 | + | - | + | + | + | + | - | - | | + | - | + | motile | + |
| HMRBI-58 | + | - | + | + | + | + | - | - | | + | - | + | motile | + |
| HMRBI-59 | + | - | + | + | + | + | - | - | | + | - | + | motile | + |
| HMRBI-60 | + | - | + | + | + | + | - | - | | + | - | + | motile | + |

# 3. APPENDIX IN FIGURES

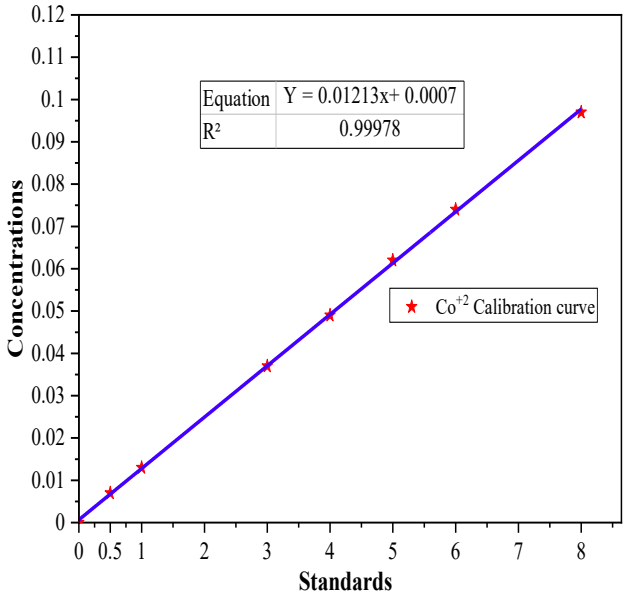


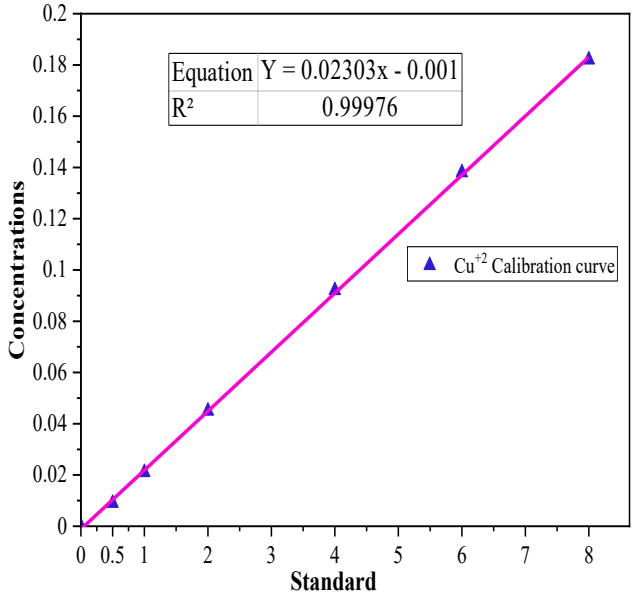


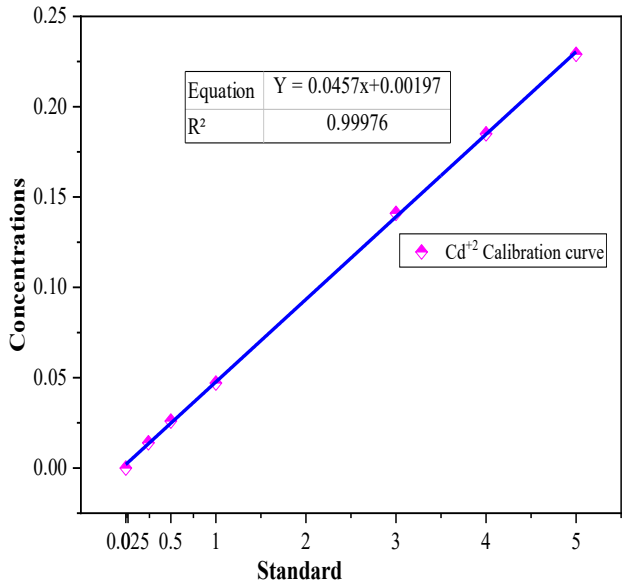


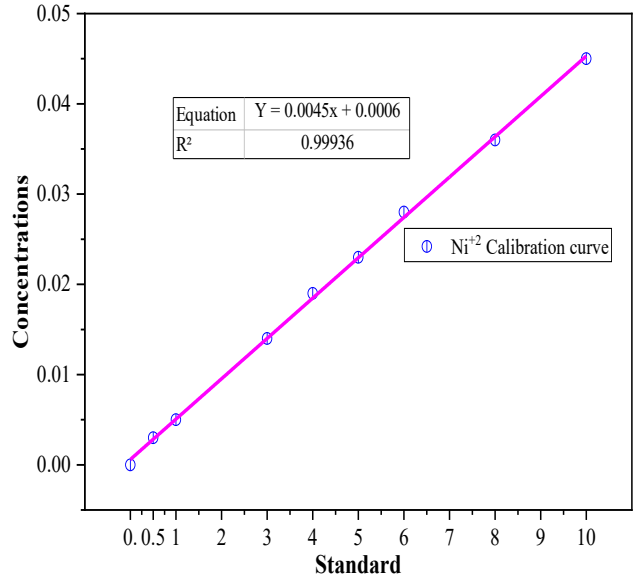

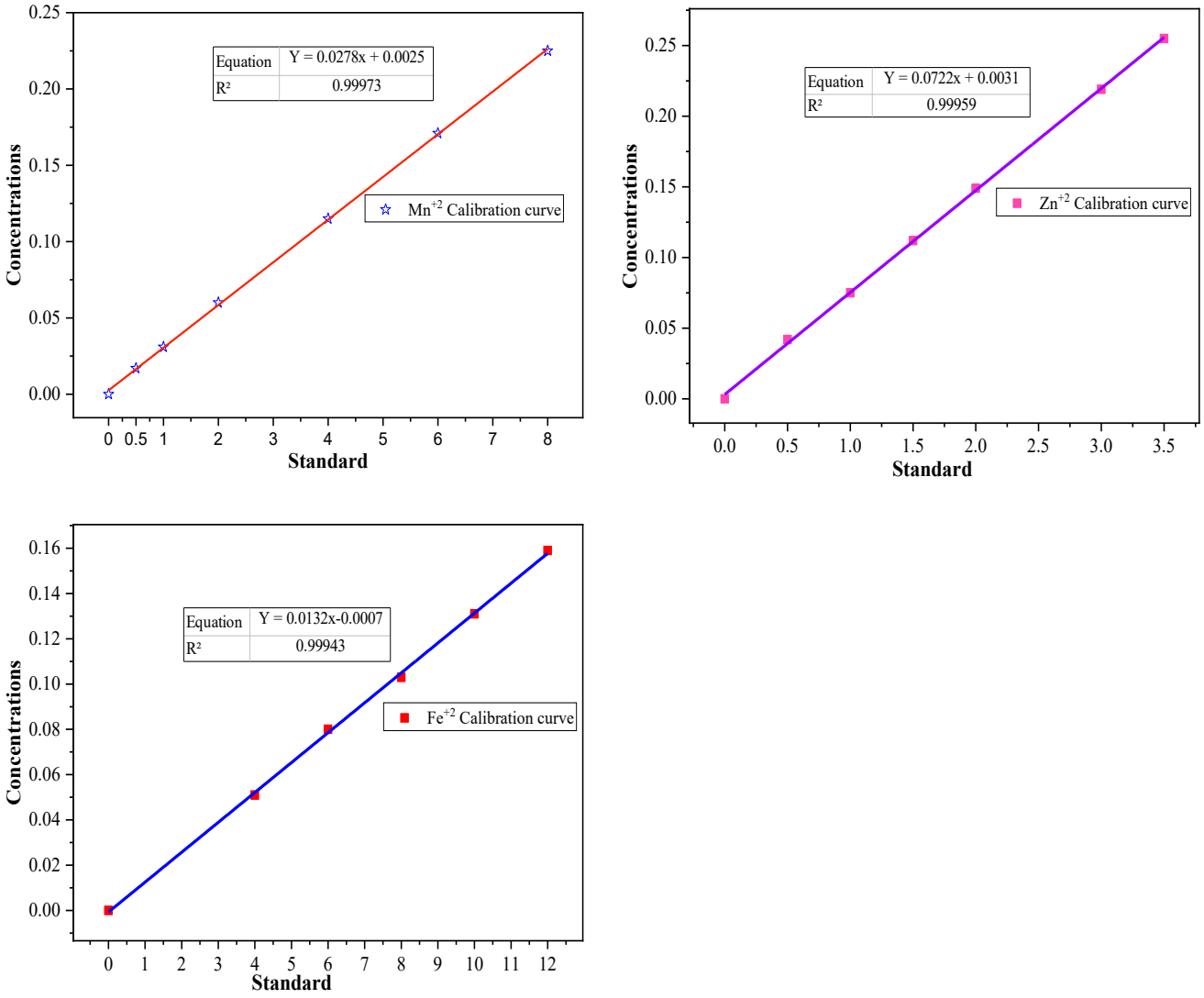


**Appendix Figure 1: Cobalt. Copper, Cadmium, Nickel, Manganese, Zinc, and Iron determination form the Bishoftu Eastern Industrial Zone soil waste calibration curve.**

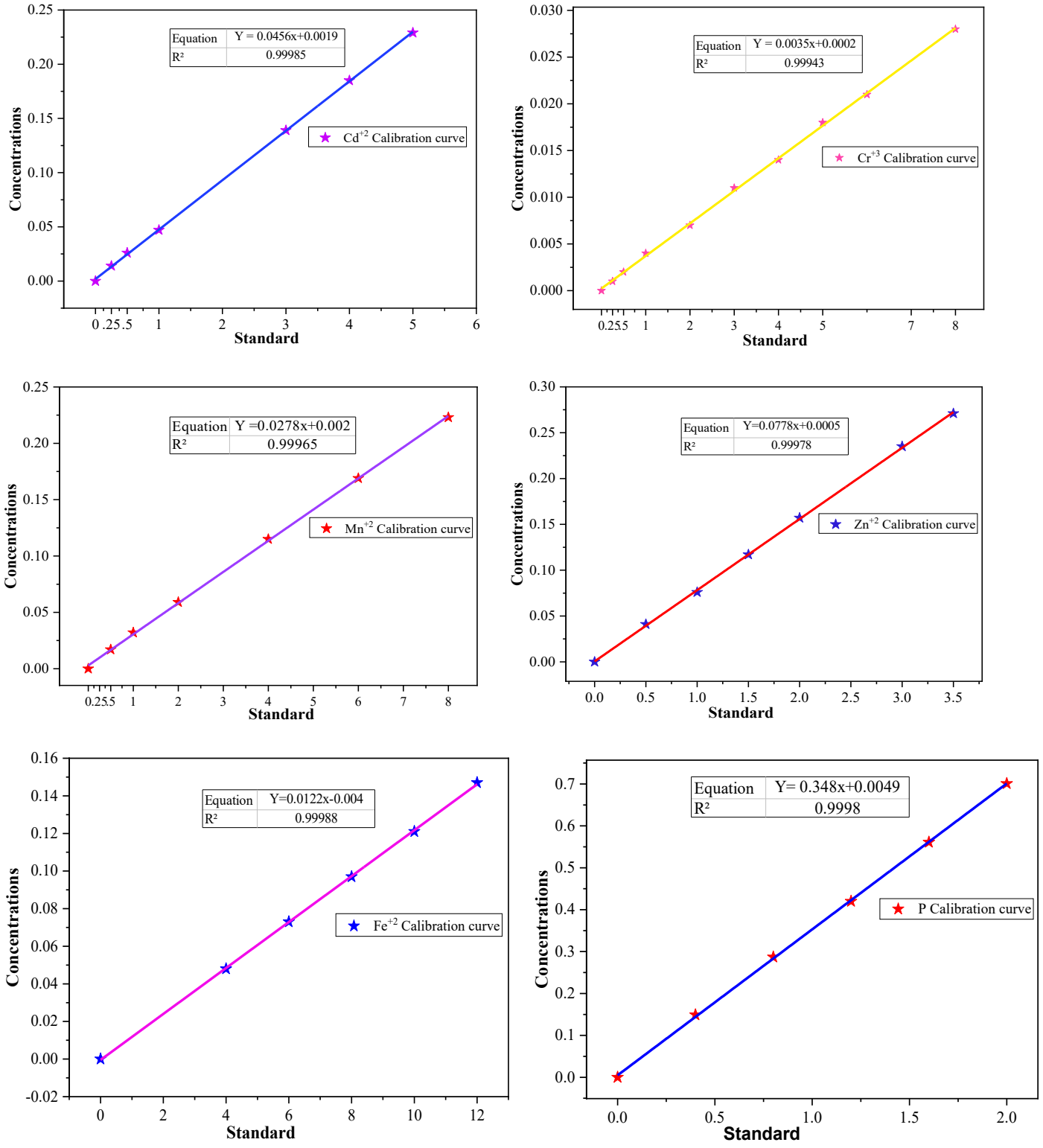


**Appendix Figure 2: Graphical Sketch Representation of Cadmium, Chromium, Manganese, Zinc, and Iron determination form the Mojo waste water calibration curve.**

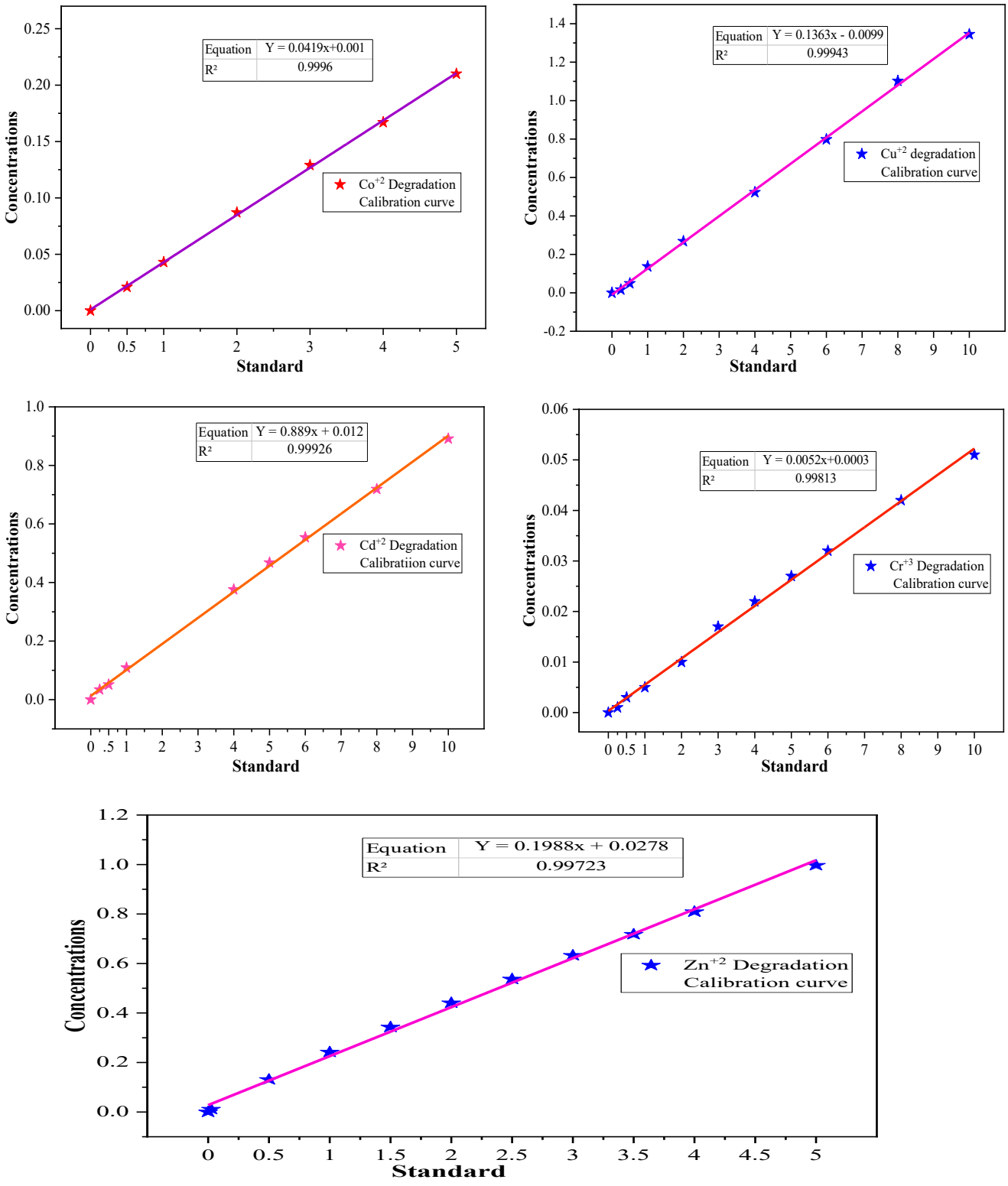


**Appendix Figure 3: Graphical Sketch Representation of Cobalt. Copper, Cadmium, and Zinc determination form the Bishoftu Eastern Industrial Zone and Mojo calibration curve.**

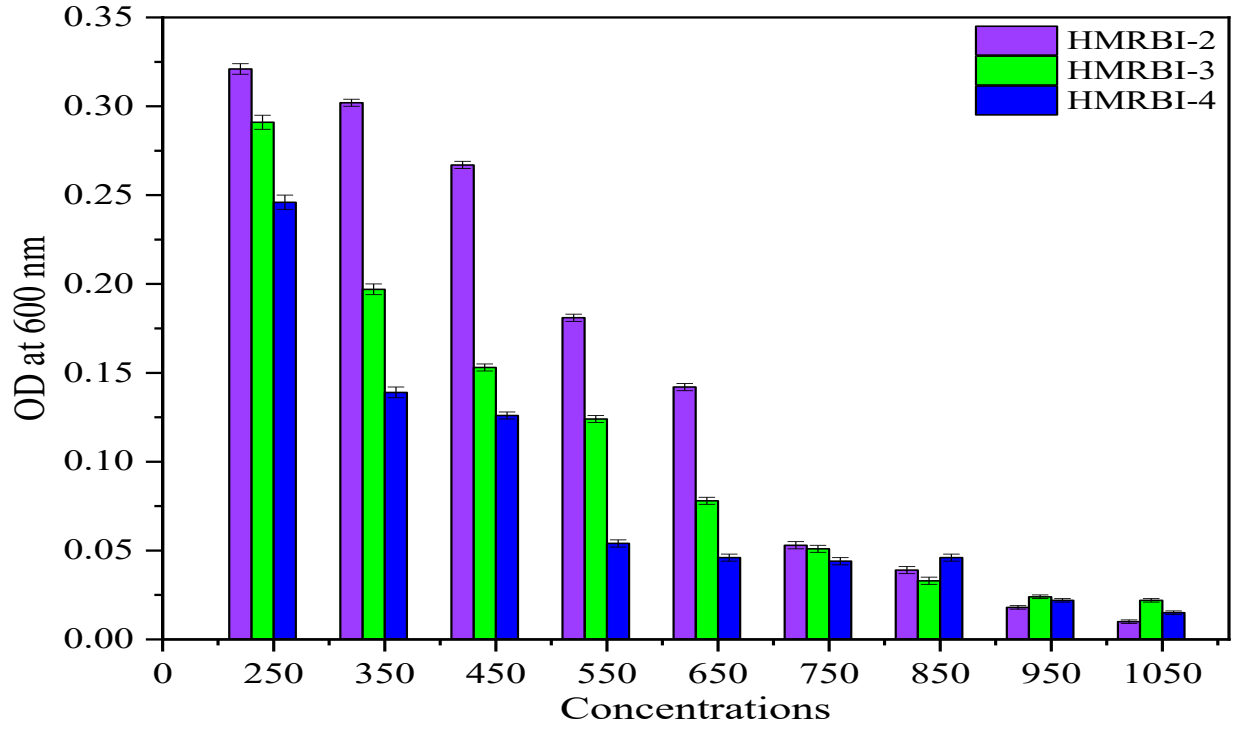


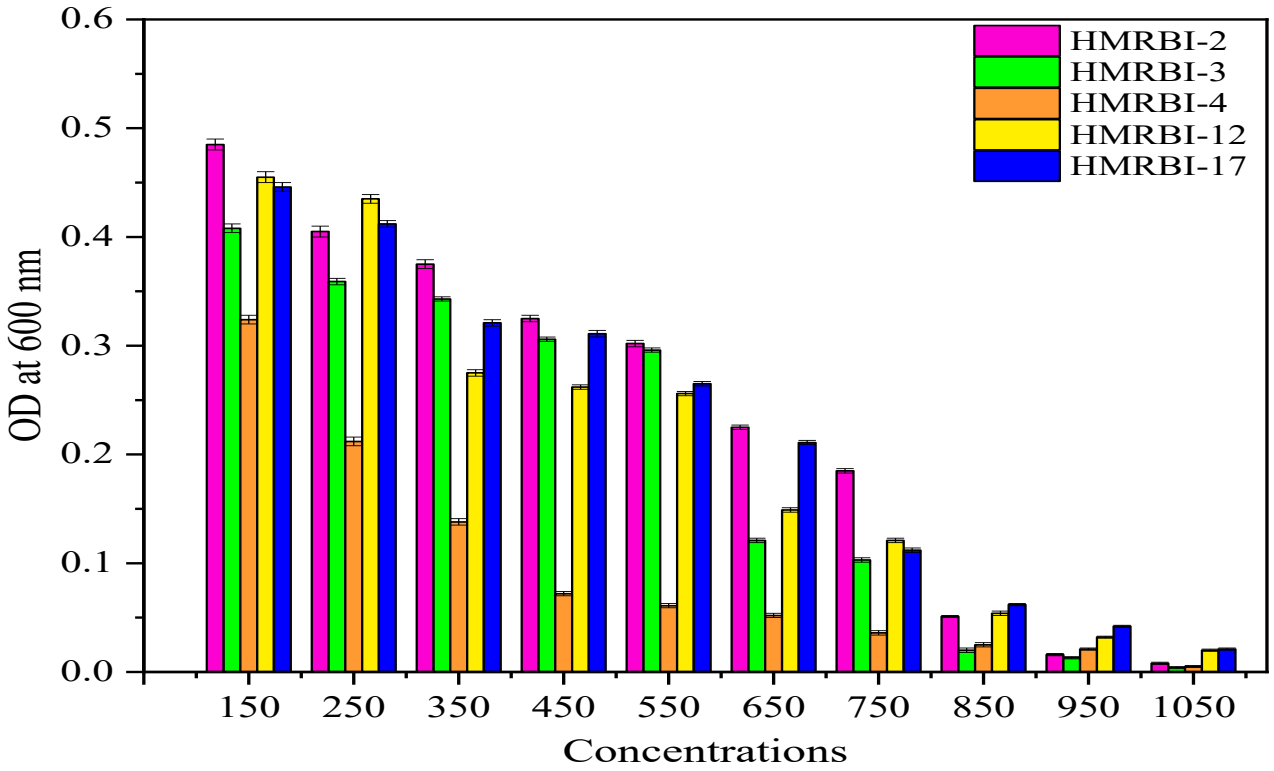


**Appendix Figure 4: Effects of HM Concentration on the Growth of Bacterial Isolates a Graphical Representation**

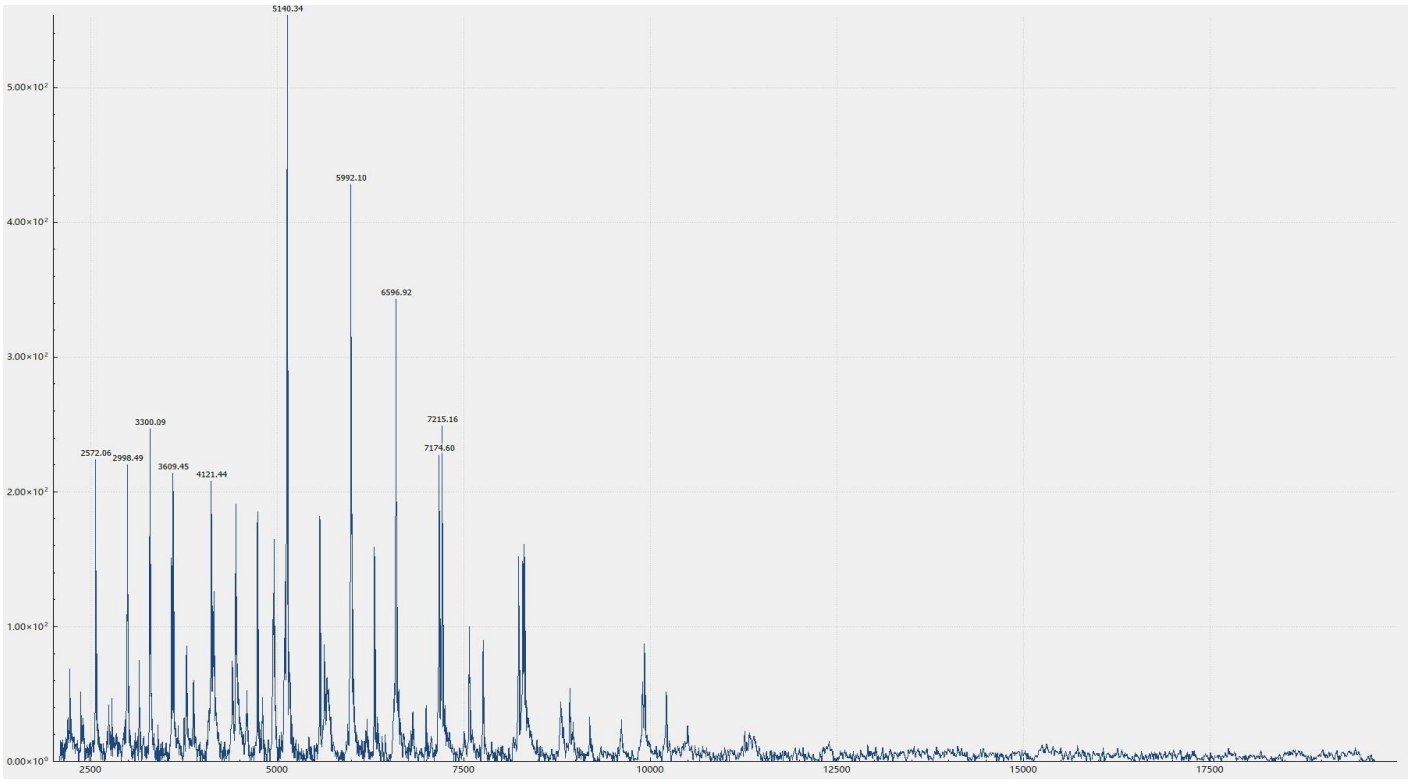


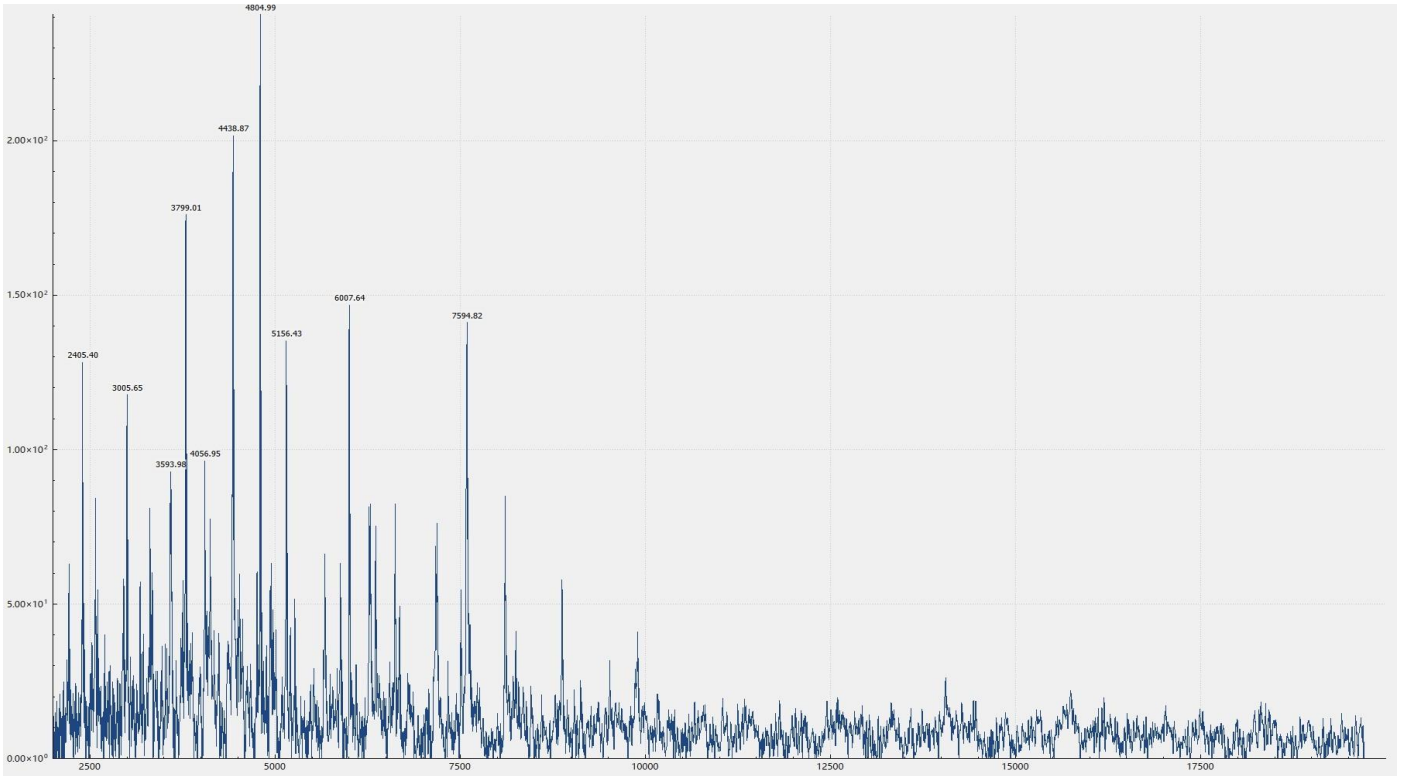


**Appendix Figure 5: Graphical Sketch Representation of *P. mosselii* and *P. oleovorans* by MALDTOF-MS respectively**

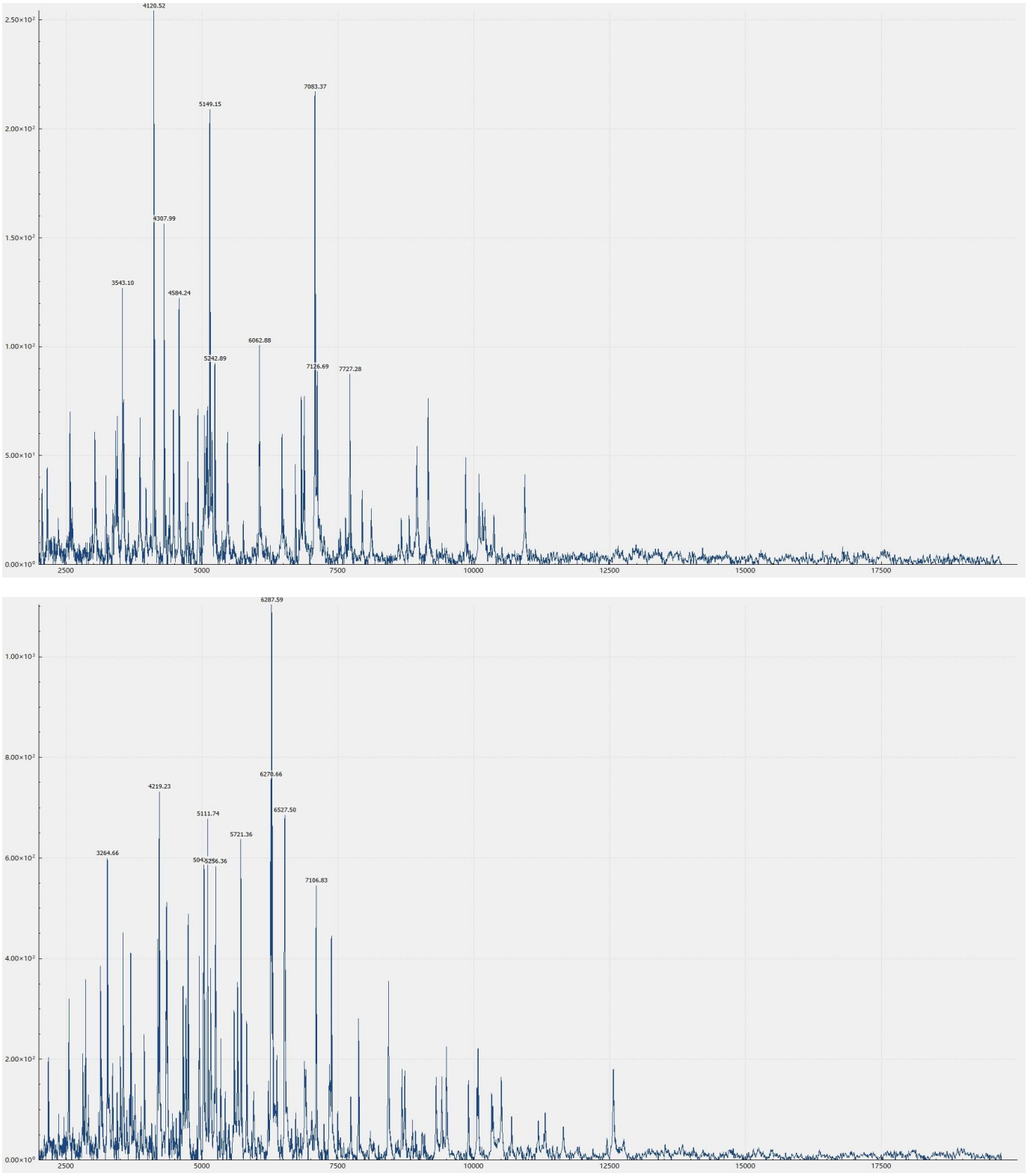


**Appendix Figure 6: Graphical Sketch Representation of *E. aurantiacum* and *Delftia acidovorans* by MALDTOF-MS respectively**

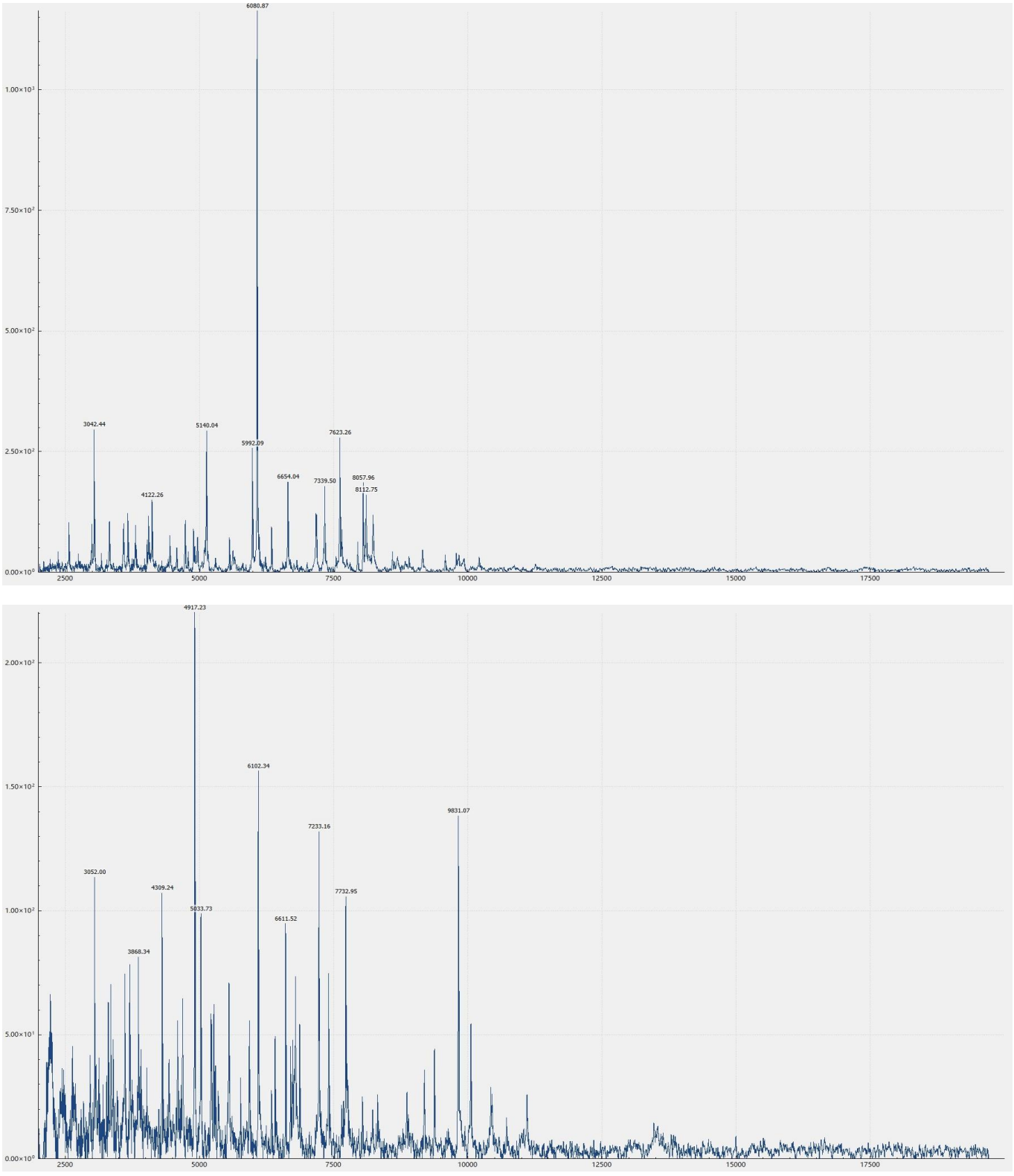


**Appendix Figure 7: Graphical Sketch Representation of *P. plecoglossicida* and *B. pumilus* Using MALDI-TOF MS respectively**

| Description | Scientific Name | Max Score | Total Score | Query Cover | E value | Per. Ident | Acc. Len | Accession |
|---|---|---|---|---|---|---|---|---|
| Paraclostridium bifermentans strain MCM B 557 16S ribosomal RNA gene, partial sequence | Paraclostridium … | 2615 | 2615 | 100% | 0.0 | 99.93% | 1455 | KT624613.1 |
| Paraclostridium sp. strain CD-H-12 16S ribosomal RNA gene, partial sequence | Paraclostridium … | 2580 | 2580 | 100% | 0.0 | 99.37% | 1457 | OP491973.1 |
| Uncultured Paraclostridium sp. clone asv_152_2131 16S ribosomal RNA gene, partial sequence; 16S-23S rib… | uncultured Para… | 2580 | 2580 | 100% | 0.0 | 99.37% | 2131 | MT967653.1 |
| Paraclostridium bifermentans strain JCM 1386 16S ribosomal RNA, partial sequence | Paraclostridium … | 2580 | 2580 | 100% | 0.0 | 99.37% | 1463 | NR_113323.1 |
| Paraclostridium bifermentans strain Cbm chromosome | Paraclostridium … | 2580 | 24053 | 100% | 0.0 | 99.37% | 3638572 | CP032452.1 |
| Paraclostridium bifermentans strain Nesulana1 16S ribosomal RNA gene, partial sequence | Paraclostridium … | 2580 | 2580 | 100% | 0.0 | 99.37% | 1472 | KJ722487.1 |
| Uncultured bacterium clone 425_TC18_122 16S ribosomal RNA gene, partial sequence | uncultured bacte… | 2580 | 2580 | 100% | 0.0 | 99.37% | 1424 | KM251041.1 |
| Clostridium sp. zx5 16S ribosomal RNA gene, partial sequence | Clostridium sp. zx5 | 2580 | 2580 | 100% | 0.0 | 99.37% | 1483 | EF052864.1 |
| Paraclostridium bifermentans strain DSM 14991 chromosome, complete genome | Paraclostridium … | 2580 | 41216 | 100% | 0.0 | 99.37% | 3304778 | CP079737.1 |
| Clostridium sp. H2 gene for 16S ribosomal RNA, partial sequence, strain: H2 | Clostridium sp. H2 | 2580 | 2580 | 100% | 0.0 | 99.37% | 1463 | LC194786.1 |
| Paraclostridium sp. strain M3-Q-101 16S ribosomal RNA gene, partial sequence | Paraclostridium … | 2580 | 2580 | 100% | 0.0 | 99.37% | 1438 | OK326205.1 |
| Paraclostridium benzoelyticum strain BL-Q-101 16S ribosomal RNA gene, partial sequence | Paraclostridium … | 2577 | 2577 | 100% | 0.0 | 99.30% | 1439 | OK326061.1 |
| Paraclostridium benzoelyticum strain B1-P-100 16S ribosomal RNA gene, partial sequence | Paraclostridium … | 2577 | 2577 | 100% | 0.0 | 99.30% | 1439 | OK271508.1 |
| Paraclostridium benzoelyticum strain B1-P-103 16S ribosomal RNA gene, partial sequence | Paraclostridium … | 2577 | 2577 | 100% | 0.0 | 99.30% | 1437 | OK271511.1 |
| Paraclostridium benzoelyticum strain Y2-Q-101 16S ribosomal RNA gene, partial sequence | Paraclostridium … | 2577 | 2577 | 100% | 0.0 | 99.30% | 1470 | OK326614.1 |
| Clostridium bifermentans strain HT2 16S ribosomal RNA gene, partial sequence | Paraclostridium … | 2577 | 2577 | 100% | 0.0 | 99.30% | 1460 | DQ978211.1 |
| [Clostridium] bifermentans strain E006 16S ribosomal RNA gene, partial sequence | Paraclostridium … | 2575 | 2575 | 100% | 0.0 | 99.30% | 1469 | JX267047.1 |
| Paraclostridium benzoelyticum strain P1-P-100 16S ribosomal RNA gene, partial sequence | Paraclostridium … | 2575 | 2575 | 100% | 0.0 | 99.30% | 1452 | OK272048.1 |
| Clostridium sp. CS2 16S ribosomal RNA gene, partial sequence | Clostridium sp. … | 2575 | 2575 | 100% | 0.0 | 99.30% | 1445 | FJ638499.1 |
| Paraclostridium bifermentans strain HD0315_2 chromosome, complete genome | Paraclostridium … | 2575 | 43747 | 100% | 0.0 | 99.30% | 3265124 | CP094933.1 |
| Uncultured bacterium clone 271H2B_15 16S ribosomal RNA gene, partial sequence | uncultured bacte… | 2575 | 2575 | 100% | 0.0 | 99.30% | 1463 | KC408481.1 |
| [Clostridium] bifermentans strain E019 16S ribosomal RNA gene, partial sequence | Paraclostridium … | 2575 | 2575 | 100% | 0.0 | 99.30% | 1474 | JX267051.1 |

**Appendix Figure 8**: The **Sequences producing significant alignments for HMRBI-1**

| Description | Scientific Name | Max Score | Total Score | Query Cover | E value | Per. Ident | Acc. Len | Accession |
|---|---|---|---|---|---|---|---|---|
| Paraclostridium sp. strain CD-H-12 16S ribosomal RNA gene, partial sequence | Paraclostridium … | 2521 | 2521 | 100% | 0.0 | 99.93% | 1457 | OP491973.1 |
| Uncultured Paraclostridium sp. clone asv_152_2131 16S ribosomal RNA gene, partial sequence; 16S-23S rib… | uncultured Para… | 2521 | 2521 | 100% | 0.0 | 99.93% | 2131 | MT967653.1 |
| Clostridium sordellii gene for 16S ribosomal RNA, partial sequence, strain: TM204 | Paraclostridium … | 2521 | 2521 | 100% | 0.0 | 99.93% | 1408 | AB448946.1 |
| Paraclostridium bifermentans strain JCM 1386 16S ribosomal RNA, partial sequence | Paraclostridium … | 2521 | 2521 | 100% | 0.0 | 99.93% | 1463 | NR_113323.1 |
| [Clostridium] bifermentans strain 0912-02001 16S ribosomal RNA gene, partial sequence | Paraclostridium … | 2521 | 2521 | 100% | 0.0 | 99.93% | 1406 | KP944171.1 |
| Paraclostridium bifermentans strain Cbm chromosome | Paraclostridium … | 2521 | 23433 | 100% | 0.0 | 99.93% | 3638572 | CP032452.1 |
| Paraclostridium bifermentans strain Nesulana1 16S ribosomal RNA gene, partial sequence | Paraclostridium … | 2521 | 2521 | 100% | 0.0 | 99.93% | 1472 | KJ722487.1 |
| Uncultured bacterium clone 425_TC18_122 16S ribosomal RNA gene, partial sequence | uncultured bacte… | 2521 | 2521 | 100% | 0.0 | 99.93% | 1424 | KM251041.1 |
| Paraclostridium bifermentans strain 2343 16S ribosomal RNA gene, partial sequence | Paraclostridium … | 2521 | 2521 | 100% | 0.0 | 99.93% | 1408 | MT604800.1 |
| Clostridium sp. zx5 16S ribosomal RNA gene, partial sequence | Clostridium sp. zx5 | 2521 | 2521 | 100% | 0.0 | 99.93% | 1483 | EF052864.1 |
| Paraclostridium bifermentans strain 2-31 16S ribosomal RNA gene, partial sequence | Paraclostridium … | 2521 | 2521 | 100% | 0.0 | 99.93% | 1416 | PP512795.1 |
| Paraclostridium bifermentans strain DSM 14991 chromosome, complete genome | Paraclostridium … | 2521 | 40271 | 100% | 0.0 | 99.93% | 3304778 | CP079737.1 |
| Clostridium sp. H2 gene for 16S ribosomal RNA, partial sequence, strain: H2 | Clostridium sp. H2 | 2521 | 2521 | 100% | 0.0 | 99.93% | 1463 | LC194786.1 |
| Paraclostridium sp. strain M3-Q-101 16S ribosomal RNA gene, partial sequence | Paraclostridium … | 2521 | 2521 | 100% | 0.0 | 99.93% | 1438 | OK326205.1 |
| Paraclostridium benzoelyticum strain BL-Q-101 16S ribosomal RNA gene, partial sequence | Paraclostridium … | 2518 | 2518 | 100% | 0.0 | 99.85% | 1439 | OK326061.1 |
| Paraclostridium benzoelyticum strain B1-P-100 16S ribosomal RNA gene, partial sequence | Paraclostridium … | 2518 | 2518 | 100% | 0.0 | 99.85% | 1439 | OK271508.1 |
| Clostridium bifermentans strain CM-C76 16S ribosomal RNA (rrs) gene, partial sequence | Paraclostridium … | 2518 | 2518 | 100% | 0.0 | 99.85% | 1406 | EU869237.1 |
| Paraclostridium benzoelyticum strain B1-P-103 16S ribosomal RNA gene, partial sequence | Paraclostridium … | 2518 | 2518 | 100% | 0.0 | 99.85% | 1437 | OK271511.1 |
| Paraclostridium benzoelyticum strain Y2-Q-101 16S ribosomal RNA gene, partial sequence | Paraclostridium … | 2518 | 2518 | 100% | 0.0 | 99.85% | 1470 | OK326614.1 |
| Clostridium bifermentans strain HT2 16S ribosomal RNA gene, partial sequence | Paraclostridium … | 2518 | 2518 | 100% | 0.0 | 99.85% | 1460 | DQ978211.1 |
| [Clostridium] bifermentans strain E006 16S ribosomal RNA gene, partial sequence | Paraclostridium … | 2516 | 2516 | 100% | 0.0 | 99.85% | 1469 | JX267047.1 |
| Paraclostridium benzoelyticum strain P1-P-100 16S ribosomal RNA gene, partial sequence | Paraclostridium … | 2516 | 2516 | 100% | 0.0 | 99.85% | 1452 | OK272048.1 |

**Appendix Figure 9: The Sequences producing significant alignments for HMRBI-3**

| Description | Scientific Name | Max Score | Total Score | Query Cover | E value | Per. Ident | Acc. Len | Accession |
|---|---|---|---|---|---|---|---|---|
| Klebsiella oxytoca strain C-S-PDA8 16S ribosomal RNA gene, partial sequence | Klebsiella oxytoca | 2198 | 2198 | 100% | 0.0 | 99.92% | 1226 | HM755642.1 |
| Klebsiella michiganensis strain K92 chromosome, complete genome | Klebsiella michiganensis | 2176 | 17411 | 100% | 0.0 | 99.58% | 6108919 | CP089315.1 |
| Klebsiella sp. AUSMSAA18 16S ribosomal RNA gene, partial sequence | Klebsiella sp. AUSMS... | 2176 | 2176 | 100% | 0.0 | 99.58% | 1510 | KP689585.1 |
| Klebsiella michiganensis strain M1, complete genome | Klebsiella michiganensis | 2176 | 17284 | 100% | 0.0 | 99.58% | 5865090 | CP008841.1 |
| Klebsiella michiganensis strain AKKL-001 chromosome, complete genome | Klebsiella michiganensis | 2176 | 17411 | 100% | 0.0 | 99.58% | 6149586 | CP060111.1 |
| Uncultured bacterium clone ncd1553a11c1 16S ribosomal RNA gene, partial sequence | uncultured bacterium | 2176 | 2176 | 100% | 0.0 | 99.58% | 1361 | JF135009.1 |
| Klebsiella michiganensis strain 8BG chromosome, complete genome | Klebsiella michiganensis | 2176 | 17411 | 100% | 0.0 | 99.58% | 6072493 | CP106658.1 |
| Klebsiella michiganensis strain JNQH491 chromosome, complete genome | Klebsiella michiganensis | 2176 | 17280 | 100% | 0.0 | 99.58% | 6039729 | CP075881.1 |
| Klebsiella michiganensis E718 chromosome, complete genome | Klebsiella michiganen... | 2176 | 17367 | 100% | 0.0 | 99.58% | 6097032 | CP003683.1 |
| Klebsiella michiganensis strain YL6-1 chromosome, complete genome | Klebsiella michiganensis | 2176 | 17345 | 100% | 0.0 | 99.58% | 6111288 | CP084415.1 |
| Klebsiella michiganensis strain 5088 chromosome, complete genome | Klebsiella michiganensis | 2176 | 17306 | 100% | 0.0 | 99.58% | 5944805 | CP103554.1 |
| Klebsiella michiganensis strain CCRI-24235 chromosome, complete genome | Klebsiella michiganensis | 2176 | 17210 | 100% | 0.0 | 99.58% | 5977739 | CP081351.1 |
| Klebsiella michiganensis strain 895358 chromosome, complete genome | Klebsiella michiganensis | 2176 | 17328 | 100% | 0.0 | 99.58% | 6130756 | CP159879.1 |
| Klebsiella michiganensis strain LH71 chromosome, complete genome | Klebsiella michiganensis | 2176 | 17343 | 100% | 0.0 | 99.58% | 5892772 | CP100497.1 |
| Uncultured Klebsiella sp. clone 3Q-38 16S ribosomal RNA gene, partial sequence | uncultured Klebsiella sp. | 2176 | 2176 | 100% | 0.0 | 99.58% | 1501 | KT461479.1 |
| Klebsiella michiganensis strain B2SmCTM4 16S ribosomal RNA gene, partial sequence | Klebsiella michiganensis | 2176 | 2176 | 100% | 0.0 | 99.58% | 1436 | MH985208.1 |
| Klebsiella pasteurii strain SPARK1448C2 16S ribosomal RNA gene, partial sequence | Klebsiella pasteurii | 2176 | 2176 | 100% | 0.0 | 99.58% | 1550 | MN104666.1 |
| Klebsiella michiganensis THO-011 DNA, complete genome | Klebsiella michiganensis | 2176 | 17317 | 100% | 0.0 | 99.58% | 5935402 | AP022547.1 |
| Klebsiella pasteurii strain AHM8C130-1I chromosome, complete genome | Klebsiella pasteurii | 2176 | 17411 | 100% | 0.0 | 99.58% | 5959193 | CP104925.1 |
| Klebsiella pasteurii strain Sb-24 chromosome, complete genome | Klebsiella pasteurii | 2176 | 17262 | 100% | 0.0 | 99.58% | 5830883 | CP073236.1 |
| Klebsiella michiganensis strain 2022CK-00623 chromosome, complete genome | Klebsiella michiganensis | 2176 | 17356 | 100% | 0.0 | 99.58% | 6301770 | CP166234.1 |
| Uncultured Klebsiella sp. clone F3jan.13 16S ribosomal RNA gene, partial sequence | uncultured Klebsiella sp. | 2176 | 2176 | 100% | 0.0 | 99.58% | 1463 | GQ417546.1 |

**Appendix Figure 10: The Sequences producing significant alignments for HMRBI-13**

| Description | Scientific Name | Max Score | Total Score | Query Cover | E value | Per. Ident | Acc. Len | Accession |
|---|---|---|---|---|---|---|---|---|
| Klebsiella michiganensis strain MIN-086 chromosome | Klebsiella michiganensis | 2410 | 19016 | 100% | 0.0 | 99.85% | 6064047 | CP086124.1 |
| Klebsiella michiganensis strain 2023CK-00457 chromosome, complete genome | Klebsiella michiganensis | 2410 | 19071 | 100% | 0.0 | 99.85% | 6062634 | CP166239.1 |
| Uncultured Klebsiella sp. clone F4jun.28 16S ribosomal RNA gene, partial sequence | uncultured Klebsiella sp. | 2410 | 2410 | 100% | 0.0 | 99.85% | 1463 | GQ418115.1 |
| Klebsiella oxytoca strain MBTC3 16S ribosomal RNA gene, partial sequence | Klebsiella oxytoca | 2410 | 2410 | 100% | 0.0 | 99.85% | 1494 | MT982728.1 |
| Uncultured Klebsiella sp. clone F1Sjun.42 16S ribosomal RNA gene, partial sequence | uncultured Klebsiella sp. | 2405 | 2405 | 100% | 0.0 | 99.77% | 1463 | GQ417205.1 |
| Klebsiella michiganensis strain M1, complete genome | Klebsiella michiganensis | 2405 | 19005 | 100% | 0.0 | 99.77% | 5865090 | CP008841.1 |
| Klebsiella pasteurii strain CM-1 chromosome | Klebsiella pasteurii | 2405 | 19090 | 100% | 0.0 | 99.77% | 5937175 | CP134211.1 |
| Uncultured Klebsiella sp. clone F1Sjun.34 16S ribosomal RNA gene, partial sequence | uncultured Klebsiella sp. | 2405 | 2405 | 100% | 0.0 | 99.77% | 1463 | GQ417197.1 |
| Uncultured Klebsiella sp. clone F4aug.36 16S ribosomal RNA gene, partial sequence | uncultured Klebsiella sp. | 2405 | 2405 | 100% | 0.0 | 99.77% | 1463 | GQ415904.1 |
| Klebsiella michiganensis strain CCRI-24235 chromosome, complete genome | Klebsiella michiganensis | 2405 | 18898 | 100% | 0.0 | 99.77% | 5977739 | CP081351.1 |
| Klebsiella michiganensis strain X2-1 chromosome, complete genome | Klebsiella michiganensis | 2405 | 18911 | 100% | 0.0 | 99.77% | 5845628 | CP051427.1 |
| Klebsiella michiganensis strain Colony517 chromosome | Klebsiella michiganensis | 2405 | 19031 | 100% | 0.0 | 99.77% | 6344682 | CP080009.1 |
| Klebsiella sp. strain F25 16S ribosomal RNA gene, partial sequence | Klebsiella sp. | 2405 | 2405 | 100% | 0.0 | 99.77% | 1502 | ON936102.1 |
| Uncultured Klebsiella sp. clone F1jun.41 16S ribosomal RNA gene, partial sequence | uncultured Klebsiella sp. | 2405 | 2405 | 100% | 0.0 | 99.77% | 1463 | GQ416907.1 |
| Klebsiella pasteurii strain Ko4 16S ribosomal RNA gene, partial sequence | Klebsiella pasteurii | 2405 | 2405 | 100% | 0.0 | 99.77% | 1550 | MN104675.1 |
| Klebsiella oxytoca strain GZC140 16S ribosomal RNA gene, partial sequence | Klebsiella oxytoca | 2405 | 2405 | 100% | 0.0 | 99.77% | 1504 | MW898652.1 |
| Klebsiella michiganensis strain Kox58 chromosome, complete genome | Klebsiella michiganensis | 2405 | 18950 | 100% | 0.0 | 99.77% | 6060346 | CP089395.1 |
| Klebsiella michiganensis THO-011 DNA, complete genome | Klebsiella michiganensis | 2405 | 18972 | 100% | 0.0 | 99.77% | 5935402 | AP022547.1 |
| Klebsiella michiganensis strain Colony351 chromosome | Klebsiella michiganensis | 2405 | 19012 | 100% | 0.0 | 99.77% | 6337738 | CP080010.1 |
| Klebsiella pasteurii strain Sb-24 chromosome, complete genome | Klebsiella pasteurii | 2405 | 19033 | 100% | 0.0 | 99.77% | 5830883 | CP073236.1 |
| Klebsiella michiganensis strain F107 chromosome, complete genome | Klebsiella michiganensis | 2405 | 18839 | 100% | 0.0 | 99.77% | 5699220 | CP024643.1 |
| Klebsiella michiganensis strain VITSW4 16S ribosomal RNA gene, partial sequence | Klebsiella michiganensis | 2405 | 2405 | 100% | 0.0 | 99.77% | 1465 | KP100328.1 |

**Appendix Figure 11:The Sequences producing significant alignments for HMRBI-14**

| Description | Scientific Name | Max Score | Total Score | Query Cover | E value | Per. Ident | Acc. Len | Accession |
|---|---|---|---|---|---|---|---|---|
| Paraclostridium sp. strain CD-H-12 16S ribosomal RNA gene, partial sequence | Paraclostridium … | 2567 | 2567 | 100% | 0.0 | 99.93% | 1457 | OP491973.1 |
| Uncultured Paraclostridium sp. clone asv_152_2131 16S ribosomal RNA gene, partial sequence; 16S-23S rib… | uncultured Para… | 2567 | 2567 | 100% | 0.0 | 99.93% | 2131 | MT967653.1 |
| Paraclostridium bifermentans strain JCM 1386 16S ribosomal RNA, partial sequence | Paraclostridium … | 2567 | 2567 | 100% | 0.0 | 99.93% | 1463 | NR_113323.1 |
| Paraclostridium bifermentans strain Cbm chromosome | Paraclostridium … | 2567 | 23928 | 100% | 0.0 | 99.93% | 3638572 | CP032452.1 |
| Paraclostridium bifermentans strain Nesulana1 16S ribosomal RNA gene, partial sequence | Paraclostridium … | 2567 | 2567 | 100% | 0.0 | 99.93% | 1472 | KJ722487.1 |
| Uncultured bacterium clone 425_TC18_122 16S ribosomal RNA gene, partial sequence | uncultured bacte… | 2567 | 2567 | 100% | 0.0 | 99.93% | 1424 | KM251041.1 |
| Clostridium sp. zx5 16S ribosomal RNA gene, partial sequence | Clostridium sp. zx5 | 2567 | 2567 | 100% | 0.0 | 99.93% | 1483 | EF052864.1 |
| Paraclostridium bifermentans strain DSM 14991 chromosome, complete genome | Paraclostridium … | 2567 | 41009 | 100% | 0.0 | 99.93% | 3304778 | CP079737.1 |
| Clostridium sp. H2 gene for 16S ribosomal RNA, partial sequence, strain: H2 | Clostridium sp. H2 | 2567 | 2567 | 100% | 0.0 | 99.93% | 1463 | LC194786.1 |
| Paraclostridium sp. strain M3-Q-101 16S ribosomal RNA gene, partial sequence | Paraclostridium … | 2567 | 2567 | 100% | 0.0 | 99.93% | 1438 | OK326205.1 |
| Paraclostridium benzoelyticum strain BL-Q-101 16S ribosomal RNA gene, partial sequence | Paraclostridium … | 2564 | 2564 | 100% | 0.0 | 99.86% | 1439 | OK326061.1 |
| Clostridium sordellii gene for 16S ribosomal RNA, partial sequence, strain: TM204 | Paraclostridium … | 2564 | 2564 | 99% | 0.0 | 99.93% | 1408 | AB448946.1 |
| Paraclostridium benzoelyticum strain B1-P-100 16S ribosomal RNA gene, partial sequence | Paraclostridium … | 2564 | 2564 | 100% | 0.0 | 99.86% | 1439 | OK271508.1 |
| [Clostridium] bifermentans strain 0912-02001 16S ribosomal RNA gene, partial sequence | Paraclostridium … | 2564 | 2564 | 99% | 0.0 | 99.93% | 1406 | KP944171.1 |
| Clostridium bifermentans strain CM-C76 16S ribosomal RNA (rrs) gene, partial sequence | Paraclostridium … | 2564 | 2564 | 100% | 0.0 | 99.86% | 1406 | EU869237.1 |
| Paraclostridium benzoelyticum strain B1-P-103 16S ribosomal RNA gene, partial sequence | Paraclostridium … | 2564 | 2564 | 100% | 0.0 | 99.86% | 1437 | OK271511.1 |
| Paraclostridium benzoelyticum strain Y2-Q-101 16S ribosomal RNA gene, partial sequence | Paraclostridium … | 2564 | 2564 | 100% | 0.0 | 99.86% | 1470 | OK326614.1 |
| Clostridium bifermentans strain HT2 16S ribosomal RNA gene, partial sequence | Paraclostridium … | 2564 | 2564 | 100% | 0.0 | 99.86% | 1460 | DQ978211.1 |
| [Clostridium] bifermentans strain E006 16S ribosomal RNA gene, partial sequence | Paraclostridium … | 2562 | 2562 | 100% | 0.0 | 99.86% | 1469 | JX267047.1 |
| Paraclostridium benzoelyticum strain P1-P-100 16S ribosomal RNA gene, partial sequence | Paraclostridium … | 2562 | 2562 | 100% | 0.0 | 99.86% | 1452 | OK272048.1 |
| Clostridium sp. CS2 16S ribosomal RNA gene, partial sequence | Clostridium sp. … | 2562 | 2562 | 100% | 0.0 | 99.86% | 1445 | FJ638499.1 |
| Paraclostridium bifermentans strain HD0315_2 chromosome, complete genome | Paraclostridium … | 2562 | 43527 | 100% | 0.0 | 99.86% | 3265124 | CP094933.1 |

**Appendix Figure 12: The Sequences producing significant alignments for HMRBI-20**

| Description | Scientific Name | Max Score | Total Score | Query Cover | E value | Per. Ident | Acc. Len | Accession |
|---|---|---|---|---|---|---|---|---|
| Citrobacter farmeri strain BT3301 16S ribosomal RNA gene, partial sequence | Citrobacter farmeri | 2536 | 2536 | 100% | 0.0 | 99.93% | 1413 | MF682949.1 |
| Citrobacter freundii complex sp. CFNIH2 chromosome, complete genome | Citrobacter freundii compl… | 2519 | 17429 | 100% | 0.0 | 99.71% | 5277996 | CP025757.1 |
| Uncultured Citrobacter sp. clone JH-77 16S ribosomal RNA gene, partial sequence | uncultured Citrobacter sp. | 2508 | 2508 | 100% | 0.0 | 99.56% | 1464 | JQ885541.1 |
| Citrobacter sp. strain ICMP 19575 16S ribosomal RNA gene, partial sequence | Citrobacter sp. | 2508 | 2508 | 99% | 0.0 | 99.64% | 1414 | MK388371.1 |
| Citrobacter farmeri strain 2024CK-01202 chromosome, complete genome | Citrobacter farmeri | 2503 | 17296 | 100% | 0.0 | 99.49% | 5417296 | CP169575.1 |
| Citrobacter farmeri strain YMU17 16S ribosomal RNA gene, partial sequence | Citrobacter farmeri | 2501 | 2501 | 99% | 0.0 | 99.49% | 1421 | MZ895023.1 |
| Citrobacter sp. strain ICMP 19576 16S ribosomal RNA gene, partial sequence | Citrobacter sp. | 2501 | 2501 | 99% | 0.0 | 99.71% | 1394 | MK388395.1 |
| Citrobacter amalonaticus strain 2023CK-01304 chromosome, complete genome | Citrobacter amalonaticus | 2497 | 17373 | 100% | 0.0 | 99.42% | 5053357 | CP140489.1 |
| Citrobacter sp. strain Gamma-79 16S ribosomal RNA gene, partial sequence | Citrobacter sp. | 2497 | 2497 | 100% | 0.0 | 99.42% | 1465 | MH703510.1 |
| Citrobacter sp. CFNIH10 chromosome, complete genome | Citrobacter sp. CFNIH10 | 2497 | 17307 | 100% | 0.0 | 99.42% | 5246201 | CP026216.1 |
| Citrobacter telavivensis strain V703 16S ribosomal RNA gene, partial sequence | Citrobacter telavivensis | 2497 | 2497 | 100% | 0.0 | 99.42% | 1437 | PP961735.1 |
| Citrobacter sp. T1 16S ribosomal RNA gene, partial sequence | Citrobacter sp. T1 | 2492 | 2492 | 100% | 0.0 | 99.35% | 1486 | JQ040542.1 |
| Uncultured Salmonella sp. clone F2jun.10 16S ribosomal RNA gene, partial sequence | uncultured Salmonella sp. | 2492 | 2492 | 100% | 0.0 | 99.35% | 1465 | GQ417394.1 |
| Citrobacter sp. TUST-S4 16S ribosomal RNA gene, partial sequence | Citrobacter sp. TUST-S4 | 2492 | 2492 | 100% | 0.0 | 99.35% | 1431 | KM186146.1 |
| Citrobacter amalonaticus strain C3H chromosome, complete genome | Citrobacter amalonaticus | 2492 | 17445 | 100% | 0.0 | 99.35% | 4847284 | CP080958.1 |
| Citrobacter sp. strain HSTU-ABk15 16S ribosomal RNA gene, partial sequence | Citrobacter sp. | 2492 | 2492 | 100% | 0.0 | 99.35% | 1552 | MW453144.1 |
| Citrobacter sp. Y3 chromosome, complete genome | Citrobacter sp. Y3 | 2492 | 17279 | 100% | 0.0 | 99.35% | 5246113 | CP050009.1 |
| Citrobacter amalonaticus strain 86 genome assembly, chromosome: CITRO86 | Citrobacter amalonaticus | 2492 | 17279 | 100% | 0.0 | 99.35% | 5048670 | LT556084.1 |
| Citrobacter amalonaticus strain CA71 chromosome, complete genome | Citrobacter amalonaticus | 2492 | 17434 | 100% | 0.0 | 99.35% | 4906411 | CP064180.1 |
| Citrobacter sp. T7(2011) 16S ribosomal RNA gene, partial sequence | Citrobacter sp. T7(2011) | 2492 | 2492 | 100% | 0.0 | 99.35% | 1467 | HQ600991.1 |
| Citrobacter amalonaticus strain g20 16S ribosomal RNA gene, partial sequence | Citrobacter amalonaticus | 2492 | 2492 | 99% | 0.0 | 99.42% | 1412 | OP114923.1 |
| Citrobacter amalonaticus strain FDAARGOS_122 chromosome, complete genome | Citrobacter amalonaticus | 2492 | 17274 | 100% | 0.0 | 99.35% | 4904719 | CP014015.2 |

**Appendix Figure 13: The Sequences producing significant alignments for HMRBI-5**

| Description | Scientific Name | Max Score | Total Score | Query Cover | E value | Per. Ident | Acc. Len | Accession |
|---|---|---|---|---|---|---|---|---|
| Citrobacter farmeri strain AFS006815 16S ribosomal RNA gene, partial sequence | Citrobacter farmeri | 2538 | 2538 | 100% | 0.0 | 99.86% | 1542 | OP986118.1 |
| Uncultured Citrobacter sp. clone F1jan.41 16S ribosomal RNA gene, partial sequence | uncultured Citrobacter sp. | 2532 | 2532 | 100% | 0.0 | 99.78% | 1465 | GQ416702.1 |
| Uncultured Citrobacter sp. clone F1jan.43 16S ribosomal RNA gene, partial sequence | uncultured Citrobacter sp. | 2532 | 2532 | 100% | 0.0 | 99.78% | 1465 | GQ416704.1 |
| Citrobacter farmeri strain AUSMDU00008141, complete genome | Citrobacter farmeri | 2532 | 17316 | 100% | 0.0 | 99.78% | 5130228 | CP022695.1 |
| Uncultured Citrobacter sp. clone F4jan.4 16S ribosomal RNA gene, partial sequence | uncultured Citrobacter sp. | 2532 | 2532 | 100% | 0.0 | 99.78% | 1465 | GQ417904.1 |
| Citrobacter farmeri strain CCRI-24236 chromosome, complete genome | Citrobacter farmeri | 2527 | 17436 | 100% | 0.0 | 99.71% | 5022624 | CP081314.1 |
| Uncultured Citrobacter sp. clone F1Sjun.22 16S ribosomal RNA gene, partial sequence | uncultured Citrobacter sp. | 2527 | 2527 | 100% | 0.0 | 99.71% | 1465 | GQ417185.1 |
| Uncultured Citrobacter sp. clone F1jun.27 16S ribosomal RNA gene, partial sequence | uncultured Citrobacter sp. | 2527 | 2527 | 100% | 0.0 | 99.71% | 1465 | GQ416893.1 |
| Uncultured Citrobacter sp. clone F1jan.40 16S ribosomal RNA gene, partial sequence | uncultured Citrobacter sp. | 2527 | 2527 | 100% | 0.0 | 99.71% | 1465 | GQ416701.1 |
| Uncultured Citrobacter sp. clone F1jan.45 16S ribosomal RNA gene, partial sequence | uncultured Citrobacter sp. | 2527 | 2527 | 100% | 0.0 | 99.71% | 1465 | GQ416706.1 |
| Uncultured Citrobacter sp. clone F1jan.44 16S ribosomal RNA gene, partial sequence | uncultured Citrobacter sp. | 2527 | 2527 | 100% | 0.0 | 99.71% | 1465 | GQ416705.1 |
| Uncultured Citrobacter sp. clone F1Sjun.25 16S ribosomal RNA gene, partial sequence | uncultured Citrobacter sp. | 2516 | 2516 | 100% | 0.0 | 99.57% | 1465 | GQ417188.1 |
| Citrobacter farmeri strain 2024CK-01202 chromosome, complete genome | Citrobacter farmeri | 2510 | 17248 | 100% | 0.0 | 99.49% | 5417296 | CP169575.1 |
| Citrobacter sp. ND-3 gene for 16S ribosomal RNA, partial sequence | Citrobacter sp. | 2507 | 2507 | 99% | 0.0 | 99.71% | 1381 | LC379574.1 |
| Citrobacter farmeri strain RCB241 16S ribosomal RNA gene, partial sequence | Citrobacter farmeri | 2503 | 2503 | 98% | 0.0 | 99.85% | 1367 | KT260453.1 |
| Citrobacter farmeri strain A11 16S ribosomal RNA gene, partial sequence | Citrobacter farmeri | 2501 | 2501 | 98% | 0.0 | 99.78% | 1396 | PP813608.1 |
| Uncultured Citrobacter sp. clone NpKsh13 16S ribosomal RNA gene, partial sequence | uncultured Citrobacter sp. | 2499 | 2499 | 100% | 0.0 | 99.35% | 1464 | JQ726794.1 |
| Citrobacter sp. ND-1 gene for 16S ribosomal RNA, partial sequence | Citrobacter sp. | 2495 | 2495 | 99% | 0.0 | 99.56% | 1398 | LC379572.1 |
| Uncultured Citrobacter sp. clone F1feb.12 16S ribosomal RNA gene, partial sequence | uncultured Citrobacter sp. | 2488 | 2488 | 99% | 0.0 | 99.34% | 1463 | GQ416744.1 |
| Citrobacter sp. ND-2 gene for 16S ribosomal RNA, partial sequence | Citrobacter sp. | 2488 | 2488 | 99% | 0.0 | 99.42% | 1385 | LC379573.1 |
| Uncultured Citrobacter sp. clone F1jun.21 16S ribosomal RNA gene, partial sequence | uncultured Citrobacter sp. | 2488 | 2488 | 100% | 0.0 | 99.20% | 1465 | GQ416887.1 |
| Uncultured Citrobacter sp. clone YN11 16S ribosomal RNA gene, partial sequence | uncultured Citrobacter sp. | 2488 | 2488 | 100% | 0.0 | 99.20% | 1464 | JQ918010.1 |

**Appendix Figure 14: The Sequences producing significant alignments for HMRBI-11**

| Description | Scientific Name | Max Score | Total Score | Query Cover | E value | Per. Ident | Acc. Len | Accession |
|---|---|---|---|---|---|---|---|---|
| Citrobacter farmeri strain AFS006815 16S ribosomal RNA gene, partial sequence | Citrobacter farmeri | 2782 | 2782 | 100% | 0.0 | 99.93% | 1542 | OP986118.1 |
| Citrobacter farmeri strain AUSMDU00008141, complete genome | Citrobacter farmeri | 2776 | 19022 | 100% | 0.0 | 99.87% | 5130228 | CP022695.1 |
| Citrobacter farmeri strain CCRI-24236 chromosome, complete genome | Citrobacter farmeri | 2771 | 19142 | 100% | 0.0 | 99.80% | 5022624 | CP081314.1 |
| Citrobacter farmeri strain 2024CK-01202 chromosome, complete genome | Citrobacter farmeri | 2754 | 18954 | 100% | 0.0 | 99.60% | 5417296 | CP169575.1 |
| Citrobacter amalonaticus strain FDAARGOS_122 chromosome, complete genome | Citrobacter amal... | 2726 | 18954 | 100% | 0.0 | 99.27% | 4904719 | CP014015.2 |
| Citrobacter farmeri strain FDAARGOS 1423 chromosome, complete genome | Citrobacter farmeri | 2721 | 18882 | 100% | 0.0 | 99.20% | 4875913 | CP077291.1 |
| Enteric Group 137 16S ribosomal RNA gene, partial sequence | Enteric Group 137 | 2713 | 2713 | 100% | 0.0 | 99.01% | 1538 | AF208013.1 |
| Citrobacter freundii complex sp. CFNIH2 chromosome, complete genome | Citrobacter freun... | 2710 | 18838 | 100% | 0.0 | 99.07% | 5277996 | CP025757.1 |
| Citrobacter farmeri strain AFS026603 16S ribosomal RNA gene, partial sequence | Citrobacter farmeri | 2704 | 2704 | 99% | 0.0 | 99.20% | 1507 | OP986241.1 |
| Citrobacter amalonaticus Y19, complete genome | Citrobacter amal... | 2704 | 18889 | 100% | 0.0 | 99.01% | 5584358 | CP011132.1 |
| Citrobacter amalonaticus strain 2023CK-01304 chromosome, complete genome | Citrobacter amal... | 2699 | 18849 | 100% | 0.0 | 98.94% | 5053357 | CP140489.1 |
| Citrobacter sp. CFNIH10 chromosome, complete genome | Citrobacter sp. ... | 2699 | 18838 | 100% | 0.0 | 98.94% | 5246201 | CP026216.1 |
| Citrobacter sp. strain ANG330 16S ribosomal RNA gene, partial sequence | Citrobacter sp. | 2699 | 2699 | 100% | 0.0 | 98.94% | 1542 | OR512202.1 |
| Uncultured Citrobacter sp. clone F1jan.41 16S ribosomal RNA gene, partial sequence | uncultured Citro... | 2695 | 2695 | 97% | 0.0 | 99.86% | 1465 | GQ416702.1 |
| Citrobacter amalonaticus strain C3H chromosome, complete genome | Citrobacter amal... | 2693 | 18854 | 100% | 0.0 | 98.87% | 4847284 | CP080958.1 |
| Citrobacter sp. Y3 chromosome, complete genome | Citrobacter sp. Y3 | 2693 | 18793 | 100% | 0.0 | 98.87% | 5246113 | CP050009.1 |
| Citrobacter amalonaticus strain CA71 chromosome, complete genome | Citrobacter amal... | 2693 | 18827 | 100% | 0.0 | 98.87% | 4906411 | CP064180.1 |
| Uncultured Citrobacter sp. clone F1Sjun.22 16S ribosomal RNA gene, partial sequence | uncultured Citro... | 2689 | 2689 | 97% | 0.0 | 99.80% | 1465 | GQ417185.1 |
| Uncultured Citrobacter sp. clone F1jan.43 16S ribosomal RNA gene, partial sequence | uncultured Citro... | 2689 | 2689 | 97% | 0.0 | 99.80% | 1465 | GQ416704.1 |
| Uncultured Citrobacter sp. clone F1jun.27 16S ribosomal RNA gene, partial sequence | uncultured Citro... | 2689 | 2689 | 97% | 0.0 | 99.80% | 1465 | GQ416893.1 |
| Uncultured Citrobacter sp. clone F1jan.40 16S ribosomal RNA gene, partial sequence | uncultured Citro... | 2689 | 2689 | 97% | 0.0 | 99.80% | 1465 | GQ416701.1 |
| Uncultured Citrobacter sp. clone F1jan.45 16S ribosomal RNA gene, partial sequence | uncultured Citro... | 2689 | 2689 | 97% | 0.0 | 99.80% | 1465 | GQ416706.1 |

**Appendix Figure 15**: **The Sequences producing significant alignments** for HMRBI-19

# Seid Mohammed Ebu

## Bioremediation Potential and Molecular Characterization of Heavy Metal-Resistance profiles of Bacterial Isolates from Ind...

Quick Submit

Quick Submit

Adama Science and Technology University

### Document Details

Submission ID
trn:oid:::1:3389015335

Submission Date
Oct 27, 2025, 10:40 PM GMT

Download Date
Oct 28, 2025, 5:08 AM GMT

File Name
Duguma_Dibbisa_28-10-2025.pdf

File Size
6.7 MB

199 Pages

60,871 Words

320,254 Characters

# 13% Overall Similarity

The combined total of all matches, including overlapping sources, for each database.

## Filtered from the Report

- Bibliography
- Cited Text
- Small Matches (less than 8 words)

## Exclusions

- 303 Excluded Matches

## Match Groups

**402** Not Cited or Quoted 13%
Matches with neither in-text citation nor quotation marks

**0** Missing Quotations 0%
Matches that are still very similar to source material

**0** Missing Citation 0%
Matches that have quotation marks, but no in-text citation

**0** Cited and Quoted 0%
Matches with in-text citation present, but no quotation marks

## Top Sources

9% Internet sources
6% Publications
2% Submitted works (Student Papers)

## Integrity Flags

**2 Integrity Flags for Review**

**Replaced Characters**
231 suspect characters on 22 pages
Letters are swapped with similar characters from another alphabet.

**Hidden Text**
40 suspect characters on 1 page
Text is altered to blend into the white background of the document.

Our system's algorithms look deeply at a document for any inconsistencies that would set it apart from a normal submission. If we notice something strange, we flag it for you to review.

A Flag is not necessarily an indicator of a problem. However, we'd recommend you focus your attention there for further review.